Breathing New Life into Living Anionic Polymerisation: The Anionic Polymerisation and Selective Functionalisation of Myrcene-Containing Polymers

LLOYD ANDREW SHAW

Breathing New Life into Living Anionic Polymerisation:

The Anionic Polymerisation and Selective Functionalisation of Myrcene-Containing Polymers

Lloyd A. Shaw

Josephine Butler College

A thesis presented in fulfilment of the requirements of Doctor of Philosophy

Declaration

I declare that:

This submission is entirely my own work and is based on research carried out within the Hutchings group at Durham University, Department of Chemistry. No part of this thesis has been submitted elsewhere for any other degree or qualification and each contribution to and quotation in this submission, which is taken from the work or works of other people, has been cited correctly.

Signed:  Date: 31/01/25

Lloyd A. Shaw

PhD Student, Hutchings (Mahon) Group

Abstract

The bio-available monomer myrcene is a highly interesting and increasingly researched chemical within the polymer chemistry community. However, many recent articles about the polymerisation of myrcene and its functionalisation have been published which have been factually incorrect. This has led to many misconceptions about what myrcene can be used for and has slowed the progression of further research. Within this report several erroneous studies reported in the literature have repeated in order to correct our understanding of the polymerisation of myrcene.

Along with reporting the homopolymerisation of myrcene, it's copolymerisation with butadiene and styrene, and the effect that polar additives – such as *N*,*N*,*N*',*N*'-tetramethylethylenediamine – have on the polymerisation kinetics, a system was devised to allow for the living anionic polymerisation of liquid monomers to be performed in a nuclear magnetic resonance tube (without the requirement of a glove box). This setup allows for the direct mapping of the incorporation of different monomers into a copolymer in real time. This approach was used for the accurate determination of the reactivity ratios of the copolymerisation of myrcene and styrene, in the presence of *N*,*N*,*N*',*N*'-tetramethylethylenediamine, to be calculated in an attempt to show that this copolymerisation is not random despite previous claims of a couple of recently published articles.

A method for the selective functionalisation of butadiene-containing polymers has also been devised, whereby it has been shown that the same bio-available monomer, myrcene, can be incorporated into butadiene containing polymers and then be used as a selective site to functionalise the polymer. It was shown that the trisubstitued pendant double bond of myrcene, which is not involved in the polymerisation reaction, can be selectively epoxidised using *m*-CPBA, in preference to any other double bonds present within the copolymerisation with butadiene. This effect, which can be enhanced by the addition of TMEDA during the copolymerisation through the increase in vinyl microstructure content, culminated in the synthesis of a model randomised styrene-butadiene rubber with 5 molar % myrcene that was epoxidised and shown to still selectively epoxidise the myrcene units.

Finally, a new method of multi-chain end functionalisation was proposed using epoxidised myrcene, whereby it was shown that due to the relatively high tolerance of the myrcene

epoxide towards nucleophilic attack, that the epoxidised myrcene could added at the end of anionic polymerisations to install 3-4 functionalised monomer units (compared to the standard 1 or 2 of traditional chain-end functionalisation methods). These epoxides can then be ring opened selectively using $LiAlH_4$ to yield the corresponding hydroxylated polymer.

Table of Contents

List of Abbreviations

AP	Anionic Polymerisation
ATRP	Atom Transfer Radical Polymerisation
CP	Cationic Polymerisation
Đ	Dispersity
DCM	Dichloromethane
DMAPP	Dimethylallyl Pyrophosphate
DPE	1,1-Diphenylethylene
DPE-OSi	1,1-Bis(4-tert-butyldimethylsiloxyphenyl)ethylene
DTHFP	Ditetrahydrofurylpropane
eFRP	Emulsion Free Radical Polymerisation
EM	Epoxidised Myrcene
ETE	Ethyl Tetrahydrofurfuryl Ether
FRP	Free Radical Polymerisation
FTIR	Fourier Transform Infra-Red
GPC	Gel Permeation Chromatography
HCl	Hydrochloric Acid
HFIP	Hexafluoro-Isopropanol
IPP	Isopentenyl Pyrophosphate
IR	Infra-Red
IUPAC	International Union of Pure and Applied Chemistry
LAP	Living Anionic Polymerisation
LDPE	Low Density Poly(Ethylene)
$LiAlH_4$	Lithium Aluminium Hydride
MCP	Metal Catalysed Polymerisation
m-CPBA	Meta-Chloroperoxybenzoic Acid
M-L	Meyer-Lowery
M_n	Number Average Molecular Weight
M_w	Weight Average Molecular Weight
n-BuLi	*n*-Butyllithium
NMP	Nitroxide Mediated Polymerisation
NMR	Nuclear Magnetic Resonance
NR	Natural Rubber
PAA	Peracetic acid
PE	Poly(Ethylene)
PET	Poly(Ethylene Terephthalate)
PFA	Performic Acid
PVC	Poly(Vinyl Chloride)
r	Reactivity Ratio
RAFT	Reversible Addition-Fragmentation chain Transfer

RDRP	Reversible-Deactivation Radical Polymerisation
ROS	Reactive Oxygen Species
RT	Room Temperature
SBR	Styrene-Butadiene Rubber
SBS	Styrene-Butadiene-Styrene
SEC	Size Exclusion Chromatography
sec-BuLi	*sec*-Butyllithium
SIS	Styrene-Isoprene-Styrene
sSBR	Solution Styrene-Butadiene Rubber
T_g	Glass Transition Temperature
THF	Tetrahydrofuran
T_m	Melting Temperature
TMEDA	*N,N,N',N'*-Tetramethylethylenediamine
UHV	Ultra-High Vacuum
X_n	Degree of Polymerisation

Acknowledgements

I would like to take this opportunity to leave a word of appreciation to all those who have contributed to this thesis or contributed to supporting me through the undertaking of this project.

Firstly, I would like to thank my project supervisor, Lian Hutchings, for his fantastic initial concept of this project, his intellectual assistance and constant support throughout my research. Not only was Lian of great support academically, but the countless Friday discussions of everything from polymers to politics have left a lasting impression of someone willing to give their time at a moment's notice, something that I hope I can emulate in my future career.

Secondly, I would like to thank Clare Mahon, my adopted project supervisor when Lian retired, for her never-ending academic and emotional support, not only for during the period of supervision, but as a constant in the Department of Chemistry. Clare's unrivalled levels of motivation and determination have been a constant beacon in finishing this research and without her support there would have been no complete thesis to present.

Next, I would like to thank both the Hutchings group – Antonella Pagliarulo, Danial Day, Natasha Boulding and Charles Tkaczyk – and the Mahon Group – Matthieu Starck, Kate Leslie, James Barclay, James Cresswell, Callum Johnson, Lydia Smith, Elle Fiandra, Jia Luo, Chloe Shilling, Emily Tate, Dalila Di Leva, Jamie Richardson and Yulia Dean – for all of their knowledge, both experimental and theoretical, and for their friendship which made working on this project a real joy (at least until it all had to be written up).

I am also incredibly grateful to all those who provide the services for the Chemistry Department of Durham University, specifically the nuclear magnetic resonance (NMR) spectroscopy service provided by Dr. Juan A Aguilar Malavia. I would also like to thank Gary Southern, Gary Oswald, Anthony Humphries and Annette Passmoor for all of the hard work that they provide to allow for the smooth running of the chemistry department.

I would also like to thank all the support staff, cleaners, technicians and lab attendants in the Chemistry Department. The department would not run without the constant hard work of these people, and I would specifically like to mention Judith, Alice, Alison, Clare and the late Ivan Smith for not only being a part of the team which keeps the department going, but also providing a friendly ear which made my time in the department so much more enjoyable.

Finally, I would like to thank all my friends and family, especially my mother and father – Ayn and Mark – and Elanor Siriwardena for their constant encouragement, emotional support and constant understanding. Elanor has been instrumental in supporting me throughout my research project and without her I would not be in the position I am today.

Chapter 1 – Introduction

1.1 History of Polymers

Synthetic polymers originated early in the 20th century with the invention of the first entirely man-made polymer, Bakelite, synthesised by Baekeland in 1907. [1] However, despite the first man-made polymer only originating in the 20th century, humans have used polymers for millennia, with one of the earliest examples of natural rubber being used by the Aztec and Mayan empires for the Mesoamerican Ballgame. [2] In 1839, following the discovery of vulcanisation by Charles Goodyear, rubber began to be produced on an industrial scale for a variety of applications including waterproof films for clothing, shoe soles and tyres. [1] Although the manufacture of polymers continued to grow through the 19th century and the beginning of the 20th century, it wasn't until 1920 that it was proposed (by Staudinger) that polymers were long chains of molecules chemically bonded together. [3] The significant variability in the chemical structure and properties of polymers and resulting versatility has resulted in polymers impacting almost every facet of human life, from being used to make tyres for transportation, drug delivery systems and medical devices, dispersants in fuel and agriculture, to packaging for food to increase its shelf life. However, in recent years, the plastic and rubber industries have received a lot of bad press, with negative representation of many products in the media and scientific articles. [4] [5] Within the rubber industry in particular, along with challenges in recycling, one of the biggest concerns is that the most widely used monomers - isoprene and butadiene - are not sustainable feedstocks, as they are sourced via the petrochemical industry. Recently, growing interest in the use of sustainable chemical feedstocks in the production of polymers has led to a surge in research into the use of bio-based monomers to replace petroleum-derived monomers. For these reasons, much of the work that will be presented within this thesis will aim to increase the use of bio-based monomers to synthesise commercially viable polymers with improved physical and chemical properties. [6]

1.2 Classification of Polymers

The word polymer comes from the Greek πολύς *(polus*) meaning many and μέρος (*meros)* meaning part. [7] IUPAC defines a polymer as a "molecule of high relative molecular mass, the structure of which essentially comprises the multiple repetition of units derived, actually or conceptually, from molecules of low relative molecular mass", adding that "a molecule can be regarded as having a high relative molecular mass if the addition or removal of one or a few of the units has a negligible effect on the molecular properties." [8]

The term polymer therefore describes a very large and diverse group of both synthetic and natural, linear and branched, simple and complex macromolecules. As a result, polymers can be classified in various ways including according to composition, properties and skeletal structure.

1.2.1 Classification by Source

Polymers can come from a variety of different sources, however, they can be categorised in terms of three main groups: natural polymers, synthetic polymers and bio-based synthetic polymers.

1.2.1.1 Natural polymers make up the fundamental building blocks of living systems. They provide the foundation for all life on earth, with: polysaccharides playing important structural roles in addition to functions in energy storage and cellular communication; poly(peptides) playing numerous structural and catalytic roles in addition to underpinning immune response; and poly(nucleic acids) enabling information storage and transmission. [9] Nature uses these polymers as the basis of existence, and as life evolved, many examples of the use of polymers can be found in ensuring an organism's survival through providing an evolutionary advantage or through using them as a defence mechanism.

1.2.1.2 Synthetic polymers are a class of material that encompasses any man-made polymers synthesised through chemical reactions. [10] Within the literature, synthetic polymers can be generally split into four main groups: organic-synthetic, inorganic-synthetic and inorganic-organic/organic-inorganic synthetic and hybrid polymers, however the definition and differentiation of each of these groups has been the topic of much debate.

Currently, a project is underway within IUPAC polymer division, aiming to clarify polymer terminology, which may lead to more defined guidelines for classification of polymers by source. [11]

1.2.1.2.1 Organic-synthetic polymers are one of the most common classifications of polymer and constitute any man-made polymer derived from organic monomers (any monomer containing carbon and hydrogen; these are generally petroleum derived), such as ethylene, propylene, butadiene and styrene. Organic-synthetic polymers have seen a wide variety of applications through multiple sectors, including applications from packaging to tyre rubbers, where the polymerisation of ethylene and propylene still constitutes around 50% of all synthetic polymers produced, for applications such as insulation, capacitors and medical implants. [12]

1.2.1.2.2 Inorganic-synthetic polymers constitute any polymer void of organic constituents (i.e. does not contain any carbon atoms) – while some definitions of inorganic-polymers are solely focused on the backbone, the focus of the definitions provided in this thesis will be on the polymer as a whole – making this classification of polymers fairly narrow. While the examples of fully inorganic polymers may be limited, several applications include the use of geopolymers (Al-O-Si polymer frameworks) for fire resistance and binders, [13] and poly(thiazyls) (S-N polymer framework) for solar cells and battery cathodes. [14]

1.2.1.2.3 Hybrid-synthetic polymers consist of both organic and inorganic components, however, they may differ in how these components make up the polymer. Examples of hybrid polymers include poly(ethylene sulfide) and poly(ethylene oxide), which have both experienced growing interest in the search for solid-state-lithium batteries. [15] Hybrid polymers may include polymers with either an inorganic backbone with organic constituents (inorganic-organic synthetic polymers), such as poly(siloxanes) – silicon-oxygen polymer backbone with alkyl substituents – which have been widely used within medical devices due to their high level of biocompatibility, [16] or polymers that have an organic backbone with inorganic constituents (organic-inorganic synthetic polymers), such as poly(acrylates) and poly(methacrylates) – carbon-based polymer backbone with oxygen substituents giving ester

or acid functional groups in the side chains of the polymer – which have seen a wide variety of uses from acrylic paints to biomaterials for functional biological tissues and drug delivery systems. [17]

1.2.1.3 Bio-based synthetic polymers are another emerging class of polymer, which have been widely studied. Bio-based synthetic polymers represent a classification of polymer that are synthetic in nature, but that are synthesised using monomers derived from natural sources or polymers that have synthesised through biological processes (e.g. enzymatic polymerisation) from man-made sources. [18] This class of materials can include everything from vulcanised natural rubber, which is probably one of earliest example of a bio-based synthetic polymer and constitutes natural rubber that has been synthetically crosslinked to improve upon its physical properties, to synthetic poly(saccharides) and poly(terpenoids), which are materials synthesised by the polymerisation of monomers found in biomass. [19]

1.2.2 Classification according to Composition

Polymers can also be classified according to their composition, whether this be the number of types of monomer used or the way in which different monomers are distributed throughout a polymer chain. [20] The simplest class of polymer is the homopolymer, which comprises only one type of monomer. When two or more different monomers are used, the polymer is classified as a copolymer (terms such as terpolymer can also be used to define copolymers with three different monomer units). Copolymers can be further sub-divided into groups that consider the sequence distribution of monomer units within the copolymer chain. The two main sub-groups of copolymer classification are block copolymers and statistical copolymers.

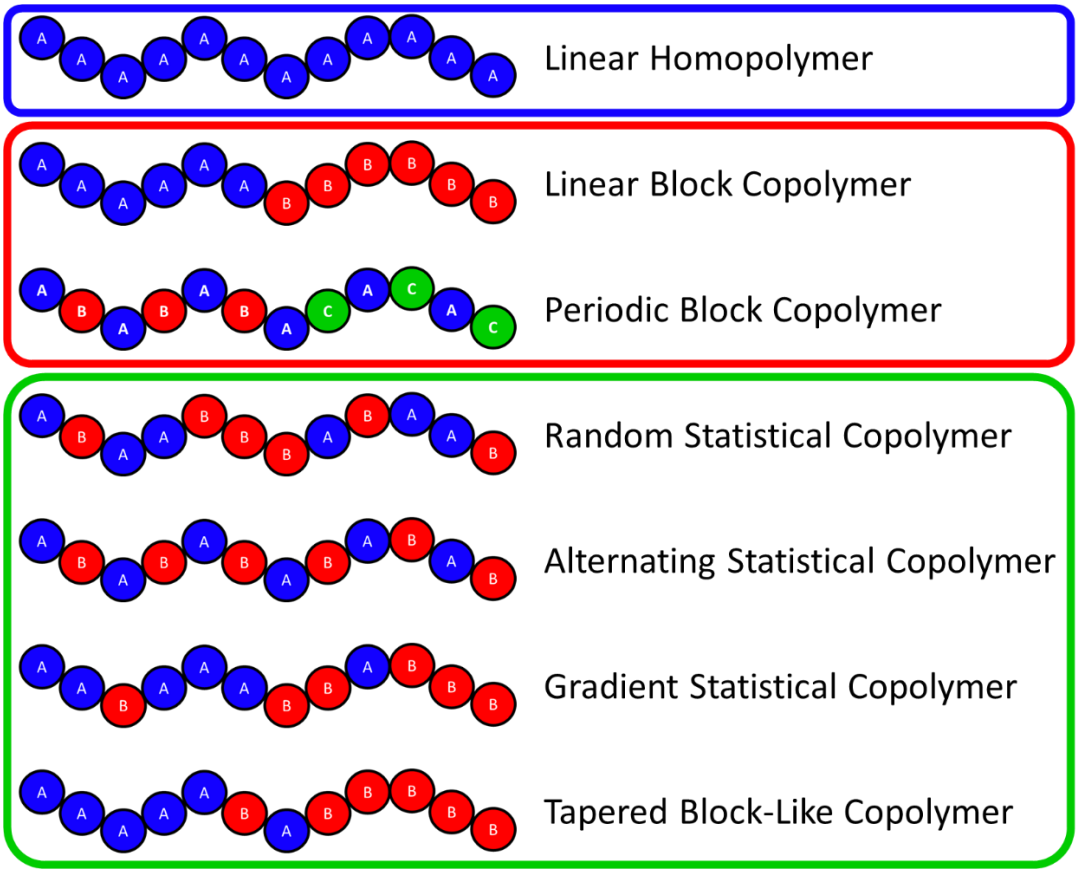

Figure 1.1: Classifications of polymers by composition, whereby the polymer within the blue box represents a homopolymer, the polymers within the red box represent block copolymers and the polymers within the green box represent statistical copolymers.

1.2.2.1 Block copolymers are copolymers that comprise two or more distinct blocks of different monomers – see Figure 1.1. The blocks can be arranged in various ways, from the simplest AB diblock copolymer to triblock copolymers (-A-B-C- or -A-B-A-), and far more complicated multiblock copolymers such as periodic block copolymers that constitute two blocks of different periodic composition.

1.2.2.2 Statistical copolymers arise when two or more monomers are polymerised simultaneously, and the resulting monomer sequence is determined by the relative reactivity of the two monomers and propagating species. Statistical copolymers can generally fall into one of four different classes, which include but are not limited to:

1.2.2.2.1 Random copolymers – These are copolymers where the sequence of monomers is completely random. This type of polymer is synthesised when there is no

selectivity between monomer ‘A’ or monomer ‘B’ when the chain is propagating, so no discernible sequence can be observed.

1.2.2.2.2 Alternating copolymers – As the name suggests, these are copolymers in which the monomer sequence strictly alternates between monomer ‘A’ and monomer ‘B’ and there is no homopolymerisation.

1.2.2.2.3 Gradient copolymers – These are copolymers where there is a gradient in composition from monomer ‘A’ to monomer ‘B’ along the polymer chain. This type of polymer arises when the initial monomer feed ratio is not maintained, and therefore changes continuously with polymer conversion, and monomer ‘A’ prefers homopolymerisation over copolymerisation with monomer ‘B’.

1.2.2.2.4 Tapered block-like copolymers are a class of copolymer where the gradient of monomer distribution is strong enough for the copolymer to exhibit block-like properties, including but not limited to the ability to microphase separate and the ability to produce copolymers with two T_gs. These are of interest to industry as the process effectively allows block copolymers to be prepared in one step rather than two, which saves both time and money. [21] The work in this thesis will mostly focus on this tapered block-like copolymer class of polymer, as the ability to control monomer sequence through the manipulation of the reactivity ratios is of significant interest to the intended application of the polymers that we synthesise (i.e. the synthesis of modified Styrene-Butadiene Rubber (SBR)).

1.2.3 Classification by Skeletal Structure

Polymers can exist in a range of different architectural configurations, from simple linear polymer chains to the highly complex hyperbranched polymers, such as Low Density Poly(Ethylene) (LDPE), which sees a yearly market share of approximately $67.5 billion for applications across multiple different sectors – the biggest of which is for the production of plastic bags and packaging. [22] The different skeletal structures of polymer chains can significantly impact a polymer’s physical properties, affecting everything from crystallinity to mechanical and rheological properties. Generally, these different polymer skeletal structures can be divided into three main categories: linear polymers (these can include linear

homopolymers, linear copolymers, etc.); branched polymers (these can include star-shaped, H-shaped, comb, brush and dendritic/hyperbranched polymers); and crosslinked polymers (these can include both high-density and low-density crosslinked polymers whereby the crosslinks themselves can be reversible or irreversible). [20] Examples for each of these different categories can be seen in Figure 1.2 below.

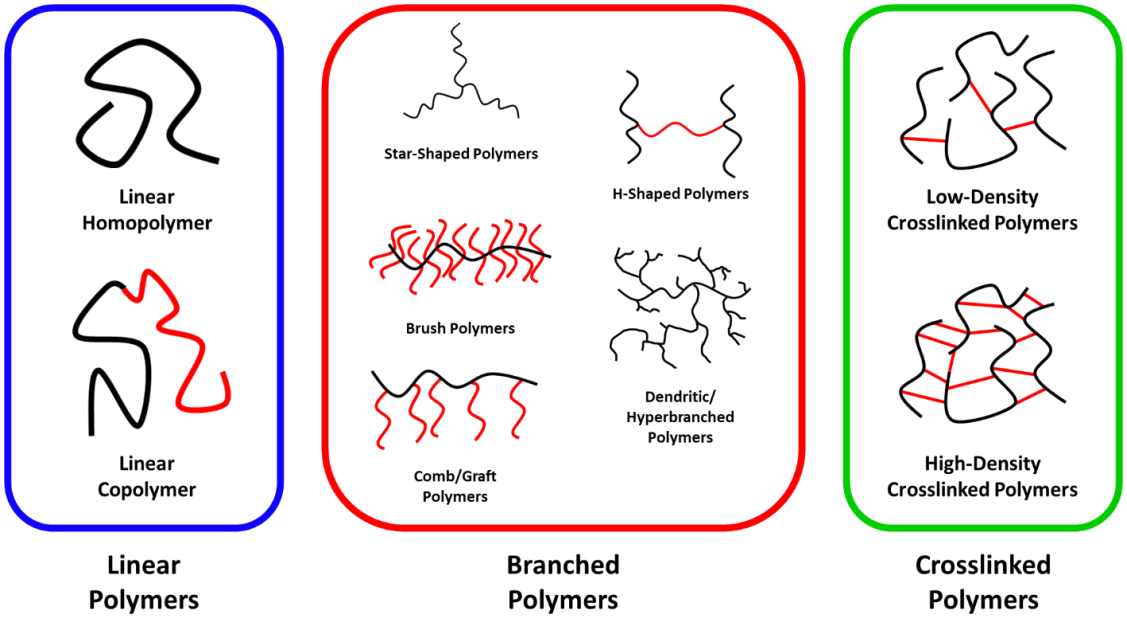

Figure 1.2: Examples of the possible classes of polymer skeletal structures.

1.2.4 Classification by Thermal-Dependant Physical Properties

Another useful way to classify polymers is according to their physical properties and specifically how key physical properties change as a function of temperature. This will have significant implications on the processability and application of the polymer. [20] Within this type of classification there are two key parameters: the melting temperature (T_m), i.e. the temperature at which polymer chains transition from being crystalline to being amorphous; and the glass transition temperature (T_g), which is the temperature at which a polymer transitions from a glassy state into a rubbery state. [23] Polymer classification by thermal-dependant physical properties can therefore be classified into three different groups: thermoplastics, elastomers and thermosets.

1.2.4.1 Thermoplastics are a class of material whereby there are no chemical crosslinks found between the polymer chains. They can be further sub-divided into amorphous – no

long-range order observed among the polymer chains, meaning that the important thermal dependant property will be the T_g – and semi crystalline – significant long-range order observed among the polymer chains resulting in crystallinity throughout the material, meaning that the important thermal-dependant properties will be the T_m and the T_g – thermoplastics. With this class of material, the glass transition temperature (T_g) – or melting temperature (T_m) if a semi-crystalline polymer is used – of the polymer is above the temperature of its intended application, meaning that it is very hard and strong. Due to the lack of chemical crosslinking between the polymer chains (which is found in both elastomers and thermosets), these materials can be heated to above their T_g (or T_m if a semi-crystalline polymer is used) and then reprocessed/recycled before cooling to allow the material to resolidify in its new shape. These thermoplastic polymers include a large range of different polymers including poly(ethylene) (PE), poly(ethylene terephthalate) (PET) and poly(vinyl chloride) (PVC), which have been used in applications from packaging and fabrics to cable and home insulation. [24]

1.2.4.2 Elastomers are a class of material whereby the polymer chains are held together by a low number/density of chemical crosslinks (which are added post-polymerisation once the shape of the material has been set). The application temperature of an elastomer is above the T_g, allowing the material to be stretched and deformed under stress and then return to its original shape when the stress is removed. These elastomeric polymers include a large range of different polymers including crosslinked natural rubber and vulcanised poly(butadiene), with typical examples of their use including as a component of car tyres and rubber bands. [25]

1.2.4.3 Thermosets are a class of material whereby during polymerisation, a large number/density of chemical crosslinks are synthesised between the polymer chains. Once crosslinked, the material can no longer be dissolved in solvent or reprocessed due to its high mechanical and chemical resistance even at elevated temperatures. Popular examples of thermosets include epoxy resins and poly(urethane) resins, which have been used in applications from surface coatings and glues to components of composite materials. [26]

1.3 Polymer Synthesis

Polymerisation is the process through which monomers are joined together, via the formation of chemical bonds, to form polymer chains. [20] There are two main categories of polymerisation mechanism – step growth and chain growth – yet within each category, there are further sub-divisions in which different types of polymerisations can be found.

1.3.1 Step-growth polymerisations – Initially, bifunctional – or trifunctional etc. – monomers are joined together through individual chemical reactions, to form dimers. These dimers can then react with another monomer unit to synthesise a trimer or react with another dimer to synthesise a tetramer. These trimer and tetramer units can then react again to form a whole host of different oligomers and then polymers as the polymerisation progresses. [27] Step-growth polymers can be subdivided into two main groups of polymerisation: polyaddition (used to synthesise poly(urethane)s, which are utilised within fabrics and coatings) – where no molecules are lost during the chemical reaction of the polymerisation – and polycondensation (used to synthesise poly(esters), poly(carbonates) and poly(amides), which are utilised within fabrics and packaging) – where a small molecule, such as water, is eliminated during each chemical reaction of the polymerisation. [28]

1.3.2 Chain-growth polymerisation occurs when a single monomer unit reacts with a propagating polymer chain end. This added monomer then becomes the reactive chain end on addition, and the polymerisation progresses. [29] All chain-growth polymerisation mechanisms have three key steps: initiation, propagation and termination (Figure 1.3).

$$I^{*}+M_A \xrightarrow{k_I} I\text{-}M_A^{*} \quad (1)$$

$$I\text{-}M_A^{*} + M_A \xrightarrow{k_P} I\text{-}M_A\text{-}M_A^{*} + (M_A)_n \rightleftarrows I\text{-}(M_A)_n\text{-}M_A^{*} \quad (2)$$

$$I\text{-}(M_A)_n\text{-}M_A^{*} \xrightarrow{k_T} I\text{-}(M_A)_n\text{-}M_A \quad (3)$$

Figure 1.3: The three main steps of chain-growth polymerisation where 1, 2 and 3 are initiation, propagation and termination respectively.

1. Initiation occurs when the first monomer (M_A) unit reacts with an initiator (I*) to form a reactive unimer (M_A*). This unimer can then go on to react with other monomers through a chain reaction (see propagation).
2. Propagation occurs immediately after initiation and involves the successive addition of individual monomer units to the reactive chain end of the polymer.
3. Termination is the final step of the chain-growth polymerisation. It occurs when reactive propagating sites are irreversibly terminated (deactivated). The precise mechanism of termination depends on the type of polymerisation and the conditions used. [30]

Within the broad class of chain-growth polymerisation, there are several different mechanisms, which include but are not limited to:

- Free Radical Polymerisation (FRP) – Covalent bonds are formed between monomers through the propagation of a radical species. FRP can be used in a variety of processes including bulk polymerisation, solution polymerisation, suspension polymerisation and emulsion polymerisation. FRP is widely exploited by industry for the synthesis of polymers, most commonly from vinyl-containing monomers. [31]
- Reversible-Deactivation Radical Polymerisation (RDRP) – Again, covalent bonds are formed between monomers through the propagation of a radical species. However, unlike FRP, a control agent, which reduces the overall number of active radical species through the establishment of an equilibrium between the active (propagating) radical and a deactivated (stable) species (whereby the equilibrium is highly skewed towards the deactivated species), is also present. There are a number of common RDRP mechanisms, which include:
    - Atom Transfer Radical Polymerisation (ATRP), where a transition metal-halide complex with two easily accessible oxidation states, separated by one electron (common examples include Cu(I)Br/Cu(II)Br_2 and Fe(II)Cl_2/Fe(III)Cl_3), is used to establish the equilibrium. [32] [33]
    - Reversible Addition Fragmentation Chain Transfer (RAFT) polymerisation, where a thiocarbonylthio RAFT agent is used to establish the equilibrium. [34]
    - Nitroxide Mediated Radical Polymerisation (NMP) polymerisation, where a persistent nitroxide radical compound is used to establish the equilibrium. [35]

- Metal Coordination Polymerisation (MCP) – The double bond of a given MCP monomer (such as ethene or propene) coordinates to a metal complex and then through migratory insertion, the polymer chain propagates. [36] MCP was first discovered when workers (Robert L. Banks and J. Paul Hogan) at Philips Petroleum realised that chromium catalysts were highly effective at polymerising ethylene at low temperatures. [37] This catalytic activity that was found for Philips catalysts was then replicated by Karl Ziegler when he discovered that combinations of titanium tetrachloride and diethyl aluminium chloride could also be used to polymerise ethylene. This principle of catalysts based on titanium compounds in combination with organoaluminium compounds was then fundamental to the work of Giulio Natta, who used crystalline titanium trichloride combined with triethylaluminium to synthesise the first isotactic poly(propylene) polymer [38] – work that was responsible for Ziegler and Natta winning the 1963 Nobel Prize in Chemistry. [39]
- Cationic Polymerisation (CP) – Covalent bonds are formed between monomers through the nucleophilic attack of the monomer to the reactive cationic site on the propagating chain. This occurs through the movement of electrons from the monomer and results in the propagation of the cationic site. [40] CP is one of the few polymerisation methods that under certain conditions (e.g. lack of any impurities, mixed solvent systems – e.g. hexane and chloroform – and temperatures below 0 ^{o}C) with certain monomers (e.g. isobutylene, Figure 1.4) can be absent of any inherent termination mechanism and therefore be described as being a “living” polymerisation – see Section 1.3.2.1 below.

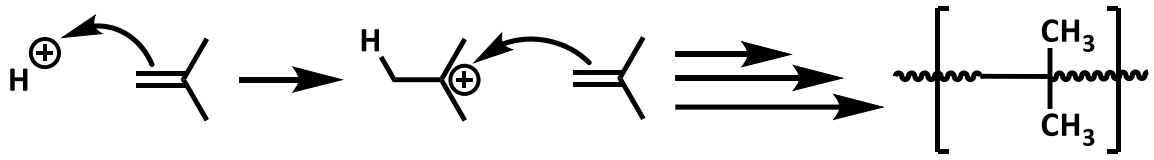

Figure 1.4: Mechanism of the "living" cationic polymerisation of isobutylene, carried out in a 1:1 hexane/chloroform binary solvent at 0 ^{o}C under ultra-high vacuum (UHV).

- Anionic Polymerisation (AP) – Covalent bonds are formed between monomers through the progression of an anionic charge, via the nucleophilic attack on monomers by the propagating anion. This propagating anion is highly reactive towards

electrophilic functional groups, meaning that extensive cleaning, drying and inert atmospheres are required for the polymerisation to occur. However, in the absence of impurities, AP can be one of the most well-controlled polymerisation methods – due to its lack of any inherent termination mechanism – making it the "gold-standard" polymerisation technique in terms of synthesising non-polar polymers with well-controlled molecular weights and weight distributions, and for the synthesis of block copolymers. In the absence of impurities, the AP mechanism can therefore be defined as being "living" – see Section 1.3.2.1. It was for the reasons detailed above that Living Anionic Polymerisation (LAP) was chosen by us as our primary research area. It will therefore be discussed further in Section 1.4 below.

1.3.2.1 Living Polymerisations

For the past 20-25 years, the term "living" with reference to a polymerisation, which was first coined by Szwarc *et al.* in 1956, has been the topic of much debate and confusion within the polymer science community. [41] The debate around this term came about after the discovery of ATRP by Mitsuo Sawamoto and by Krzysztof Matyjaszewski independently in 1995, which many in the community termed a "living" radical polymerisation; a view that was not shared by many others, especially users of anionic and cationic polymerisation. This led to many inaccuracies in the literature with claims of "living" polymerisations, which despite being determined as incorrect by the polymer community, still represents one of the leading inaccuracies that can be found within the literature of RDRPs. The criteria for a "living" polymerisation - which were presented in 1956 by Szwarc [41] – are:

1. The polymerisation continues as long as a monomer is present, and if additional monomer is then added, the polymerisation will proceed once more.
2. The number average molecular weight (M_n) and number average degree of polymerisation (X_n) are directly proportional to the monomer conversion.
3. The number of propagating chains is constant throughout the reaction and is therefore independent of the conversion.
4. The M_n of the final polymer can be controlled by the initial molar ratios of monomer and initiator.
5. Polymers with a low dispersity (<1.1) are synthesised.

6. Block copolymers can be synthesised through the sequential addition of different monomers once the previous block has been polymerised.
7. Chain-end functionalisation can be achieved in quantitative yield through controlled termination reactions. [30]

Most polymer scientists have now agreed that RDRP techniques are not living due to the inherent termination step which, although suppressed compared to FRP, is not eliminated entirely, meaning that typical RDRP mechanisms do not meet all of the 7 criteria that have been set out to define a living system. These types of radical polymerisation processes can therefore be thought of as “controlled” or “quasi-living” instead.

1.4 Living Anionic Polymerisation (LAP)

As mentioned previously, LAP is a chain-growth polymerisation mechanism and one of the few polymerisation methods that, in the absence of impurities, can be described as a "living" polymerisation technique. This is because in the absence of impurities LAP meets all 7 of the criteria for "living" polymerisation due to the absence of inherent termination reactions (Section 1.3.2.1). LAP was first discovered by Szwarc *et al.* in 1956 when they observed the persistent deep red colour of "living" polystyrene after initiation of styrene with sodium naphthalide (see Figure 1.5 below). [41] [42]

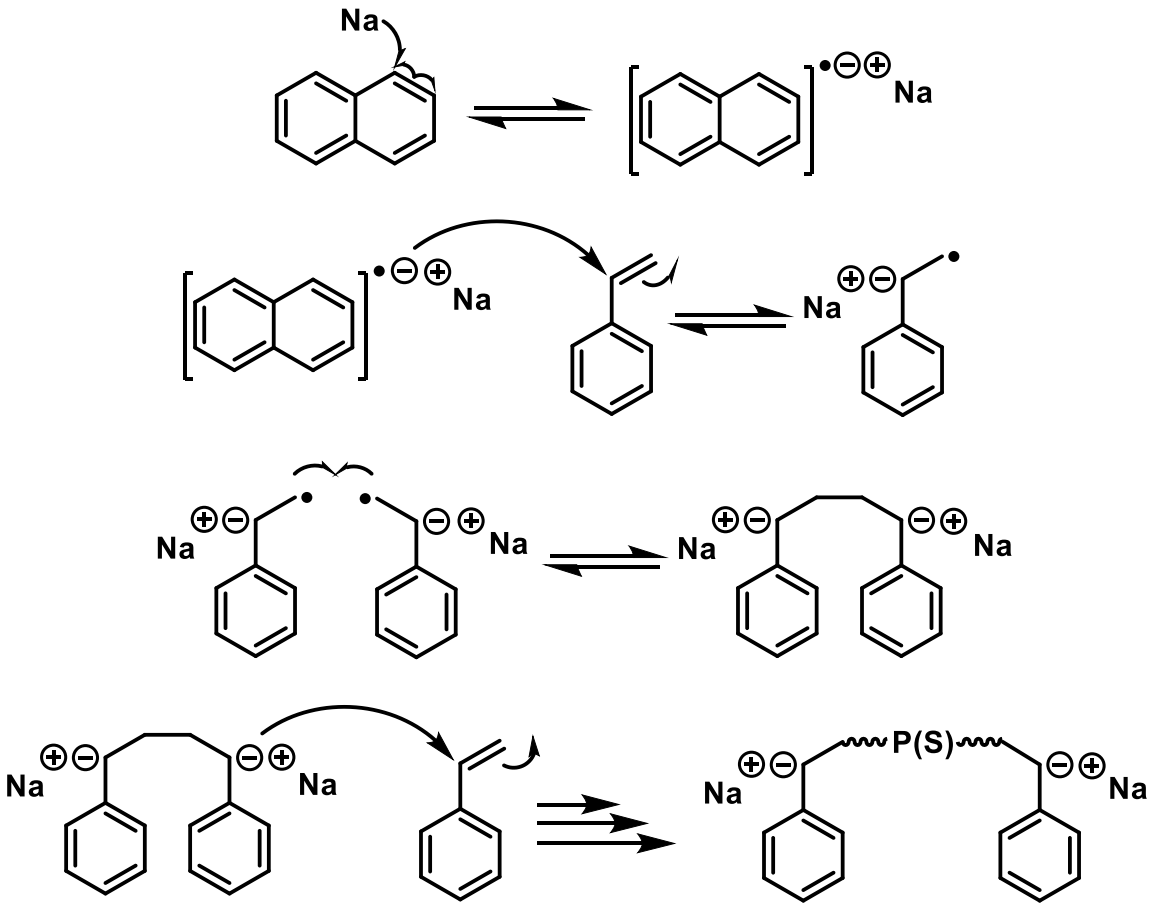

Figure 1.5: Reaction scheme showing the first example of "living" anionic polymerisation by Szwarc, carried out in THF. *[41]*

Since its discovery, LAP has been of great interest to polymer scientists due to its ability to form block copolymers through sequential monomer addition and its ability to synthesise polymers with a large degree of control over the target number-average molecular weight (M_n), monomer distribution, microstructure, and dispersity (Đ) – which will be generally less

than 1.1. The subsequent realisation that organolithium species could be successfully used as initiators in non-polar solvents resulted in widespread adoption of LAP by industry for the synthesis of highly controlled homopolymers, statistical copolymers and block copolymers, despite the difficult reaction conditions, such as extensive cleaning and drying, and the requirement for an inert atmosphere. This requirement for inert conditions and high purity comes about due to the highly reactive propagating carbanions, which are both very basic and very nucleophilic, and so will react rapidly with any species carrying a remotely acidic proton (water, alcohols, acids and even primary/secondary amines) and electrophiles (halides, oxygen, carbon dioxide). Thus, the environmental impurities (water, O_2 and CO_2) need to be excluded, meaning the reactions need to be carried out under a vacuum or inert atmosphere. [30]

The highly reactive carbanionic site present during LAP also limits the functional group tolerance of the technique. For LAP, the only monomers that can generally be used are unfunctionalised vinyl-containing monomers, which can stabilise the negative charge through substituent effects (electron withdrawing, resonance or hyperconjugation). Common industrial examples of monomers utilised within LAP include styrene, butadiene and isoprene (see Figure 1.6 below). Other monomers that contain functionality – such as methacrylates, acrylates, vinyl pyridine and a wide range of styrene derivatives – can be used within LAP but generally require unfavourable conditions – such as being run at reduced temperatures – which may not be practical/financially viable for industry. [30]

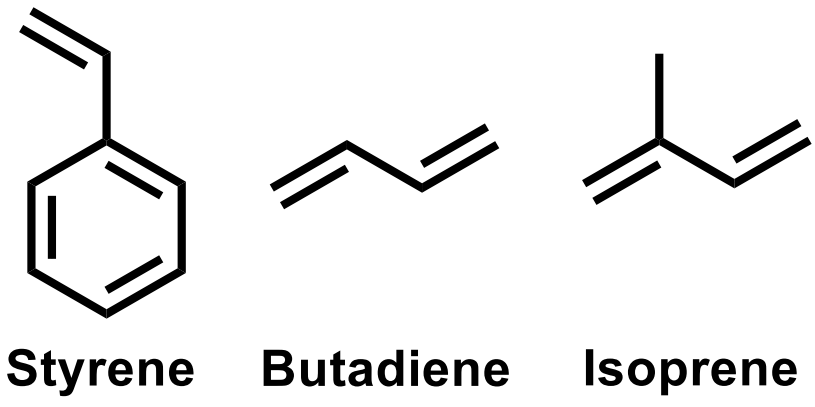

Figure 1.6: Three commonly used monomers in LAP.

As a chain-growth polymerisation, LAP has three main stages to its mechanism: initiation, propagation and termination.

1.4.1 Initiation of Living Anionic Polymerisations

During LAP, initiation is usually achieved using a group 1 metal alkyl initiator, meaning that the living polymer chain has a highly reactive negative charge – which is both highly basic and nucleophilic – at the chain end. Originally, LAP initiation was achieved through electron transfer from a radical anion, as shown in the mechanism proposed by Szwarc (Figure 1.5). As previously mentioned, however, one of the most important factors in the adoption of LAP by industry was the development whereby organolithium compounds, such as *n*-butyllithium (*n*-BuLi) and *sec*-butyllithium (*sec*-BuLi), were used to initiate anionic polymerisations, providing the polymerisation with far greater control over the target molecular weight and molecular weight distribution due to the high rate of initiation that could be achieved (resulting in a rate of initiation that can be far greater than the rate of propagation).

1.4.1.1 Nature of the Carbon-Lithium Bond

The carbon-lithium bond is an extraordinary example of a polar-covalent bond and fundamental to the level of control achieved within LAP. This polar-covalent bond is brought about due to the electronegativity difference between lithium and carbon being only 1.57, meaning that the bond has characteristics of both a covalent and ionic bond, two models of which can be seen in Figure 1.7 below. This results in the precise nature of the C-Li bond being highly dependent on the external environment, the factors and effect of which will be discussed in Section 1.4.1.4 below. [43]

Figure 1.7: The two models that can be used to describe the bonding of lithium to carbon depending on the environmental conditions. (Left: Covalent model in non-polar solvents. Right: Ionic model in polar solvents).

1.4.1.2 Aggregation of Organolithium Compounds in Non-Polar Solvents

When using an organolithium initiator (such as *n*-BuLi) in a non-polar solvent, aggregates of the carbanion and their cationic lithium counterparts will form in the reaction mixture. This is due to the energy minimum associated with the balance between the electrostatic repulsion

of the lithium cations; the electrostatic attraction of the carbanion components to the lithium cations; the enthalpy of solvation; and the association energy of the aggregates. The most favourable degree of aggregation will generally depend on the nature of the anionic charge – i.e. whether the anion is primary, secondary or tertiary and whether there are any substituents that can stabilise the anionic charge – with primary anions on linear alkyl chains (e.g. *n*-BuLi) generally leading to larger aggregates (e.g. hexamers) and secondary/tertiary anions or those next to an aromatic group (e.g. *sec*-BuLi) generally leading to smaller aggregates, such as tetramers or dimers. If the most favourable aggregate for the lithium is a tetramer, this will mean that most of the lithium will be in a tetrameric aggregate. However, this aggregate will be in equilibrium (Figure 1.8) with lithium dimers and unaggregated alkyllithium unimers in non-polar solvents – with the potential for a very small number of aggerates with an even greater degree of aggregation.

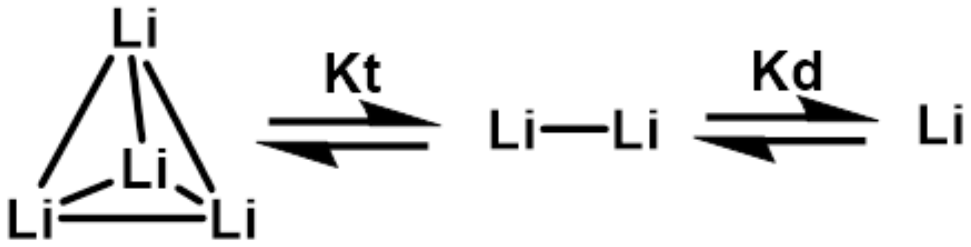

Figure 1.8: Equilibrium for the dissociation of lithium aggregates in solution, where the organic anionic components and associated charges have been excluded for clarity but would be present at the faces of each of the aggregates.

In the literature, there have been two arguments proposed on the effect of these aggregates (1. initiation can only occur in the unaggregated organolithium unimers and 2. polymerisation is greatly reduced in the aggregated form); however, both suggest that at least the majority of polymerisation occurs when the lithium is in the unaggregated state due to the steric hindrance associated with the angle of attack of the new monomer being added onto the chain. [30]

1.4.1.3 Mechanism of Initiation of Living Anionic Polymerisations

As previously mentioned, the majority of initiation that occurs during LAP happens when the organolithium initiator is present in its unaggregated state. This means that when looking at

the mechanism for the initiation of LAP, the dissociation of the lithium aggregates must not only be presented in the mechanism itself (Figure 1.9) but is also fundamental to the rate of initiation equation that has been determined (equation 1.1).

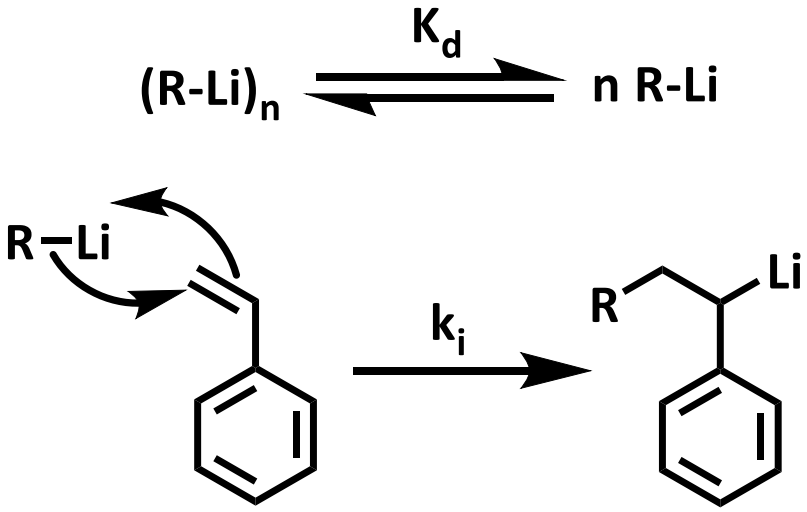

Figure 1.9: Mechanism for the LAP initiation of styrene, in a non-polar solvent, using an organolithium initiator, whereby K_d represents the dissociation constant for the organolithium aggregates and k_i represents the rate constant for initiation.

The LAP initiation of styrene in a non-polar solvent (Figure 1.9) begins with the dissociation of the organolithium aggregates whereby n represents the degree of aggregation – which will be dependent on the initiator that was used, as described in Section 1.4.1.2 – and K_d represents the equilibrium constant between the organolithium aggregates and the unaggregated organolithium. Upon dissociation, the anionic organic component of the organolithium compound can initiate nucleophilic attack on the electrophilic carbon of a vinyl monomer, providing the monomer has a substituent that can stabilise the propagating anion through electron withdrawing effects, resonance or hyperconjugation. Upon attack of the monomer, the anion of the initiator will progress through the vinyl group of the monomer whereby another monomer can be attacked resulting in progression to the propagation stage of the polymerisation or the lithium can reaggregate (generally with a decreased aggregation number due to the increased sterics and increased carbon-lithium bond length).

Due to the occurrence of aggregation of organolithium compounds, the rate of initiation calculation must therefore include an inverse order dependence with relation to the aggregation number of initiator (Equation 1.1).

$$R_i = k_i K_d [\text{R-Li}]^{1/n} [\text{M}]$$

Equation 1.1: Rate of initiation (R_i) in aromatic non-polar solvents, whereby k_i represents the rate constant for initiation, K_d represents the equilibrium constant between the aggregated and unaggregated states of the initiator, [R-Li] represents the concentration of the initiator, n represents the most favourable aggregation state of the initiator and [M] represents the concentration of the monomer.

Equation 1.1 describes the rate of initiation for anionic polymerisations carried out in a non-polar aromatic solvent, but it fails to adequately describe the corresponding initiation process in aliphatic solvents. This discrepancy is most likely due to the incomplete dissociation of the aggregates in aliphatic solvents and the formation of cross-association species, due to the massively reduced rates of initiation, although a detailed discussion is beyond the scope of this thesis. Equation 1.1 can be further simplified through the exclusion of constants to show the impact of each variable on the rate of initiation (Equation 1.2).

$$R_i \propto [\text{R-Li}]^{1/n}$$

$$R_i \propto [\text{M}]$$

Equation 1.2: Proportionality of the rate of initiation (R_i) shown in relation to the concentration of the initiator ([R-Li]), the most favourable aggregation state of the initiator (n), and the concentration of the monomer ([M]).

In non-polar aromatic solvents, the rate of initiation is directly proportional to the initiator concentration to the power of inverse n, whereby n is the aggregation number of the initiator used in the selected solvent, and directly proportional to the monomer concentration.

1.4.1.4 Factors Influencing the Initiation of Living Anionic Polymerisations

It can readily be seen that the rate of initiation of an anionic polymerisation is increased by increasing the monomer concentration and the organolithium initiator concentration, or by decreasing the aggregation number of the initiator used (Equation 1.2). However, what might not be as evident are the factors that can influence the aggregation number and the rate constant for initiation (k_i), leading to a change in the rate of initiation. The rate of initiation is greatly affected by temperature, due to increases in collisional frequency between initiator

units and monomers, and the reduction in the aggregation number of the organolithium initiator. The final – and probably most influential – factor that can influence the rate of initiation by a significant degree is the polarity of the solvent in which the polymerisation is performed. The C-Li bond is a polar-covalent bond (Section 1.4.1.1) and therefore the polarity of the solvent can influence how covalent/ionic the bond is. In a non-polar solvent, the bond can be thought of as being covalent in nature, whereas in polar solvents, the bond can be thought of as being ionic in nature. [44] [45] Due to the increased bond length in polar solvents, the rate of initiation will generally increase with increasing solvent polarity. As solvent polarity is increased, the extent of dissociation of the organolithium initiator will also be increased (and therefore n will decrease) due to the increased stabilisation of the charged ions through solvation. This stabilisation of the ions also leads to three further states of the organolithium initiator complex which are not possible in non-polar solvents – contact lithium-carbanion ion pairs, solvent separated lithium-carbanion ion pairs and free lithium-carbanion ions (Figure 1.10) – which will greatly increase the rate of initiation. A similar effect on both the rate and aggregation number can be observed with the addition of a polar modifier (Section 1.4.2.1.3).

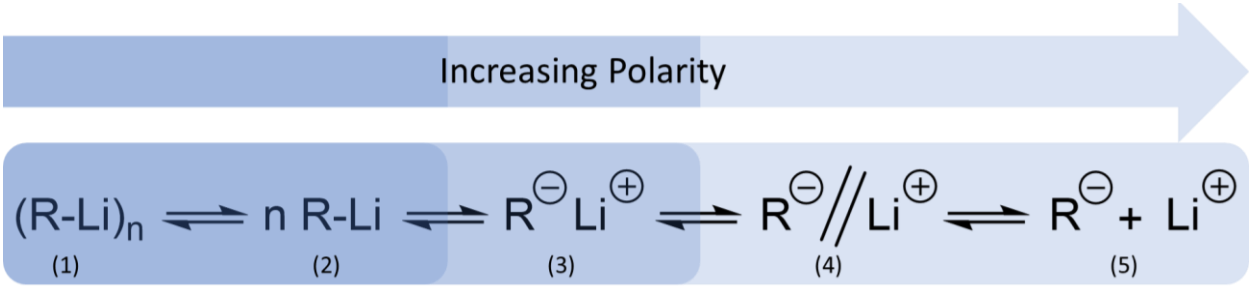

Figure 1.10: The different species of organolithium initiator complex that can be found in LAP, with increasing polarity, featuring: (1) aggregated lithium-carbanion complexes, (2) unaggregated lithium-carbanion complexes, (3) contact lithium-carbanion ion pairs, (4) solvent separated lithium-carbanion ion pairs, (5) free lithium-carbanion ions. [30]

1.4.2 Propagation of Living Anionic Polymerisations

In LAP, propagation occurs immediately after initiation and involves any additional attack of monomer by the propagating polymer chain (Figure 1.11).

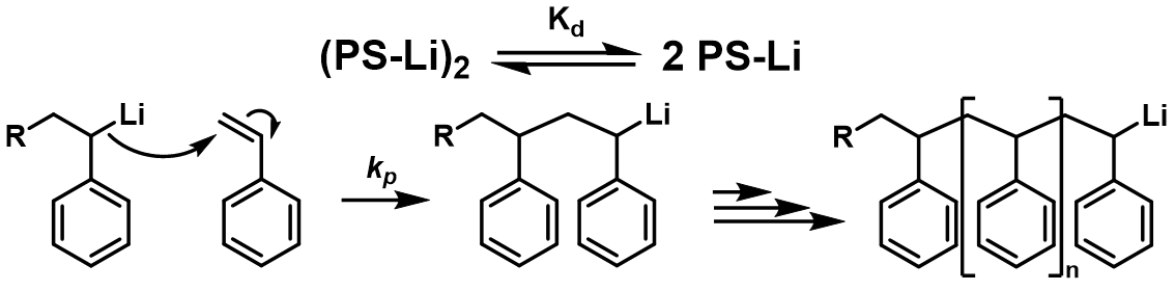

Figure 1.11: Mechanism for the LAP propagation of styrene, in a non-polar solvent, using an organolithium initiator, whereby K_d represents the equilibrium constant for the propagating species aggregates and k_p represents the rate constant for propagation.

During propagation in non-polar solvents, there is once again a dissociation step of the lithium aggregates – which form to minimise the free energy of the system – before monomers are added to the growing unaggregated polymer chain through the nucleophilic attack of the monomer by the anionic site. This results in the propagation of the anionic site as the polymerisation progresses (Figure 1.11). The dissociation step shown from a dimer to unimer represents the dissociation from the most favourable aggregation state of poly(styryl)lithium to the unaggregated species – i.e. n for this system is 2. However, if another monomer is used (such as butadiene), this step would involve the dissociation from whatever the most favourable aggregation state is (which could be a tetramer or dimer depending on the active centre concentration for poly(butyl)lithium (Section 1.4.2.1.1).

Once again, due to the occurrence of aggregates of organolithium compounds being formed, the rate of propagation calculation must include an inverse order dependence with relation to the aggregation number of propagating polymer chain. The rate of propagation for LAP of styrene in a non-polar solvent can therefore be calculated (Equation 1.3). [30]

$$R_p = -d[S]/dt = k_p[PS\text{-}Li][S]$$

$$R_p = k_p(K_d/2)^{1/2}[PS\text{-}Li]_o^{1/2}[S]$$

$$R_p = k_{obs}[PS\text{-}Li]_o^{1/2}[S]$$

Equation 1.3: Rate of propagation (R_p) of styrene in non-polar solvents, whereby k_p represents the rate constant for propagation, K_d represents the equilibrium constant between the aggregated and unaggregated states of the propagating chains, k_{obs} represents the observed rate constant for propagation, [PS-Li] represents the concentration of active chain ends, $[PS\text{-}Li]_o$ represents the total concentration of chain ends, and [S] represents the concentration of the styrene monomer.

As shown in Equation 1.3, the rate of propagation of styrene during LAP in non-polar solvents has an inverse order dependence with relation to the aggregation number of poly(styryl)lithium (n = 2). Due to the low concentration of the unaggregated species at any given point, it is very difficult to measure the dissociation constant of the system (K_d) and therefore obtain a value for the rate constant for propagation (k_p). This means that generally the observed single rate constant (k_{obs}) is used to compare rates of reaction, including both the dissociation constant and the rate constant for propagation.

1.4.2.1 Propagation of Dienes by Living Anionic Polymerisation

While the LAP propagation step of styrene in non-polar solvents represents one of the most well-understood monomer systems due to its simplicity, this thesis and the wider LAP industry generally deals more with dienes rather than styrenic monomers. The diene class of monomer encompasses a whole host of different chemicals, whereby the propagation step of the polymerisation occurs through the diene functional group (CH_2=CH-CH=CH_2). Three of the most commonly used dienes within academia and industry – butadiene, isoprene and myrcene – are shown (Figure 1.12).

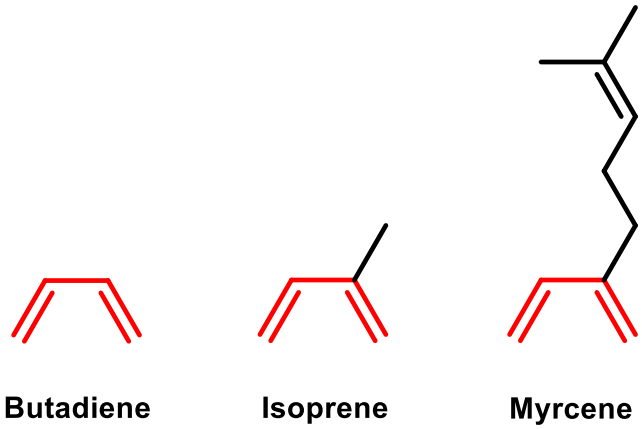

Figure 1.12: Three examples of commonly used diene monomers (butadiene, isoprene and myrcene) whereby the diene functionality has been highlighted in red.

The propagation of diene monomers brings about added complexity due not only to the addition of variable aggregation states but also to the fact that different microstructures for dienes can be observed, both of which will be discussed in the subsequent sections.

1.4.2.1.1 Propagation Mechanism of Dienes by Living Anionic Polymerisation

The mechanism for the propagation of dienes begins with the dissociation of the poly(dienyl)lithium aggregates. However, within diene systems, the dissociation constant varies with chain end concentration due to the different aggregation states that become favourable at different chain end concentrations. This means that there are two possible mechanisms for the polymerisation of dienes by LAP, as shown in Figure 1.13 by the inclusion of a second dissociation step for larger aggregates at higher concentrations of chain ends.

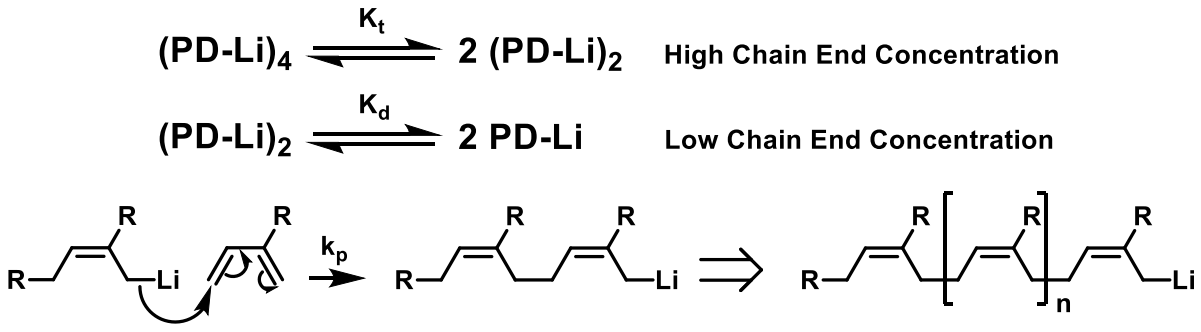

Figure 1.13: Mechanism for the LAP propagation of dienes, in a non-polar solvent, using an organolithium initiator, whereby K_d and K_t represent the equilibrium constants for the propagating species aggregates and k_p represents the rate constant for propagation.

As it can be seen in the mechanism shown in Figure 1.13 above, the propagation of diene monomers is very similar to that of styrene, whereby lithium aggregates are first dissociated before the diene monomers are added to the growing unaggregated polymer chain through the nucleophilic attack of the diene by the anionic site. There are, however, two main differences between the propagation of styrene compared to the propagation of dienes. The first difference is that, as mentioned, the propagating diene chains aggregate into different aggregation numbers depending on the concentration of active chain ends.

$$R_p = -d[D]/dt = k_{obs}[D]$$

$$R_p \text{ (at high conc.)} = k_p K_t^{1/4} K_d^{1/2} [\text{PD-Li}]^{1/4} [D]$$

$$R_p \text{ (at low conc.)} = k_p K_d^{1/2} [\text{PD-Li}]^{1/2} [D]$$

Equation 1.4: Rate of propagation (R_p) of dienes in non-polar solvents at both high and low concentrations of chain ends, whereby k_p represents the rate constant for propagation, K_d and K_t represent the equilibrium constant between the aggregated and unaggregated states of the propagating chains, k_{obs} represents the observed rate constant for propagation, [PD-Li] represents the concentration of active chain ends, and [D] represents the concentration of the diene monomer.

As shown (Equation 1.4), it is not only the mechanism that differs at different chain end concentrations, but as a consequence, the rates of propagation also vary depending on the most favourable aggregation state of the poly(dienyl)lithium chains. At low concentrations of chain ends, mostly dimeric aggregates will be present in the reacting mixture. This results in a single dissociation step from dimers to unimers – which is represented by a single dissociation constant (K_d) and the concentration of active chain ends being raised to the inverse of 2 within Equation 1.4 – before the dissociated species goes on to react with the next diene monomer. However, at high concentrations of chain ends, the most favourable aggregation state within the reaction mixture will be the tetramer. [30] This means that the dissociation step involves first the breakdown of tetramers to dimers, before the dimers dissociate into unimers – which is represented by two dissociation constants (K_d and K_t) and the concentration of active chain ends being raised to the inverse of 4 within Equation 1.4. These unimers can then go on to react with the next monomer unit.

1.4.2.1.2 Microstructure of Poly(dienes) Synthesised by Living Anionic Polymerisation

The second way in which the propagation of dienes is more complex than that of styrene is due to the charge distribution within the propagating chain, which leads to a variety of different microstructures. The microstructure of a polymer can be defined as the physical and spatial arrangement of the repeating subunits along the backbone of a polymer chain [46] including: the tacticity (orientation) of the monomers in the polymer chain; which isomer the repeat unit is in (e.g. cis/trans if isomerisation is possible); and through which bond(s) the polymerisation has occurred. Using a generic diene – with the formula CH_2=CH-CR=CH_2 – all of the different possible microstructures of a poly(diene) synthesised by LAP have been shown in Figure 1.14 below.

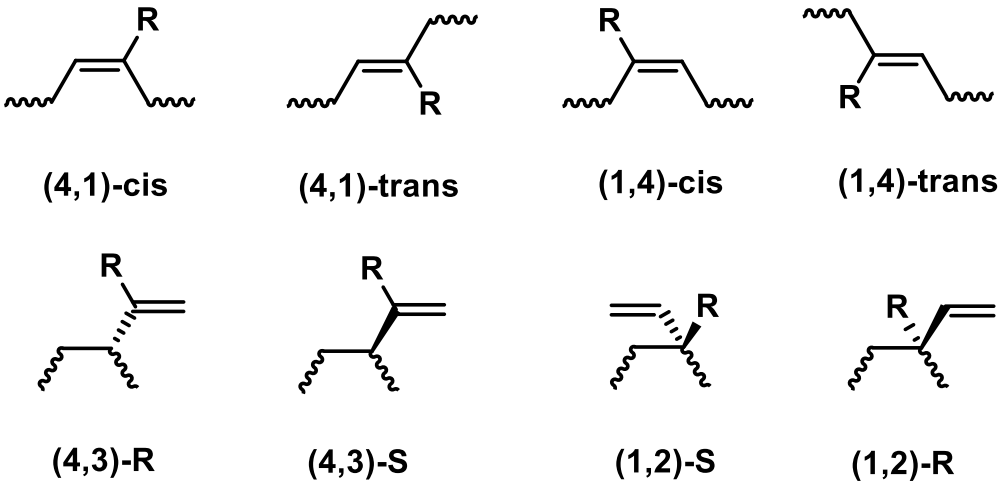

Figure 1.14: The 8 possible microstructures of a generic diene with the formula CH2=CH-CR=CH2.

While all of these different microstructures are possible, LAP not only gives the user control over the M_n and the molecular weight distribution, but also a large degree of control over the microstructure of dienes due to the relative stabilisation of the carbanion and due to the partial complexation of diene molecules with the counter cation of LAP (see Figure 1.15 below). This is highly important with dienes where many of the polymer properties – including crystallinity, solubility, T_g, etc. – are highly dependent on the microstructure of each subunit. The microstructure can be affected by: the polarity of the solvent, the pressure the reaction is carried out at, the type of monomer, the countercation, the temperature, and the presence of any polar modifiers/additives. [30]

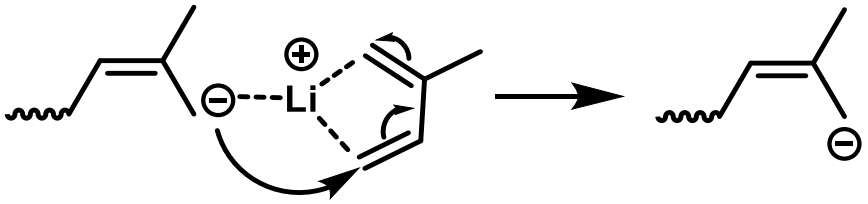

Figure 1.15: Mechanism of the LAP of isoprene, showing the isoprene-lithium complexation, which leads to the high 4,1-cis microstructure percentage in non-polar solvents.

The atomic radius of lithium (157 pm) is much larger than that of carbon (77 pm), and in a non-polar solvent, in the absence of a polar modifier, the carbon-lithium bond displays more covalent character than ionic character. This means that at the propagating chain end, lithium is more likely to be bonded to the terminal carbon, [47] and most of the electron density will lie on the carbon at the end of the propagating chain and therefore this will be the carbon that is most likely to react. This is part of the reason for the high (1,4) microstructure that is commonly found for dienes polymerised in non-polar solvents. Changing the R group from hydrogen to bulkier groups generally leads to an increased (1,4) microstructure content relative to butadiene. [30]

1.4.2.1.3 The Effect of Polar Modifiers on the Microstructure of Polymers Synthesised by Anionic Polymerisations

While the microstructure of a polymer synthesised by LAP in non-polar solvents using lithium as the countercation is largely dictated by the nature of the monomer that is being polymerised (temperature, concentration and pressure can also affect the microstructure but to a lesser extent), changes to the polarity of the solvent or addition of polar modifiers can be used to tailor the microstructure percentages of the polymer for its required application.

The polar modifiers used in LAP contain heteroatoms with a high affinity for the counter ion used in LAP - in most cases lithium. The most common polar modifiers are oxygen-containing ethers, such as ditetrahydrofurylpropane (DTHFP), and tertiary amines, such as *N,N,N',N'*-tetramethylethylenediamine (TMEDA).

As the commonly used polar modifiers prove, most polar modifiers contain either oxygen or nitrogen, both of which have a lone pair of electrons that are able to coordinate to the lithium counter cations, which are bound to the propagating chain end. A partial donation of electron density from the polar modifier to the lithium cation results in the delocalisation of the

positive charge across both the lithium cation and the coordinated polar modifier. This delocalisation of charge results in an increase in ionic character of the carbon-lithium bond (and therefore an associated increase in bond length), leading to greater resonance character in the propagating polymer chain end. This increase in resonance character of the propagating chain end means that more of the electron density of the anionic charge is situated on carbon 2 (Figure 1.16) relative to the electron density distribution found in the propagating polymer chain end of an unmodified polymerisation. This redistribution of electron density, along with an increase in steric hindrance at the propagating chain end due to the increased size of the polar modifier-lithium complex relative to the lithium countercation generally results in an increase in the (1,2) and (4,3) microstructure percentages.

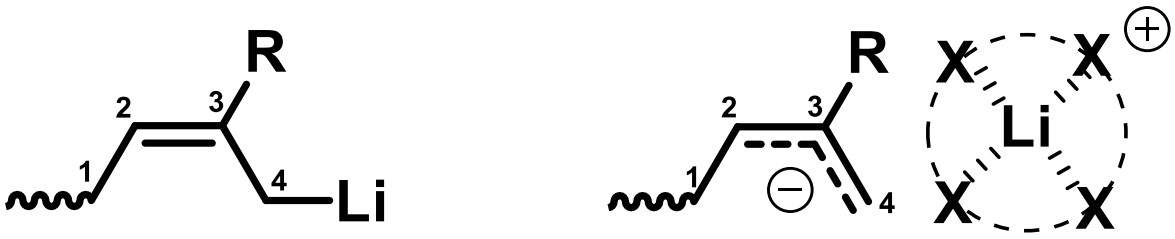

Figure 1.16: The two models that can be used to describe the bonding of lithium to carbon on a propagating diene chain, showing the effect that polar modifiers have on the charge distribution across the monomeric unit at the chain end. (Left: Covalent model in absence of polar modifiers. Right: Ionic model in presence of polar modifiers).

1.4.2.2 Copolymerisation by Living Anionic Polymerisation

LAP of copolymers (statistical and block) is a topic of enduring interest to both academia and industry. Variation in both synthetic methodology and monomer reactivity means that the sequence of monomers in a copolymer is almost infinitely variable. However, the vast array of possible sequences can be broadly divided into two main classes of copolymer: block copolymers and statistical copolymers, as discussed previously (Section 1.2.2). When investigating monomer reactivity, and therefore the relative rate of incorporation of monomers into statistical copolymers, it is therefore vital to discuss the copolymerisation kinetics.

1.4.2.2.1 Copolymerisation Kinetics within Living Anionic Polymerisation

During copolymerisation of two different monomers, the copolymer composition and monomer sequence of statistical copolymers is governed by the reactivity ratios of each of the monomers used and their relative concentrations. The reactivity ratios of two monomers – 'A' and 'B' – are determined by first considering the four possible propagation reactions that may occur during the copolymerisation, each of which has a unique rate constant (see Figure 1.16 below).

$$M_A^* + M_A \xrightarrow{k_{AA}} M_A M_A^*$$

$$M_A^* + M_B \xrightarrow{k_{AB}} M_A M_B^*$$

$$M_B^* + M_A \xrightarrow{k_{BA}} M_B M_A^*$$

$$M_B^* + M_B \xrightarrow{k_{BB}} M_B M_B^*$$

Figure 1.17: The 4 possible propagation reactions in a statistical copolymerisation, with associated rate constants, whereby the * signifies the progression of the propagating chain end – which in the case of LAP would be the propagating anion.

The reactivity ratios (r) are defined as the ratio of the rate constant for self-propagation (homopolymerisation) to the rate constant for cross-propagation (copolymerisation). (Equation 1.5)

$$r_A = \frac{k_{AA}}{k_{AB}} \qquad r_B = \frac{k_{BB}}{k_{BA}}$$

Equation 1.5: Reactivity ratios of monomers 'A' and B'.

Reactivity ratios can be used in conjunction with the instantaneous concentration of each monomer to define the Mayo-Lewis equation (Equation 1.6), which can be used to calculate the copolymer composition. [48]

$$\frac{d[M_A]}{d[M_B]} = \frac{[M_A](r_A[M_A]+[M_B])}{[M_B](r_B[M_B]+[M_A])}$$

Equation 1.6: Mayo-Lewis equation (copolymer equation), whereby [M_A] represents the moles of monomer A in the feed and [M_B] represents the moles of monomer B in the feed.

The above equation enables the determination of reactivity ratios, but due to the effect of monomer concentration on the rate of its incorporation, only the initial 5-10 % conversion of the copolymers can used for investigation, to prevent the effects of a gradient shift in the feed ratio.

During LAP, the reactivity ratios of different monomers can be tuned by changing the polarity of the solvent used or by adding a polar modifier to the polymerisation mixture. This means that different types of copolymers and sequencing can be achieved when using the same monomers.

1.4.2.2.2 Methods for Calculating Reactivity Ratios

The established method of calculating reactivity ratios uses the Mayo-Lewis equation or slight derivations of the Mayo-Lewis equation. [48] However, this treatment is not completely accurate, especially for special cases of copolymerisation – such as alternating and block – and requires many experiments with different feed ratios with a low conversion. There have, however, been several advances and new models devised for determining reactivity ratios, including integrated methods. This includes the Meyer-Lowery method (Equation 1.7), which allows use of composition data at all conversions to be used – rather than only data at low conversion. This ability to utilise the composition data at all conversions arises due to the use of instantaneous feed ratios, by "real-time" analysis of composition, along with the initial monomer feed ratio, in the equation. This means that the low monomer conversions between each sampling point can be calculated at the instantaneous monomer feed ratio and also means that less experimental work is required, as the copolymerisation does not have to be repeated at many different feed ratios. However, for this method to work, the number of active chains within the system must remain constant and the reaction should be run to full

conversions of the monomer, meaning that any substantial termination that occurs during the reaction can lead to inaccuracies in the measured reactivity ratios. [49]

$$\mathbf{Conv} = \mathbf{1} - \left(\frac{\mathbf{f_A}}{\mathbf{f_A^0}}\right)^{\mathbf{r_B}/(\mathbf{1}-\mathbf{r_B})} \left(\frac{\mathbf{1}-\mathbf{f_A}}{\mathbf{1}-\mathbf{f_A^0}}\right)^{\mathbf{r_A}/(\mathbf{1}-\mathbf{r_A})} \times \left(\frac{\mathbf{f_A}(\mathbf{2}-\mathbf{r_A}-\mathbf{r_B})-\mathbf{r_B}-\mathbf{1}}{\mathbf{f_A^0}(\mathbf{2}-\mathbf{r_A}-\mathbf{r_B})-\mathbf{r_B}-\mathbf{1}}\right)^{(\mathbf{r_A r_B}-\mathbf{1})/(\mathbf{1}-\mathbf{r_A})(\mathbf{1}-\mathbf{r_B})}$$

Equation 1.7: Meyer-Lowery equation for determining reactivity ratios of a copolymerisation.

1.4.2.3 The Effect of Polar Modifiers on the Kinetics of Living Anionic Copolymerisation

As well as impacting the rate of reaction and the microstructure of diene polymers (as discussed in Section 1.4.2.1.3), solvent polarity and the addition of polar modifiers significantly impacts copolymerisation kinetics and reactivity ratios. For example, in the commercial production of solution styrene-butadiene rubber (sSBR) copolymers, polar modifiers are used to randomise the incorporation of styrene and butadiene, by changing the reactivity ratios of the monomers so they are both approximately equal to 1. [50] [51]

The co-ordination of the polar modifier has the effect of reducing the average number of lithium cations in each aggregate, most likely due to both the reduced charge density and the increased steric hindrance associated with each cation. This brings about a secondary feature of the addition of polar modifiers, whereby the rate of polymerisation can also generally be increased due to the reduced number of dissociative steps required to form the unaggregated lithium complex. The lithium-polar modifier complex and propagating polymer chain are effectively broken up into solvated ion pairs. In polar solvents, these aggregates can be found in two further dissociation states (solvent separated ion pairs and free ions – see Figure 1.10), which can have enhanced effects on the reactivity rates of different monomers. [30]

The chelation of the polar modifiers to the lithium and the resulting change in the C-Li bond length/strength at the end of the propagating chain changes the relative rate of incorporation of the two monomers. This is because the increase in ionicity and therefore the solvation of the resulting ions changes the homopolymerisation and cross-polymerisation rate constants. In the solvated ionic state of the propagating polymer chain, the reactivity ratios of both styrene and butadiene will be approximately equal to each other, resulting in the synthesis of an almost completely random copolymer. This change in the reactivity ratios could be the

result of decreased substituent effect on the alkyl lithium bond due to the increased iconicity of the bond, where the substituent effects will have the greatest impact on covalent bonds due to hyperconjugation and inductive effects. [52] [53] Although not fully understood in the literature, there is growing evidence that the addition of a polar modifier can also change the local concentration of monomers around the propagating chain end, which may have an impact on monomer incorporation. [54]

1.4.3 Termination of Living Anionic Polymerisations

Due to the lack of inherent termination mechanisms within LAP, termination of the propagating anion must occur through the addition of a terminating agent, usually a protic solvent such as an alcohol, or weak acid, commonly acetic acid (see Figure 1.18).

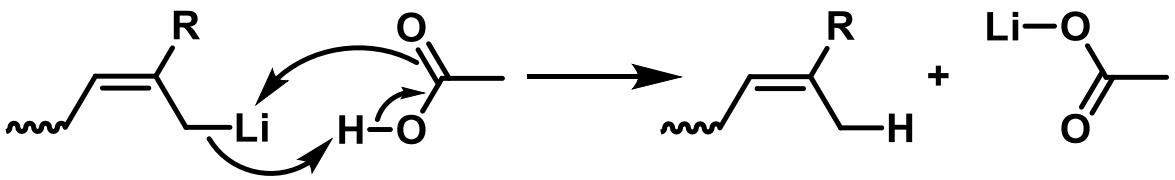

Figure 1.18: Mechanism for the termination of the LAP of a generic diene, in a non-polar solvent, using acetic acid as the terminating agent.

This absence of an inherent termination mechanism offers the opportunity to introduce chain-end functionalisation via a controlled termination/functionalisation reaction.

1.4.3.1 Functionalisation of Polymers Synthesised by LAP

Due to the reactive nature of the propagating carbanion in LAP, the polymer chains that are synthesised by LAP are very limited in their functionality. This is because the carbanion must attack almost all electron deficient or polar functional groups, which can terminate the reaction if an acidic proton is present or cause an unwanted microstructure if the polymerisation proceeds through one of these functional groups (ultimately terminating the reaction if the reaction progresses through a carbonyl due to the formation of a Li-O covalent bond). This restricts LAP to the use of non-functional, non-polar monomers, such as styrene, butadiene and isoprene, and means that other methods, such as post-polymerisation functionalisation, must be used in order to produce polar, hydrophilic polymers.

Functionalisation of polymers synthesised by LAP may be achieved through the use of monomers, initiators or terminating agents containing protected functional groups, or through post-polymerisation functionalisation strategies. The addition of new functional groups into the polymer can affect the polymer's physical and chemical properties. For example, the polymer could be made more polar through the addition of functional groups such as hydroxyl or carbonyl groups, which could in turn have effects on water permeability and adhesion. [55] There are two main types of polymer functionalisation: chain-end functionalisation and in-chain functionalisation.

1.4.3.1.1 Chain-End Functionalisation

Chain-end functionalisation, as the name suggests, is where a functional group is introduced into the polymer at either or both ends of the polymer chain. Where both ends are functionalised, the two functional groups can be either the same or different, leading to a diverse range of possible functionalities for the polymer. Further modification of these functional groups can then be carried out if required. [56] [57]

For LAP, chain-end functionalisation can generally be achieved via initiation and/or termination steps (Figure 1.19). Again, due to the challenges associated with the reactivity of the carbanion, functional groups that are added during initiation or termination will need to be protected to prevent attack by the carbanion. Due to the nature of LAP, in the absence of impurities, chain-end functionalisation is frequently quantitative, leading to typically much higher end group fidelities than can be accessed via many polymerisation techniques (e.g. RDRP). [58]

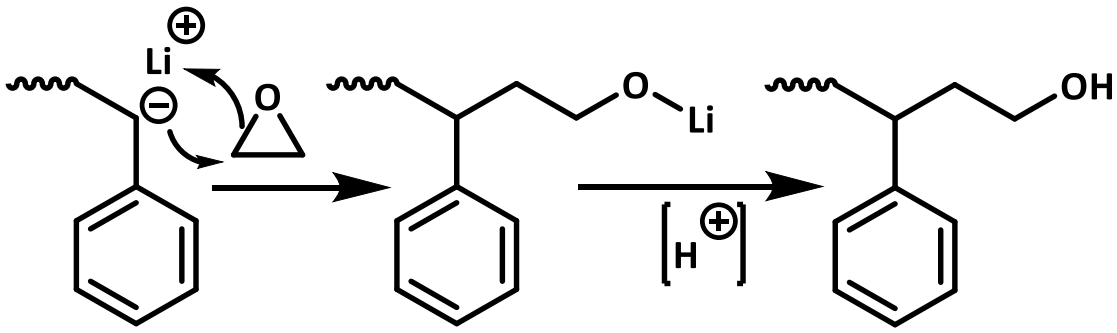

Figure 1.19: Example of a chain-end functionalisation method – mechanism of hydroxyl chain-end termination of a "living" poly(styrene) chain end. *[59]*

1.4.3.1.2 In-Chain Functionalisation

In-chain functionalisation is a method of functionalisation where, as the name suggests, the functional groups are added along the chain, either on the backbone or on side chains of the polymer. For this to occur, the monomers that are used for polymerisation must contain at least one functional group that is not involved in the polymerisation. For LAP, this can be relatively difficult due to the reactivity of the propagating species, which can attack a large variety of functional groups, such as carbonyl and hydroxyl groups, so they cannot be present in the monomers unless protected. Functional groups that are inert to attack by the propagating species, such as mono-alkene groups present after the LAP of dienes, can also be used as a precursor to other functional groups through post-polymerisation modification reactions. [60] Common in-chain functionalisation approaches include thiol-ene conjugation [61] (Figure 1.20) and malenisation, the introduction of maleimide units that can be ring opened to produce dicarboxylate units, changing the solubility parameters of the resultant polymer. [62] [63] Industrially, vulcanisation, the introduction of inter-chain chemical crosslinks (most commonly disulphide linkages), [64] is important to optimise the material properties of polymers to be used in tyres, construction materials and consumer goods. [65]

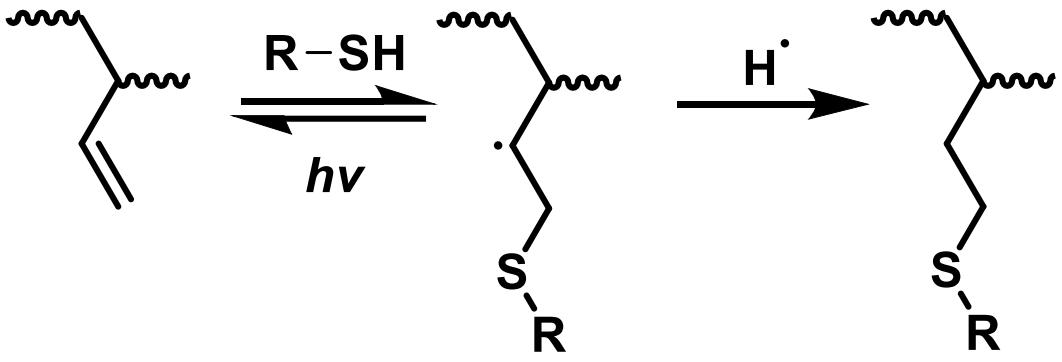

Figure 1.20: Example of a post-polymerisation in-chain functionalisation method – mechanism of thiol-ene in-chain functionalisation of a poly(butadiene) polymer, synthesised by LAP.

1.4.3.1.3 Advantages and Disadvantages of Each Functionalisation Method

There are of course advantages and disadvantages of each functionalisation method, which should be taken into consideration. A summary of the advantages and disadvantages of both chain-end functionalisation methods and in-chain functionalisation methods is shown (Table 1.1).

Table 1.1: Advantages and disadvantages of the two main methods of functionalisation used with LAP.

Chain-End Functionalisation	Conventional In-Chain Functionalisation
Advantages: Quantitative – can ensure each chain has one or two functional groups. Little impact on the polymer backbone properties such as T_g and rheological properties. Two different functionalities can (in theory) be introduced if a different functionality is used for initiator and terminator.	**Advantages:** Many functionalities can be added to the polymer chain, offering scope to modify polymer properties. Greater scope for the manipulation of the polymer's physical and chemical properties due to the number of functional groups that can be added.
Disadvantages: A maximum of two functional groups can be added to each chain so it has limited ability to change the properties of the polymer. (Multifunctional group initiating and terminating groups can be used but the functional group tolerance is limited.) The functional groups of both the functionalised initiator and terminator usually must be protected to prevent attack by the cation. Protected groups require a further reaction to remove the protecting group, which costs time and money.	**Disadvantages:** Must be carried out as a second step after polymerisation. Previously, in-chain functionalisation has been fairly limited to diene-containing polymers, which reduces the scope of polymers and applications that this type of functionalisation can be used for. Can have large effects on the polymer backbone properties, as the functionality is usually added to the remaining diene backbone double bond. Generally, very little control over where the functionality occurs.

1.4.3.1.4 Living Anionic Polymerisation of Functionalised Monomers

As discussed previously, it is possible to polymerise functional monomers by LAP, although these polymerisations either require fairly extreme conditions that are unfeasible for industry, or use of protected monomers, both of which increase the cost of the polymerisation. The most commonly investigated functional monomers that are polymerised by LAP are methyl methacrylate-based monomers, ethylene oxide derivatives and functionalised styrene derivatives. [66] [67] [68]

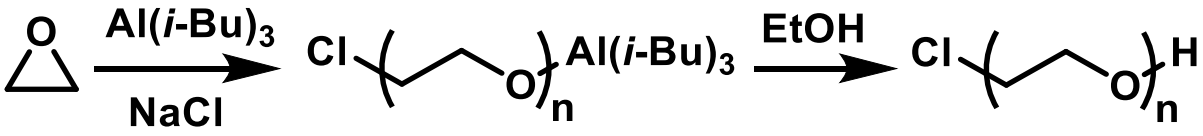

Figure 1.21: LAP of ethylene oxide. *[69]*

However, much like RDRP, all of these processes require conditions/monomers/processes that are far too expensive for industry and thus far have been fairly limited to academia and some small-scale companies who synthesise medical devices.

Some monomers with protected functional groups have also been investigated including the polymerisation of benzoyloxy protected hydroxylated styrene derivatives (Figure 1.22). [70] However, these polymers still require further modification (i.e. deprotection) post-polymerisation. [66]

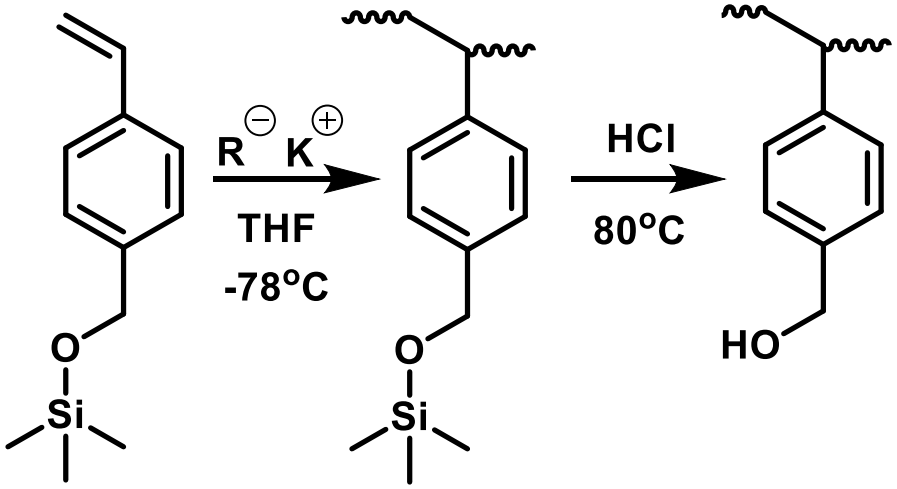

Figure 1.22: The LAP and deprotection of alkyl silyl protected of 4-[2-(hydroxyethyl)styrene. *[71]*

1.5 Industrial Applications

Although LAP on an industrial scale is largely (but not exclusively) limited to the use of three monomers – styrene, butadiene and isoprene – the ability to control monomer sequence distribution (via reactivity ratios) and diene microstructure means that (co)polymers manufactured by LAP find use in many varied applications.

One of the leading industries that utilises LAP is the tyre industry and specifically copolymers for tyre treads. A key copolymer used in the manufacture of tyre treads is solution styrene-butadiene rubber (sSBR), although sSBR being a non-polar copolymer lacking in any functionality creates some challenges during the manufacturing process.

1.5.1 Solution Styrene-Butadiene Rubber

sSBR is a copolymer produced by LAP, which can be employed like natural rubber (NR) for many uses in the industrialised world. NR is an elastomer that is prepared by washing, pressing and drying/smoking the precipitation collected from acidified latex, a milky fluid collected from certain tropical trees. [72] This process has several drawbacks related to the fact that the rubber is collected from trees, which have a maximum daily yield totalling 5 kg annually per tree. This means that to increase the amount of NR that can be produced each year, more trees must be planted, which requires more space. It also takes about 5 years for the trees to reach maturity, before which time the latex can be extracted. [73] This means that there is a 5-year time delay between an increased need for NR and the time at which the need can be met. This has resulted in the production of synthetic rubbers, including sSBR, to meet increased demand for rubber products in the modern world. Synthetic rubbers can be produced in such a way, through the manipulation of the monomers used or their relative ratios, which results in a rubber that can have mechanical or chemical properties that may be superior to that of NR for the use in the field for which they are required.

This means that the production of sSBR in industry is increasing, especially for applications such as pneumatic tyres, shoe soles, gaskets and chewing gum. [74]

1.5.1.1 Use of Silica Additives

Developments in the manufacturing processes of pneumatic tyres, for improving wet-grip and rolling-resistance properties, has led to the addition of polar compounds, such as silica, to

sSBR. [75] However, due to the non-polar nature of sSBR, there is very little control in the dispersion of these polar additives. This means that the added molecules can coagulate during their incorporation, which causes the rubber to harden. This in turn results in increased manufacture costs – to break up coagulates – and potential fracture points in the tyres themselves – where coagulates are not broken up and are incorporated into the tyre. [76]

1.5.1.2 Methods for Breaking up the Additive Aggregates

Apart from the obvious mechanical solutions – increased mixing of the rubber-additive matrix/finer particles when the additives are being added – for breaking up or preventing additive aggregate formation, many research groups have been looking at chemical solutions to provide filler dispersion.

One solution that has been adopted by industry is the addition of polar groups to the polymer chains to aid dispersion of the filler molecules. However, the small pool of monomers that can be used for anionic polymerisation has generally limited the research to chain-end modifications. [77] These modifications, although promising, can be challenging to perform on an industrial scale and may not provide the required polarity for the dispersion to be carried out effectively. One way through which polarity can be added to polymers synthesised by LAP is through the post-polymerisation in-chain functionalisation of the polymer chains. Several groups have also looked at the in-chain functionalisation of sSBR, through functionalisation methods such as epoxidation. [78] However, one issue with in-chain functionalisation for these systems is that functionalisation is generally unspecific, meaning the functionalisation can occur anywhere along the polymer chains, and the functionalisation itself can cause an increase in the glass transition temperature (T_g) of the rubber, meaning that the rubber will have a smaller operating temperature and may not be suitable to be used in low temperature environments. If in-chain functionalisation is to become a viable method of providing polarity in sSBR, a method for allowing the functionalisation to occur selectively to limit the effect that functionalisation has on the polymer's T_g while providing the most beneficial properties must be developed.

1.5.2 LAP of Terpenes

One type of monomer that has multiple alkene groups and can therefore be functionalised after polymerisation is terpenes such as β-myrcene (hereby termed myrcene). Myrcene

(Figure 1.12) is a naturally occurring terpene that is biosynthesised through the combination of isoprene subunits. These subunits come from the two isoprene phosphate isomers: isopentenyl pyrophosphate (IPP) and dimethylallyl pyrophosphate (DMAPP) (Figure 21). [79] Myrcene is found in many different species of plants and can be found in high yields in many different plant oils including hops, barley and cardamom. [80]

Whilst myrcene can be extracted from plant oils and synthesised on small scales, issues with purity and a high degree of thermal initiation mean it has not been used industrially as a monomer for many years. [80] However, more recently the industrial scale pyrolysis of β-pinene [81] and the microbial synthesis of myrcene using metabolically engineered bacteria [82] have led to renewed interest and research from academia and industry into myrcene's potential applications, including as a monomer.

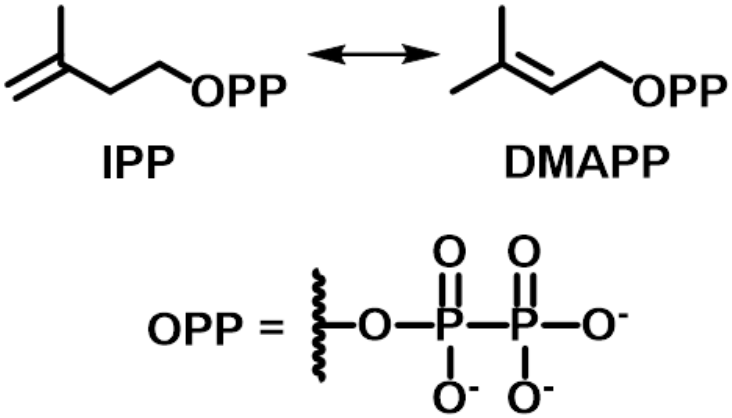

Figure 1.23: The two isoprene phosphate isomers used in terpene biosynthesis.

1.5.2.1 Polymerisation of Myrcene

Myrcene was initially investigated as a monomer in the 1940s, as a component of tank-tread rubber, with the aim of replacing the dwindling natural rubber supplies. [83] However, due to the difficult synthesis of the monomer and its high degree of thermal initiation [80], myrcene was subsequently largely overlooked by the polymer industry for about 60 years until the 2010s. However, in the past 10 years, myrcene has become, once again, a monomer of interest. Recent reports describe the polymerisation of myrcene by LAP [84] [85], RAFT [86], MCP [87] and emulsion free radical polymerisation (eFRP) [88].

1.5.2.2 Myrcene Copolymers as Butadiene Substitutes

As well as being homopolymerised by a variety of different polymerisation techniques, several different copolymers of myrcene have been synthesised by various methods of polymerisation. For example, a copolymer of myrcene and dibutyl itaconate has been synthesised via persulfate initiated emulsion polymerisation. [60] Moreover, myrcene has also been investigated as a substitute for butadiene in butadiene-styrene rubbers synthesised by LAP [89] and via persulfate initiated emulsion polymerisation. [89] In both cases, the authors of these studies subjected the poly(styrene-*co*-myrcene) to dynamic mechanical analysis to investigate the physical and mechanical properties of the copolymers, including tensile strength and glass transition temperature (T_g). In both cases, the myrcene-styrene copolymer was found to have properties that were comparable, if not superior to butadiene-styrene copolymers, in so much as they have improved traction and reduced rolling resistance over the butadiene-styrene copolymers.

Within the tyre industry, it is established that properties with regards to the rolling resistance and wear resistance properties are optimised when the butadiene-styrene copolymers are completely random (and ideally with no adjacent styrene units). [51] For this reason, a number of studies have been conducted into the synthesis of random copolymers of myrcene and styrene. As discussed (see Section 1.4.2.3), polar additives are frequently used to influence the comonomer sequence and to randomise butadiene and styrene in sSBR, thus there are a small number of reports in the literature of the use of TMEDA [90] and ethyl tetrahydrofurfuryl ether (ETE) [91] as polar additives in the anionic copolymerisation of myrcene and styrene. Despite reports that polar modifiers can induce random copolymerisation in mixtures of myrcene and styrene, data presented in support of these claims is incomplete and possibly misinterpreted. [90] [91]

1.5.2.3 Functionalisation of Myrcene-Containing Polymers

There has been a limited number of reports describing the functionalisation of polymyrcene or myrcene-containing copolymers. However, both chain-end and in-chain functionalisation of the homopolymer have been reported in the literature. For the chain-end functionalisation of poly(myrcene), amine capped homopolymers have been synthesised through the termination of “living” chains with *N*-benzylidenetrimethylsilylamine. [92] A number of

methods for in-chain functionalisation of polymyrcene have been reported, such as functionalisation via thiol-ene reactions and then thiol-based click reactions (similar to the reaction seen in Figure 1.20). [85] Several reports have also been published describing the epoxidation of poly(myrcene) and subsequent ring-opening of this epoxide. Zhou *et al.* used hydrogen peroxide and formic acid as epoxidising agents (which generally result in a higher yield at the cost of several side reactions) in order to utilise the hydroxylated poly(myrcene) as a macroinitiator for poly(lactide) copolymerisation. [93] Matic *et al.* also showed that poly(myrcene) could be epoxidised using *m*-CPBA prior to epoxide ring opening under acidic conditions. [94] In both of these examples, the epoxidation was only carried out on homopolymers of poly(myrcene). Having reviewed these papers, some concerns about the accuracy of the reported data were noted, however, this will be discussed further in Section 3.2.6.2. Finally, several articles detailing the polymerisation and copolymerisation of polar-modified myrcene by LAP have been published recently. Tavtorkin *et al.* detailed the modification of myrcene with trisubstituted amine and ether groups [95] before its subsequent polymerisation by LAP, while Frey *et al.* showed that silyl-protected myrcenol and acetyl-protected di-hydroxy myrcene could be polymerised and copolymerised by LAP. [96] [54] In both of these examples, however, the authors detail how the dispersity of the resulting polymer is slightly higher than would be otherwise expected for LAP.

One of the biggest issues discovered upon examination of the literature surrounding myrcene polymerisation is that many publications contain factual inaccuracies. These inaccuracies range from incorrectly characterised progression of polymerisation [85] to incorrectly described copolymerisation kinetics, [90] [91] and wrongly identified functionalisation reactions. [93] [94] These factors frustrate the accurate review of the literature of myrcene and highlight the challenges in advancing the field until inaccuracies in the literature have been resolved.

1.5.2.4 Myrcene as a Selective Site of Functionalisation

One potential method could be through the incorporation and selective functionalisation of the bio-available monomer myrcene. If the introduction of myrcene into sSBR can lead to the selective functionalisation of the polymer and thus an increase in polarity, then the addition of silica to the polymer could be more controlled. This in turn could result in lower

manufacturing costs in the production of high grip and low rolling resistance tyres. In this thesis, we will investigate the polymerisation and functionalisation of bio-derived myrcene-containing polymers to understand the impact myrcene could potentially have in the polymer industry as a replacement for petroleum-derived butadiene and isoprene.

1.6 References

[1] G. Patterson, A Prehistory of Polymer Science, Heidelberg: Springer Berlin, 2012.

[2] J. Tully, The Devil's Milk, New York: Monthly Review Press, 2011.

[3] H. Staudinger, “Über Polymerisation,” Berichte der deutschen chemischen Gesellschaft, vol. 53, pp. 1073-1085, 1920.

[4] A. Cózara, F. Echevarría, J. I. González-Gordillo, X. Irigoien, B. Úbeda, S. Hernández-León, Á. T. Palma, S. Navarro, J. García-de-Lomas, A. Ruiz, M. L. Fernández-de-Puelles and C. M. Duarte, “Plastic debris in the open ocean,” Proc. Natl. Acad. Sci. U.S.A., vol. 111, no. 28, pp. 10239-10244, 2014.

[5] C. Wilcox, E. Van Sebille and B. D. Hardesty, “Threat of plastic pollution to seabirds is global, pervasive, and increasing,” PNAS, vol. 112, no. 38, pp. 11899-11904, 2015.

[6] G. Hayes, M. Laurel, D. MacKinnon, T. Zhao, H. A. Houck and C. R. Becer, “Polymers without Petrochemicals: Sustainable Routes to Conventional Monomers,” Chemical Reviews, vol. 123, pp. 2609-2734, 2023.

[7] B. Bailey, “List of Latin and Greek Roots,” Bulletin of The Malacological Society of London , vol. 32, pp. 6-7, 1999.

[8] A. D. McNaught and A. Wilkinson, IUPAC. Compendium of Chemical Terminology, 2nd ed. (the "Gold Book"), Oxford: Blackwell Scientific Publications, 1997.

[9] S. Thomas, P. M. Visakh and A. P. Mathew, Advances in Natural Polymers - Composites and Nanocomposites, Heidelberg: Springer-Verlag Berlin, 2013.

[10] A. Shrivastava, “Introduction to Plastics Engineering,” in Introduction to Plastics Engineering, Oxford, William Andrew Publishing, 2018, pp. 1-16.

[11] P. Division, “IUPAC - Polymer Terminology Project,” Thee Digital, 1 June 2013. [Online]. Available: https://iupac.org/project/2012-048-3-400. [Accessed 21 November 2022].

[12] R. Geyer, J. R. Jambeck and K. L. Law, “Production, use, and fate of all plastics ever made,” Science Advances, vol. 3, no. 7, e1700782, 2017.

[13] W. M. Kriven, “Geopolymers and Geopolymer-Derived Composites,” in Encyclopedia of Materials: Technical Ceramics and Glasses, Elsevier, pp. 424-438, 2021.

[14] A. G. MacDiarmid, C. M. Mikulski, M. S. Saran, P. J. Russo, M. J. Cohen, A. A. Bright, A. F. Garito and A. J. Heeger, “Synthesis and Selected Properties of Polymeric Sulfur Nitride,

(Polythiazyl), (SN)x," in Inorganic Compounds with Unusual Properties, Washington, D. C., American Chemical Society, pp. 63-72, 1976.

[15] G. Homann, L. Stolz, J. Nair, I. C. Laskovic, M. Winter and J. Kasnatscheew, "Poly(Ethylene Oxide)-based Electrolyte for Solid-State-Lithium Batteries with High Voltage Positive Electrodes: Evaluating the Role of Electrolyte Oxidation in Rapid Cell Failure," Scientific Reports, vol. 10, no. 4390, 2020.

[16] R. G. Hill, "Biomedical polymers," in Biomaterials, Artificial Organs and Tissue Engineering, Woodhead Publishing Limited, pp. 97-106, 2005.

[17] O. S. Manoukian, N. Sardashti, T. Stedman, K. Gailiunas, A. Ojha, A. Penalosa, C. Mancuso, M. Hobert and S. G. Kumbar, "Biomaterials for Tissue Engineering and Regenerative Medicine," in Encyclopedia of Biomedical Engineering, Elsevier, pp. 462-482, 2019.

[18] F. S. Al-Jahwari and T. Pervez, "The Potential of Environmental-Friendly Biopolymers as an Alternative to Conventional Petroleum-Based Polymers," in Encyclopedia of Renewable and Sustainable Materials, Elsevier, pp. 200-206, 2020.

[19] M. Delbianco and P. H. Seeberger, "Materials science based on synthetic polysaccharides," Materials Horizons, vol. 7, pp. 963-969, 2020.

[20] R. J. Young, Introduction to Polymers, Michigan: Chapman and Hall, 2010.

[21] E. Grune, T. Johann, M. Appold, C. Wahlen, J. Blankenburg, D. Leibig, A. H. E. Müller, M. Gallei and H. Frey, "One-Step Block Copolymer Synthesis versus Sequential Monomer Addition: A Fundamental Study Reveals That One Methyl Group Makes a Difference," Macromolecules, vol. 51, pp. 3527-3537, 2018.

[22] O. Guirdham, "Low-Density Polyethylene Global Market Report 2021: COVID-19 Impact and Recovery to 2030- Product Image," The Business Research Company, 2021.

[23] J. B. Clarke, J. W. Hastie, L. H. E. Kihlborg, R. Metselaar and M. M. Thackeray, "Definitions of terms relating to phase transitions of the solid state (IUPAC Recommendations 1994)," Pure and Applied Chemistry, vol. 66, no. 3, pp. 577-594, 1994.

[24] M. Biron, Material Selection for Thermoplastic Parts, Elsevier Ltd., 2016.

[25] S. Datta, "Elastomer Blends," in The Science and Technology of Rubber, Elsevier Inc. pp. 547-589, 2013.

[26] D. Ratna, Recent Advances and Applications of Thermoset Resins, Elsevier Inc., 2022.

[27] J. K. Stille, "Step-Growth Polymerization," Journal of Chemical Education, vol. 58, no. 11, pp. 862-866, 1981.

[28] L. Biller, D. Fournier and F. Du Prez, “Step-growth polymerization and ‘click’ chemistry: The oldest polymers rejuvenated,” Polymer, vol. 50, pp. 3877-3886, 2009.

[29] S. Ito, “Chain-growth polymerization enabling formation-introduction of arylene groups into polymer main chains,” Polymer Journal, vol. 48, pp. 667-677, 2016.

[30] H. L. Hsieh and R. P. Quirk, Anionic Polymerization: Principles and Practical Applications, New York: Marcel Dekker, 1996.

[31] W.-F. Su, “Radical Chain Polymerization,” in Principles of Polymer Design and Synthesis, Berlin, Springer, pp. 137-183, 2013.

[32] K. Matyjaszewski, “Atom Transfer Radical Polymerization (ATRP): Current Status and Future Perspectives,” Macromolecules, vol. 45, pp. 4015-4039, 2012.

[33] K. Matyjaszewski, “Atom Transfer Radical Polymerization: From Mechanisms to Applications,” Israel Journal of Chemistry, vol. 52, pp. 206-220, 2012.

[34] N. Ten Brummelhuis and M. Weck, “RAFT Polymerization of Alternating Styrene-Pentafluorostyrene Copolymers,” Polymer Chemistry, vol. 52, pp. 1556-1559, 2014.

[35] A. C. Greene and R. B. Grubbs, “Nitroxide-Mediated Polymerization of Methyl Methacrylate and Styrene with New Alkoxyamines from 4-Nitrophenyl 2-Methylpropionat-2-yl Radicals,” Macromolecules, vol. 43, pp. 10320-10325, 2010.

[36] A. Shrivastava, “Polymerization,” in Introduction to Plastics Engineering, William Andrew Publishing, pp. 17-48, 2018.

[37] J. P. Hogan and R. L. Banks, “Polymers and production thereof”. United States Patent US2825721A, 4 March 1958.

[38] W.-F. Su, “Coordination Polymerization,” in Principles of Polymer Design and Synthesis, Berlin, Springer, pp. 219-232, 2013.

[39] “ The Nobel Prize in Chemistry 1963,” Nobel Prize Outreach AB 2022, [Online]. Available: https://www.nobelprize.org/prizes/chemistry/1963/summary/. [Accessed 23 November 2022].

[40] J. P. Kennedy, “Living Cationic Polymerization of Olefins. How Did the Discovery Come About,” Polymer Science Part A. Polymer Chemistry, vol. 37, pp. 2285-2293, 1999.

[41] M. Szwarc, “Living Polymers,” Nature, vol. 178, pp. 1168-1169, 1956.

[42] M. Szwarc, M. Levy and R. Milkovich, “Polymerization Initiated by Electron Transfer to Monomer. A New Method of Formation of Block Polymers,” Communications to the Editor, vol. 78, pp. 2636-2637, 1956.

[43] R. J. Ouellette and J. D. Rawn, “Structure of Organic Compounds,” in Principles of Organic Chemistry, Elsevier, pp. 1-32, 2015.

[44] L. Pauling, The Nature of the Chemical Bond, London: Oxford University Press, 1939.

[45] R. Waack, L. D. McKeever and M. A. Doran, “The nature of carbon–lithium bonding in benzyl-lithium and its variation with solvent,” Journal of the Chemical Society D: Chemical Communications, pp. 117b-118, 1969.

[46] A. D. Jenkins, P. Kratochvil, R. F. T. Stepto and U. W. Suter, “Glossary of basic terms in polymer science (IUPAC Recommendations 1996),” Pure and Applied Chemistry, vol. 68, no. 12, p. 2287–2311, 1996.

[47] A. F. Wells, Structural Inorganic Chemistry, Oxford: Clarendon Press, 1984.

[48] F. R. Mayo and F. M. Lewis, “Copolymerization. I. A Basis for Comparing the Behavior of Monomers in Copolymerization; The Copolymerization of Styrene and Methyl Methacrylate,” American Chemical Society, vol. 66, pp. 1594-1601, 1944.

[49] N. A. Lynd, R. C. Ferrier Jr. and B. S. Beckingham, “Recommendation for Acurate Experimental Determination of Reactivity Ratios in Chain Copolymerization,” Macromolecules, vol. 52, pp. 2277-2285, 2019.

[50] T. A. Antkowiak, A. E. Oberster, A. F. Halasa and D. P. Tate, “Temperature and concentration effects on polar-modified alkyllithium polymerizations and copolymerizations,” Journal of Polymer Science - Part A Polymer Chemistry , vol. 10, pp. 1319-1334, 1972.

[51] A. F. Halasa and W. L. Hsu, “Preparation and characterization of a perfectly random solution SBR using modified organolithium catalyst,” in American Chemical Society, Polymer Preprints, Division of Polymer Chemistry, Orlando, 1996.

[52] R. F. W. Bader, T. S. Slee, D. Cremer and E. Kraka, “Description of Conjugation and Hyperconjugation in Terms of Electron Distributions,” Journal of the American Chemical Society, vol. 105, no. 15, pp. 5061-5068, 1983.

[53] J. I.-C. Wu and P. v. R. Schleyer, “Hyperconjugation in hydrocarbons: Not just a “mild sort of conjugation”,” Pure and Applied Chemistry, vol. 85, no. 5, pp. 921-940, 2013.

[54] C. Wahlen, M. Rauschenbach, J. Blankenburg, E. Kersten, C. P. Ender and H. Frey, “Myrcenol-Based Monomer for Carbanionic Polymerization: Functional Copolymers with Myrcene and Bio-Based Graft Copolymers,” Macromolecules, vol. 53, no. 20, pp. 9008-9017, 2020.

[55] L. Li, S. Li and D. Cui, “Highly Cis-1,4-Selective Living Polymerization of 3 Methylenehepta1,6-diene and Its Subsequent Thiol−Ene Reaction: An Efficient Approach to Functionalized Diene-Based Elastomer,” Macromolecules, vol. 49, pp. 1242-1251, 2016.

[56] A. Pagliarulo and L. R. Hutchings, “End-Functionalized Chains via Anionic Polymerization: Can the Problems with Using Diphenylethylene Derivatives be Solved by using Bisphenol F?,” Macromolecular Chemistry and Physics, vol. 219, p. 1700386, 2017.

[57] J. Jagur-Grodzinski, “Functional polymers by living anionic polymerization,” Journal of Polymer Science A Polymer Chemistry, vol. 40, pp. 2116-2133, 2002.

[58] M. A. Peters, A. M. Belu, R. W. Linton, L. Dupray, T. J. Meyer and J. M. DeSimone, “Termination of Living Anionic Polymerizations Using Chlorosilane Derivatives: A General Synthetic Methodology for the Synthesis of End-Functionalized Polymers,” Journal of American Chemistry Society , vol. 117, pp. 3380-3388, 1995.

[59] T. Ishizone and R. Goseki, “Anionic Addition Polymerization (Fundamental),” in Encyclopedia of Polymeric Nanomaterials, Berlin, Springer, pp. 23-33, 2015.

[60] P. Sarkar and A. K. Bhowmick, “Green Approach toward Sustainable Polymer: Synthesis and Characterization of Poly(myrcene-co-dibutyl itaconate),” Sustainable Chemistry and Engineering, vol. 4, pp. 2129-2141, 2016.

[61] A. B. Lowe, “Thiol-ene “click” reactions and recent applications in polymer and materials synthesis,” Polymer Chemistry, vol. 1, pp. 17-36, 2010.

[62] J. J. Fong, “Waterborne maleinized polybutadiene emulsion coating composition”. United States Patent US5552228A, 03 September 1996.

[63] Y. Nakayama, “Maleinization process”. United States Patent US3778418A, 11 December 1973.

[64] J. V. Alemán, A. V. Chadwick, J. He, M. Hess, K. Horie, R. G. Jones, P. Kratochvíl, I. Meisel, I. Mita, G. Moad, S. Penczek and R. F. T. Stepto, “Definitions of terms relating to the structure and processing of sols, gels, networks, and inorganic-organic hybrid materials (IUPAC Recommendations 2007),” Pure and Applied Chemistry, vol. 79, no. 10, pp. 1801-1829, 2007.

[65] J. Kruželák, R. Sýkora and I. Hudec, “Sulphur and peroxide vulcanisation of rubber compounds – overview,” Chemical Papers, vol. 70, no. 12, pp. 1533-1555, 2016.

[66] A. Hirao, R. Goseki and T. Ishizone, “Advances in Living Anionic Polymerization: From Functional Monomers, Polymerization Systems, to Macromolecular Architectures,” Macromolecules , vol. 47, pp. 1883-1905, 2014.

[67] D. Baskaran, “Strategic developments in living anionic polymerization of alkyl (meth)acrylates,” Progress in Polymer Science, vol. 28, pp. 521-581, 2003.

[68] J. Herzberger, K. Niederer, H. Pohlit, J. Seiwert, M. Worm, F. R. Wurm and H. Frey, “Polymerization of Ethylene Oxide, Propylene Oxide, and Other Alkylene Oxides: Synthesis, Novel Polymer Architectures, and Bioconjugation,” Chemical Reviews, vol. 116, pp. 2170-2243, 2016.

[69] V. Rejsek, P. Desbois, A. Deffieux and S. Carlotti, “Polymerization of ethylene oxide initiated by lithium derivatives via the monomer-activated approach: Application to the direct synthesis of PS-b-PEO and PI-b-PEO diblock copolymers,” Polymer, vol. 51, no. 24, pp. 5674-5679, 2010.

[70] S. Nakahama and A. Hirao, “Protection and Polymerization of Functional Monomers - Anionic Living Polymerization of Protected Monomers,” Progress in Polymer Science, vol. 15, pp. 299-335, 1990.

[71] A. Hirao, A. Yamamoto, K. Takenaka, K. Yamaguchi and S. Nakahama, “Protection and polymerization of functional monomers: 8. Anionic living polymerization of 4-[2-(trialkyl)silyloxyethyl]styrene as protected 4-(2-hydroxyethyl)styrene,” Polymer, vol. 28, no. 2, pp. 303-310, 1987.

[72] T. Renner and L. Pék, “Comparing Strength Properties of Natural Rubber and Synthetic Rubber Mixtures,” Sustainable Construction and Design, vol. 1, pp. 134-141, 2011.

[73] H. De Livonniere, “Idustrial Natural Rubber Collection and Control Procedures,” Clinical Reviews in Allergy, vol. 11, no. 3, pp. 310-323, 1993.

[74] W. Obrecht, J. Lambert, M. Happ, C. Oppenheimer-Stix, J. Dunn and R. Krüger, “Rubber, 4. Emulsion Rubbers,” Ullmann's Encyclopedia of Industrial Chemistry, 2011.

[75] J. Gheller Jr, M. V. Ellwanger and V. Oliveira, “Polymer–filler interactions in a tire compound reinforced with silica,” Elastomer and Plastics, vol. 48, no. 3, pp. 217-226, 2016.

[76] W. Kaewsakul, K. Sahakaro, W. K. Dierkes and J. W. M. Noordermeer, “Factors influencing the flocculation process in silica-reinforced natural rubber compounds,” Journal of Elastomers, vol. 48, no. 5, p. 426, 2016.

[77] E. Kim, E. Lee, I. Park and T. Chang, “End Functionalization of Styrene–Butadiene Rubber with Poly(ethylene glycol)–poly(dimethylsiloxane) Terminator,” Polymer Journal, vol. 34, no. 9, pp. 674-681, 2002.

[78] K. Sengloyluan, K. Sahakaro, W. Dierkes and J. W. M. Noordermeer, “Silica-reinforced tire tread compounds compatibilized by using epoxidized natural rubber,” European Polymer Journal, vol. 51, pp. 69-79, 2014.

[79] E. Oldfield and F.-Y. Lin, “Terpene Biosynthesis: Modularity Rules,” Angewandte Chemie, vol. 51, no. 5, pp. 1124-1137, 2012.

[80] A. Behr and L. Johnen, “Myrcene as a Natural Base Chemical in Sustainable Chemistry: A Critical Review,” ChemSusChem, vol. 2, pp. 1072-1095, 2009.

[81] X. Yang, C. Wang, S. Li, K. Huang, M. Li, W. Mao, S. Cao and J. Xia, “Study on the synthesis of bio-based epoxy curing agent derived from myrcene and castor oil and the properties of the cured products,” RSC Advances, vol. 7, pp. 238-247, 2017.

[82] E.-M. Kim, J.-H. Eom, Y. Um, Y. Kim and H. M. Woo, “Microbial Synthesis of Myrcene by Metabolically Engineered Eschericha coli,” Agricultural and Food Chemistry, vol. 63, pp. 4606-4612, 2015.

[83] A. J. Johanson, M. F. L. and L. A. Goldblatt, “Emulsion Polymerization of Myrcene,” Industrial and Engineering Chemistry, vol. 40, no. 3, pp. 500 - 502, 1948.

[84] E. Grune, J. Bareuther, J. Blankenburg, M. Appold, L. Shaw, A. H. E. Muller, G. Floudas, L. R. Hutchuings and H. Frey, “Towards bio-based tapered block copolymers: the behaviour of myrcene in the statistical anionic copolymerisation,” Polymer Chemistry, vol. 10, pp. 1213-1220, 2019.

[85] A. Matic and H. Schlaad, “Thiol-ene photofuctionalization of 1,4-polymyrcene,” Polymer International, vol. 67, pp. 500-505, 2018.

[86] J. Hilschmann and G. Kali, “Bio-based polymyrcene with highly ordered structure via solvent free controlled radical polymerization,” European Polymer Journal, vol. 73, pp. 363-373, 2015.

[87] W. Li, J. Zhao, X. Zhang and D. Gong, “Capability of PN3 type Cobalt Complexes toward Selective (Co-)Polymerization of Myrcene, Butadiene, and Isoprene: Access to Biosourced Polymers,” Industrial and Engineering Chemistry Research , vol. 58, pp. 2792-2800, 2019.

[88] P. Sarkar and A. K. Bhowmick, “Synthesis, characterization and properties of a bio-based elastomer: polymyrcene.,” Royal Society of Chemistry Advances, vol. 4, pp. 61343-61354, 2014.

[89] P. Sarkar and A. K. Bhowmick, “Terpene Based Sustainable Elastomer for Low Rolling Resistance and Improved Wet-Grip Application: Synthesis, Characterization and Properties of Poly(styrene-co-myrcene).,” Americal Chemical Society Sustainable Chemistry 7 Engineering, vol. 4, no. 10, pp. 5462-5474, 2016.

[90] S. Zhang, L. Han, H. Ma, P. Liu, H. Shen, L. Lei, C. Li, L. Yang and Y. Li, “Investistigation on Synthesis and Application Performance of Elastomers with Bioogenic Myrcene,” Industrial & Engineering Chemistry Research , vol. 58, pp. 12845-12853, 2019.

[91] J. Zhang, J. Lu, K. Su, D. Wang and B. Han, “Bio-based Beta-myrcene-modified solution-polymerized styrene-butadiene rubber for improving carbon black dispersion and wet skid resistance,” Applied Polymer Science, vol. 136, pp. 48159-48169, 2019.

[92] A. Ávila-Ortega, M. Aguilar-Vega, M. I. L. Bastarrachea, C. Carrera-Figueiras and M. Campos-Covarrubias, “Anionic synthesis of amine ω-terminated β-myrcene polymers,” Polymer Research, vol. 22, no. 11, pp. 226-234, 2015.

[93] C. Zhou, Z. Wei, C. Jin, Y. Wang, Y. Yu, X. Leng and Y. Li, “Fully biobased thermoplastic elastomers: Synthesis of highly branched linear comb poly(beta-myrcene)-graft-poly(L-lactide) copolymers with tuneable mechanical proberties,” Polymer, vol. 138, pp. 57-64, 2018.

[94] A. Matic, A. Hess, D. Schanzenbach and H. Schlaad, “Epoxidized 1,4-polymyrcene,” Polymer Chemistry, vol. 11, pp. 1364-1368, 2020.

[95] A. N. Tavtorkin, I. F. Gavrilenko, N. N. Kostitsyna, S. A. Korchagina, M. S. Chinova, A. V. Shlyakhtin, I. E. Nifant’ev, A. M. Vagizov and K. G. R., “Synthesis of Diene–Styrene (Co)polymers Modified by Myrcene-Based Diene Polar Monomers,” Polymer Science, vol. 61, no. 1, pp. 1-7, 2019.

[96] C. Hahn, M. Wagner, A. H. E. Müller and H. Frey, “MyrDOL, a Protected Dihydroxyfunctional Diene Monomer Derived from β-Myrcene: Functional Polydienes from Renewable Resources via Anionic Polymerization,” Macromolecules, vol. 55, no. 10, pp. 4046-4055, 2022.

Chapter 2 – The Living Anionic Polymerisation and Copolymerisation of β-Myrcene

2.1 Introduction

Solution Styrene Butadiene Rubber (sSBR) has been used in many different areas in industry for applications such as shoe soles, gaskets and chewing gum. [1] Most interestingly, sSBR is used within the pneumatic tyre industry for tyre treads, to increase the wear resistance. To improve the wet-grip and rolling-resistance properties of tyres, compounds such as silica and carbon black are added. This approach, however, has led to difficulties in the manufacturing process, and additives can coagulate during their incorporation, which causes the rubber to harden. This in turn results in increased manufacture costs – to break up coagulates – and potential fracture points in the tyres themselves – where coagulates are not broken up and are incorporated into the tyre. [2] One potential solution is the addition of polar groups to the chain termini to aid the dispersion of the filler molecules. [3] [4] However, the lack of possible monomers that can be used for anionic polymerisation has generally limited the research to chain-end modifications, which, although promising, can be challenging to perform on an industrial scale and which may not provide the required polarity for the dispersion to be carried out effectively. One way through which polarity can be added to polymers synthesised by living anionic polymerisation (LAP) is through the post-polymerisation in-chain functionalisation. Several groups have explored the in-chain functionalisation of sSBR, [5] including using tertiary amine substituted vinyl monomers to increase the interaction of silica to the non-polar sSBR, [6] and through curing the sSBR in the presence of bis[3-(triethoxysilyl) propyl] tetrasulfide to provide covalent interactions between the silica and sSBR. [7] An issue with in-chain functionalisation for these systems, however, is that functionalisation is generally unspecific – meaning the functionalisation can occur anywhere along the polymer chains – and the functionalisation itself can cause an increase in the glass transition temperature (T_g) of the rubber – meaning that the rubber will have a smaller operating range of temperatures and may not be suitable to be used in low-temperature environments. [8] If in-chain functionalisation is to become a viable method of providing polarity in sSBR, a method for allowing the functionalisation to occur selectively

while having little impact on the T_g must be found. One potential method could be through the incorporation and selective epoxidation of the bio-available monomer myrcene. Although the polymerisation of myrcene was first investigated as a potential component in the manufacture of tank-tread rubber in the 1940s, [9] it was largely forgotten about until the 2010s, since which the polymerisation of myrcene has been increasingly explored due to the requirement to move away from depleted petrochemical-based monomers towards sustainable bio-based monomers. [10] Recent advancements in the production of myrcene, including the industrial scale pyrolysis of β-pinene [10] and the microbial synthesis of myrcene using metabolically engineered bacteria [11], have also led to increased interest and research into myrcene's applications from industry as it becomes more commercially viable. Myrcene can be polymerised under standard LAP procedures, [12] [13] Metal Catalysed Polymerisation (MCP) [14] and Reversible Addition-Fragmentation Transfer (RAFT) polymerisation. [15] Myrcene has also been shown to be easily copolymerised with styrene, via LAP, producing polymers with mechanical properties that are desirable for the use in tyre treads. [16] [17] These properties, along with fact that when polymerised by LAP, poly(myrcene) displays a pendant trisubstituted double bond (not involved in the polymerisation mechanism) that has the potential to be epoxidised to provide polarity and a platform for further functionalisation, suggest that myrcene could be a potential solution to some of the problems encountered by the tyre industry.

In this study, we examine the polymerisation mechanism of myrcene, previously improperly described, [13] along with presenting qualitative kinetic studies into the copolymerisation of myrcene with both the commonly used monomers styrene and butadiene before a terpolymer of all three is synthesised. This chapter will also detail a qualitative study into the effect of *N,N,N',N'*-tetramethylethylenediamine (TMEDA) on the homopolymerisation, copolymerisation and terpolymerisation of myrcene with butadiene and styrene.

This Chapter was a direct continuation of the Master's project that was started previously within the Hutchings group [18] and many of the results presented have been used to support the claims of a previously published patent [19]:

L. Shaw, "The synthesis, characterisation and functionalisation of myrcene (co)polymers prepared by living anionic polymerisation.," University of Durham, 2018.

L. R. Hutchings, "Method of Epoxidation". International Patent WO2020212492A1, 22 October 2020.

2.2 Results and Discussion

Despite previous reports of the homopolymerisation of myrcene, the beginning of this project describes the homopolymerisation of β-myrcene in an attempt to build upon the research already available and to provide insight into some of the misconceptions that are often associated with the polymerisation of β-myrcene (and many other dienes) by LAP.

2.2.1 The Living Anionic Homopolymerisation of Myrcene

Myrcene has already been homopolymerised by LAP by several different research groups including by R. Quirk and T. Huang in 1984, [20] and by J. Bolton, M. Hillmyer and T. Hoye more recently in 2014. [21]

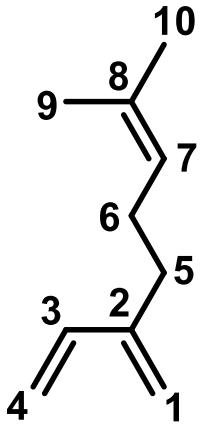

Figure 2.1: β-myrcene, showing conventional numbering assigned to each carbon (and the hydrogens on said carbon).

One of the misconceptions that is found most regularly within the literature concerns the propagation of terpenes. We have found that in most literature reports describing the LAP of myrcene, the mechanism of the polymerisation has been wrongly identified. In many papers, the LAP of myrcene has been identified as propagating in a 1,4 direction. This is a common misconception with not only myrcene but most substituted dienes, including one of the most commonly used monomers, isoprene. [22] [23] [24]

Due to the fact that the stability of carbanions in non-polar solvents is fairly low, and considering the resonance structures of the carbanion, it is widely accepted that carbons 1 and 4 are the only viable sites of attack. However, most papers have identified the propagation of myrcene as occurring in a 1,4 direction, whereas we believe that there is not

just one but two reasons that mean that the polymerisation actually occurs primarily in the 4,1 direction.

The first reason is based on the electron density of the double bonds in the myrcene (Figure 2.1). Hyperconjugation from adjacent sp^3 C-H bonding orbitals to the alkene π system increases the electron density of the 1,2 double bond, [25] decreasing the likelihood of attack of the 1,2 double bond by the carbon anion of the living polymer chain. This means that we believe the most readily available carbon for attack, based on the lowest activation energy barrier (i.e. most susceptible for attack), is carbon 4, which is the first reason for our proposed 4,1 propagation mechanism. The second reason for our proposed propagation direction is based on the stability of the resulting carbanion after attack of the myrcene monomer. As is commonly known and reported in literature, the stability of a carbanion decreases with increasing substitution. [26]

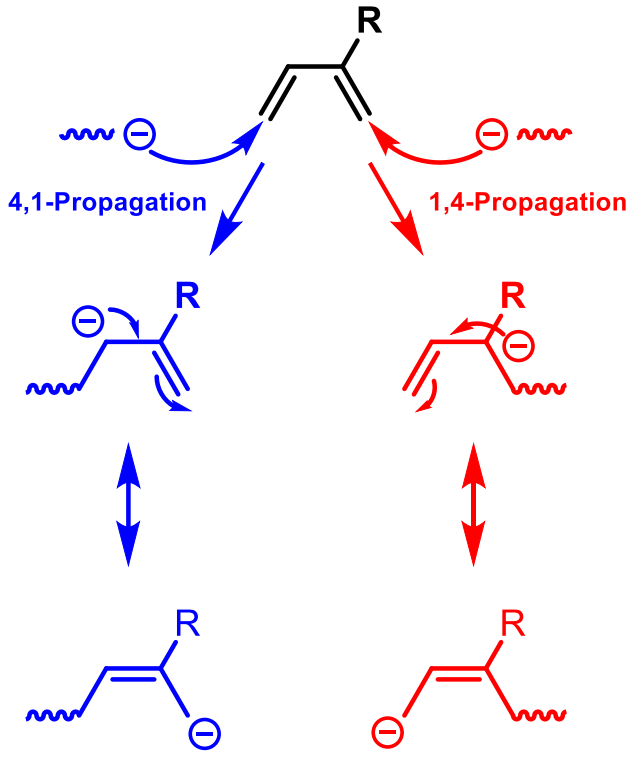

Figure 2.2*:* Mechanism showing the potential positions of anionic attack of a generic diene and the subsequent resonance structures after attack, whereby the blue pathway indicates the resonance structures of 4,1-propagation and the red pathway indicates the resonance structures of 1,4-propagation.

Upon attack of carbon 1 (Figure 2.2; red pathway) the resulting anions are primary and tertiary, however, the anions resulting from reaction at carbon 4 (blue pathway) are primary

and secondary. This means that the stability of the propagating species is likely to be greater upon attack of carbon 4 relative to carbon 1. This would suggest that the barrier to attack of carbon 1 is much greater than the barrier of attack to carbon 4, suggesting that 4,1 propagation will be favoured in the case of myrcene (and by extension isoprene, farnescene, etc.).

To investigate the homopolymerisation of myrcene, a sample of poly(myrcene) – (PM1) – was synthesised in benzene at room temperature, with a target M_n of 40,000 g mol^{-1} (Figure 2.3).

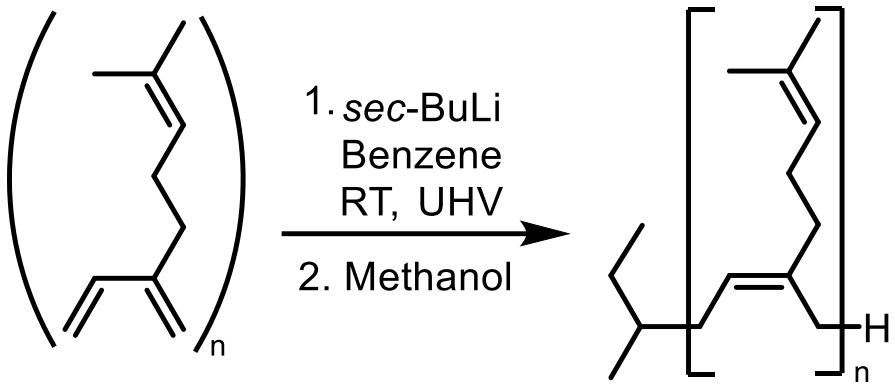

Figure 2.3: Homopolymerisation of myrcene by LAP using *sec*-BuLi as the initiator.

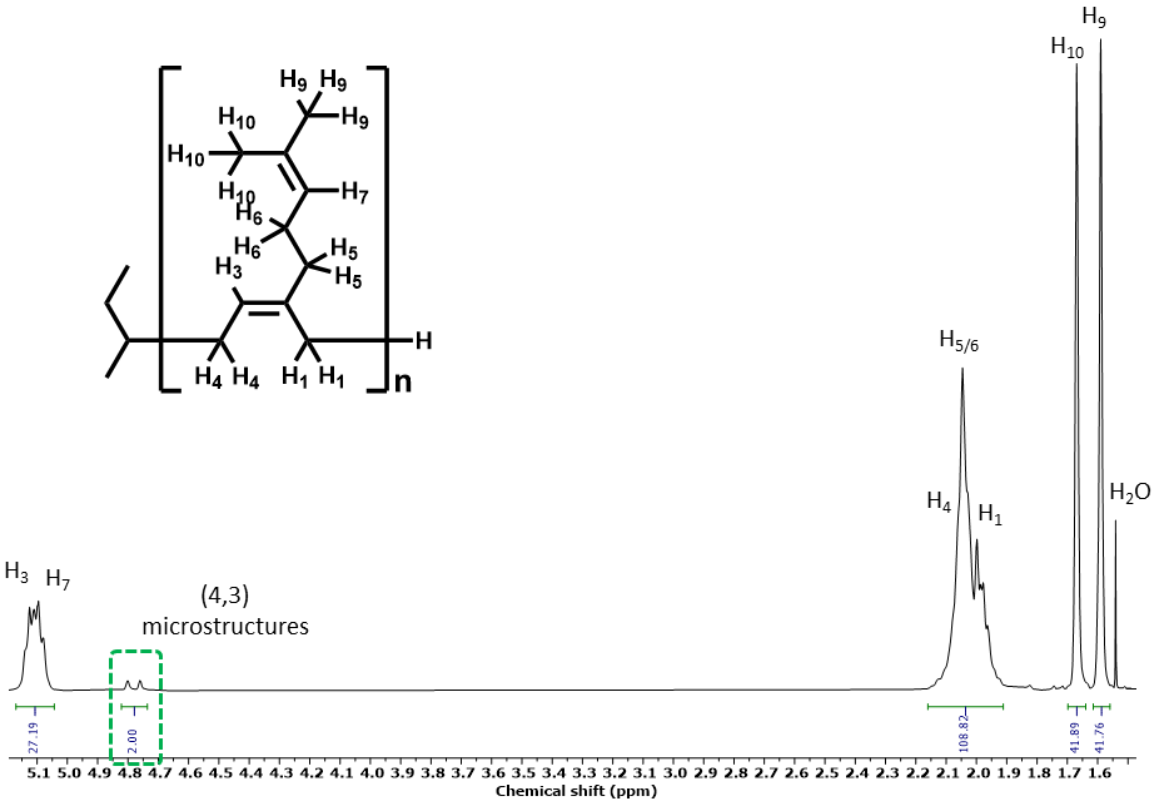

Figure 2.4: ^{1}H NMR spectrum (400 MHz, $CDCl_3$) of PM1, with associated proton assignment.

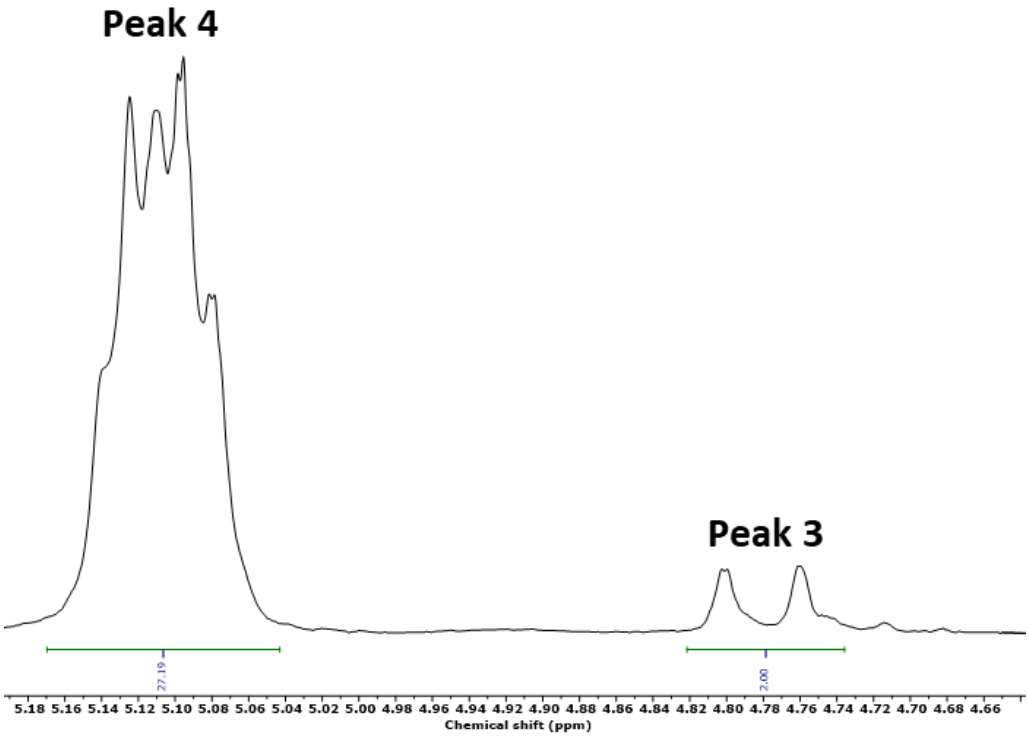

Figure 2.5: Expanded ^{1}H NMR spectrum (400 MHz, $CDCl_3$) of PM1, showing the alkene region of the spectrum (4.65 – 5.20 ppm; green dashed box in Figure 2.4) and the associated peak numbering assignment.

As discussed previously in Section 1.4.2.1.2, the microstructure composition of a poly(diene) (Figure 2.6) plays a vital role in determining the overall physical properties of the synthesised polymer. As such, the microstructure composition of the sample was analysed using ^{1}H NMR spectroscopy.

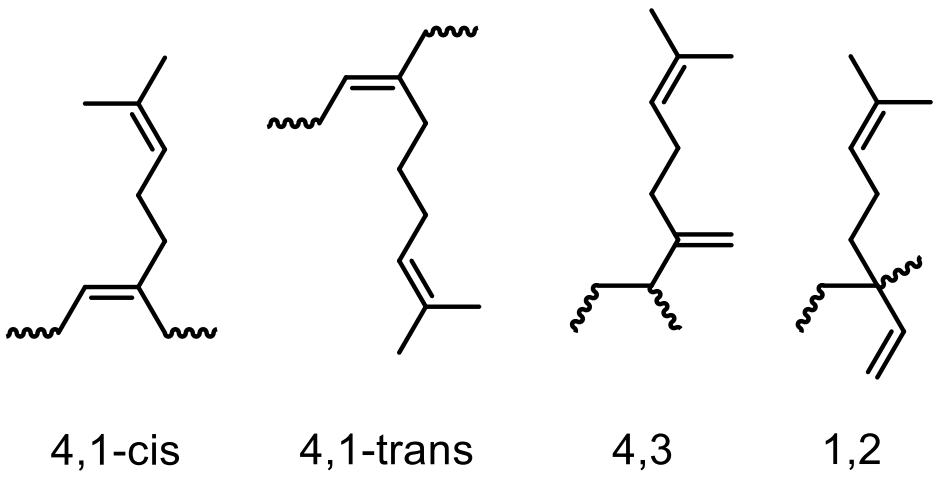

Figure 2.6: The 4 possible microstructures of myrcene synthesised by LAP, whereby polymerisations occurring in the 1,4 direction would also be likely but in smaller quantities, due to reasons that were discussed previously.

In non-polar solvents, in agreement with the literature surrounding isoprene, the 1,2-microstructure of poly(myrcene) is not observed within the ^{1}H NMR spectrum. In the ^{1}H NMR spectra of poly(myrcene) samples (Figure 2.4), it can be seen that unlike for spectra of poly(butadiene), the signals for the 4,1-cis and 4,1-trans alkene peaks are completely indistinguishable from each other. This means that the microstructure composition for poly(myrcene) samples, polymerised in non-polar solvents (and in the absence of polar modifiers) can be calculated using Equation 2.1 below.

$$\%\ 4{,}1\ \text{microstructure} = \frac{\text{Integral Peak 4} - \left(\frac{\text{Integral Peak 3}}{2}\right)}{\text{Integral Peak 4} - \left(\frac{\text{Integral Peak 3}}{2}\right) + \text{Integral Peak 3}} \times 100\ \%$$

Equation 2.1: Equation used to calculate the percentage of 4,1 microstructures in a sample of poly(myrcene) prepared in a non-polar solvent.

Using the integrals for PM1 in Figure 2.4 we get:

$$\%\ \mathbf{4{,}1\ microstructure} = \frac{\mathbf{27.19} - \left(\frac{\mathbf{2.00}}{\mathbf{2}}\right)}{\mathbf{27.19} - \left(\frac{\mathbf{2.00}}{\mathbf{2}}\right) + \mathbf{2.00}} \times \mathbf{100}\ \% = \mathbf{92.9}\ \%$$

$$\%\ 4{,}3\ \text{microstructures} = 100\ \% - 92.9\ \% = 7.1\ \%$$

Equation 2.2: Equations used to calculate the microstructure composition percentages of PM1.

A very small proportion of (4,3) microstructures was observed (approximately 7%) during the homopolymerisation of myrcene in benzene at room temperature using lithium as the counterion. This is similar to the (4,3) composition of poly(isoprene) when polymerised under the same conditions, which is also approximately 6%. [27] These (4,3) compositions are both lower than the observed (4,3) composition observed for poly(butadiene) synthesised under the same conditions, which is approximately 11%. [28] This difference could potentially be explained by the increased steric hindrance associated with the monomer being polymerised at carbon 3 in myrcene and isoprene compared to the steric hindrance associated with butadiene.

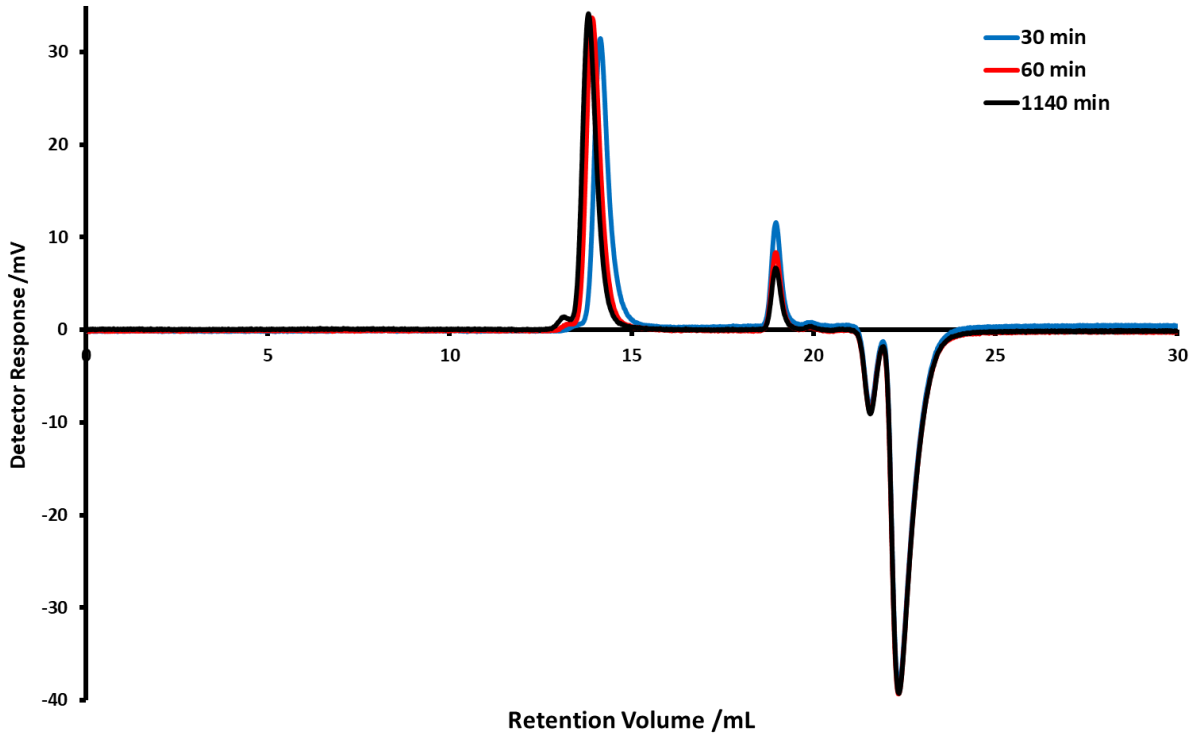

Figure 2.7: SEC curves of the 3 samples collected during the polymerisation of PM1 (THF, 1 mL/min) whereby the sample collected at 1140 min (19 hours) was the trace of the final polymer – PM1.

Table 2.1: Instantaneous microstructure composition, Đ and molar mass for the homopolymerisation of PM1 as a function of time.

Sampling time / min	M_n /g mol^{-1}	Đ	Conversion*/ %
30	33200	1.06	73
60	40600	1.04	89
1140	45400	1.03	100

* Calculated using the M_n values obtained by SEC assuming sample at 1140 represents 100 % conversion.

Based on the assumption that the homopolymerisation went to completion, it can be observed from Figure 2.7 and the accompanying data in Table 2.1 above, that after 60 minutes, 89% of polymerisation had already occurred. From this qualitative kinetic investigation, we can see that the rate of homopolymerisation of myrcene is far quicker relative to the rate of the homopolymerisation of butadiene [28] and much closer to the rate of homopolymerisation of isoprene. [27] This can potentially be explained by the increased nucleophilicity of the propagating anion due to the donation of electron density from the alkyl

substituent. A similar effect is observed in the polymerisation of electronically similar isoprene molecules. [29]

Looking at the SEC curves in Figure 2.7, we can see that while the curves themselves are fairly narrow and Gaussian (a characteristic of polymers synthesised by LAP) resulting in low Đ observed, they each display a significant shoulder to the left-hand side of the trace – corresponding to polymer chains with a molecular weight of approximately twice the M_n. While this is a problem that has previously been reported in the literature [26] for LAP of other monomers (particularly dienes), the size of this peak is very noticeable for polymerisations involving myrcene. In the literature, this presence of a 2 x M_n peak has been attributed to three potential mechanisms (see Figure 2.8):

1. Oxygen coupling of two living chain ends – an electron transferred from a Reactive Oxygen Species (ROS) to the propagating chain end results in an anionic-radical (much like that described in the mechanism shown by Michael Szwarc in the initiation of styrene using sodium). If two of these anionic-radical species are generated, the subsequent radical termination of these two chains results in a polymer with twice the M_n of the initial chains.
2. Nucleophilic attack of carbon dioxide – nucleophilic attack of carbon dioxide by a propagating polymer chain can result in the functionalisation of the chain end by a carboxylic acid, which can then in turn be attacked by a second propagating chain, resulting in a polymer with twice the M_n and a ketone functionality in the middle (this ketone can in turn be attacked by another 1 or 2 chains resulting in polymers with a M_n of up to 4 times the expected M_n). [30]
3. Degradation of the propagating chain – the carbon-lithium bond has been shown to degrade over time and at elevated temperatures, leading to termination of the propagating polymer and resulting in a diene functionality being present at the end of the polymer chain. If present during the polymerisation, this diene functionality can be attacked by and incorporated into another propagating polymer, resulting in this polymer having over twice the M_n of the initial polymer. [26]

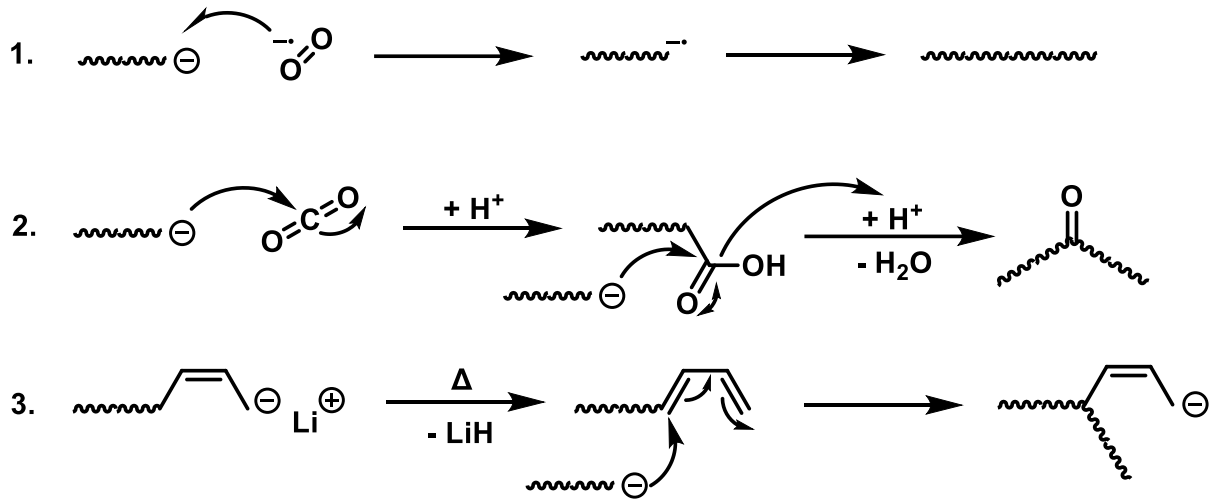

Figure 2.8: Three potential mechanisms to explain how polymers with a molecular weight of 2M_n can be introduced during Living Anionic Polymerisation.

Despite having three potential mechanisms, it is believed that the increase in the amount of myrcene (and other R-substituted dienes) polymers with 2 × M_n is once again a result of the decreased stability of the carbanion, resulting from hyperconjugation from the bonding orbitals of the sp^3 hybridised carbon 5 into the propagating π bond. This decreased stability means that intramolecular termination through degradation is much more likely, and also upon termination (through the addition of a protic solvent), the active chain ends will be much more susceptible to termination through any air impurities, which will generally be a higher energy pathway to termination than termination caused by the protic solvent and can still be added during addition even when the protic solvents are deoxygenated. This increased air termination susceptibility along with the fact that these air impurities will diffuse through the system quicker than the protic solvent (a fact supported by the proportion of 2 × M_n increasing with increasing molecular weight – and therefore viscosity – of the polymer) means that a higher proportion of the chain ends will be terminated through the coupling mechanisms shown in Figure 2.8 above. While the literature regarding which of the three mechanisms of termination might dominate is limited, due to the observations that were made regarding the fact that this shoulder is almost completely absent when polystyrene is the propagating species and due to the fact that the shoulder appeared to increase with increasing molecular weight and therefore reaction time, it is proposed that for LAP systems (especially those involving myrcene and isoprene) that mechanism 3 will dominate in resulting in the 2 x M_n shoulder, although all three mechanisms have been reported in the literature.

2.2.1.1 The Effect of Polar Additives on the Anionic Polymerisation of Myrcene

Within the context of LAP, polar modifiers (termed “randomisers” in some older literature [31] [32]) and polar solvents have large implications on not only the kinetics of the polymerisation but also the microstructures present of the resulting polymers when dienes are polymerised. [33] [34] [35] These polar additives are extremely important in the field of LAP, especially within industry, as they not only allow for direct control of a polymer’s glass transition temperature (T_g) – through the control of the amount of vinyl microstructure present – but also allow for the reactivity ratios within copolymerisations, terpolymerisations, etc. to be manipulated. This manipulation of reactivity ratios is probably best shown within the example of the synthesis of “random” diene-styrene copolymers, [36] [37] which represent a massive industry within commercial polymers synthesised by LAP including for the synthesis of polymers used in car tyre rubbers, insoles and tubing. [38]

It was due to the effects on microstructure and the importance of polar modifiers in the synthesis of many commercial polymers that it was decided that *N*,*N*,*N’*,*N’*-tetramethylethylenediamine (TMEDA – Figure 2.9) would be used within the homopolymerisation of myrcene so that its effect could be investigated.

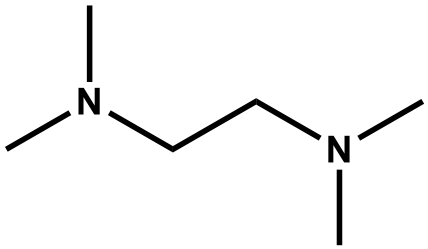

Figure 2.9: Chemical structure of TMEDA.

In order to understand the effects that polar additives have on the polymerisation of myrcene, it is helpful to examine previous literature to explore the effects of polar modifiers within other polymerisations. While there is plenty of literature regarding the use of polar modifiers, there are few papers that examine the underlying mechanism of action, and therefore we will also present some potential explanations for these effects.

As discussed in Section 1.4.1.2, butyl lithium compounds are unstable in non-polar solvents. It is for this reason that within non-polar solvents, these butyl lithium compounds aggregate

to reduce the overall energy potential, with the aggregation number determined by the balance of the electrostatic repulsion of the lithium cations; the electrostatic attraction of the negatively charged alkyl/polymer chains to the lithium cations; the energy of solvation; and the enthalpy of aggregation. The most favourable degree of aggregation will generally depend on the steric bulk of the alkyl fragment at the propagating chain end, with unbranched, linear chains leading to larger aggregates, such as hexamers, and branched or bulky aromatic chains leading to smaller aggregates, such as tetramers or dimers. However, this will be in equilibrium with lithium dimers and unaggregated alkyllithium unimers (Figure 1.8). As discussed previously, it is believed polymerisation can only occur in the unaggregated alkyllithium unimers, due to the steric hindrance associated with the angle of attack of the new monomer being added onto the chain. [26]

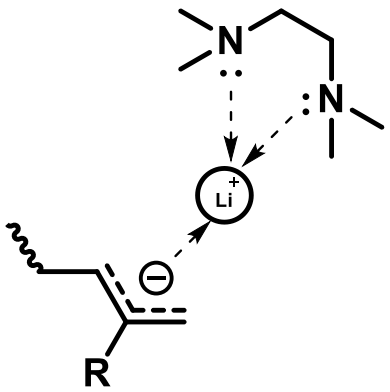

Figure 2.10: Coordination of TMEDA to the lithium counterion of a propagating generic diene during LAP.

TMEDA contains two nitrogen atoms, each with a lone pair of electrons that are able to coordinate to the lithium counter cations associated with the propagating chain end (Figure 2.10). A partial donation of electron density from the TMEDA to the lithium cation results in the delocalisation of the positive charge across both the lithium cation and the coordinated TMEDA. This reduces the charge density of the lithium cation, resulting in an increase in the ionicity of the bond between the lithium cation and the propagating chain end, which causes the aggregates to be broken up into effectively solvated ion pairs (see Section 1.4.1.4). This in turn leads to a lengthening of the lithium-oligomer/polymer bond, resulting in a decrease in its strength, which ultimately results in different rates of any homopolymerisation and cross-polymerisation rate constants for the monomers being polymerised. This change in the reactivity ratios could be the result of decreased substituent effect on the alkyl lithium bond

due to the increased iconicity of the bond, where the substituent effects will have the greatest impact on covalent bonds due to hyperconjugation and induction. Due to the lithium aggregates being broken up into effectively solvated ion pairs, the addition of a polar modifier is generally always seen to be accompanied by an increase in the rate of polymerisation.

The rate of polymerisation, however, is not the only characteristic of the polymerisation that is affected by the addition of a polar modifier – TMEDA – whereby in the polymerisation of dienes the microstructure composition of the final polymer is also affected and thus must be considered. This change in the microstructure composition is most likely explained by the shift in charge density caused by the shift in bonding from a covalent model in the absence of TMEDA to a more ionic model in the presence of TMEDA.

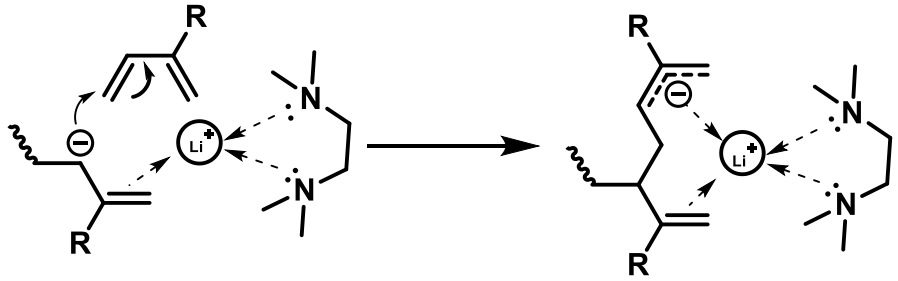

Figure 2.11: Mechanism of 4,3-propagation of a generic mono-substituted diene during LAP in the prensence of the polar modifier

In the polymerisation of myrcene, the coordination of TMEDA to the lithium counterion and the effective solvation of the ion pairs results in a shift in the position of the electron density (negative charge) of the propagating chain, meaning that a greater proportion of the electron density is now situated on the kinetically preferred, more substituted carbon 3 (despite being more substituted this carbon is more accessible than carbon 1 due to the presence of the large lithium-TMEDA complex which will still be situated closer to carbon 1 despite the increase in C-Li bond length), relative to the thermodynamically preferred carbon 1, which is favoured in the absence of TMEDA in non-polar solvents when lithium is used as the counterion (Figure 2.11). This leads to an increase in propagation occurring through carbon 3, leading to a greater proportion of 4,3 microstructures.

To investigate the impact of TMEDA on the microstructure of a sample of polymyrcene, a homopolymerisation of myrcene in the presence of 2 molar equivalents of TMEDA with respect to the amount of initiator used was conducted (PM2).

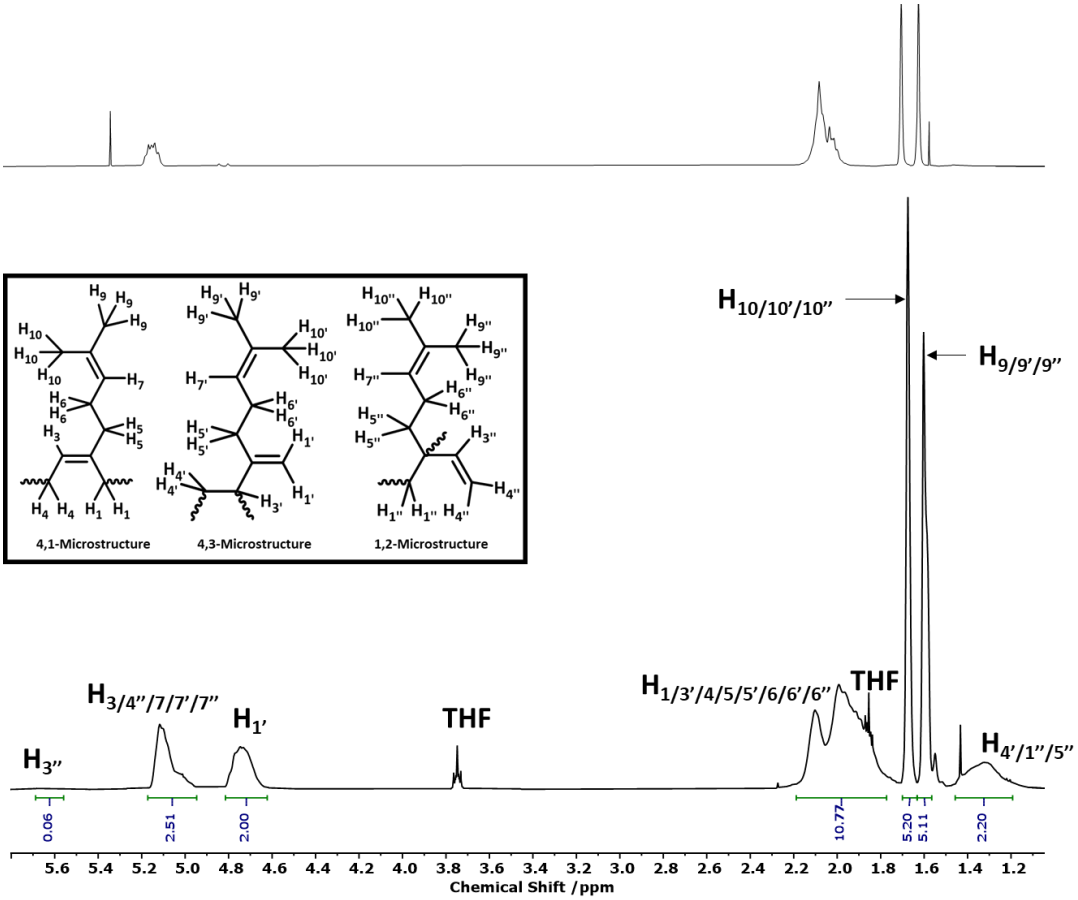

Figure 2.12: ^{1}H NMR spectrum (400 MHz, $CDCl_3$) of PM2 with hydrogen assignments of the peaks observed, whereby the trace of PM1 has been overlaid above for reference to show the change in microstructure associated with polymerisation in the presence of TMEDA.

As can be seen in Figure 2.12, the coordination of TMEDA to the lithium cation can dramatically alter the microstructure composition of poly(myrcene). What is also evident from Figure 2.12 is that in the presence of TMEDA, a (1,2) microstructure – as evidenced by the presence of a small peak in the region between 5.55 – 5.75 ppm, which arises due to the presence of protons $H_{3''}$ in the ^{1}H NMR spectrum of PM2 – which is completely inaccessible during the polymerisation in non-polar solvents in the absence of TMEDA, is also present in very small but appreciable yields. This (1,2) propagation leads to an anion that is much less stable than the anion present when nucleophilic attack occurs at carbon 4 due to the electron density being localised on carbon 2 – a tertiary carbon and therefore the least stable (and the most sterically hindered) carbanion – meaning that under normal conditions in non-polar solvents (whereby a more covalent model of C-Li bond is present) the activation energy barrier is too great to overcome and only the (4,1) and (4,3) microstructures will be seen. This accessible (1,2) microstructure when myrcene is polymerised in the presence of a polar

modifier is an effect that can also be observed in the polymerisation of isoprene whereby in the presence of a polar modifier or polar solvent (1,2), propagation can also occur, which is not the case for the polymerisation of isoprene in non-polar solvents in the absence of a polar modifier. [39] [40] This extra microstructure that is accessible means that for the calculation of microstructure compositions of polymyrcene samples prepared in the presence of TMEDA, a new set of equations must be derived.

The microstructure of PM2 can be calculated using the integrals of peaks 3, 4 and 5 (see Figure 2.13) as follows:

- Peak 3 (4.45-4.85 ppm), which corresponds to 2 protons from 4,3 repeat units ($H_{1'}$)
- Peak 4 (4.85-5.20 ppm), which corresponds to 2 protons from 4,1 repeat units (H_3 and H_7) and 1 proton from 4,3 repeat units (again H_7 – which is common to all microstructures) and 3 protons from the 1,2 repeat units ($2 \times H_{4''} + H_{7''}$)
- Peak 5 (5.55-5.75 ppm), which corresponds to 1 proton from 1,2 repeat units ($H_{3''}$)

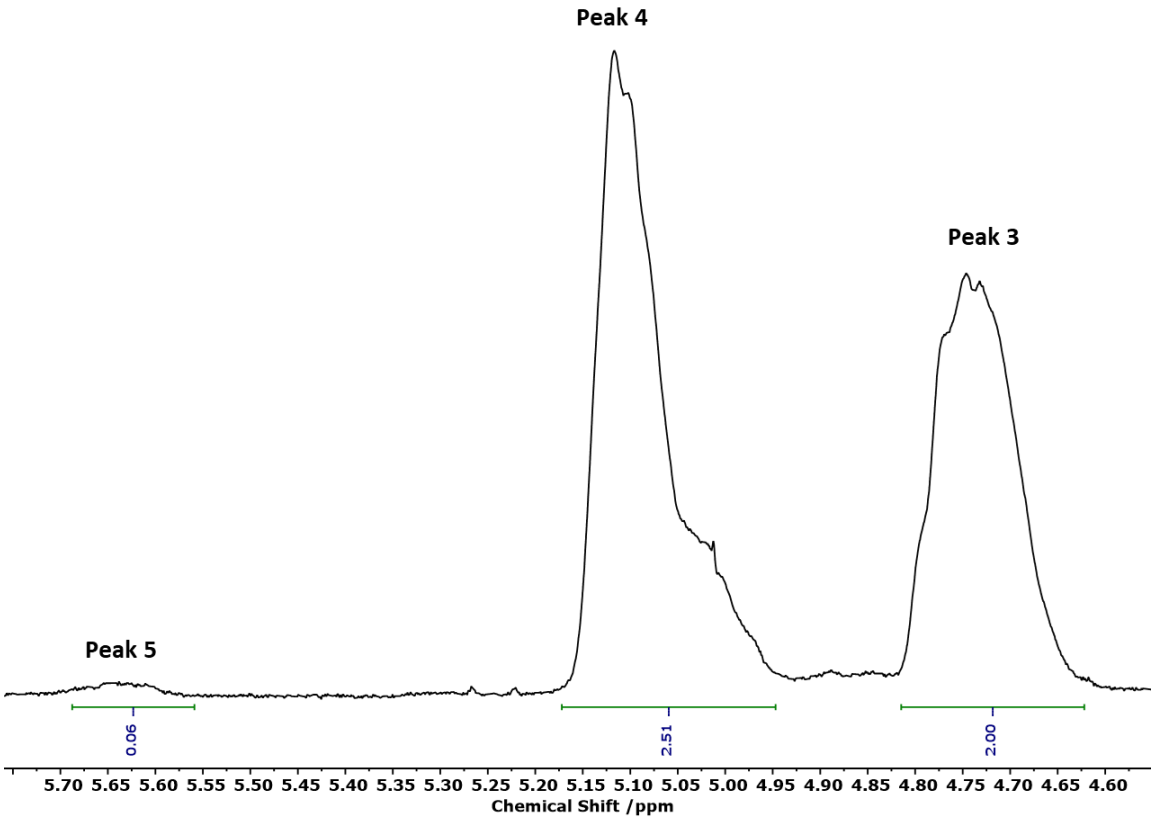

Figure 2.13: Expanded ^{1}H NMR spectrum (400 MHz, $CDCl_3$) of PM1, showing the alkene region of the spectrum (4.55 – 5.80 ppm) and the associated peak numbering assignment.

Thus, the integral equivalent to 2 protons from 4,1 repeat units is given by Equation 2.3.

$$2H_{4,1} = \text{Integral Peak 4} - \frac{\text{Integral Peak 3}}{2} - (3 \times \text{Integral Peak 5})$$

$$2H_{4,1} = 2.51 - \frac{2.00}{2} - (3 \times 0.06) = 1.33$$

Equation 2.3: Equation used to calculate the equivalent protons of 4,1 microstructures in a sample of Poly(myrcene) prepared in the presence of TMEDA.

The integral equivalent to 2 protons from 4,3 repeat units is equal to the integral of Peak 3 (2.00) and the integral equivalent to 2 protons from 1,2 repeat units is given by 2 × the integral of Peak 5 (0.12). These values can be used to calculate the % 4,1-, % 4,3- and % 1,2-units using Equations 2.4, 2.5 and 2.6 respectively.

$$\%\ 4{,}1\ \text{microstructure} = \frac{2H_{4,1}}{2H_{4,1} + \text{Integral Peak 3} + 2 \times \text{Integral Peak 5}} \times 100\ \%$$

$$\%\ 4{,}1\ \text{microstructure} = \frac{1.33}{1.33 + 2.00 + 0.12} \times 100\ \% = 38.5\%$$

Equation 2.4: Equation used to calculate the percentage of 4,1 microstructures in a sample of poly(myrcene) prepared in the presence of TMEDA.

$$\%\ 4{,}3\ \text{microstructure} = \frac{\text{Integral Peak 3}}{2H_{4,1} + \text{Integral Peak 3} + 2 \times \text{Integral Peak 5}} \times 100\ \%$$

$$\%\ 4{,}3\ \text{microstructure} = \frac{2.00}{1.33 + 2.00 + 0.12} \times 100\ \% = 58.0\ \%$$

Equation 2.5: Equation used to calculate the percentage of 4,3 microstructures in a sample of poly(myrcene) prepared in the presence of TMEDA.

$$\%\ 1{,}2\ \text{microstructure} = \frac{2 \times \text{Integral Peak 5}}{2H_{4,1} + \text{Integral Peak 3} + 2 \times \text{Integral Peak 5}} \times 100\ \%$$

$$\%\ 1{,}2\ \text{microstructure} = \frac{0.12}{1.33 + 2.00 + 0.12} \times 100\ \% = 3.5\ \%$$

Equation 2.6 Equation used to calculate the percentage of 1,2 microstructures in a sample of poly(myrcene) prepared in the presence of TMEDA.

Using Equations 2.3, 2.4, 2.5 and 2.6, the microstructure percentages of PM2 could be calculated as being 39% (4,1), 58% (4,3) and 3% (1,2) and when compared to the microstructure composition of PM1 – 93% (4,1) and 7 % (4,3) – the stark impact of TMEDA on the microstructure can be observed. As discussed previously, this change is most likely due to the increased size of the charge species and its subsequently decreased charge density, which results in the alkyl lithium bond moving from the stronger covalent model to the weaker ionic model. This change in iconicity means that the thermodynamically favourable (4,1) propagation occurs less, as the increased steric hindrance associated with lithium-TMEDA complex, along with the greater delocalisation of anionic charge across the propagating diene, results in more anionic attack from carbon 3. This means that (4,3) propagation occurs more readily, which results in more vinyl microstructures being present in the synthesised polymer.

2.2.2 The Statistical Copolymerisation of Myrcene and Butadiene

As discussed previously, one of the main motivations for this research was the investigation into using bio-available myrcene as a potential replacement or part replacement for petroleum-derived butadiene. As such, it was important to investigate not only the anionic polymerisation of myrcene but also its copolymerisation with monomers in which it could potentially be formulated as a copolymer. For this reason, it was decided that copolymers of butadiene and myrcene would be prepared in both the absence and presence of TMEDA to investigate how the copolymerisation kinetics are affected by the addition of 2 equivalents of TMEDA – as it could be expected that within many applications, the addition of a polar modifier may be used and therefore its effect must be understood.

In order to obtain an understanding of the initial copolymerisation kinetics, it was decided that a myrcene-butadiene copolymer with a target molar composition of approximately 50% of each monomer (actual ratio of 57% butadiene and 43% myrcene) would be synthesised with sampling in order to determine the molar composition of each sample and subsequently gain a qualitative understanding into how myrcene and butadiene copolymerise. Once again, samples were collected at the reported time intervals, worked up using standard conditions (see Experimental Section 2.4.5) and then analysed by SEC and ^{1}H NMR spectroscopy in order to determine the molar composition of each sample. The assigned ^{1}H NMR spectrum of the final copolymer that was collected can be seen in Figure 2.14.

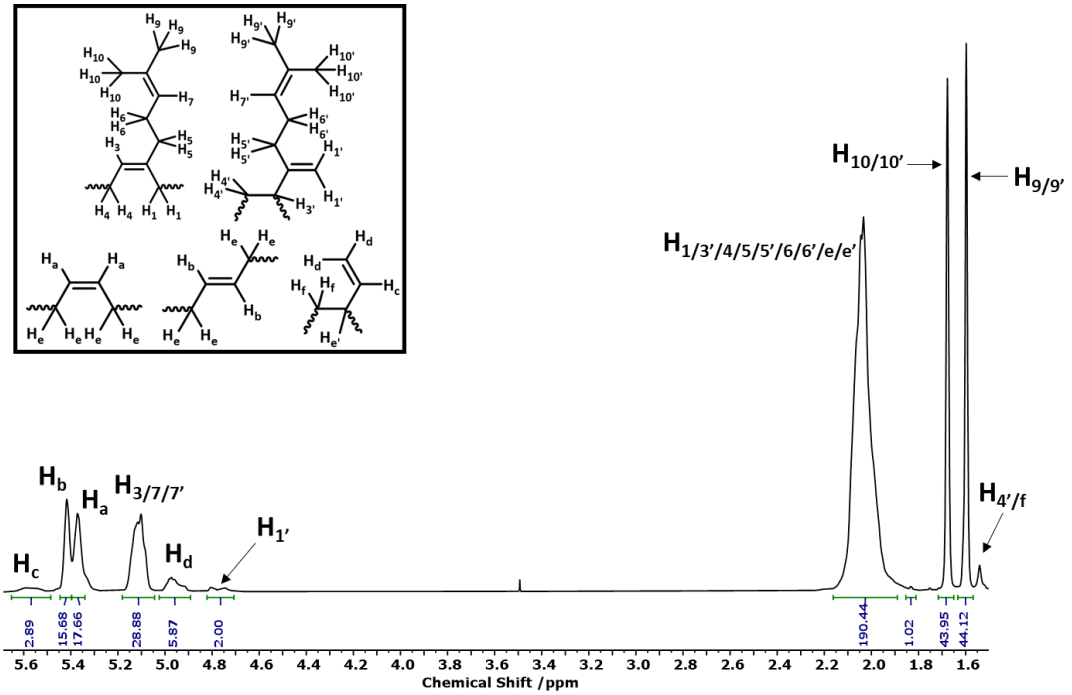

Figure 2.14: ^{1}H NMR spectrum (400 MHz, $CDCl_3$) of PMB1, with associated proton assignment.

In order to determine the molar composition of myrcene-butadiene copolymers, a new set of equations was once again required whereby the additional peaks present for butadiene also required assignment and analysis in order to determine the microstructure content of each of the two dienes present in the sample.

The molar composition and microstructure of PMB1 can be calculated using the integrals of peaks 3, 5, 6, 7 and 8 (see Figure 2.15) as follows:

- Peak 3 (4.70-4.83 ppm), which corresponds to 2 protons from myrcene 4,3 repeat units ($H_{1'}$)
- Peak 5 (5.05-5.18 ppm), which corresponds to 2 protons from myrcene 4,1 repeat units (H_3 and H_7) and 1 proton from 4,3 repeat units (again H_7 – which is common to all microstructures)
- Peak 6 (5.33-5.39 ppm), which corresponds to 2 protons from butadiene 1,4-cis repeat units (H_a)
- Peak 7 (5.39-5.45 ppm), which corresponds to 2 protons from butadiene 1,4-trans repeat units (H_b)
- Peak 8 (5.58-5.65 ppm), which corresponds to 1 proton from butadiene 1,2 repeat units (H_c)

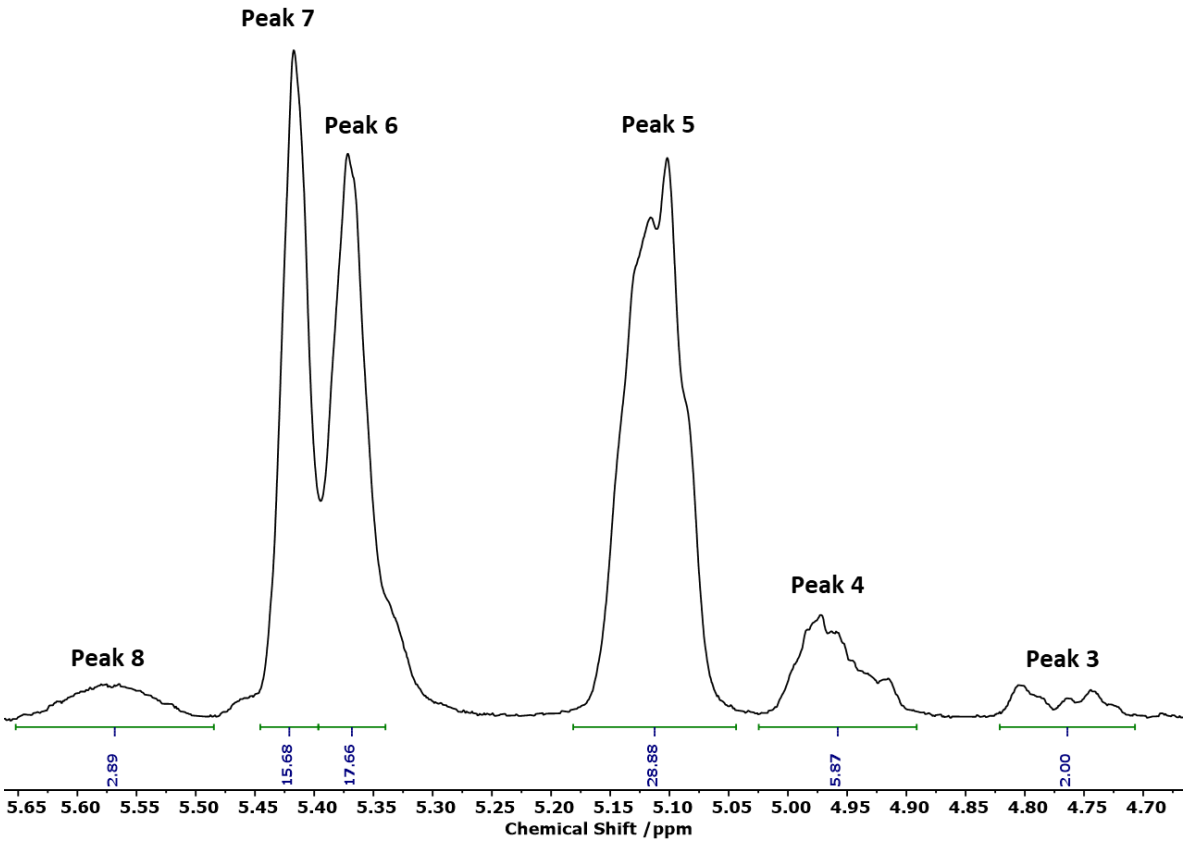

Figure 2.15: Expanded ^{1}H NMR spectrum (400 MHz, $CDCl_3$) of PMB1, showing the alkene region of the spectrum (4.70 – 5.70 ppm) and the associated peak numbering assignment.

Thus, the integral equivalent to 2 protons from myrcene repeat units is given by Equation 2.7 below.

$$2H_{Myr} = \text{Integral Peak 5} - \frac{\text{Integral Peak 3}}{2} + \text{Integral Peak 3}$$

$$2H_{Myr} = 28.88 - \frac{2.00}{2} + \mathbf{2.00} = 29.88$$

Equation 2.7: Equation used to calculate 2 equivalent protons of myrcene in a sample of poly(myrcene-*co*-butadiene).

And the integral equivalent to 2 protons from butadiene repeat units is given by Equation 2.8 below.

$$2H_{But} = \text{Integral Peak 6} + \text{Integral Peak 7} + 2 \text{ x Integral Peak 8}$$

$$2H_{But} = 17.66 + 15.68 + 2 \times 2.89 = 39.12$$

Equation 2.8: Equation used to calculate 2 equivalent protons of butadiene in a sample of poly(myrcene-*co*-butadiene).

Using the 2 equivalent protons of myrcene and butadiene calculated using Equations 2.7 and 2.8 respectively, the molar composition of myrcene and butadiene within PMB2 can be calculated using Equation 2.9 below.

$$\text{Myrcene Molar \%} = \frac{2\text{H}_{\text{Myr}}}{2\text{H}_{\text{Myr}} + 2\text{H}_{\text{But}}} \times 100\%$$

$$\text{Myrcene Molar \%} = \frac{29.88}{29.88 + 39.12} \times 100\ \% = 43.3\%$$

$$\text{Butadiene Molar \%} = \frac{39.12}{29.88 + 39.12} \times 100\% = 57.7\%$$

Equation 2.9: Equation used to calculate molar composition of poly(myrcene-*co*-butadiene).

While the microstructure of the myrcene within butadiene-myrcene copolymers can be calculated using a slightly modified version of Equation 2.1 (whereby the appropriate peak integral is utilised), the calculations used to calculate the microstructure composition of butadiene were required and are detailed in Equations 2.10, 2.11 and 2.12 below.

$$\%\ 1{,}2\ \text{microstructure} = \frac{2 \times \text{Integral Peak 8}}{2\text{H}_{\text{But}}} \times 100\%$$

$$\%\ 1{,}2\ \text{microstructure} = \frac{2\ \text{x}\ 2.89}{39.12} \times 100\% = 14.7\%$$

Equation 2.10: Equation used to calculate the percentage of butadiene (1,2) microstructures in a copolymer of myrcene and butadiene.

$$\%\ 1{,}4\text{-trans microstructure} = \frac{\text{Integral Peak 7}}{2\text{H}_{\text{But}}} \times 100\%$$

$$\%\ 1{,}4\text{-trans microstructure} = \frac{15.68}{39.12} \times 100\ \% = 40.1\%$$

Equation 2.11: Equation used to calculate the percentage of butadiene (1,4-trans) microstructures in a copolymer of myrcene and butadiene.

$$\%\ 1{,}4\text{-cis microstructure} = \frac{\text{Integral Peak 6}}{2\text{H}_{\text{But}}} \times 100\%$$

$$\%\ 1{,}4\text{-cis microstructure} = \frac{17.66}{39.12} \times 100\% = 45.2\%$$

Equation 2.12: Equation used to calculate the percentage of butadiene (1,4-cis) microstructures in a copolymer of myrcene and butadiene.

In order to determine a conversion for each sample, SEC analysis was chosen whereby the conversion would be based upon the M_n of each sample relative to the final M_n, which was assumed to correlate to 100% conversion. Due to the potential for the monomers to be incorporated into the copolymer in a block-like or gradient-like fashion, it was decided that the molar composition of each sample would be analysed first by ^{1}H NMR spectroscopy before this molar composition was used in conjugation with the dn/dc values for each of the individual homopolymers (polybutadiene and polymyrcene) to determine a weighted dn/dc value for each individual copolymer. These individual weighted dn/dc values were then used to analyse each respective sample by SEC in order to try to obtain molecular weight information that is most representative of each sample. The overlaid SEC curves of each sample collected during the copolymerisation can be seen in Figure 2.16 below.

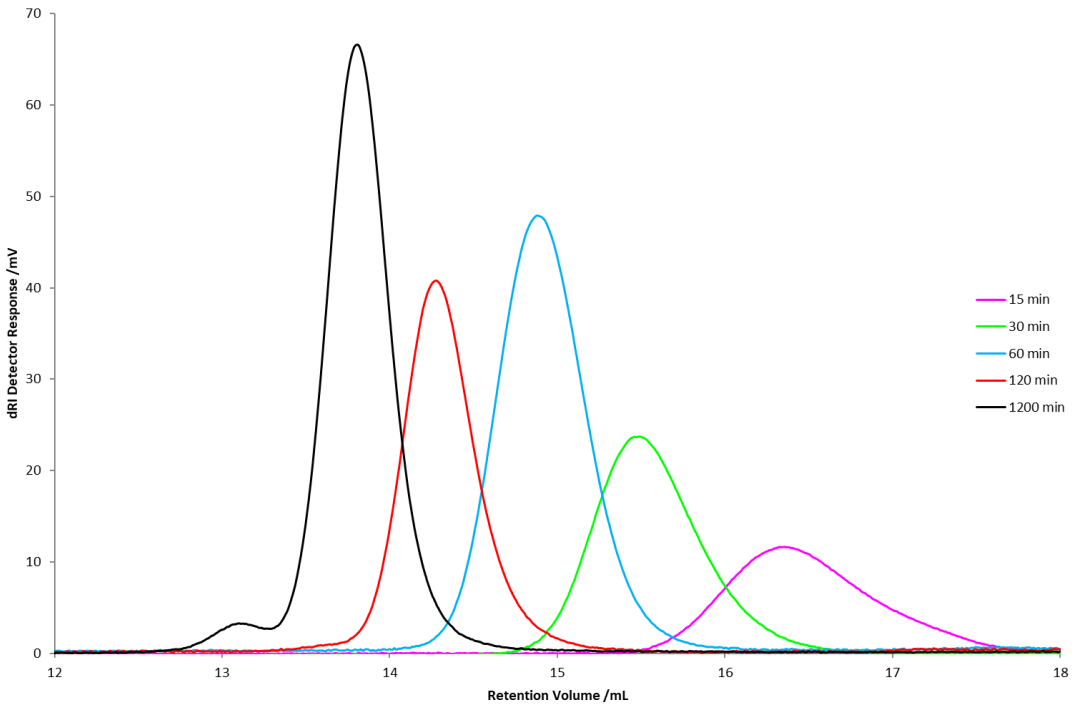

Figure 2.16: SEC curves of the 3 samples collected during the polymerisation of PMB1 (THF, 1 ml/min) whereby the sample collected at 1200 min (20 hours) was the trace of the final polymer – PMB1.

From the analysis of the ^{1}H NMR spectra data collected for each of the intermediate samples of PMB1, using Equations 2.1 and Equations 2.7-2.12, and the associated data from the SEC curves, the M_n, Đ, polymer composition and the microstructure compositions for each sample of PMB1 were determined and are reported in Table 2.2 below.

Table 2.2: Instantaneous copolymer composition, microstructure and molar mass for the statistical copolymerisation of PMB1 as a function of time.

Time /min	M_n /g mol^{-1}	Đ	Copolymer Composition /mol %		Butadiene Microstructure /%			Myrcene Microstructure /%	
			Butadiene	Myrcene	(1,2)	(1,4) Cis	(1,4) Trans	(4,1)	(4,3)
15	3000	1.08	51	49	14	47	39	94	6
30	6600	1.09	53	47	15	45	40	94	6
60	12200	1.05	53	47	15	45	40	94	6
120	22700	1.04	53	47	13	47	40	94	6
1200	36100	1.03	57	43	15	45	40	93	7

The final M_n of PMB1 was determined to be 36,100 g mol^{-1}, which was in good agreement with the target M_n of 30 kg mol^{-1}. Based on the assumption that the copolymerisation went to completion, it can be seen from the data presented in Table 2.2 that after 15 minutes, 8% of the copolymerisation had occurred in PMB1, leading to a copolymer with a molar composition of 51% butadiene and 49% myrcene. From the polymer composition percentages shown in Table 2.2, it can be seen that as the copolymerisation of myrcene and butadiene progresses, there is actually a slight shift in the composition as a function of conversion from 51 molar % butadiene at 15 min to 57 molar % at 1200 min, with a higher percentage of myrcene in the earlier samples. This suggests that there is a slight preference for the incorporation of myrcene over butadiene during the copolymerisation, resulting in a slightly gradient shifted copolymer. This observation was quite unexpected as based on the literature regarding butadiene and isoprene, it would be expected that butadiene would be incorporated preferentially (r_{But} = 3.6, r_{iso} = 0.5 in benzene at 40 ^{o}C). [41] This is even more surprising when one of the arguments to suggest why this occurs is due to the crossover propagation rate constants of butadiene and isoprene, which is believed to limit the rate of incorporation of isoprene, despite isoprene generally having a quicker rate of homopolymerisation than butadiene. The reduced steric hinderance associated with butadiene along with the greater degrees of symmetry compared to isoprene have been attributed to the reasoning behind this reduced rate of Butadiene → Isoprene and enhanced rate of Isoprene → Butadiene crossover kinetics. The electronic nature of the diene in both isoprene and myrcene is extremely similar whereby they both have a monosubstituted diene

with an alkyl substituent occurring on carbon 2 and, as such, it was initially believed that while the slight increase in nucleophilicity of myrcene – due to the increased length of alkyl substitution – might result in a slightly reduced gradient distribution, it would still be expected that, due to the cross-over propagation rate constants, butadiene would be incorporated preferentially. As shown above, this was not the case, however, when the copolymerisation of myrcene and isoprene was conducted in collaboration with Holger Frey *et al.,* [12] the rate of myrcene incorporation was greater than that of isoprene with reactivity ratios (r_{Myr} = 4.4, r_{iso} = 0.23 in cyclohexane at RT), which showed even greater disparity compared to those reported for butadiene and isoprene. This suggests that either the slight increase in nucleophilicity of the myrcene carbanion – leading to enhanced rates of homopolymerisation – is enough to counteract the slow cross-over rate constants to myrcene from butadiene, or that the alkene present in the myrcene that is not involved in the polymerisation plays a role in increasing the local concentration of myrcene around the lithium cation through partial coordination – a concept that will be explored further in Section 4.2.3 in which further evidence of this potential phenomenon was found.

2.2.2.1 The Effect of Polar Additives on the Copolymerisation of Myrcene and Butadiene

As mentioned previously, the use of polar modifiers in industry is vital to allow polymers to be synthesised with very specific compositions and microstructures in order to match the required physical, chemical and thermal properties of the intended use with the greatest efficiency. As a result, it was decided that a copolymer of myrcene and butadiene be prepared in the presence of two molar equivalents of TMEDA with respect to the *sec*-BuLi in order to investigate how the incorporation of myrcene into the copolymer was affected by the addition of polar modifiers. As before, samples were taken at predetermined time intervals (15, 60 and 1200 min), worked up under standard conditions and dried before being analysed by SEC (THF, 1 mL min^{-1}) and ^{1}H NMR spectroscopy. The assigned ^{1}H NMR spectrum of the final copolymer – PMB2 – can be seen in Figure 2.17.

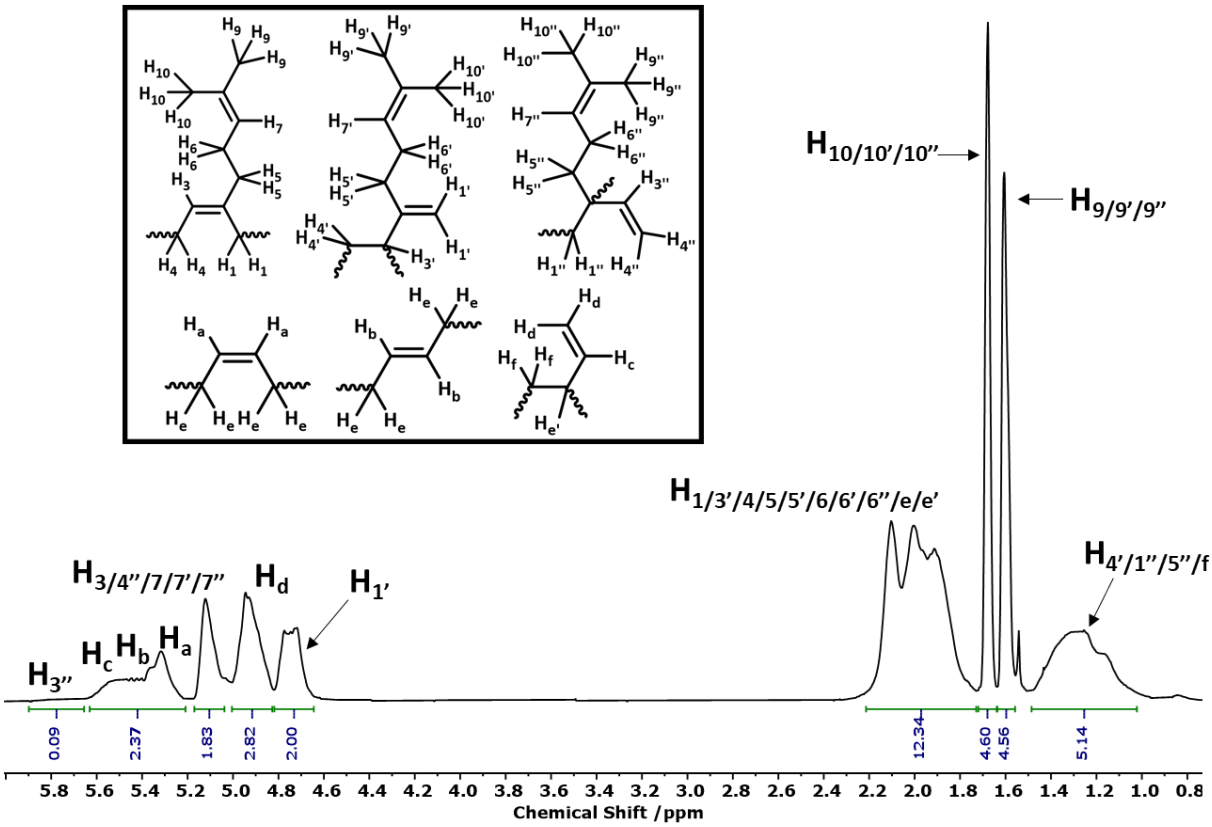

Figure 2.17: ^{1}H NMR spectrum (400 MHz, $CDCl_3$) of PMB2, with associated proton assignment.

The microstructure composition of both the butadiene and myrcene has been vastly impacted by the addition of TMEDA, leading to significant peak broadening in the ^{1}H NMR spectrum due to the increased number and prevalence of different diad and triad pairs/trios of subunits that can occur along the polymer chain. As such, analysis of the polymer becomes much more difficult, as defined peaks are no longer present for the microstructures of butadiene. This means that to calculate $2H_{Myr}$ and $2H_{But}$, different equations must be proposed in order to work out the composition of each of the individual samples. In this case, where separate peaks for the different microstructures of butadiene are indistinguishable, we have defined different regions/peaks compared to the regions/peaks of PMB1 as follows:

- Peak 3 (4.65-4.82 ppm), which corresponds to 2 protons from myrcene 4,3 repeat units ($H_{1'}$)
- Peak 4 (4.83-5.00 ppm), which corresponds to 2 protons from butadiene 1,2 repeat units (H_d)

- Peak 5 (5.05-5.18 ppm), which corresponds to 2 protons from 4,1 repeat units (H_3 and H_7), 1 proton from 4,3 repeat units (again H_7 – which is common to all microstructures) and 3 protons from the 1,2 repeat units (2 x $H_{4''}$ + $H_{7''}$)
- Peak 6 (5.33-5.39 ppm), which corresponds to 2 protons from butadiene 1,4-Cis repeat units (H_a), 2 protons from butadiene 1,4-trans repeat units (H_b) and 1 proton form the 1,2 butadiene repeat units (H_c)
- Peak 7 (5.58-5.65 ppm), which corresponds to 1 proton from myrcene 1,2 repeat units ($H_{3''}$)

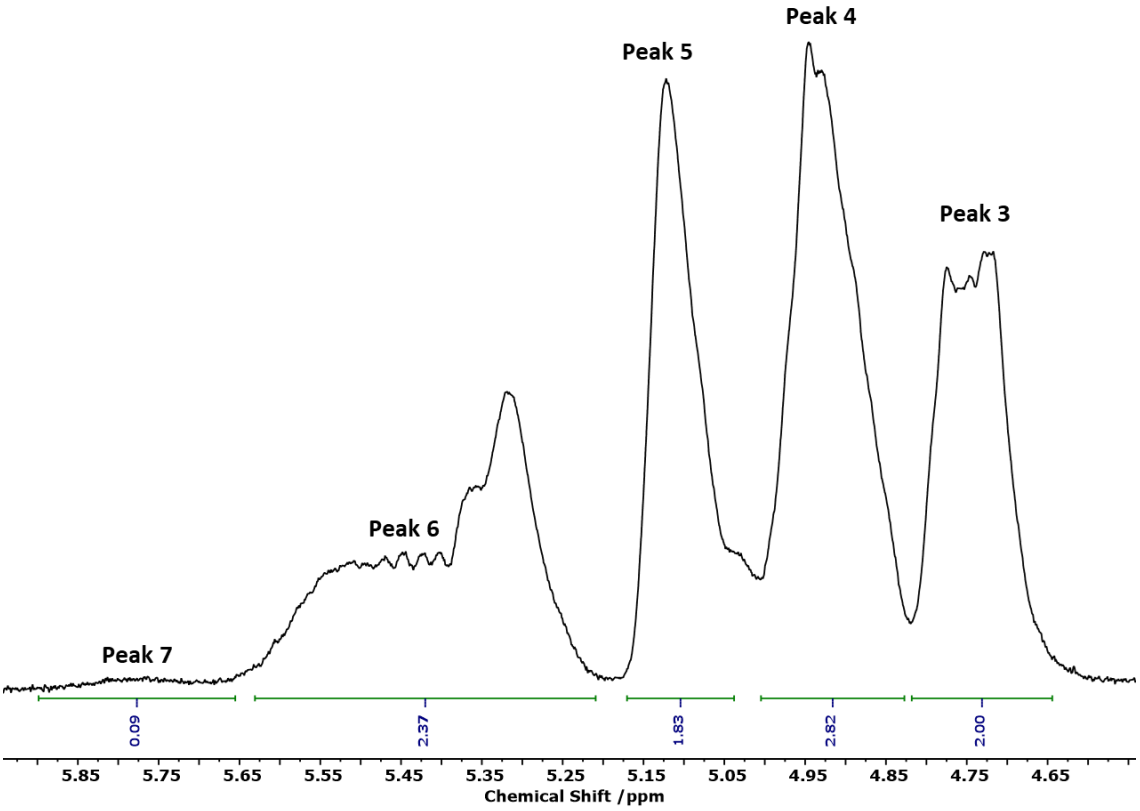

Figure 2.18: Expanded ^{1}H NMR spectrum (400 MHz, $CDCl_3$) of PMB2, showing the alkene region of the spectrum (4.60 – 5.90 ppm) and the associated peak numbering assignment.

Having assigned these regions within the ^{1}H NMR spectrum**,** the integral equivalent to 2 protons from myrcene repeat units ($2H_{Myr}$) and the integral equivalent to 2 protons from butadiene repeat units ($2H_{But}$) are given by Equations 2.13 and 2.14 below.

$$2\mathrm{H}_{\mathrm{Myr}} = \frac{\text{Integral Peak 3}}{2} + \text{Integral Peak 5 - Integral Peak 7}$$

$$2\mathrm{H}_{\mathrm{Myr}} = \frac{2.00}{2} + \mathbf{1.83} - \mathbf{0.09} = \mathbf{2.74}$$

Equation 2.13: Equation used to calculate 2 equivalent protons of myrcene in a sample of poly(myrcene-*co*-butadiene) prepared in the presence of a polar modifier.

$$2\mathrm{H}_{\mathrm{But}} = \text{Integral Peak 6} + \frac{\text{Integral Peak 4}}{2}$$

$$2\mathrm{H}_{\mathrm{But}} = 2.37 + \frac{2.82}{2} = 3.78$$

Equation 2.14: Equation used to calculate 2 equivalent protons of butadiene in a sample of poly(myrcene-*co*-butadiene) prepared in the presence of a polar modifier.

These values for $2\mathrm{H}_{\mathrm{Myr}}$ and $2\mathrm{H}_{\mathrm{But}}$ can then be used with Equation 2.9 in order to calculate the molecular composition of the given sample. The results for the ^{1}H NMR spectroscopic molecular composition analysis for each sample collected during the copolymerisation and the associated molecular weights calculated by SEC (THF, 1 mL/min) can be seen in Table 2.3.

Table 2.3: Instantaneous copolymer composition and molar mass for the statistical copolymerisation, in the presence of TMEDA, of PMB2 as a function of time.

Time /min	M_n /g mol^{-1}	Conversion /%	Copolymer Composition /mol %	
			Butadiene	Myrcene
15	25600	64	73	27
60	34300	86	63	37
1200	39800	100	58	42

The first thing that can be noticed in Table 2.3 is that the presence of TMEDA within the copolymerisation appears to significantly enhance the rate of polymerisation – as expected due to the breaking up of lithium aggregates – as evidenced by the fact that after 15 min, the conversion of PMB2 was at 64% compared to a conversion of 8% in the polymerisation of PM1 (in the absence of TMEDA) after 15 min. The second factor that can be noticed about the addition of TMEDA to the copolymerisation is that it appears that the slight preferential uptake of myrcene that was observed in the absence of TMEDA has been completely inverted,

leaving butadiene to have a strong preferential uptake and leading to a tapered “block-like” copolymer. This result was less surprising than for the case of PMB1, as it has been shown for isoprene that the addition of TMEDA supresses the rate of homopolymerisation, [42] whereby an enhanced rate of homopolymerisation for butadiene is observed in the presence of TMEDA. [43] It has also been shown that as a result, it is almost impossible to synthesise random chains of poly(isoprene-co-butadiene) – whereby gradient block-like copolymers with an isoprene rich block at the chain end are almost always achieved [44] – and, as such, it could be expected that the presence of TMEDA in the copolymerisation of myrcene and butadiene would result in a tapered block-like copolymer with a myrcene rich block at the chain end. What is surprising, however, is the degree to which the rate of myrcene incorporation has been reduced, as the gradient observed under these conditions is greater than the perceived gradient of butadiene-isoprene copolymers synthesised under the same conditions. One potential hypothesis for this is that the added steric hindrance of the myrcene alkyl substituent, relative to the alkyl substituent of isoprene, supresses the rate of homopolymerisation of myrcene to a greater extent than that of the rate isoprene. This results in much greater disparity between the rates of incorporation of myrcene and butadiene compared to the analogous isoprene-butadiene copolymerisation.

2.2.3 The Statistical Copolymerisation of Myrcene and Styrene

Industrially, dienes – such as butadiene and isoprene – are found in many different copolymer compositions. However, in the field of LAP, two of the most important copolymer classes are random SBR (Styrene-Butadiene Rubber) and SBS/SIS (Styrene-Butadiene/Isoprene-Styrene) – both of which are diene-styrenic based copolymers. As mentioned previously, SBR finds use in applications such as chewing gum, shoe soles and within the tread of car tyres, [1] while SBS and SIS are two of the most commonly used examples of thermoplastic elastomers, used in applications such as tool grips, adhesives and asphalt modifications. [45] As such, a large amount of time was dedicated in order to try to determine how myrcene and styrene copolymerise in both the absence and presence of a polar modifier – TMEDA – especially due to the fact that two articles were published in peer-reviewed journals obtaining results that were significantly different to the results obtained during this study. The first article by Bingyong Han *et al.* suggested that in the presence of 0.8 equivalents of ethyl

tetrahydrofurfuryl ether (ETE) with respect to the amount of BuLi initiator used, random myrcene-styrene copolymers and random butadiene-myrcene-styrene terpolymers could be synthesised. [16] In this work, a styrene-blockiness calculation was used as part of the underpinning rationale, which will be examined and explained further in Section 2.2.3.2. While this work did not directly disagree with the results obtained during the study (as a different polar modifier was used), the rationale behind some of the arguments used required further work in this study to prove invalid. The second article by Yang Li *et al.* suggested that in the presence of 2 equivalents of TMEDA with respect to the amount of BuLi initiator used, random myrcene-styrene copolymers could be synthesised. [46] These results were in direct disagreement with the results presented in this section, despite the exact same conditions being used for the copolymerisation, and as such, three separate methods were used to try to establish whether copolymers of myrcene and styrene synthesised in the presence of two molar equivalents of TMEDA with respect to the amount of initiator used produced random copolymers or tapered block-like structures. This section has been based on and adapted upon the following peer-reviewed article that was published during the period of this research [47]:

L. Shaw and L. R. Hutchings, "Tales of the unexpected. The non-random statistical copolymerisation of myrcene and styrene in the presence of a polar modifier," *Polymer Chemistry,* vol. 11, no. 44, pp. 7020-7025, 2020.

2.2.3.1 Terminal Method for Sample Collection During Copolymerisation

To investigate the effect of TMEDA on the modification of myrcene and styrene copolymerisations, two copolymers were prepared by LAP, one without TMEDA – PMS1 – and one with 2 molar equivalents of TMEDA with respect to the *sec*-BuLi – PMS2. Each polymerisation had an initial molar monomer feed ratio of 49% myrcene and 51% styrene and were performed in benzene at room temperature, with sampling at 15, 60 and 1200 minutes. Each sample was terminated with nitrogen-sparged methanol, precipitated into methanol, and dried before being characterised by SEC and ^{1}H NMR spectroscopy (see Figures 2.19 and 2.20 below for the ^{1}H NMR spectra of the final polymer collected for each). The full experimental details of the preparation of these polymers can be found in Section 2.4.5.

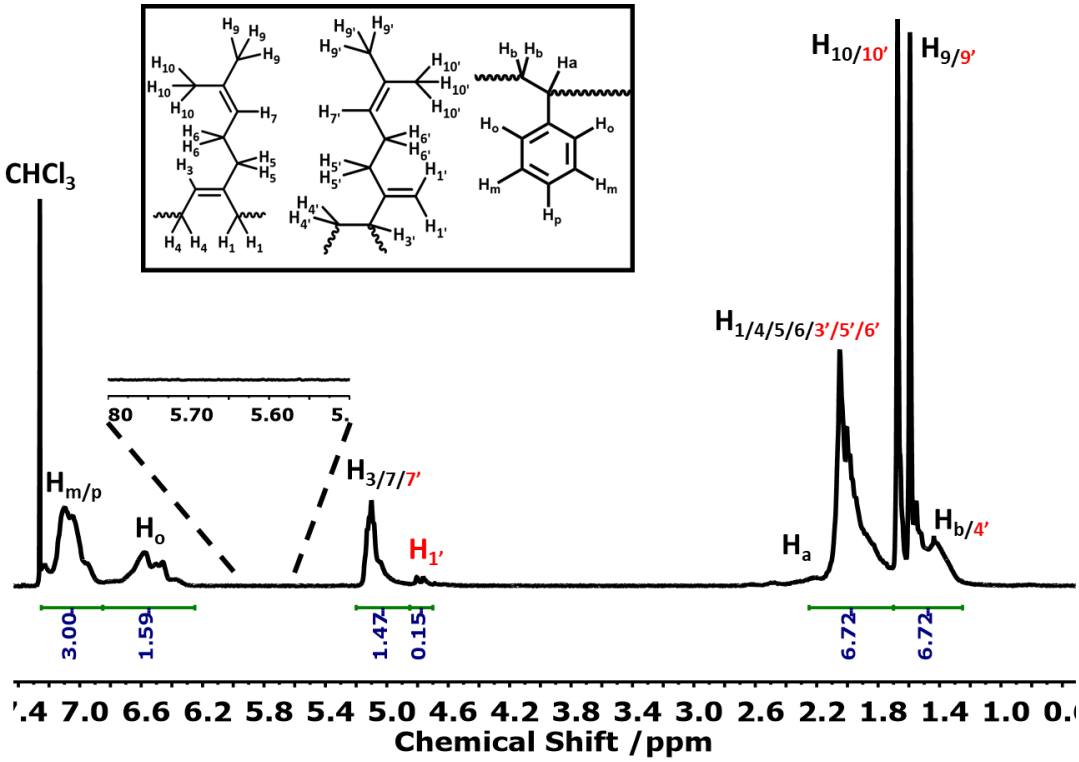

Figure 2.19: ^{1}H NMR spectrum (400 MHz, $CDCl_3$) of PMS1 with hydrogen assignment of each of the peaks.

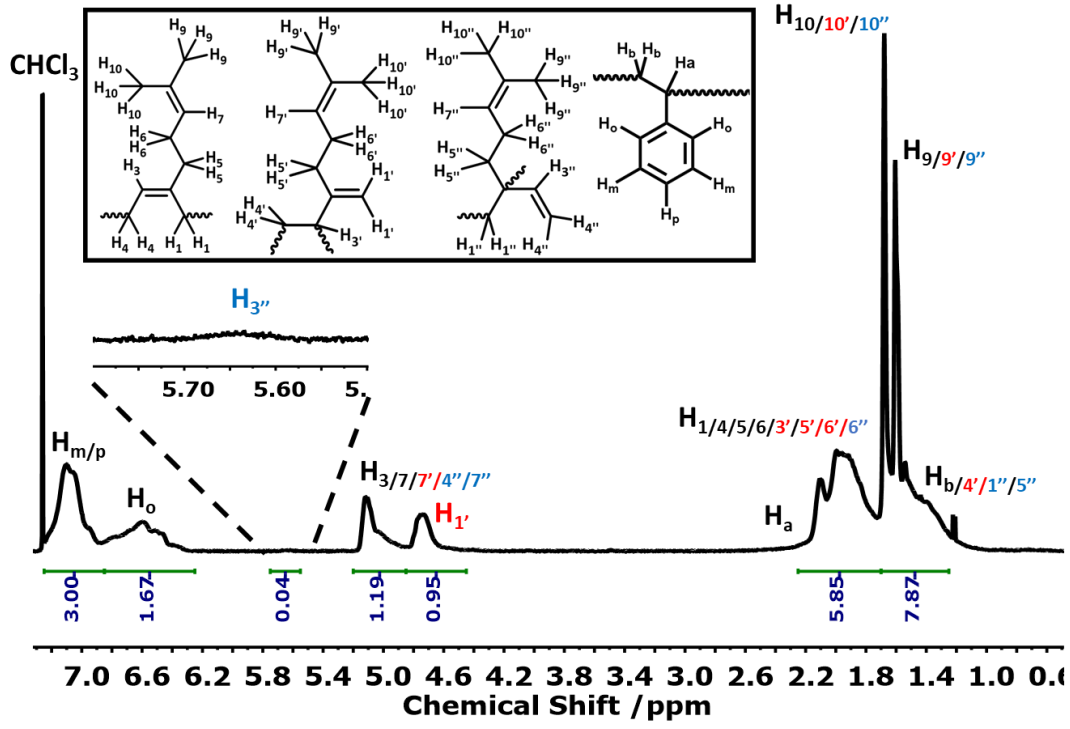

Figure 2.20: ^{1}H NMR spectrum (400 MHz, $CDCl_3$) of PMS2 with hydrogen assignment of each of the peaks.

Upon comparison of the ^{1}H NMR spectra in Figures 2.19 and 2.20 above, the once again evident change in microstructure of the myrcene is observed – along with substantial peak

broadening as expected – upon addition of two equivalents of TMEDA. Using the respective equations for the calculation of myrcene's microstructure composition in both the absence of (Equations 2.1 and 2.2) and presence of (Equations 2.3-2.6) TMEDA, the microstructure of the myrcene within PMS1 and PMS2 can be calculated respectively, the results of which can be seen in Table 2.4.

Table 2.4: Summary of the myrcene microstructure composition for PMS1 and PMS2.

Copolymer	Myrcene microstructure composition /%		
	(4,1)	**(4,3)**	**(1,2)**
PMS1	90.3	9.7	0.0
PMS2	38.1	57.1	4.8

Due to the use of a new monomer in this copolymerisation (styrene), a new equation in order to calculate the integral equivalent to 2 protons from styrene repeat units ($2H_{Sty}$) was derived and reported below.

$$2H_{Sty} = \frac{2 \times \text{Integral of Peaks between 6.25-7.25 ppm}}{5}$$

$$2H_{Sty} = \frac{2 \text{ x } 4.59}{5} = \mathbf{2.74}$$

Equation 2.15: Equation used to calculate 2 equivalent protons of styrene in a sample of poly(myrcene-*co*-styrene).

While in theory the peak at 6.25-6.85 ppm could be used to represent the integral equivalent to 2 protons from styrene repeat units ($2H_{Sty}$) as it is the peak of the two *ortho*- protons in polystyrene, it was decided that Equation 2.15 would give a more accurate representation of the integral equivalent of two protons due to the fact that this peak can shift and merge with the other styrene peak between 6.85-7.25 ppm under certain conditions that will be discussed in Section 2.2.3.2. Having calculated $2H_{Myr}$ and $2H_{Sty}$ using equations 2.13 and 2.15 respectively, a slightly modified version of Equation 2.9 (whereby $2H_{Sty}$ replaces $2H_{But}$) can be used in order to calculate the molar composition of each sample. The data for the molecular composition for each sample of the two different copolymerisations, along with the SEC molecular weight data (THF, 1 mL min^{-1}), can be seen in Table 2.5.

Table 2.5: Comparison of the composition of two myrcene-styrene copolymers, PMS1 and PMS2, as a function of polymerisation reaction time.

Time	Composition of PMS1 /mol %			Composition of PMS2 /mol %		
/min	Myrcene	Styrene	M_n /kg mol^{-1}	Myrcene	Styrene	M_n /kg mol^{-1}
0	49	51	-	49	51	-
15	91	9	12.7	8	92	11.9
60	90	10	33.3	35	65	25.8
1200	49	51	80.7	45	55	32.6

The molar composition of each sample from both of the two copolymerisations was plotted as a function of the molecular weight of each sample as a percentage of the final molecular weight – representative of conversion in LAP due to the lack of inherent termination reactions – in order to visualise the incorporation of myrcene as the copolymerisation progresses. It was hypothesised that if a random copolymer of myrcene and styrene was synthesised under the conditions that were used, as suggested by the literature **[46]**, the percentage of myrcene within the copolymer would remain constant throughout the progression of the polymerisation, as represented by the horizontal green line in Figure 2.21 below.

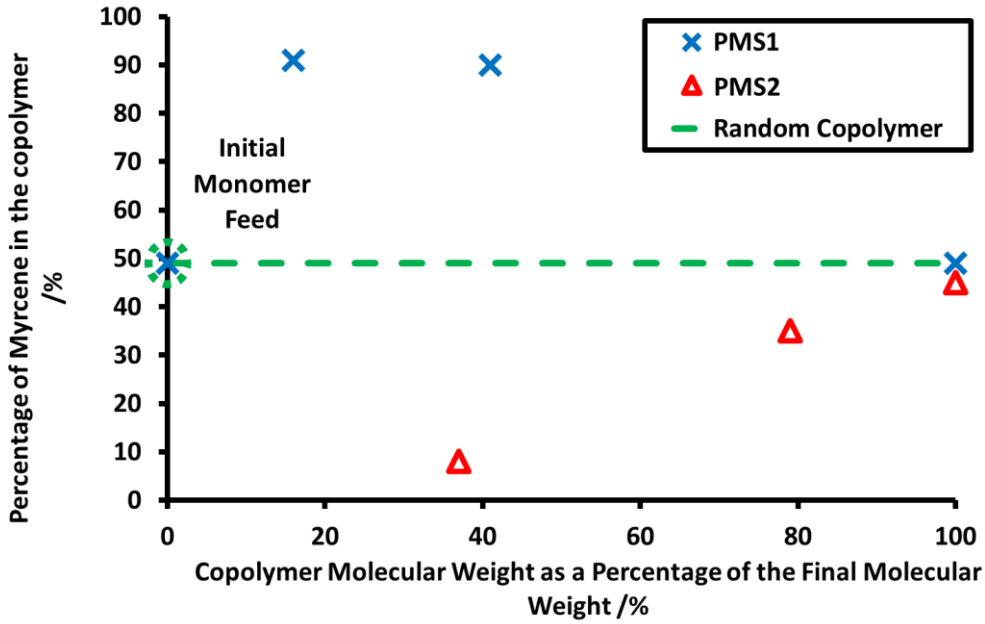

Figure 2.21 The percentage of myrcene that each sample collected during the polymerisation contained as a function of the total conversion of all the monomers, whereby the horizontal green line signifies an idealised random copolymerisation.

Both sets of polymerisations that were performed were not random copolymerisations (Table 2.5, Figure 2.21) as the percentage of myrcene did not remain consistent throughout the copolymerisation. From the data presented, it appears that the reactivity ratios that have been observed for myrcene and styrene in the absence of TMEDA in cyclohexane (r_{myr} = 36 and r_s = 0.028 [12]) were almost completely inverted for the polymerisation of myrcene and styrene in the presence of TMEDA. This observation suggests that rather than a random copolymer being synthesised, a tapered block-like copolymer is synthesised where the styrene is incorporated preferentially to form a styrene-rich block followed by a tapered region and a myrcene-rich block.

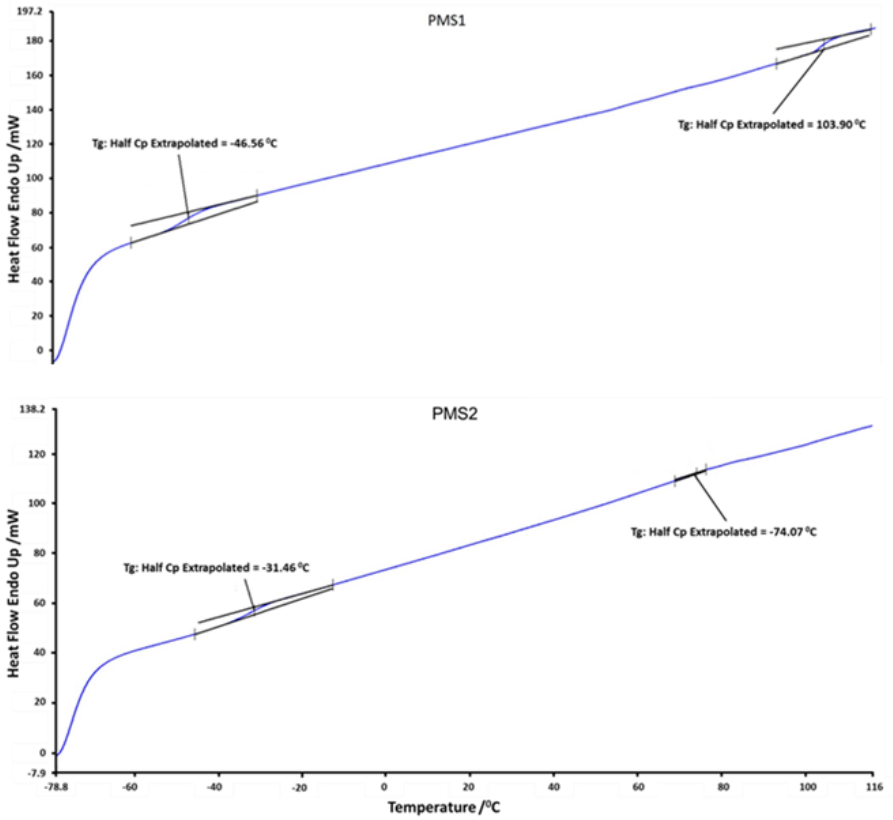

Figure 2.22 DSC analysis of PMS1 (Top) and PMS2 (Bottom) with the extrapolated T_g values that were calculated provided for each transition, whereby trace shown had a heating rate of 100 °C/min.

The block-like nature of PMS1 and PMS2 was further supported through the characterisation of these polymers by DSC analysis (See Figure 2.22). Both statistical copolymers showed two individual T_g values related to a myrcene-rich block and a styrene-rich block whereby PMS1 had T_g values of -46.6 °C and 103.9 °C, and PMS2 had T_g values of -31.5 °C and 74.1 °C. The fact that both of these polymers show two distinct T_g values signifies that there is enough of

a gradient in the incorporation of the two monomers, whereby the polymers are acting as block copolymers to give two regions with very different thermal properties.

Whilst these observations represent fairly strong evidence to suggest that the recently published literature [16] [46] may not be correct, to convince the reader, further evidence will be presented below.

2.2.3.2 ^{1}H NMR Spectroscopic "Blockiness" Calculation

As briefly mentioned, ^{1}H NMR data can also be used to determine the "blockiness" of styrene in styrene-diene copolymers. [48] This approach attempts to determine the proportion of styrene units that appear next to another styrene unit but is generally only valid when 3 or 4 or more styrene units are adjacent in a block. This approach uses ^{1}H NMR signals from the styrenic aromatic protons and specifically the chemical shift of the ortho protons, which is highly sensitive to the nature of adjacent monomer units. Thus, when a styrene unit is found in a block of three or more styrene molecules, the ortho signal is found at 6.25 - 6.85 ppm (defined herein as Peak [B]) and the para/meta signals are found at 6.85 - 7.25 ppm (defined herein as Peak [A]). See Figures 2.23 and 2.24 which show the ^{1}H NMR spectra of a polystyrene and poly(myrcene-*block*-styrene) – which was synthesised by sequential addition and polymerisation of styrene after the initial myrcene had been fully polymerised.

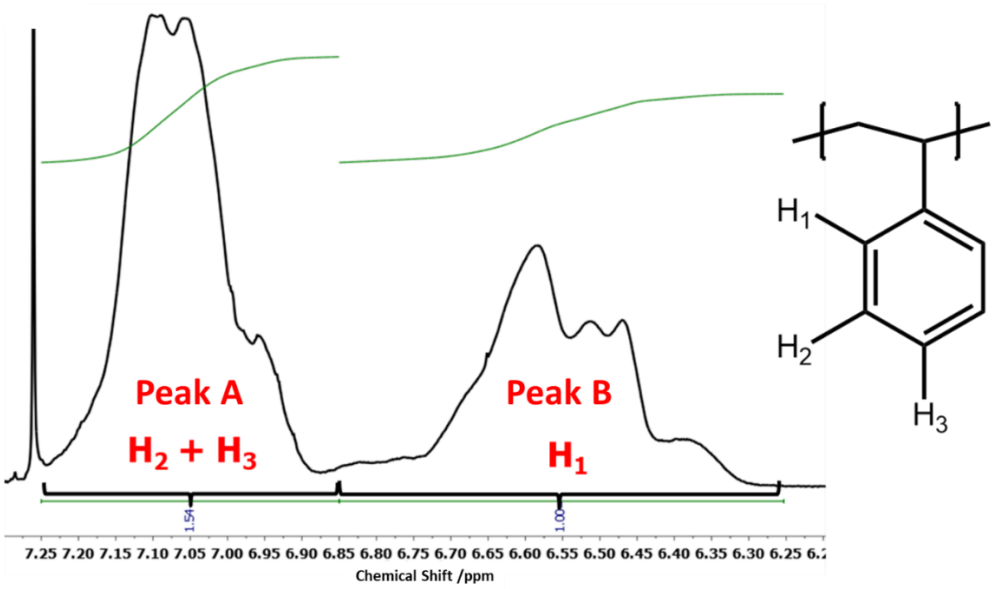

Figure 2.23: ^{1}H NMR spectrum (400 MHz, $CDCl_3$) of polystyrene homopolymer indicating chemical shifts of *ortho*- (H_1), *meta*- (H_2) and *para*- (H_3) protons of polystyrene.

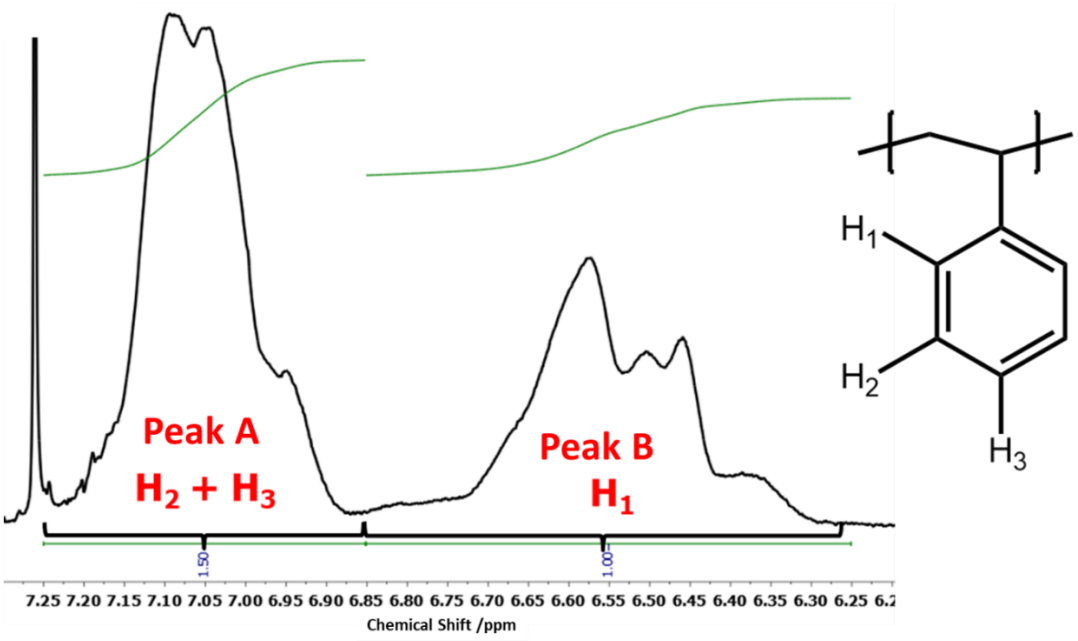

Figure 2.24: ^{1}H NMR spectrum (400 MHz, $CDCl_3$) of poly(myrcene-*block*-styrene) indicating chemical shifts of *ortho*- (H_1), *meta*- (H_2) and *para*- (H_3) protons of polystyrene block.

However, when a styrene unit is not found in a block of three styrene molecules, as would be expected for a random styrene-diene copolymer, the ortho proton signal is shifted down-field so that the peak is found in the same region as the meta and para signals (see Figure 2.25) – note that in Figure 2.25, chemical shift is measured in τ rather than ppm and thus the ortho proton signal appears at 3.5 τ and the meta/para signals at 3.0 τ.

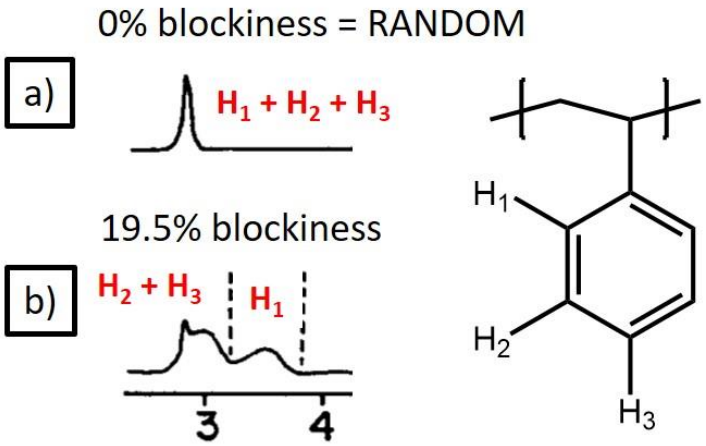

Figure 2.25: ^{1}H-NMR spectra of butadiene-styrene copolymers with varying composition and degree of blockiness a) 17 % styrene, 0 % blockiness (i.e. random); b) 28 % styrene, 19.5 % blockiness. Figure adapted from ref [48]**.**

Based on this observation, an equation to calculate the "randomness/blockiness" of styrene has been devised, [49] (Equation 2.16) but what this calculation actually defines is the proportion of styrene units that are found in a block of three or more styrene units.

$$\text{"Randomness" percentage} = \frac{[A]-1.5[B]}{[A]+[B]} \times 100\ \%$$

$$\text{"Blockiness" percentage} = 100 - \text{"Randomness" Percentage}$$

Equation 2.16: Equation used to calculate the proportion of styrene units that are found in a block of three or more styrene units – "Blockiness".

To demonstrate that the myrcene-styrene copolymers PMS1 and PMS2 are both block-like, the percentage "blockiness" of each was calculated using ^{1}H NMR data from the spectra in Figures 2.26 and 2.27 below.

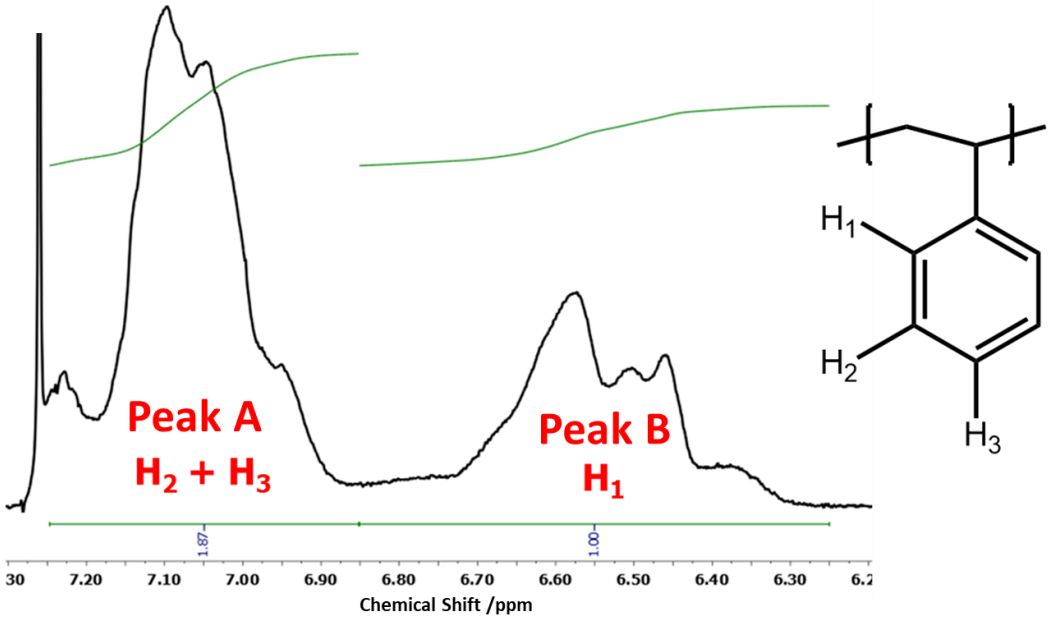

Figure 2.26: ^{1}H NMR spectrum (400 MHz, $CDCl_3$) of PMS1 (poly(myrcene-*stat*-styrene) - no TMEDA) indicating chemical shifts of ortho (H_1), meta (H_2) and para (H_3) protons of styrene repeat units.

PMS1 has a molar ratio of 54 % styrene and 46 % myrcene with a M_n of 80,700 g mol^{-1}.

Ratio of Peak [A] to Peak [B] = 1.87 : 1 therefore degree of randomness = (0.37/2.87)*100 = 12.89 %. Thus c. 87% of the styrene units are found in a block of 3 or more styrene units.

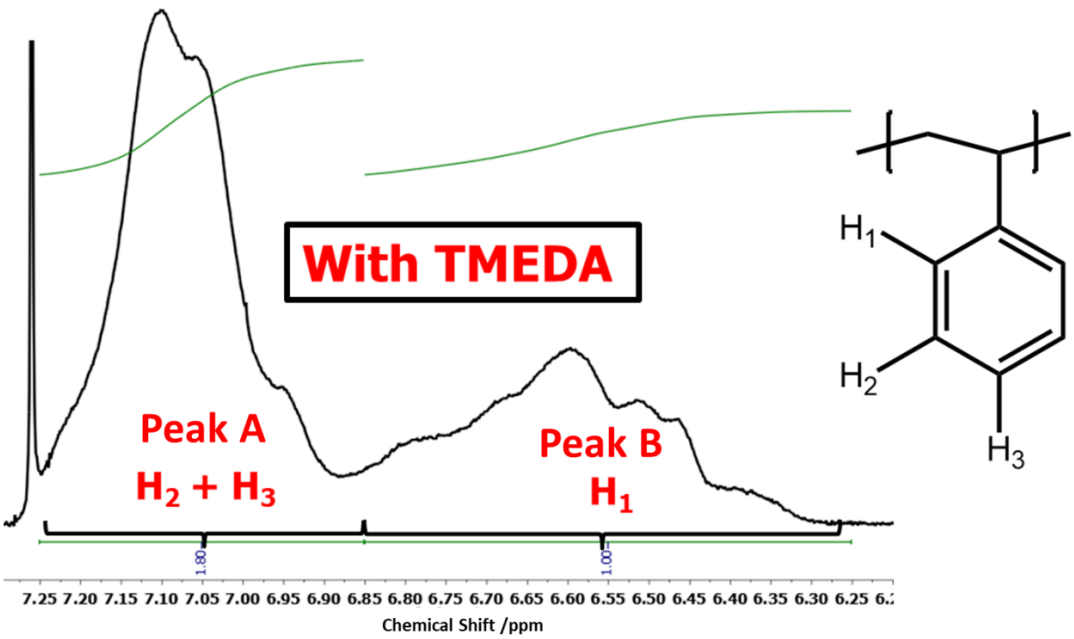

Figure 2.27: ^{1}H NMR spectrum (400 MHz, $CDCl_3$) of PMS2 (poly(myrcene-*stat*-styrene) – with TMEDA) indicating chemical shifts of *ortho*- (H_1), *meta*- (H_2) and *para*- (H_3) protons of styrene repeat units.

PMS2 has a molar ratio of 53 % styrene and 47 % myrcene with M_n of 32,600 g mol^{-1}.
Ratio of Peak [A] to Peak [B] = 1.8 : 1 therefore degree of randomness = (0.3/2.8)*100 = 10.71 %. Thus 89 % of the styrene units are found in a block of 3 or more styrene units.

As it can be determined via the ^{1}H NMR spectra and associated calculations, both of these copolymers would be defined as being block-like, even though there appears to be a slight up-field shift of the ortho peak. This, along with the previously calculated reactivity ratios for myrcene-styrene copolymerisations in cyclohexane of r_{myr} = 36 and r_s = 0.028, [12] which was defined as a tapered block copolymer, suggests that the PMS2 copolymer is also a tapered block-like copolymer.
However, whilst this equation has been used to show that these copolymers are not random, its definition and improper use in the literature has led to a large amount of confusion about what can actually be defined by carrying out this calculation. This confusion may have led to incorrect conclusions within the recently published literature on random myrcene-styrene copolymers. [16] [46] In both of these publications, only the “blockiness” equation had been used to conclude the copolymer was random, but in the ^{1}H NMR spectra that were presented, there still appears to be a peak between 6.25 ppm to 6.85 ppm, which suggests that the copolymer is not random. However, according to these two publications, the signal

corresponding to *ortho*- protons disappeared when the proportion of myrcene to styrene was increased. From this observation, these publications, [46] [16] and countless others using the same technique conclude that the disappearance of the signal corresponding to *ortho*-protons implies that the polymer is therefore random. However, the observations made during terminal sample collection experiments suggest that the copolymer is not random. Based on the other authors' ^{1}H NMR spectroscopic data, it is clear that the number of large styrene blocks has decreased, yet this does not indicate a copolymer's randomness. Instead, it is proposed that the copolymer sample that each of these groups has in fact synthesised will still have a gradient of inclusion of styrene, based on the observations that have been presented, whereby more styrene is incorporated initially. However, due to the proportion of myrcene present, the likelihood of styrene blocks being synthesised is relatively small.

These findings suggest that this calculation cannot be used independently of calculating reactivity ratios or sampling to determine whether a copolymer is random – especially when uneven molar feed ratios are used i.e. whenever the feed ratio of each monomer is not 0.5. These findings would also suggest that if the other groups carried out sampling analysis during their copolymerisations, the overall percentage of styrene in their copolymer samples would decrease as the polymerisation progressed.

2.2.3.3 Real-Time In-Situ ^{1}H NMR Spectroscopy Polymerisation

Due to the existence of the two previously published articles on the randomisation of myrcene-styrene copolymers, a third method, whereby accurate reactivity ratios for the copolymerisation of styrene and myrcene in the presence of TMEDA could be determined, was devised and used to ensure that results that have already been presented in this thesis were completely accurate and that the myrcene and styrene were not in fact randomised.

To do this, the use of *in-situ* ^{1}H NMR spectroscopic monitoring of LAP was employed. This *in-situ* ^{1}H NMR spectroscopic technique to monitor LAP, which was developed by Professor Holger Frey, Dr. Frederik R. Wurm and Professor Axel Müller, had been previously used within the Hutchings group in collaboration with Eduard Grune, whereby the reactivity ratios for the copolymerisation of myrcene and styrene/4-methylstyrene were calculated. [12] Using this technique, the copolymerisation of the two monomers can be mapped by looking at the depletion of the ^{1}H NMR signals corresponding to each monomer.

2.2.3.3.1 Experimental Method Design

Initially it was decided to devise a system in which an NMR spectroscopy tube could be used as a polymerisation vessel, with reaction mixtures prepared using a Schlenk line to avoid the requirement for glovebox manipulation. This approach requires a method to allow the NMR spectroscopy tube to first be evacuated under ultra-high vacuum (UHV) for 24 h, before being flushed with purified argon for 2 h. An ideal system would subsequently allow for the dry mixture of monomer and deuterated solvent to be added under an argon atmosphere without exposure to external elements. The prepared NMR spectroscopy tube could then be taken to the NMR spectrometer, and the reaction initiated before the progress of the polymerisation be followed *in situ* by monitoring the depletion of the monomeric signals by ^{1}H NMR spectroscopy so that the reactivity ratios could be determined. The schematic design of the system developed and the actual system are shown in Figure 2.28 below.

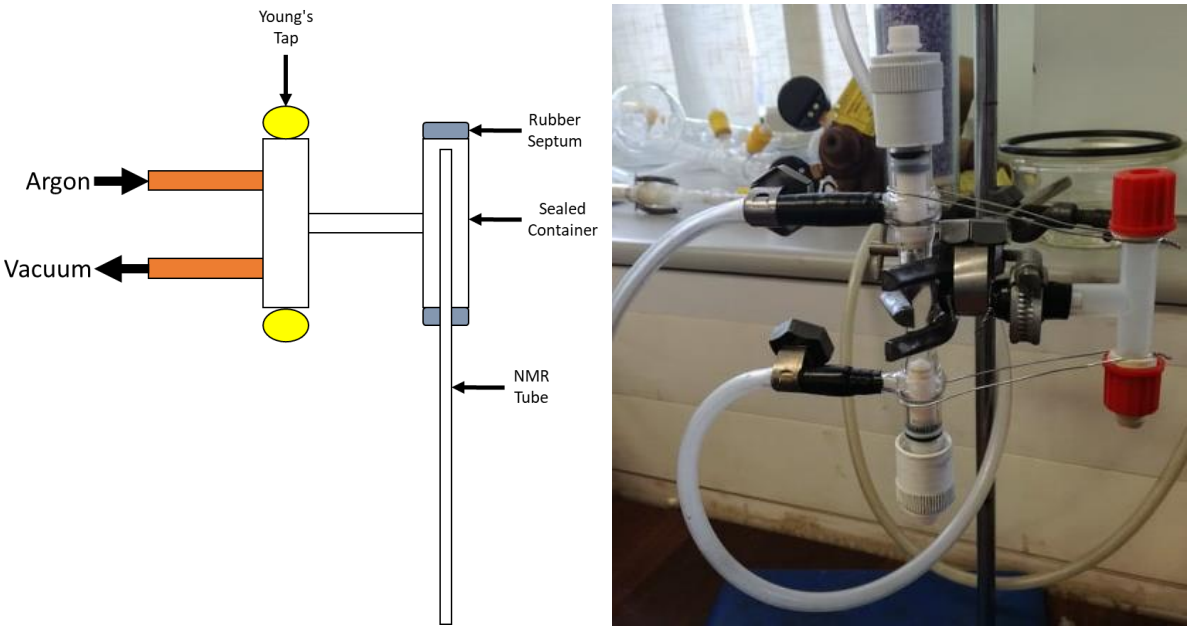

Figure 2.28: Schematic design (left) and actual picture of equipment (right) used to prepare NMR spectroscopy tubes for LAP kinetic experiments.

2.2.3.3.2 Test Polymerisations

To ensure that the expensive deuterated solvent was not wasted, a number of different polymerisations were carried out in the NMR spectroscopy tube before being worked up and characterised. Initially, styrene was used due to its dark red colour when polymerisation is living (Figure 2.29), but focus was switched to myrcene for the optimisation process to ensure

that a relatively high M_n and low Đ could be achieved. The NMR spectroscopy tube was first prepared as discussed previously, before the solvent-monomer mixture – which had been dried over CaH_2 – was injected. The tube was then sealed with a new septum, the required amount of *sec*-BuLi was injected and the polymerisation was left at room temperature. The molecular weights of polymers prepared are shown (Table 2.6).

Table 2.6: Summary of the test NMR spectroscopy tube polymerisations, whereby M_n was calculated by triple detection SEC (THF, 1 mL min^{-1}).

Polymer	Code	Target M_n /g mol^{-1}	Actual M_n /g mol^{-1}	Actual M_w /g mol^{-1}	Đ
Poly(styrene)	PS(NMR)1	-*	1,900	2,000	1.05
Poly(myrcene)	PM(NMR)1	-*	2,200	2,700	1.23
Poly(myrcene)	PM(NMR)2	2,000	3,100	3,600	1.16
Poly(myrcene)	PM(NMR)3	20,000	12,400	17,000	1.37
Poly(myrcene)	PM(NMR)4	10,000	22,000	30,200	1.37
Poly(myrcene)	PM(NMR)5	10,000	35,300	43,200	1.22

***Initial tests were carried out without a specific volume being used, 1 drop of sec-BuLi was added.**

Figure 2.29: Example of LAP of styrene in an NMR spectroscopy tube – showing the characteristic red colour of living poly(styrene).

The LAP of both styrene and myrcene could be carried out with reasonable consistency (Table 2.6). The higher-than-expected M_n values were due to the fact that only a small amount of *sec*-BuLi is used to initiate the polymerisation, meaning any termination/loss of the initiator has a large impact on the final M_n. The Đ is also slightly higher than expected for LAP potentially due to the accumulation of initiator at the surface of the reaction mixture before mixing and due to the lack of stirring as the polymerisation proceeds.

2.2.3.3.3 Real-Time In-Situ ^{1}H NMR Spectroscopic Polymerisation Analysis

For the investigation of reactivity ratios for a copolymer of myrcene and styrene prepared in the presence of TMEDA, a mixture of myrcene and styrene in equal volumes, giving a molar ratio of 2:3 myrcene:styrene, and two equivalents of TMEDA to *sec*-BuLi were used. The polymerisation was carried out in deuterated cyclohexane under an argon atmosphere. The first ^{1}H NMR spectrum was taken approximately 1.5 min after the reaction had been initiated and then every 2.5 min afterwards.

The monomer depletion of the myrcene-styrene copolymerisation, in the presence of TMEDA, can be seen in the stacked ^{1}H NMR spectra below (See Figure 2.30).

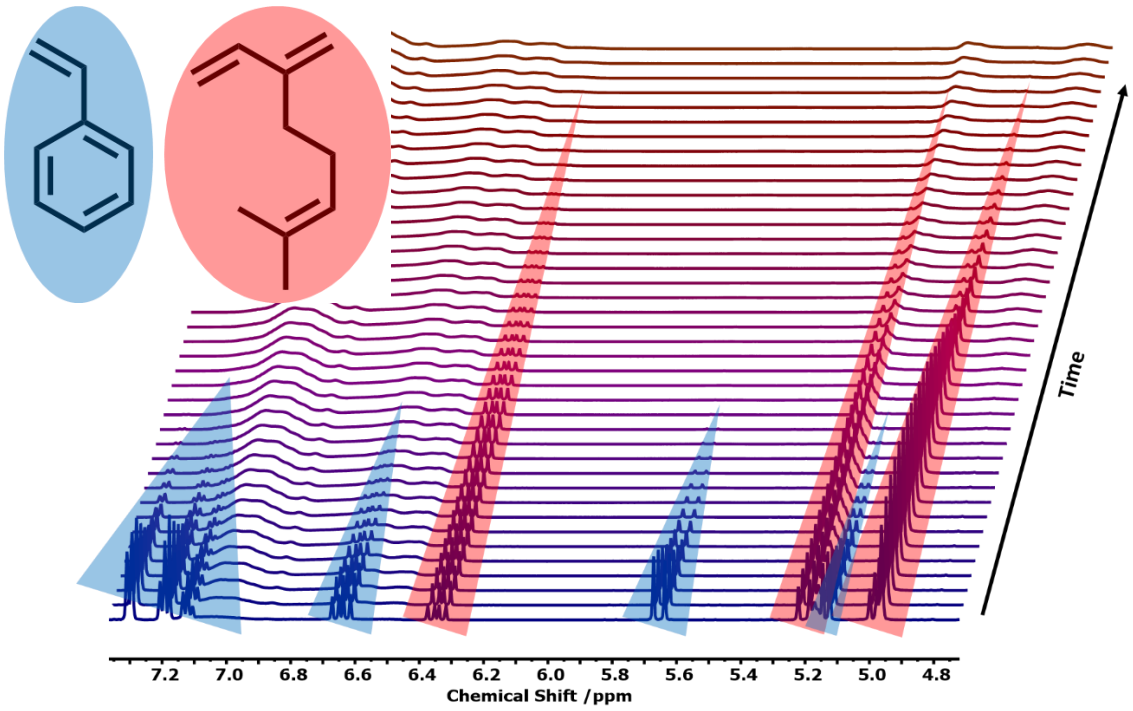

Figure 2.30: ^{1}H NMR (500 MHz, C_6D_{12}) spectra recorded during the real-time ^{1}H NMR spectroscopy polymerisation experiment. Monomer depletion has been highlighted by the triangles shown, to guide the reader's eye.

Using the integrals of the signals associated with each monomer in the ^{1}H NMR spectra, it was possible to calculate the percentage of each monomer remaining – and therefore the percentage of each monomer that had been incorporated into the copolymer – and the total monomer conversion. To reduce any error arising from the impact of a non-zero integral value due to baseline noise, a baseline subtraction was first applied to the integral values used for the calculation of the reactivity ratios. Thus, integral data was "normalised" such that the regions of the spectrum where the monomer peaks (would) appear in the final ^{1}H NMR spectrum in the series – where no residual monomer is present – are given a total integral value of zero.

The signal associated with the myrcene monomer that was used to calculate its depletion overlapped slightly with the growing peak of one of the aromatic signals of polymeric styrene. Specifically, the peak for the myrcene monomer proton H_1 at 6.27-6.37 ppm, which was used to calculate myrcene monomer depletion, overlaps with the emerging peak for the ortho phenyl protons of polystyrene (Figure 2.31). This overlap introduces a potential error, and a correction was made in an attempt to rectify the error. For this correction, the magnitude of the integral for the specific portion of the peak arising from the *ortho*- aromatic proton (6.27-6.37 ppm) that overlaps with the myrcene monomer proton H_3 at 6.27-6.37 ppm was estimated, for each NMR integral that was used. Figure 2.32 shows the final ^{1}H NMR spectrum from the series of stacked spectra in Figure 2.30 and in this case, there is no overlap because there is no unreacted myrcene monomer and 100 % of the styrene has reacted. We estimated the integral of the portion that would overlap in this case (0.73) and then scaled the integral as a function of styrene conversion. Thus, the assumption is that if the integral value of the overlapping portion at 100 % styrene conversion is 0.73, then at 57% styrene conversion the integral value of the overlapping portion will be 0.73 × 0.57, which equals 0.416.

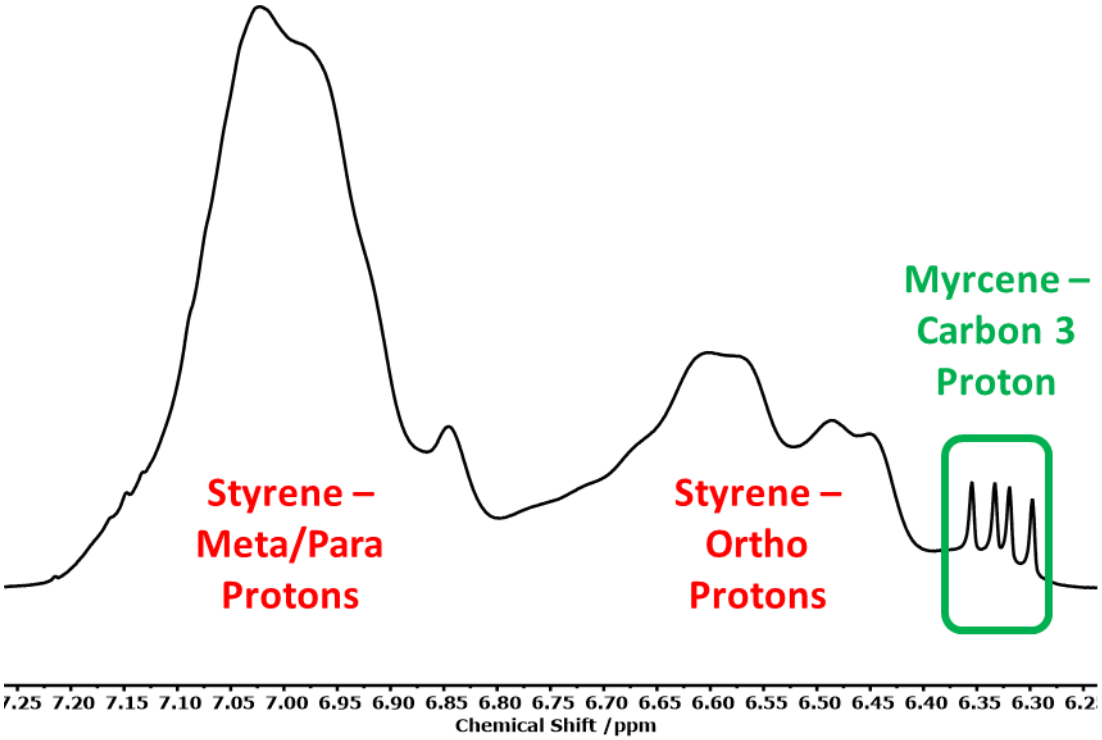

Figure 2.31: Partial ^{1}H NMR spectrum of PMS(NMR)1 showing the styrenic region as the polymerisation is progressing, illustrating that the polystyrene *ortho*- proton peak (6.8 – 6.25 ppm) overlaps with the myrcene monomer peak at 6.27 – 6.37 ppm.

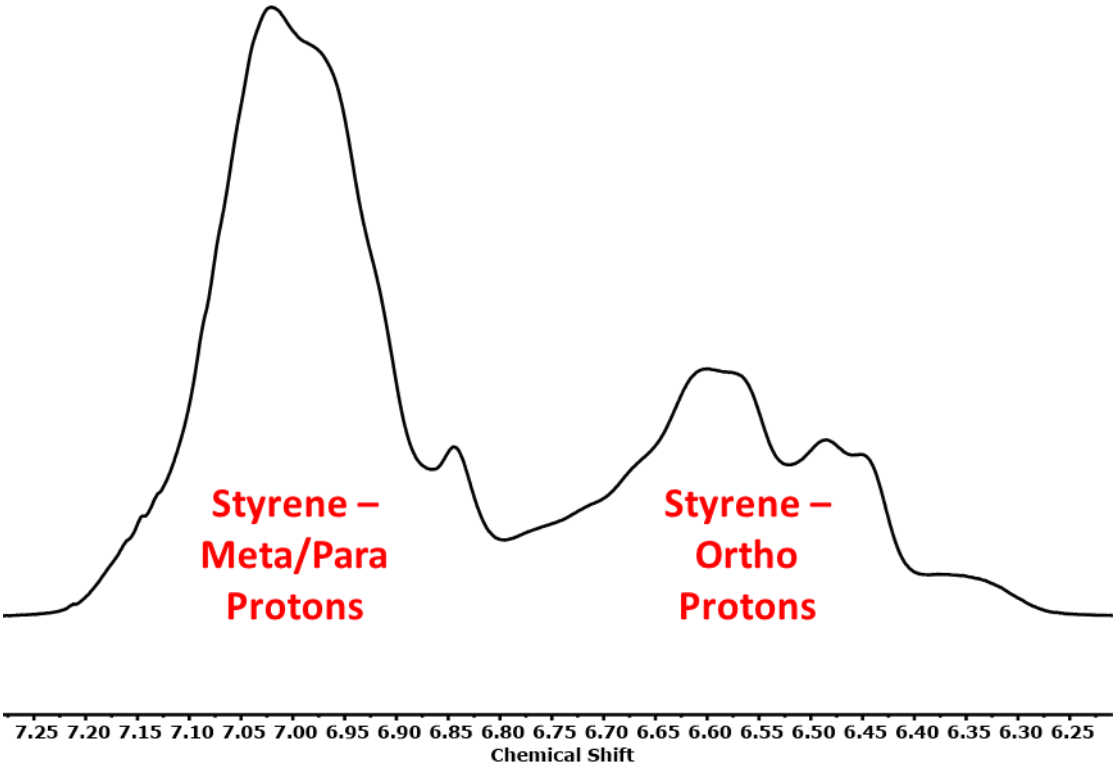

Figure 2.32: Partial ^{1}H NMR spectrum of PMS(NMR)1 showing the styrenic region after the polymerisation has occurred to show the magnitude of the peak that overlaps with the myrcene monomer peak.

This value was then subtracted from the integral of the myrcene peak in each spectrum to obtain a more accurate representation of the actual amount of myrcene monomer left. Having obtained normalised and corrected integral values for each sample of the polymerisation, a plot of incorporation of each monomer can be presented as a function of the total monomer conversion to see the relative rate of incorporation of each (see Figure 2.33 below).

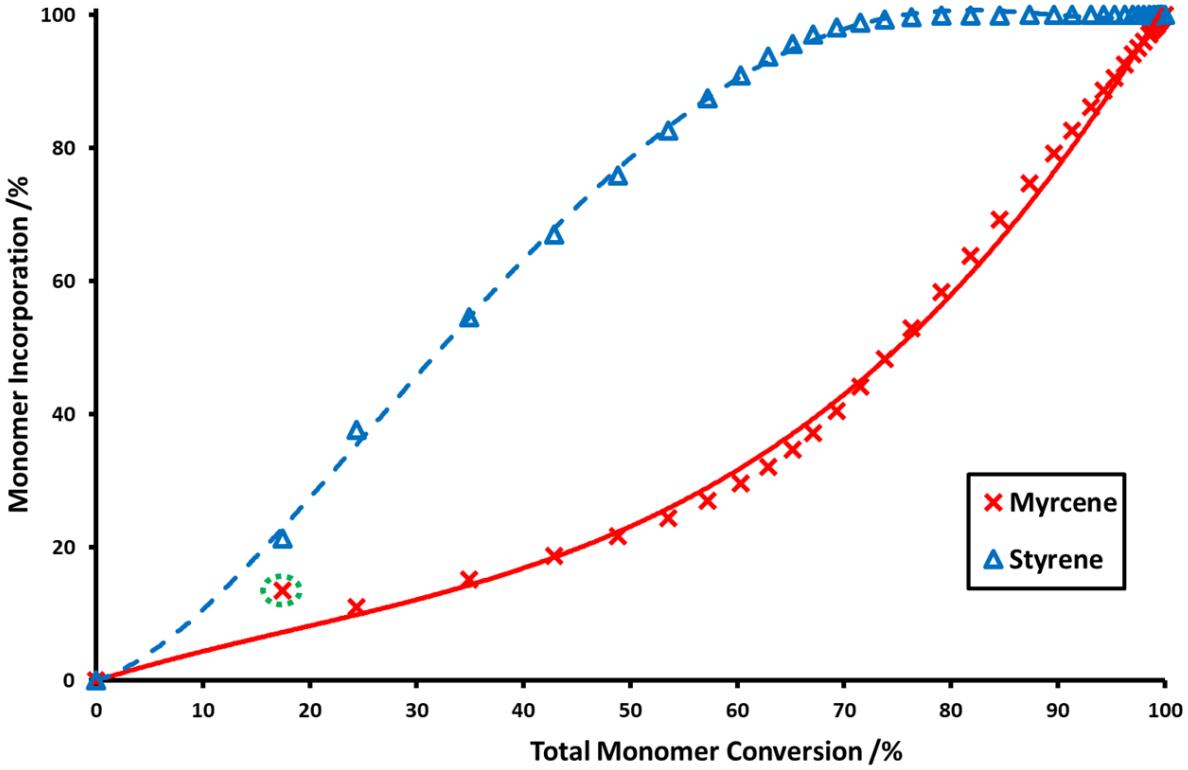

Figure 2.33: Comparison of the incorporation of both myrcene and styrene as a function of the total monomer conversion, where the trendlines presented have been added to guide the eye of the reader. The point highlighted by the green circle appears to be anomalous, potentially due to an overcorrection caused by the styrene polymer correction.

Having obtained corrected values for the integrals of each of the individual ^{1}H NMR spectra the reactivity ratios for the copolymerisation of myrcene and styrene in the presence of TMEDA can be calculated. The Meyer-Lowry (M-L) approach was chosen for the calculation of the reactivity ratios as it allows data at all monomer conversions to be used, rather than just data at low (< 5%) conversion, as required by widely-used linear estimation methods such as the Fineman–Ross [50] and Kelen–Tüdös [51] methods. [137] [12] Moreover, such linear

methods have been shown to lack statistical rigour for all systems. The M-L approach also means that data from a single copolymerisation reaction can be used to estimate reactivity ratios, rather than needing to repeat the copolymerisation using several different feed ratios. The Meyer-Lowry equation can be seen in Equation 2.17 below.

$$\mathbf{Conv} = \mathbf{1} - \left(\frac{\mathbf{f_A}}{\mathbf{f_A^0}}\right)^{\mathbf{r_B}/(\mathbf{1-r_B})} \left(\frac{\mathbf{1-f_A}}{\mathbf{1-f_A^0}}\right)^{\mathbf{r_A}/(\mathbf{1-r_A})} \times \left(\frac{\mathbf{f_A(2-r_A-r_B)-r_B-1}}{\mathbf{f_A^0(2-r_A-r_B)-r_B-1}}\right)^{(\mathbf{r_A r_B-1})/(\mathbf{1-r_A})(\mathbf{1-r_B})}$$

Equation 2.17: Meyer-Lowry equation which was used for determining the reactivity ratios of the copolymerisation where f_A is the feed ratio of monomer A, f_A^0 is the initial monomer feed ratio of A, r_A is the reactivity ratio of monomer A and r_B is the reactivity ratio of monomer B. [138]

The (experimental) instantaneous monomer feed ratios obtained by ^{1}H NMR spectroscopy and assumed reactivity ratios were used within the Meyer-Lowry equation to estimate a (calculated) total monomer conversion and the process iterated to minimise the difference between the calculated and experimental monomer conversion. Reactivity ratios of r_{Sty} = 16.67 and r_{Myr} = 0.14 were obtained. The agreement between experimental and calculated conversion data is extremely good, indicting a good fit with an R^2 value of 0.991806. A plot of i) the experimental monomer conversion from the ^{1}H NMR spectroscopy data and ii) conversion calculated using the estimated reactivity ratios versus f_A – the mole fraction of styrene in the instantaneous feed ratio – is shown below (Figure 2.34).

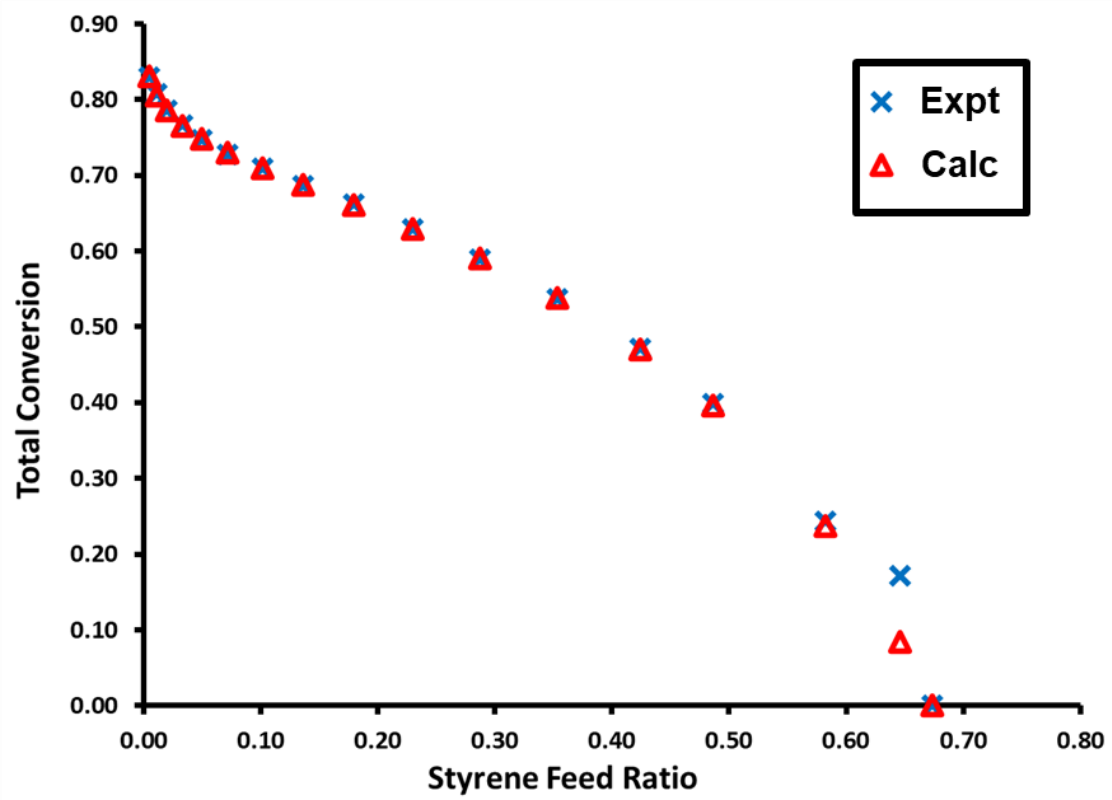

Figure 2.34: Experimental total monomer conversion (blue crosses) and monomer conversion calculated using estimated reactivity ratios (red triangles) at varying values of mole fraction styrene in instantaneous monomer feed ratio.

As previously mentioned, there is a significant discrepancy between the experimental and the calculated total monomer conversion for the first set of ^{1}H NMR spectroscopy data where the fraction of styrene in the instantaneous feed has reduced to 0.65. Thus, whilst experimental conversion based on raw NMR data is c. 18%, the conversion value calculated using the estimated reactivity ratios is a little less than 10%. The source of this discrepancy could be experimental or analytical, and is not immediately obvious. However, the significant difference between experimental and calculated does impact on the iteration process – which seeks to minimise differences – and the reactivity ratios obtained. The process of estimating reactivity ratios was therefore repeated, whilst excluding the aforementioned data point, giving values of r_{Sty} = 17.52 and r_{Myr} = 0.15. The agreement between experimental and calculated monomer conversion was extremely good, indicating an improved (excellent) fit with an R^2 value of 0.999908.

Once again, the data presented (Figures 2.33 and 2.34) suggests that the initial observations that were presented in this study on monomer incorporation during copolymerisation were

in fact correct. It can clearly be seen that the styrene monomer is consumed preferentially in the initial stages of the polymerisation before the myrcene is incorporated in the later stages. This along with the significant disparity between the obtained reactivity ratios (r_{Sty} = 17.52 and r_{Myr} = 0.15) supports the claim that what in fact is being polymerised during this copolymerisation is a tapered block-like copolymer and not a random copolymer as suggested in the previous literature. [46]

2.2.3 The Terpolymerisation of Myrcene, Butadiene and Styrene in the Absence and Presence of TMEDA

As mentioned previously, one of the main motivations of this project was to investigate the use of myrcene as a potential replacement for or part replacement of butadiene. Also, one of the main industrial applications of LAP is in the synthesis of sSBR for use in tyre tread formulations. In the synthesis of sSBR, polar additives are added in order to randomise the sequence distribution of butadiene and styrene. This ensures that the number of styrene units found in a block are minimised as much as possible, as blocky regions of styrene have been shown to have a negative impact on the performance of the tyre. [54]

Thus, it was decided to synthesise a terpolymer of myrcene, butadiene and styrene in benzene at room temperature, with the addition of 2 equivalents of TMEDA with respect to the amount of BuLi used (a ratio that has been used to synthesise random sSBR [55]) to try to synthesise a terpolymer with styrene and butadiene that is randomised while also investigating how the myrcene is incorporated, as this may determine how effective a part replacement of the butadiene with myrcene would be. This would then be compared to the terpolymerisation of myrcene, butadiene and styrene in the absence of TMEDA to try to fully understand the effect that TMEDA has on the relative rates of incorporation of each monomer.

An initial monomer feed ratio of approximately 33 % of each monomer was chosen in order to determine the preference of which monomer was incorporated across the polymerisation, with samples being taken, worked up and analysed at 15, 60 and 1440 mins. Based upon the observations presented previously for the copolymerisation of myrcene with styrene/butadiene in the presence of TMEDA and based upon the literature regarding the synthesis of random butadiene-styrene copolymers, [55] it was hypothesised that the synthesis of a terpolymer of myrcene, styrene and butadiene in the presence of TMEDA would

result in a gradient-type copolymer moving from a random styrene-butadiene rich block to a myrcene-rich block, while the terpolymer synthesised in the absence of TMEDA would also result in a tapered block copolymer whereby a slightly gradient shifted myrcene-butadiene rich section would be followed by a styrene-rich block.

The final assigned ^{1}H NMR spectra of PMBS1 (a terpolymer of myrcene, butadiene and styrene synthesised in the absence of TMEDA) and PMBS2 (a terpolymer of myrcene, butadiene and styrene synthesised in the presence of 2 equivalents of TMEDA with respect to the amount of BuLi) can be seen in Figures 2.35 and 2.36 respectively below.

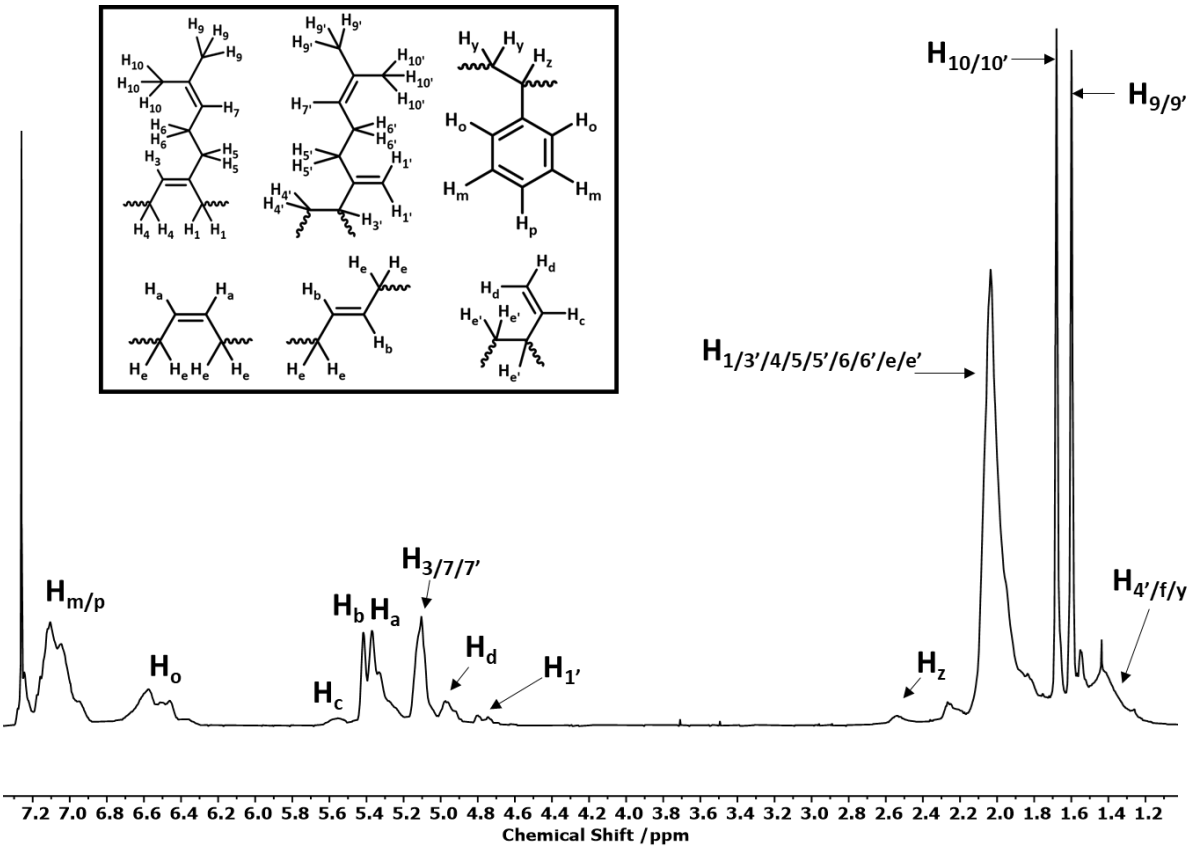

Figure 2.35: ^{1}H NMR spectrum (400 MHz, $CDCl_3$) of PMBS1 with hydrogen assignment of each of the peaks.

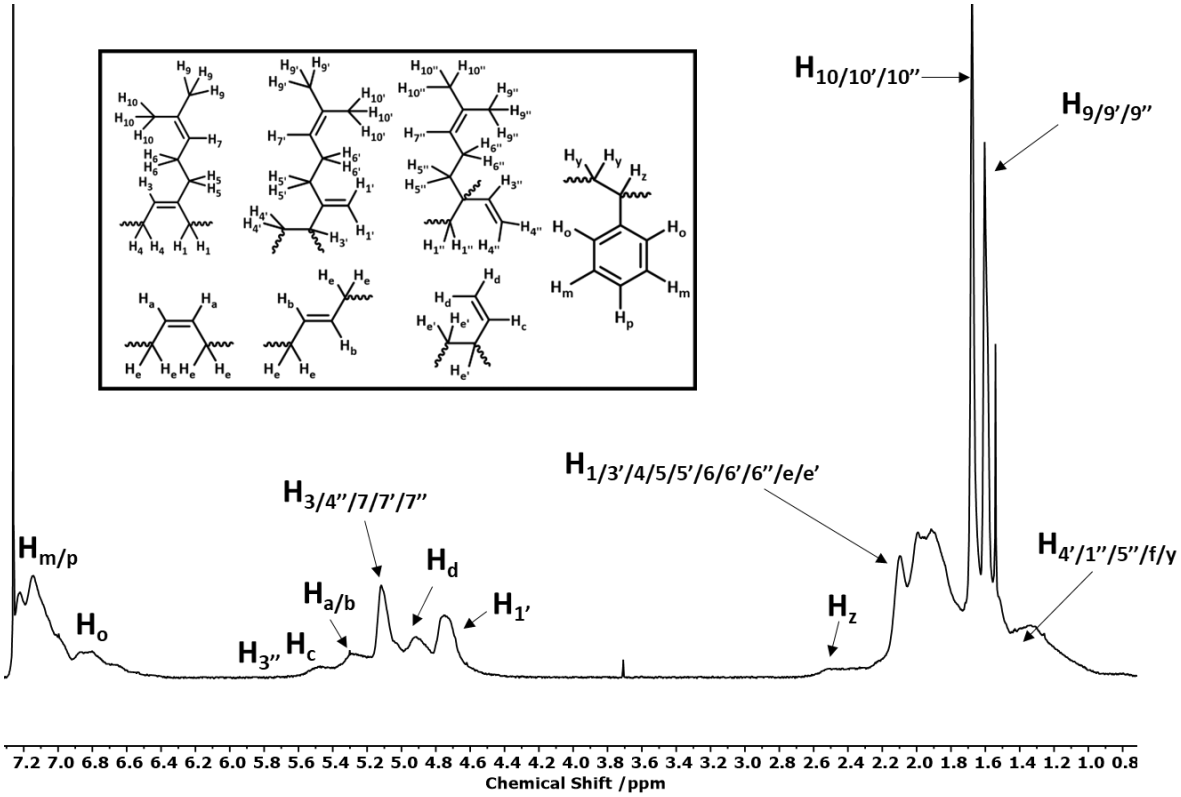

Figure 2.36: ^{1}H NMR spectrum (400 MHz, $CDCl_3$) of PMBS2 with hydrogen assignment of each of the peaks.

Once again, as shown in the spectra above, the addition of TMEDA during the terpolymerisation has caused a significant amount of peak broadening, to the extent that in PMBS2 the peaks became so broad – due to the large variation of possible diad and triad monomeric pairs/trios – that accurate investigation of the microstructure composition found within PMBS2 was nigh-on impossible to achieve. Thus, during this investigation, only the effect of TMEDA on the rate of incorporation was investigated, with the assumption that while the microstructure cannot be calculated from this sample directly, the composition of microstructures would have a similar distribution as to those found for PM2 – 58% (4,3), 39 % (4,1) and 3 % (1,2).

The compositional analysis of each sample collected during the terpolymerisations to generate PMBS1 and PMBS2 can be seen in Table 2.7 below, with a visual representation of the composition of each sample found in Figures 2.37 and 2.38.

Table 2.7: Comparison of the instantaneous composition of two terpolymers, one synthesised in the absence of TMEDA (PMBS1) and one synthesised in the presence of TMEDA (PMBS2), as a function of time.

Time Sample was Collected	Terpolymer Composition without TMEDA - PMBS1 /mol %			Terpolymer Composition with TMEDA – PMBS2 /mol %		
	Butadiene	Styrene	Myrcene	Butadiene	Styrene	Myrcene
15 min	55	7	38	45	41	14
60 min	54	7	39	40	34	26
1440 min	38	34	28	33	32	35

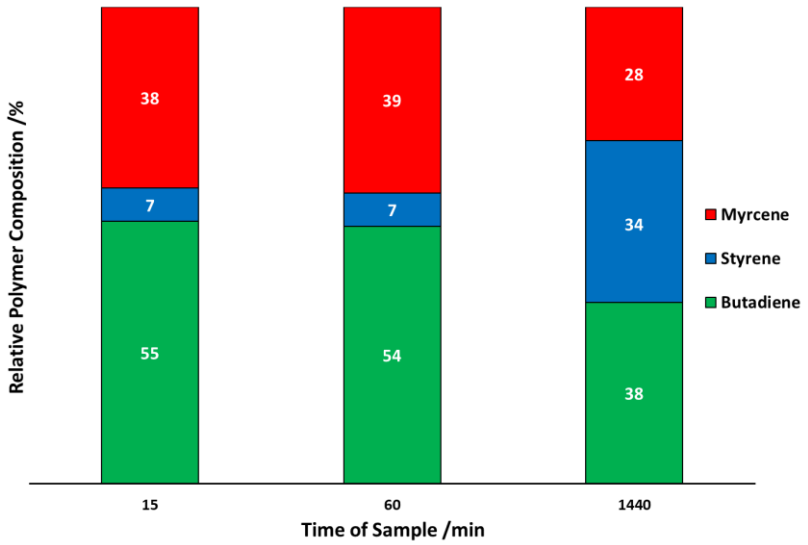

Figure 2.37: Visual representation of the compositional analysis (from Table 2.7) of each sample collected during the terpolymerisation of PMBS1.

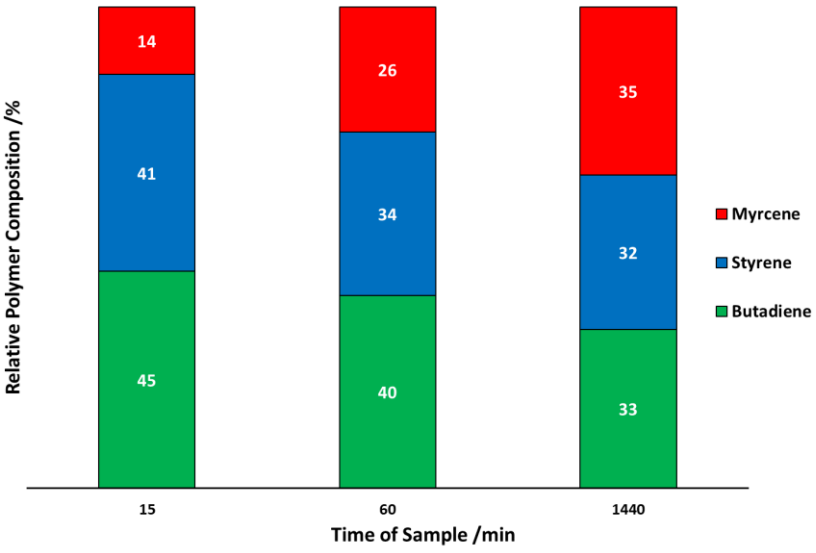

Figure 2.38: Visual representation of the compositional analysis (from Table 2.7) of each sample collected during the terpolymerisation of PMBS2.

As it can be seen in Table 2.7 and Figure 2.37 above, the synthesis of PMBS1 followed the general hypothesis that was proposed based on the previous observations of the different copolymerisations of myrcene with styrene/butadiene. As it can be seen, the rate of incorporation of styrene appears to be much reduced compared to the rate of incorporation of butadiene and myrcene, suggesting that a tapered block-like copolymer was synthesised with a myrcene-butadiene rich block followed by a taper region and a styrene-rich block. If the ratio between the myrcene and butadiene is calculated, it can be found that this ratio remains pretty much constant throughout the polymerisation (1.44 at 15 mins, 1.38 at 60 mins and 1.36 at 1440 mins) with only a very slight preference for butadiene incorporation observed at the earlier stages of the terpolymerisation. While this observation is slightly unexpected based upon the results collected during the copolymerisation to generate PMB1, it could be as a result of the added error associated with the analysis of these terpolymers, as additional peak overlap occurs due to the broadening of peaks observed upon the addition of a third monomer. In both cases, the extent of preferential uptake of one of the monomers was very slight, so any error in the interpretation of the ^{1}H NMR spectra could result in the inversion of which monomer was seen to be incorporated first.

From Table 2.7 and Figure 2.38, it can also be seen that the synthesis of PMBS2 also followed the proposed hypothesis, whereby it can be seen that the rate of incorporation of myrcene appears to be significantly reduced compared to the rate of incorporation of butadiene and myrcene, suggesting that a tapered block-like copolymer was synthesised with a styrene-butadiene rich block followed by a taper region and a styrene-rich block. In this terpolymer, if the ratio between the styrene and butadiene is calculated, it can be found that this ratio remains constant – within the errors associated with ^{1}H NMR spectroscopy – throughout the polymerisation (1.10 at 15 mins, 1.18 at 60 mins and 1.03 at 1440 mins), a finding consistent with the previously reported literature which suggests that in the presence of 2 equivalents of TMEDA with respect to the amount of BuLi, random styrene-butadiene copolymers are synthesised. [36] [37] It is once again proposed that due to the alkyl substitution of myrcene, the steric hindrance associated with attack from a propagating chain – with a lithium counterion which is co-ordinated to TMEDA – suffers from a large energy barrier, which reduces the rate of incorporation of myrcene relative to the rate of incorporation of the butadiene and the styrene.

2.3 Conclusion

Through the data presented in this Chapter, it has been shown that myrcene can be successfully polymerised – in both the absence and presence of TMEDA – whereby the addition of TMEDA was shown to impact the microstructure of the myrcene in the polymer from approximately 93% (4,1) and 7% (4,3) in the absence of TMEDA to approximately 39% (4,1), 58% (4,3) and 3% (1,2) in the presence of TMEDA.

In each of the individual copolymerisations conducted, a slight preference for the incorporation of myrcene was observed relative to butadiene, with a substantial preference for its incorporation over styrene – as confirmed by the reactivity ratios of myrcene and styrene being determined as $r_{Myr} = 36$ and $r_{Sty} = 0.028$. [12] However, this preferential uptake of the myrcene monomer is completely lost in the presence of 2 molar equivalents of TMEDA, with respect to the amount of BuLi used, as it was shown that for both myrcene/butadiene and myrcene/styrene copolymerisations, the rate of myrcene polymerisation is greatly reduced in the presence of TMEDA, resulting in a preferential incorporation of either the butadiene or the styrene.

The preferential uptake of styrene in the copolymerisation of myrcene in the presence of TMEDA was investigated in detail due to the claims of several literature reports that suggested that myrcene and styrene sequence distribution would be randomised in the polymer synthesised under the conditions used. [16] [46] Using three separate methods of investigation, it was shown that these previously published articles were in fact incorrect. This was categorically proven by the determination of the reactivity ratios of myrcene and styrene copolymerised in the presence of two molar equivalents of TMEDA (with respect to the initiator used) as the ratios were calculated as $r_{Sty} = 17.52$ and $r_{Myr} = 0.15$, suggesting the synthesis of a tapered-block copolymer whereby the first block would be styrene rich followed by a tapered region and then a myrcene-rich block.

Finally, in the terpolymerisation of myrcene, styrene and butadiene, it was shown that the butadiene and myrcene polymerise almost randomly in preference to styrene in the absence of TMEDA, but when TMEDA was added, it was shown that styrene and butadiene polymerised almost randomly in preference to the myrcene. While the ultimate aim of this project was to investigate the use of myrcene as a potential butadiene replacement, the stark differences in reactivity with styrene in both the absence and presence of TMEDA compared

to the butadiene suggest that while a wider range of potential architectures might possible in one pot with styrene and myrcene, through the variation of the amount of polar additive added, it may be much more difficult to randomise the monomer sequence distribution without the requirement for continuous addition of monomer. In the cases of random styrene-diene copolymers, it was therefore proposed that rather than using the myrcene as a replacement – as the properties may be massively reduced due to the increased likelihood of styrene blocks – additional myrcene would be added to the random styrene-diene copolymer. From the investigations of this chapter, it would be hypothesised that the addition of a small amount myrcene in the random copolymerisation of butadiene and styrene – whereby a polar additive /solvent is most likely to be used – would result in a random styrene-butadiene copolymer with a small myrcene-rich tail. It was then proposed that the trisubstituted alkene of myrcene not involved in the polymerisation could be selectively functionalised over any other butadiene-related alkene to allow functionality to be localised at/near the chain end of the polymer – a property of functionality within sSBR that has shown to have enhanced added benefit over random functionalisation of the polymer. [56] [57] This hypothesis was investigated in Chapter 3.

2.4 Experimental

2.4.1 Materials

β-myrcene (≥ 95 %, Sigma Aldrich UK), ReagentPlus styrene (≥ 99 %, Sigma Aldrich UK), TMEDA (≥ 99.5%, Sigma Aldrich UK), cyclohexane-D_{12} (≥ 99.6 atom% D, Sigma Aldrich UK) and anhydrous benzene (99.8 %, Sigma Aldrich UK) were dried and degassed, using extra pure calcium hydride (93 %, 0 – 2 mm grain size, Acros Organics) and the freeze-pump-thaw method. 1,3-butadiene (≥ 99.6%, Sigma Aldrich UK) was purified by passing through molecular sieves before being sacrificially initiated with *n*-butyllithium solution (*n*-BuLi) (2.5 M in hexanes, Sigma Aldrich UK) prior to distillation. *Sec*-butyllithium (*sec*-BuLi) (1.4 M in cyclohexane, Sigma Aldrich UK), laboratory reagent grade propan-2-ol (99.5%, Fisher Scientific UK), chloroform-D (> 99.8 atom% D, Apollo Scientific Limited) and analytical reagent grade methanol (99.99%, Fisher Scientific UK) were all used as supplied.

2.4.2 ^{1}H NMR Spectroscopy

^{1}H NMR spectroscopy was carried out using a Bruker Advance III 400 MHz spectrometer with an operating frequency of 400.130 MHz for ^{1}H, using deuterated chloroform ($CDCl_3$) as the solvent. The ^{1}H NMR kinetic spectroscopy experiment was carried out using a Varian DD2-500 MHz spectrometer with an operating frequency of 499.520 MHz for ^{1}H, using deuterated cyclohexane (C_6D_{12}) as the solvent.

2.4.3 SEC Measurements and DSC Analysis

Triple detection SEC was carried out using a Viscotek GPC max VE2001 solvent/sample module and a Viscotek Triple Detector Array 302 in THF at 35 ^{o}C with a 1 mL min^{-1} flow rate. A dn/dc value of 0.131 mL g^{-1} [58] was used for polymyrcene in THF**,** a dn/dc value of 0.124 mL g^{-1} [59] was used for polybutadiene in THF, and a dn/dc value of 0.185 mL g^{-1} was used for polystyrene in THF [59]. A weighted average dn/dc value was calculated for each copolymer based on copolymer composition data obtained by ^{1}H NMR spectroscopy.

Glass transition temperature analysis was carried out using a Perkin Elmer DSC 8500. Each sample was subjected to a heat-cool-reheat cycle and glass transitions were measured on a reheat cycle, with a heating rate of 100 ^{o}C/ min.

2.4.4 Preparation of glassware used during LAP

To prepare the purification flask (1A), the glassware was first oven-dried (80 °C) for 16 h before being evacuated under ultra-high vacuum. Dry, degassed benzene (30 mL) and dry, degassed styrene (2 g) were then distilled into the reaction flask before another freeze pump-thaw-cycle was carried out. The solution was then allowed to thaw to room temperature, before the flask was flushed with a continuous flow of nitrogen. The tap (1B) of the flask was taken off before *sec*-BuLi (3 mL) was injected in before the tap was replaced, and the solution stirred. One final freeze-pump-thaw cycle was then carried out. This flask was then used to purify benzene, distilled from CaH_2, directly before use as a polymerisation's solvent.

To prepare the glassware that was used for each polymerisation reaction - "Christmas Tree" – (2A), the glassware was first cleaned with methanol, THF and acetone, before being evacuated under ultra-high vacuum for 2 hours at room temperature. The glassware was then washed with a "living" styrene solution, which had been prepared in the "Christmas Tree" previously, using the same method as for the preparation of the purification flask, and stored under vacuum in one of the side flasks (2B). Benzene from this living solution was then distilled into another side arm (2C) and used to return the rest of the living solution back to the original side arm flask. This was repeated several times, until all the living solution had been returned to the side arm flask (2B). The "Christmas Tree" was then left under ultra-high vacuum for 16 h at room temperature before it was ready to use.

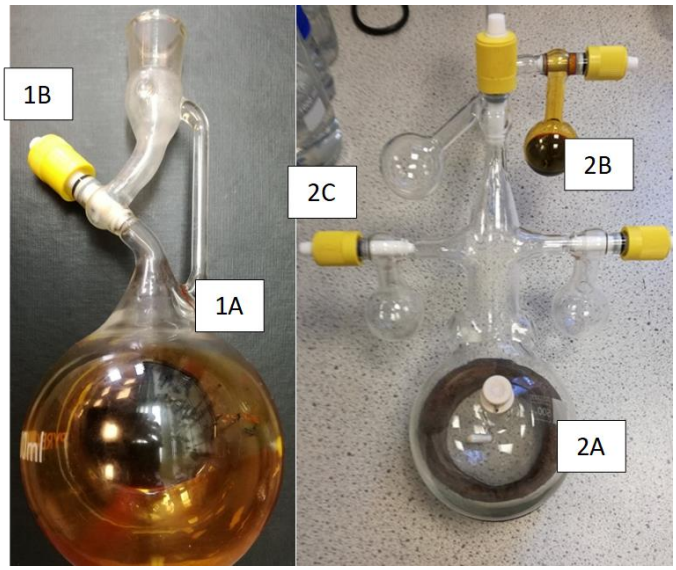

Figure 2.38: Image of the glassware used for the preparation of dry solvents (left) and the "Christmas Tree" used for anionic polymerisations (right).

2.4.5 Polymer Synthesis

PM1 was synthesised by "living" anionic polymerisation (LAP) in benzene at room temperature, under ultra-high vacuum conditions. Dry, degassed myrcene (3.24 g, 23.8 mmol) was mixed with dry, degassed benzene (~20 wt%) before being initiated with *sec*-BuLi (0.058 mL, 81 µmol), injected *via* syringe, to synthesise a polymer with a target M_n of 40,000 g mol^{-1}. The solution was then left to stir for 1140 min at room temperature, ensuring full monomer conversion, before the polymerisation was terminated *via* the injection of an excess of sparged methanol. PM1 (a clear viscous liquid) was precipitated into a large excess of methanol, washed and dried under reduced pressure (2.89 g, 89% yield). M_n – 45,400 g mol^{-1}, M_w – 46,800 g mol^{-1}, Đ – 1.03, 93% (4,1), 7% (4,3).

PM2 was synthesised by LAP in benzene at room temperature, under ultra-high vacuum conditions. Dry, degassed myrcene (4.05 g, 29.7 mmol) was mixed with dry, degassed benzene (~20 wt%) and TMEDA (0.02 mL, 130 µmol) before being initiated with sec-BuLi (0.07 mL, 100 µmol), injected *via* syringe, to synthesise a polymer with a target M_n of 45,000 g mol^{-1}. The solution was then left to stir for 360 min at room temperature, ensuring full monomer conversion, before the polymerisation was terminated *via* the injection of an excess of sparged methanol. PM2 (a clear very viscous liquid) was precipitated into a large excess of methanol, washed and dried at reduced pressure (3.22 g, 80% yield). M_n – 70,800 g mol^{-1}, M_w – 74,100 g mol^{-1}, Đ – 1.05; 39% (4,1), 58% (4,3), 3% (1,2).

PMB1 was synthesised by LAP in benzene at room temperature, under ultra-high vacuum conditions. Dry, degassed myrcene (3.81 g, 28.0 mmol) was mixed with butadiene (1.98 g, 36.6 mmol) before dissolution in dry, degassed benzene (~100 mL). The polymerisation was then initiated with sec-BuLi (0.138 mL, 193.2 µmol) to synthesise a statistical copolymer, with a target M_n of 30,000 g mol^{-1}. The solution was left to stir for 1200 min at room temperature before being terminated *via* the injection of an excess of sparged methanol. PMB1 (a clear viscous liquid) was recovered by precipitation into a large excess of methanol, washed and dried in *vacuo* to yield poly(myrcene-*co*-butadiene) (4.80 g, 83 %). M_n – 36,100 g mol^{-1}, M_w – 37,200 g mol^{-1}, Đ – 1.03 (as determined by SEC using a dn/dc value of 0.127); 57% butadiene (15% (1,2), 45% (1,4)-cis, 40% (1,4)-trans), 43% myrcene (93% (4,1), 7% (4,3)).

PMB2 was synthesised by LAP in benzene at room temperature, under ultra-high vacuum conditions. Dry, degassed myrcene (5.15 g, 37.8 mmol) was mixed with butadiene (2.4 g, 44 mmol) and TMEDA (0.09 mL, 600 µmol) before dissolution in dry, degassed benzene (~100 mL). The polymerisation was then initiated with 180 µL (252 µmol) of *sec*-BuLi to synthesise a statistical copolymer, with a target M_n of 30,000 g mol^{-1}. The solution was left to stir for 1200 min at room temperature before termination *via* the injection of an excess of sparged methanol. PMB2 (a clear very viscous liquid) was recovered by precipitation into a large excess of methanol, washed and dried in *vacuo* to yield poly(myrcene-*co*-butadiene) (6.22 g, 82% yield); M_n – 39,800 g mol^{-1}, M_w – 41,000 g mol^{-1}, Đ – 1.03 (as calculated by SEC using a dn/dc value of 0.127); 57% butadiene, 43% myrcene.

PMS1 was synthesised by LAP in benzene at room temperature, under ultra-high vacuum conditions. Dry, degassed myrcene (3.21 g, 23.6 mmol) was mixed with dry, degassed styrene (2.58 g, 24.8 mmol) before dissolution in dry, degassed benzene (~100 mL). The polymerisation was then initiated with *sec*-BuLi (59 µL, 83 µmol) to synthesise a statistical copolymer, with a target M_n of 70,000 g mol^{-1}. The solution was left to stir for 1200 min at room temperature before termination *via* the injection of an excess of sparged methanol. PMS1 (a white solid) was recovered by precipitation into a large excess of methanol, washed and dried in *vacuo* to yield poly(myrcene-*co*-styrene) (4.81 g, 83% yield); M_n – 80,700 g mol^{-1}, M_w – 86,800 g mol^{-1}, Đ – 1.08 (as calculated by SEC using a dn/dc value of 0.159); 54% styrene, 46 % myrcene (90% (4,1), 10% (4,3)).

PMS2 was synthesised by LAP in benzene at room temperature, under ultra-high vacuum conditions. Dry, degassed myrcene (4.80 g, 5.2 mmol) was mixed with dry, degassed styrene (3.82 g, 36.7 mmol) and TMEDA (86 µL, 58 µmol), before dissolution in dry, degassed benzene approximately (~100 mL). The polymerisation was then initiated with *sec*-BuLi (205 µL, 287 µmol) to synthesise a statistical copolymer, with a target M_n of 30,000 g mol^{-1}. The solution was left to stir for 1200 min at room temperature before termination *via* the injection of an excess of sparged methanol. PMS2 (a white sticky solid) was recovered by precipitation into a large excess of methanol, washed and dried in *vacuo* to yield poly(myrcene-*co*-styrene) (6.38 g, 74%); M_n – 32,600 g mol^{-1}, M_w – 35,300 g mol^{-1}, Đ – 1.08 (as calculated by SEC using a dn/dc value of 0.161); 53% styrene, 47% myrcene (38% (4,1), 57% (4,3), 5% (1,2)).

PMS(NMR)1 was synthesised by LAP in an NMR spectroscopy tube in C_6D_{12} at room temperature, under argon. Myrcene (80 µL, 470 µmol) was mixed with styrene (80 µL, 700 µmol), TMEDA (4 µL, 30 µmol) and cyclohexane (640 µL) and degassed over CaH_2 before being injected into an NMR spectroscopy tube that had been dried under ultra-high vacuum and then filled with argon using the apparatus described in Section 2.2.3.3.1. The solution was then initiated with *sec*-BuLi (10 µL, 14 µmol), injected *via* syringe, to synthesise a copolymer with a target M_n of approximately 10,000 g mol^{-1}, and immediately placed in an NMR spectrometer. The solution was then left for 3 h at 298 K, ensuring full monomer conversion, where an ^{1}H NMR spectrum was taken every 150 s before the polymerisation was terminated *via* the injection of an excess of sparged isopropanol. PMS(NMR)1 (a white sticky solid) was precipitated into a large excess of isopropanol, washed and dried in vacuo. M_n – 15,900 g mol^{-1}, M_w – 17,400 g mol^{-1}, Đ – 1.09 (as calculated by SEC using a dn/dc value of 0.167); 67% styrene, 33% myrcene (34% (4,1), 61% (4,3), 5% (1,2)).

PMBS1 was synthesised by LAP in benzene at room temperature, under ultra-high vacuum conditions. Dry, degassed myrcene (5.10 g, 37.4 mmol) was mixed with butadiene (2.76 g, 51.0 mmol) and styrene (4.88 g, 46.9 mmol) before dissolution in dry, degassed benzene (~100 mL). The polymerisation was then initiated with *sec*-BuLi (114 µL, 160 µmol) synthesise a statistical copolymer, with a target M_n of 80,000 g mol^{-1}. The solution was left to stir for 1440 min at room temperature before termination *via* the injection of an excess of sparged methanol. PMBS1 (a white solid) was recovered by precipitation into a large excess of methanol, washed and dried in *vacuo* to yield poly(myrcene-*co*-butadiene-*co*-styrene) (9.73 g, 76%); M_n – 95,300 g mol^{-1}, M_w – 100,100 g mol^{-1}, Đ – 1.05 (as calculated by SEC using a dn/dc value of 0.147); 34% styrene, 38% butadiene (17% (1,2), 50% (1,4)-cis, 33% (1,4)-trans), 28% myrcene (89% (4,1), 11% (4,3)).

PMBS2 was synthesised by LAP in benzene at room temperature, under ultra-high vacuum conditions. Dry, degassed myrcene (4.12 g, 30.2 mmol) was mixed with butadiene (1.55 g, 28.7 mmol), styrene (2.85 g, 27.4 mmol) and TMEDA (63 µL, 420 µmol), before dissolution in dry, degassed benzene (~100 mL). The polymerisation was then initiated with *sec*-BuLi (152 µL, 213 µmol) to synthesise a statistical terpolymer, with a target M_n of 40,000 g mol^{-1}. The solution was left to stir for 1200 min at room temperature before termination *via* the injection

of an excess of sparged methanol. PMBS2 (a clear very viscous liquid which solidified on drying) was recovered by precipitation into a large excess of methanol, washed and dried in *vacuo* to yield poly(myrcene-*co*-butadiene-*co*-styrene) (7.18 g, 84 % yield); M_n – 41,100 g mol^{-1}, M_w – 42,900 g mol^{-1}, Đ – 1.04 (as calculated by SEC using a dn/dc value of 0.146); 32% styrene, 33% butadiene, 35% myrcene.

2.5 References

[1] W. Obrecht, J. Lambert, M. Happ, C. Oppenheimer-Stix, J. Dunn and R. Krüger, “Rubber, 4. Emulsion Rubbers,” *Ullmann's Encyclopedia of Industrial Chemistry,* 2011.

[2] W. Kaewsakul, K. Sahakaro, W. K. Dierkes and J. W. M. Noordermeer, “Factors influencing the flocculation process in silica-reinforced natural rubber compounds,” *Journal of Elastomers,* vol. 48, no. 5, p. 426, 2016.

[3] L. Wang, S. Zhao, A. Li and X. Zhang, “Study on the structure and properties of SSBR with large-volume functional groups at the end of chains,” *Polymer ,* vol. 51, no. 9, pp. 2084-2090, 2010.

[4] M. Hassanabadi, M. Najafi, G. H. Motlagh and S. S. Garakani, “Synthesis and characterization of end-functionalized solution polymerized styrene-butadiene rubber and study the impact of silica dispersion improvement on the wear behavior of the composite,” *Polymer Testing,* vol. 85, p. 10643, 2020.

[5] R. Bisschop, F. Grunert, S. Ilisch, T. Stratton and A. Blume, “Influence of molecular properties of SSBR and BR types on composite performance,” *Polymer Testing,* vol. 99, p. 107219, 2021.

[6] W. P. Francik, C. L. Alwardt, M. J. Rachita and S. Rodewald, “Rubber composition and tire containing functionalized polybutadiene and functionalized styrene/butadiene elastomers”. Europe Patent EP2607103A2, 27 April 2016.

[7] M. A. Sattar and A. Patnaik, “Role of Interface Structure and Chain Dynamics on the Diverging Glass Transition Behavior of SSBR-SiO2-PIL Elastomers,” *ACS Omega,* vol. 5, no. 33, pp. 21191-21202, 2020.

[8] R. J. Young and P. A. Lovell, Introduction to Polymers, Boca Raton: CRC Press, 2011.

[9] A. J. Johanson, M. F. L. and L. A. Goldblatt, “Emulsion Polymerization of Myrcene,” *Industrial and Engineering Chemistry,* vol. 40, no. 3, pp. 500 - 502, 1948.

[10] X. Yang, C. Wang, S. Li, K. Huang, M. Li, W. Mao, S. Cao and J. Xia, “Study on the synthesis of bio-based epoxy curing agent derived from myrcene and castor oil and the properties of the cured products,” *RSC Advances,* vol. 7, pp. 238-247, 2017.

[11] E.-M. Kim, J.-H. Eom, Y. Um, Y. Kim and H. M. Woo, “Microbial Synthesis of Myrcene by Metabolically Engineered Eschericha coli,” *Agricultural and Food Chemistry,* vol. 63, pp. 4606-4612, 2015.

[12] E. Grune, J. Bareuther, J. Blankenburg, M. Appold, L. Shaw, A. H. E. Muller, G. Floudas, L. R. Hutchuings and H. Frey, “Towards bio-based tapered block copolymers: the behaviour of myrcene in the statistical anionic copolymerisation,” *Polymer Chemistry,* vol. 10, pp. 1213-1220, 2019.

[13] A. Matic and H. Schlaad, “Thiol-ene photofuctionalization of 1,4-polymyrcene,” *Polymer International,* vol. 67, pp. 500-505, 2018.

[14] W. Li, J. Zhao, X. Zhang and D. Gong, “Capability of PN3-type Cobalt Complexes toward Selective (Co-)Polymerization of Myrcene, Butadiene, and Isoprene: Access to Biosourced Polymers,” *Industrial and Engineering Chemistry Research ,* vol. 58, pp. 2792-2800, 2019.

[15] J. Hilschmann and G. Kali, “Bio-based polymyrcene with highly ordered structure via solvent free controlled radical polymerization,” *European Polymer Journal,* vol. 73, pp. 363-373, 2015.

[16] J. Zhang, J. Lu, K. Su, D. Wang and B. Han, “Bio-based β-myrcene-modified solution-polymerized styrene–butadiene rubber for improving carbon black dispersion and wet skid resistance,” *J. Appl. Polym. Sci.,* vol. 136, p. 48159, 2019.

[17] P. Sarkar and A. K. Bhowmick, “Terpene Based Sustainable Elastomer for Low Rolling Resistance and Improved Wet Grip Application: Synthesis, Characterization and Properties of Poly(styrene-co-myrcene),” *ACS Sustainable Chemistry & Engineering ,* vol. 4, no. 10, pp. 5462-5474, 2016.

[18] L. Shaw, “The synthesis, characterisation and functionalisation of myrcene (co)polymers prepared by living anionic polymerisation.,” University of Durham, 2018.

[19] L. R. Hutchings, “Method of Epoxidation”. International Patent WO2020212492A1, 22 October 2020.

[20] R. P. Quirk and T.-L. Huang, “Alkyllithium-Initiated Polymerization of Myrcene New Block Copolymers of Styrene and Myrcene,” in *New Monomers and Polymers*, Boston, Springer, pp. 329-330, 1984.

[21] J. M. Bolton, M. A. Hillmyer and T. R. Hoye, “Sustainable Thermoplastic Elastomers from Terpene-Derived Monomers,” *ACS Macro Letters,* vol. 3, no. 8, pp. 717-720, 2014.

[22] S. Ayano and S. Yabe, “Anionic Polymerization of Isoprene. I. Polymerization of Isoprene,” *Polymer Journal,* vol. 1, no. 6, pp. 700-705, 1970.

[23] X. Jia, X. Zhang and D. Gong, “1,2 Enriched polymerization of isoprene by cobalt complex carrying aminophosphory fused (PN3) ligand,” *J. Polym. Sci. Part A: Polym. Chem.,* vol. 56, pp. 2286-2293, 2018.

[24] M. Zhao, Q. Mahmood, C. Jing, L. Wang, G. Zhu, X. Zhang and Q. Wang, “Isoprene Polymerization: Catalytic Performance of Iminopyridine Vanadium(III) Chloride versus Vanadium(III) Chloride,” *Polymers,* vol. 11, p. 1122, 2019.

[25] L. G. Wade Jr., Organic Chemistry, Upper Saddle River : Peason Education, 2010.

[26] H. L. Hsieh and R. P. Quirk, Anionic Polymerization: Principles and Practical Applications, New York: Marcel Dekker, 1996.

[27] J. A. Tenorio-López, J. J. Benvenuta-Tapia, E. Vivaldo-Lima, M. Á. Ríos-Enriquez and M. Lourdes de Nieto-Peña, “Modeling of polymerization rate and microstructure in the anionic polymerization of isoprene using n-butyl lithium and N,N,N’,N’-tetramethylethylenediamine considering different reactivities of the structural units,” *Journal of Polymer Research,* vol. 19, no. 9909, p. 7, 2012.

[28] H. L. Hsieh, “Kinetics of Polymerization of Butadiene, Isoprene, and Styrene with Alkyllithiums. Part I. Rate of Polymerization,” *Journal of Polymer Science,* vol. 3, pp. 153-161, 1965.

[29] M. Morton, E. E. Bostick, R. A. Livigni and L. J. Fetters, “Homogeneous anionic polymerization. IV. Kinetics of butadiene and isoprene polymerization with butyllithium,” *Journal of Polymer Science: Part A,* vol. 1, no. 5, pp. 1735-1747, 1963.

[30] K. Pérez, S. Leveneur, F. Burel, J. Legros and D. Vuluga, “Anionic synthesis and end-functionalization of polymyrcene in a flow microreactor system,” *Reaction Chemistry & Engineering,* vol. 8, pp. 432-441, 2022.

[31] R. D. Bayley, T. R. Hoffend, T. J. Fuller and S. K. Ahuja, “Random copolymers made by anionic polymerization, toners incorporating these copolymers and method for the manufacture thereof”. United States of America Patent US5532327A, 27 February 1995.

[32] R. Quirk, “Anionic Polymerization,” in *Handbook of Polymer Synthesis, Characterization, and Processing*, John Wiley & Sons, Inc., pp. 127-162, 2013.

[33] Y. Rogan, S. Beal and D. Rhodes, “Microstructure modification of polydienes using polar modifiers”. United Kindom Patent GB2516233A, 15 July 2013.

[34] R. Kozak and M. Matlengiewicz, “Influence of polar modifiers on microstructure of polybutadiene obtained by anionic polymerization. Part 3: Lewis acid alkoxide (μ) and Lewis base amine, amine-ether, and ether mixed-type (σ+μ) polar modifiers,” *International Journal of Polymer Analysis and Characterization ,* vol. 21, no. 1, pp. 44-58, 2016.

[35] D.-C. Huang and R. C.-C. Tsiang, “Effects of Tetrahydrofuran as a Structure Modifier in Preparation of SBS Thermoplastic Block Copolymers in Cyclohexane,” *Journal of Applied Polymer Science,* vol. 61, no. 2, pp. 333-342, 1996.

[36] A. F. Halasa, C. Jasiunas, B. Hsu, S. Henning and K. S. Seo, “Synthesis of random or tapered solution styrene–butadiene copolymers in the presence of sodium dodecylbenzene sulfonate as a polar modifier,” *International Journal of Applied Polymer Science,* vol. 127, no. 3, pp. 2116-2120, 2012.

[37] R. P. Quirk, Y. J. Lee, J. A. Schwindeman and R. J. Letchford, “Compositions providing improved functionalization of terminal anions and processes for improved functionalization of terminal anions”. United States of America Patent US6605564B1, 28 April 1999.

[38] R. R. Lattime, “Styrene-Butadiene Rubber,” *Kirk-Othmer Encyclopedia of Chemical Technology,* pp. 1-17, 2000.

[39] D. A. H. Fuchs, S. P. Wadgaonkar, A. H. E. Müller and H. Frey, “Effect of tetrahydrofuran on the anionic copolymerization of 4-trimethylsilylstyrene with isoprene,” *Polymer Advanced Technologies,* vol. 35, no. 6, p. e6478, 2024.

[40] S. Dumas, J. Sledz, F. Schue, S. Raynal, S. Bywater and D. J. Worsfold, “Anionic polymerization of isoprene by the complexes oligoisoprenyllithium/tertiary polyamines in cyclohexane: 3. Structural study of the polymers by 1H n.m.r. at 100 MHz,” *Polymer,* vol. 24, no. 10, pp. 1291-1293, 1983.

[41] J. Furukawa, T. Mieda and K. Irako, “Copolymerization of butadiene and isoprene with n-butyllithium.,” *Journal of Industrial Chemistry,* vol. 65, no. 12, pp. 2079-2081, 1962.

[42] C. C. Chang, A. F. Halasa and J. W. Miller JR., “The reaction engineering of the anionic polymerization of isoprene,” *Journal of Applied Polymer Science,* vol. 47, no. 9, pp. 1589-1599, 1993.

[43] Q. Wang, M. Liao, Y. Wang and C. Zhang, “Effects of 1,2-butadiene on the anionic copolymerization of styrene and 1,3-butadiene in the presence of polar additives,” *Polymer International,* vol. 56, pp. 1021-1028, 2007.

[44] A. F. Halasa and W. L. Hsu, “Synthesis of high vinyl elastomers via mixed organolithium and sodium alkoxide in the presence of polar modifier,” *Polymer,* vol. 43, no. 25, pp. 7111-7118, 2002.

[45] N. R. Legge, G. Holden and H. E. Schroeder, Thermoplastic Elastomers: A Comprehensive Review, Hanser Publishers, 1987.

[46] S. Zhang, L. Han, H. Ma, P. Liu, H. Shen, L. Lei, C. Li, L. Yang and Y. Li, “Investistigation on Synthesis and Application Performance of Elastomers with Bioogenic Myrcene,” *Industrial & Engineering Chemistry Research ,* vol. 58, pp. 12845-12853, 2019.

[47] L. Shaw and L. R. Hutchings, “Tales of the unexpected. The non-random statistical copolymerisation of myrcene and styrene in the presence of a polar modifier,” *Polymer Chemistry,* vol. 11, no. 44, pp. 7020-7025, 2020.

[48] V. D. Mochel, “NMR Composition Analysis of Copolymers,” in *Rubber Chemistry and Technology*, Montreal, Canada, 1967.

[49] A. F. Halasa, C. Jusinas, W.-L. Hsu and D. J. Zanzig, “Random low vinyl styrene-isoprene copolymers,” *European Polymer Journal,* vol. 46, pp. 2013-2018, 2010.

[50] M. Fineman and S. D. Ross, “Linear Method for Determining Monomer Reactivity Ratios in Copolymerization,” *Journal of Polymer Science,* vol. 5, no. 2, pp. 259-265, 1949.

[51] T. Kelen and F. Tudos, “Analysis of the Linear Methods for Determining Copolymerization Reactivity Ratios A New Improved Linear Graphic Method,” *Journal of Macromolecular Science: Part A - Pure and Applied Chemistry,* vol. 9, no. 1, pp. 1-27, 1975.

[52] N. A. Lynd, R. C. Ferrier Jr. and B. S. Beckingham, “Recommendation for Accurate Experimental Determination of Reactivity Ratios in Chain Copolymerization,” *Macromolecules,* vol. 52, pp. 2277-2285, 2019.

[53] V. E. Meyer and G. G. Lowry, “Integral and Differential Binary Copolymerization Equations,” *Journal of Polymer Science: Part A,* vol. 3, pp. 2843-2851, 1965.

[54] M. L. Kerns, Z. Xu and S. M. Christian, “Synthesis of styrene-butadiene rubber”. United States of America Patent US6372863B1, 18 July 2000.

[55] Y. Hattori, H. Morita and Y. Inoki, “Random styrene-butadiene copolymer rubber”. United States of America Patent US4547560A, 18 March 1983.

[56] T. Yuasa, M. Iwano, T. Sone and T. Tominaga, “Improved Silica Dispersibility with functionalised s-SBR for Lower Rolling Resistance,” in *The International Tire Exhibition and Conference*, Ohio, 2008.

[57] D. Kim, G. Yeom, H. Joo, B. Ahn, H.-J. Paik, H. Jeon and W. Kim, “Effect of the Functional Group Position in Functionalized Liquid Butadiene Rubbers Used as Processing Aids on the Properties of Silica-Filled Rubber Compounds,” *Polymers,* vol. 13, no. 16, p. 2698, 2021.

[58] R. P. Quirk and T.-L. Huang, “Alyllithium-Initiated Polymerization of Myrcene,” in *New Monomers and Polymers*, New York, Springer US, pp. 329-355, 1984.

[59] L. R. Hutchings, P. P. Brooks, D. Parker, J. A. Mosely and S. Sevinc, “Monomer Sequence Control via Living Anionic Copolymerization: Synthesis of Alternating, Statistical, and Telechelic Copolymers and Sequence Analysis by MALDI ToF Mass Spectrometry,” *Macromolecules,* vol. 48, no. 3, pp. 610-628, 2015.

[60] V. E. Meyer and G. G. Lowry, “Integral and Differential Binary Copolymerization Equations,” *Journal of Polymer Science,* vol. 3, pp. 2843-2851, 1965.

[61] J. Geng, Y. Sun and J. Hua, “1,2- and 3,4-Rich Polyisoprene Synthesized by Mo(VI)-Based Catalyst with Phosphorus Ligand,” *Polymer Science, Series B,* vol. 58, no. 5, pp. 495-502, 2016.

[62] S. Georges, M. Bria, P. Zinck and M. Visseaux, “Polymyrcene microstructure revisited from precise high-field nuclear magnetic resonance analysis,” *Polymer,* vol. 55, pp. 3869-3878, 2014.

Chapter 3 – The Selective Epoxidation of Poly(Myrcene) and Myrcene-Containing Copolymers

3.1 Introduction

As discussed previously, one of the motivations for this project is to explore the use of bio-available monomers in copolymers for applications such as the production of tyre treads. Tyre treads are produced from complex formulations, including fillers – such as silica and carbon black – which are added to the formulation to improve the physical properties of the tyre tread. The key physical properties are antagonistic in so much as the tyre should have a very high friction coefficient during braking (grip) but a very low friction coefficient when rolling (i.e. low rolling resistance). Although seemingly contradictory, silica and carbon black fillers can be used to improve both properties due to the frequency of distortion that occurs during rolling and braking being very different. [1] [2]

However, whilst the use of fillers can result in great improvements in physical properties, there exist challenges when it comes to incorporating and dispersing the filler into the tyre rubber formulation, even when functionalisation methods are used due to the large majority of the polymer remaining unfunctionalised and non-polar. Both silica and carbon black are polar in nature – due to the presence of polar functional groups on their surface – meaning that when they are added to the inherently non-polar polymers, the filler particles aggregate to reduce the free energy of the system, which reduces the overall property improvement and can also lead to 'hardpoints' within the tyre, which can contribute to fractures/punctures, unless expensive milling and rubber processing are carried out. [3]

One way in which the added benefits of filler particles can be increased is through increasing the interaction of the non-polar polymers with the polar filler particles. This can be achieved through several different strategies – including the costly plasma treatment of the polar additives to remove polar functional groups on the surface and increase non-covalent interactions between the filler and polymer chains – with one of the easiest and most commonly used mechanisms being through the functionalisation of the non-polar polymer chains. As discussed in Chapter 1.4.3.1, functionalisation of polymers synthesised by LAP can be achieved in many ways to give both chain-end and in-chain functional groups, which can

be used to increase the polymers' interaction with the silica through covalent and non-covalent/hydrogen bonding. While both chain-end functionalisation and in-chain functionalisation have been shown to further improve upon the rolling resistance properties added by the addition of polar filler particles – due to the better interaction of the additives to the polymer chains leading to reduced aggregate size and greater dispersion of the additive – it has been shown that functionalisation that occurs at or near the chain end improves properties to a greater extent, when the degree of functionalisation is roughly the same. This behaviour has been attributed to the added benefit of 'tying up' the chain ends – through interaction with the polar additive – which has the effect of reducing energy loss at low frequencies of distortion, improving the rolling resistance properties of the rubber. [4] [5]

Although the use of fillers to improve the properties of rubbers and elastomers is not limited to tyre rubber applications, we have chosen to explore the functionalisation of myrcene with a view to using small fractions of myrcene in a typical sSBR polymer with the expectation that the functionalisation of sSBR will enhance the interaction of the polymer with the filler, reducing/preventing aggregation of the additive and therefore leading to a greater overall property improvement. It should be pointed out that this study focusses only on the synthesis of said polymers, and an investigation into the physical properties of tyre rubber formulations is beyond the scope of this thesis.

3.1.1 The Functionalisation of Polymers Produced by Anionic Polymerisation

As discussed in Chapter 1.4.3.1, there are various different strategies that can be used to functionalise polymers synthesised by LAP, with advantages and disadvantages for each strategy (Table 1.1). Due to the presence of alkene moieties along the polymer chain when dienes – such as butadiene and isoprene – are polymerised, alkenes represent one of the most commonly used functionalities for post-polymerisation, in-chain functionalisation. Several strategies whereby the alkene moieties of polymerised dienes have been targeted for post-polymerisation in-chain functionalisation have been investigated in the literature, with some of the most common functionalisation reactions including: ionic addition of an aldehyde in the presence of a Lewis acid; [6] concerted ene addition of maleic anhydride; [7] and the free radical addition of thiol. [8]

3.1.2 The Epoxidation of Poly(Dienes)

Probably one of the most well-known and studied strategies for post-polymerisation in-chain functionalisation is through the epoxidation of alkene-containing polymers. Epoxidation of diene-containing polymers represents a highly dependable functionalisation strategy due to its ease of use, diverse range of epoxidising agents (several of which can be bought on an industrial scale at relatively low prices), general lack of side reactions (unless hydrogen peroxide is used) and the ability of the epoxide formed to be ring-opened by a large variety of different nucleophiles, allowing the epoxide to act as a site for a diverse range of different functionalities. These favourable characteristics of epoxidation reactions for polymer functionalisation have resulted in a large number of both publications of epoxidation of diene-containing polymers and patents for the synthesis of epoxidised polymers to be used within rubber formulations. The vast literature that can be found for the epoxidation of diene-containing polymers includes but is not limited to: epoxidation of styrene/butadiene star block copolymers using *m*-chloroperoxybenzoic acid (*m*-CPBA), peracetic acid (PAA), performic acid (PFA) and hexafluoro-isopropanol (HFIP); [9] partial epoxidation of poly(isoprene) prior to metal catalysed methyl methacrylate grafting; [10] epoxidation of polymyrcene using *m*-CPBA; [11] and a patent for the epoxidation of unsaturated polymers using hydrogen peroxide in the present of a one-phase-transfer catalyst. [12]

One further benefit of epoxidation reactions is the level of selectivity towards different alkene bonds, which the reaction can provide. This selectivity of reaction has been well documented in the literature and comes about due to the relative rate of epoxidation of the various epoxidising agents to different alkene bonds of varying substitution degree (and therefore electron density of the double bond), where generally the relative rate of epoxidation increases with increasing levels of alkene substitution (Figure 3.1). [13]

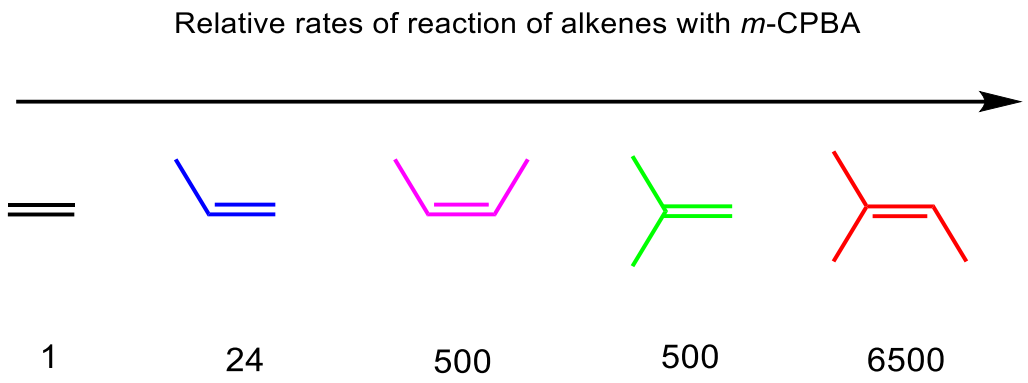

Figure 3.1: Relative rates of alkene epoxidation using *m*-CPBA. *[13]*

Epoxidation of an alkene is a concerted electrophilic addition reaction, whereby the alkene acts as a nucleophile and the peroxyacid acts as an electrophile. The reaction involves the nucleophilic attack of the weakly polarised O-O peroxide bond by the electron rich π-orbitals of the alkene bond, prior to attack of the alkene by the same oxygen that was attacked, via a butterfly transition state, in a concerted reaction (Figure 3.2).

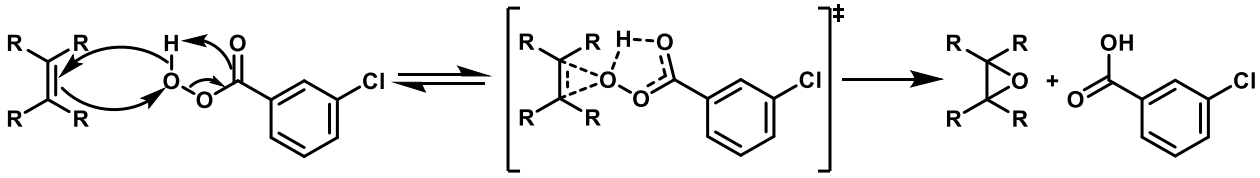

Figure 3.2: Mechanism for alkene epoxidation using *m*-CPBA. *[13]*

The selectivity of epoxidation (Figure 3.1), is brought about due to the nucleophilic attack of the weakly polarised O-O peroxide bond, whereby increasing the substitution of the alkene increases the electron density of the alkene through sp^3 to π-orbital partial electron donation.

Again, this Chapter was direct continuation of the Master's project that was started previously within the Hutchings group [14] and many of the results presented have been used to support the claims of a previously published patent [15]:

L. Shaw, "The synthesis, characterisation and functionalisation of myrcene (co)polymers prepared by living anionic polymerisation," University of Durham, 2018.

L. R. Hutchings, "Method of Epoxidation". International Patent WO2020212492A1, 22 October 2020.

3.2 Results and Discussion

It was believed that due to the high selectivity that epoxidation can provide towards alkenes with higher degrees of substitution, and due to the reactivity rates, which were found for myrcene copolymerisations in the presence of a polar modifier (as was discussed in Chapter 2.2), myrcene could be incorporated into sSBR in very small quantities before being selectively epoxidised, to provide functionality at/near the chain-end of the sSBR rubber. This would have the advantage of using a post-polymerisation in-chain functionalisation method to add tailored functionality to the SBR to allow for increased interaction with any additives that are added to the tyre formulation – relative to the interaction that is provided by chain-end functionalisation methods – while also maintaining any benefits that are provided by tying up the chain ends.

Initially, work began with the epoxidation of simple homopolymers of poly(butadiene) and poly(myrcene) in order to help with subsequent characterisation of copolymers of the two when investigations into the selectivity of epoxidation were started.

3.2.1 The Epoxidation of Poly(Butadiene)

Initially to find a method for the epoxidation of diene-containing polymers, we turned to the literature, taking into consideration the solubility of polymers in solution that we were to use. Using the previous work of Pandit *et al.* [9], a general experimental of which can be seen in Chapter 3.4 below, we started our investigations by epoxidising a simple poly(butadiene) homopolymer.

The amount of *m*-CPBA required to epoxidise each target degree of epoxidation was calculated using Equation 3.1 below.

$$m\text{-CPBA required} = \frac{\text{Purity } m\text{-CPBA} \times M_r \text{ of } m\text{-CPBA} \times \text{Mass Polymer} \times \text{mol \% Target Epoxidation}}{M_r \text{ of Polymer Repeat Unit}}$$

Equation 3.1: Equation used to calculate the amount of *m*-CPBA required for the chosen Target Epoxidation.

Initially, the epoxidation of a sample of polybutadiene (M01122 – a sample of polybutadiene that was synthesised previously within the group by Dr. Matthew Oti – 12 % (1,2), 88 % (1,4)) was attempted, to give a target epoxidation of approximately 19.6 % of the double bonds, in

part to compare (EPB1) with the results in previously published reports, but also to help with the subsequent characterisation of poly(butadiene-myrcene) copolymers. In general, a nominal 10 – 30 % total double bond epoxidation was targeted to present a compromise between the signals being observable and accurate by ^{1}H NMR spectroscopy and the solubility of the epoxidised polymer, but also to limit the available bond distribution change as those that are greater in substitution get used up. The full experimental of the epoxidation of poly(butadiene) can be found in Section 3.4.

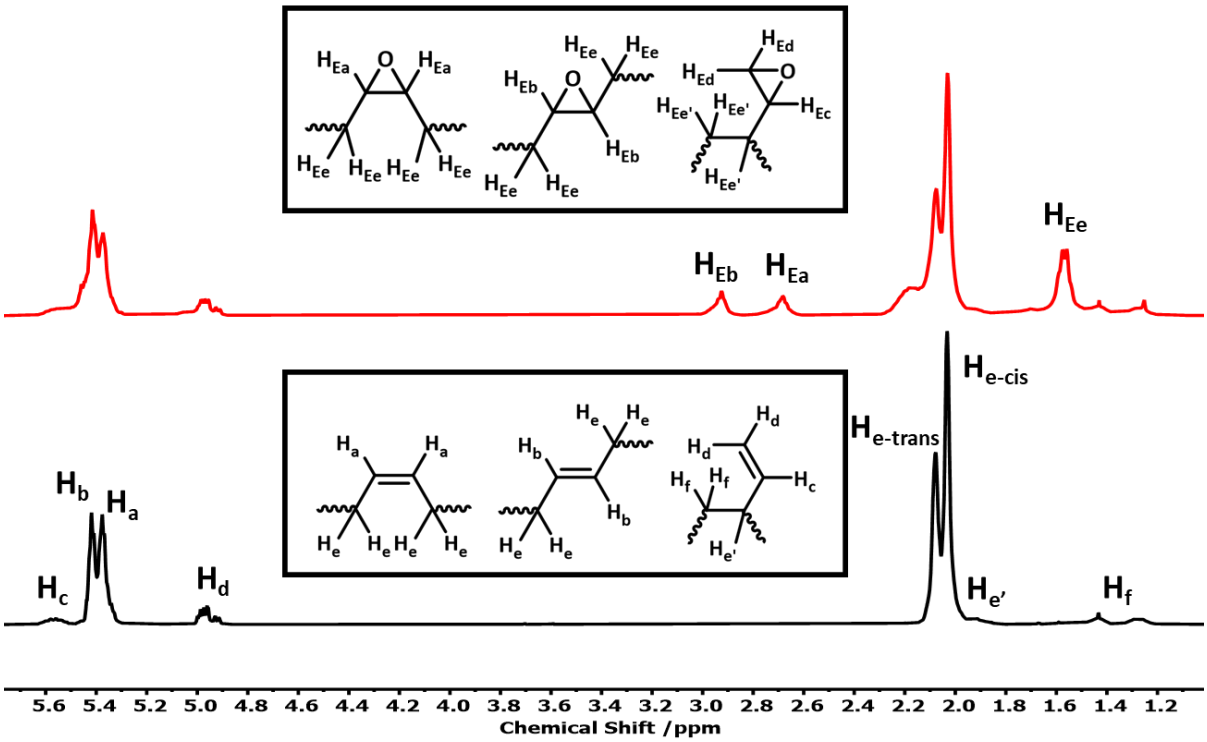

Figure 3.3: Partial ^{1}H NMR spectra (400 MHz, $CDCl_3$) of poly(butadiene) (bottom-black) and epoxidised poly(butadiene) (red-top).

As can be seen in the stacked ^{1}H NMR spectra in Figure 3.3, the epoxidation of poly(butadiene) was successful, as evidenced by the appearance of new ^{1}H NMR peaks at 2.65 ppm and 2.92 ppm, which are attributed (both by ourselves and others [16]) to the protons on the 2,3-epoxide ring (H_{Ea} and H_{Eb}), and the peak at 1.57 ppm, which we have attributed to the backbone protons (H_{Ee}) of an epoxidised butadiene unit. Whilst there is some debate as to whether these two peaks arise due to the presence of the two different isomers of the epoxide i.e. cis-2,3-epoxide and trans-2,3-epoxide, or whether the peaks correspond to the two protons on the same epoxide ring, we believe that the most likely explanation is that the

two peaks arise due to the two different isomers formed. However, for the most part, the explanation does not affect any of the calculations subsequently carried out as, in general, both peaks will have similar if not the same integration values (this can be seen in Table 3.1 below whereby B1 and B2 are within 5 % of each, which could be explainable purely though the error associated with these integrals or due to the slight initial asymmetrical distribution of available double bonds within poly(butadiene) - 57 % cis and 43 % trans). What may also be noticeable to the reader is that the peaks at 5.37 and 5.41 ppm have changed shape and a peak at 2.18 ppm has also appeared in the epoxidised sample. Both of these changes to the ^{1}H NMR spectrum can be attributed to a change in the potential dyads and triads that will be present throughout the backbone of the polymer due to the new epoxidised subunits that have now been synthesised.

Based on previous reports, the chemoselectivity that could be expected for the epoxidation of the 3,4-vinyl double bond (the relative rate of epoxidation for which would be 21 times less than that for the relative rate of a 2,3-backbone double bond) present when (1,2) polymerisation occurs, along with the low percentage of this microstructure in the sample (~ 12 %), would suggest that miniscule amounts of the 3,4-vinyl double bond would be epoxidised. This results in the peaks, which would correspond to the 3,4-epoxidations being indistinguishable from the noise of the ^{1}H NMR spectrum. [17] [13]

In order to calculate the extent of epoxidation of this polybutadiene sample, the integrals of each assigned environment must be considered – see Table 3.1.

Table 3.1: Summary of integral data for the epoxidised poly(butadiene) sample from the ^{1}H NMR spectrum in Figure 3.3.

Assigned Region	Chemical Shift Range /ppm	Proton Assignment	Integration
B1	2.63 – 2.80	H_{Ea}	1.85
B2	2.88 – 3.00	H_{Eb}	1.78
B3	4.85 – 5.10	H_d	2.00
B4	5.28 – 5.50	$H_a + H_b$	11.56

The integration values may then be used to calculate the extent of epoxidation using the equations below. Equation 3.2 gives an integral value equivalent to 1H for all butadiene units (butadiene + epoxidised butadiene):

$$|\text{Butadiene Units}| = \frac{|\text{B1}|+|\text{B2}|+|\text{B3}|+|\text{B4}|}{2}$$

$$|\text{Butadiene Units}| = \frac{1.85+1.78+2.00+11.56}{2} = 8.60$$

Equation 3.2: Equation used to calculate a nominal integral for the relative number of butadiene subunits.

Equation 3.3 can then be used to provide an integral value equivalent to 1H for all epoxidised units.

$$|\text{Epoxidised Butadiene Units}| = \frac{|\text{B1}|+|\text{B2}|}{2} = \frac{1.85+1.78}{2} = 1.82$$

Equation 3.3: Equation used to calculate a nominal integral for the relative number of epoxidised butadiene subunits.

Thus, the percentage of butadiene units which have been epoxidised is given by Equation 3.4.

$$\text{Percentage of Butadiene Units Epoxidised} = \frac{|\text{Epoxidised Butadiene Units}|}{|\text{Butadiene Units}|} \text{ X } 100\ \%$$

$$\text{Percentage of Butadiene Units Epoxidised} = \frac{1.82}{8.60} \text{ X } 100\ \%$$

$$\text{Percentage of Butadiene Units Epoxidised} = 21\ \%$$

Equation 3.4: Equation used to calculate the percentage of butadiene subunits that have been epoxidised.

As can be seen from the calculation above, 21 % of butadiene units have been epoxidised, which is in excellent agreement with target extent of epoxidation (20%).

3.2.2 The Epoxidation of Poly(Myrcene)

The same procedure was used to epoxidise poly(myrcene) - PM1. Two polymyrcene samples with different microstructures were used. A key aim of these experiments was to investigate the chemoselectivity of the epoxidation reaction towards the different types of alkene bonds present in polymyrcene.

3.2.2.1 The Epoxidation of Poly(Myrcene) Prepared in a Non-Polar Solvent – P(M)1

PM1 is a sample of poly(myrcene) that was synthesised in benzene and as such is expected to have a high 4,1 microstructure. ^{1}H NMR analysis of the homopolymer precursor suggests that the polymer had a microstructure composition of 93 % 4,1 and 7 % 4,3 and SEC analysis gave a molecular weight of 45,400 g mol^{-1} with a dispersity of 1.03. A target epoxidation of 10 % of all of the double bonds (representing 20 % of all myrcene units) was chosen for the selectivity analysis and it was expected that, due to the chemoselectivity of the epoxidation reaction, approximately 50 % of the epoxidation would occur on the 7,8-double bond and approximately 50 % of the epoxidation would occur on the 3,2-double bond, with no observable 2,1-double bond epoxidation being detected. The full experimental of the epoxidation of PM1 – EPM1 – can be found in Section 3.4.

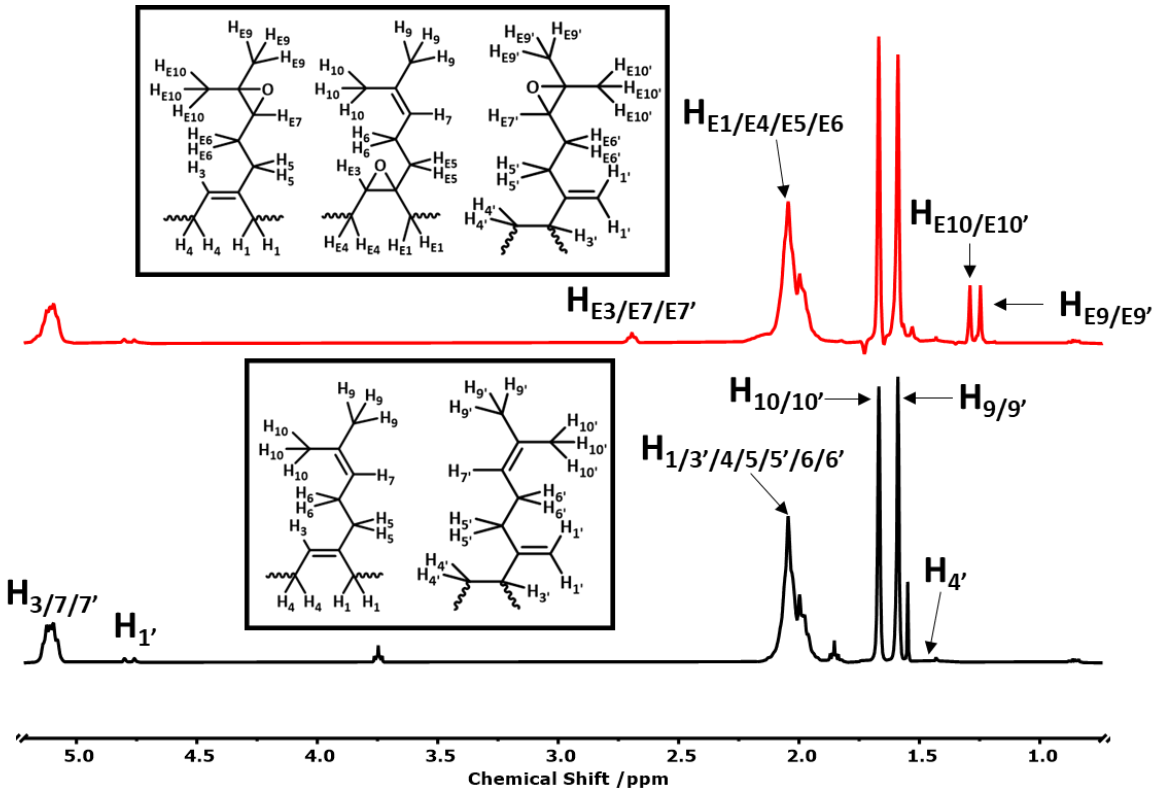

Figure 3.4: Stacked ^{1}H NMR spectra (400 MHz, $CDCl_3$) of poly(myrcene) (bottom-black) and epoxidised poly(myrcene) (red-top).

As it can be seen in the stacked ^{1}H NMR spectra in Figure 3.4 above, it is clear that the epoxidation reaction was successful. This is evidenced by the appearance of a peak at 2.69

ppm, which corresponds to i) H_{E3}, the ring hydrogen of the 3,2-epoxide derived from epoxidation of the backbone alkene of a 4,1 myrcene repeat unit (*cis or trans)* and ii) both H_{E7} and $H_{E7'}$, the ring hydrogens of the 7,8-epoxide derived from epoxidation of the pendant 7,8 alkene of either a 4,1 or 4,3 myrcene repeat unit. Moreover, the appearance of two new peaks at 1.25 ppm and 1.29 ppm can also be seen in Figure 3.4, which correspond to the hydrogens ($H_{E9/9'}$ and $H_{E10/E10'}$) of the two methyl groups beside the 7,8-epoxide in both the (4,1) and the (4,3) microstructure of poly(myrcene). It is worth noting that the low relative reactivity/chemoselectivity of epoxidation towards the 1,1-disubstituted 2,1-alkene bond present when 4,3 enchainment occurs, coupled with the low percentage (7 %) of this microstructure in PM1, means that the extent of epoxidation of the 2,1-alkene bond is expected to be insignificant (Figure 3.5) and as such any new peaks arising due to 2,1 epoxidation are expected to be indistinguishable from the baseline noise of the ^{1}H NMR spectrum. [13]

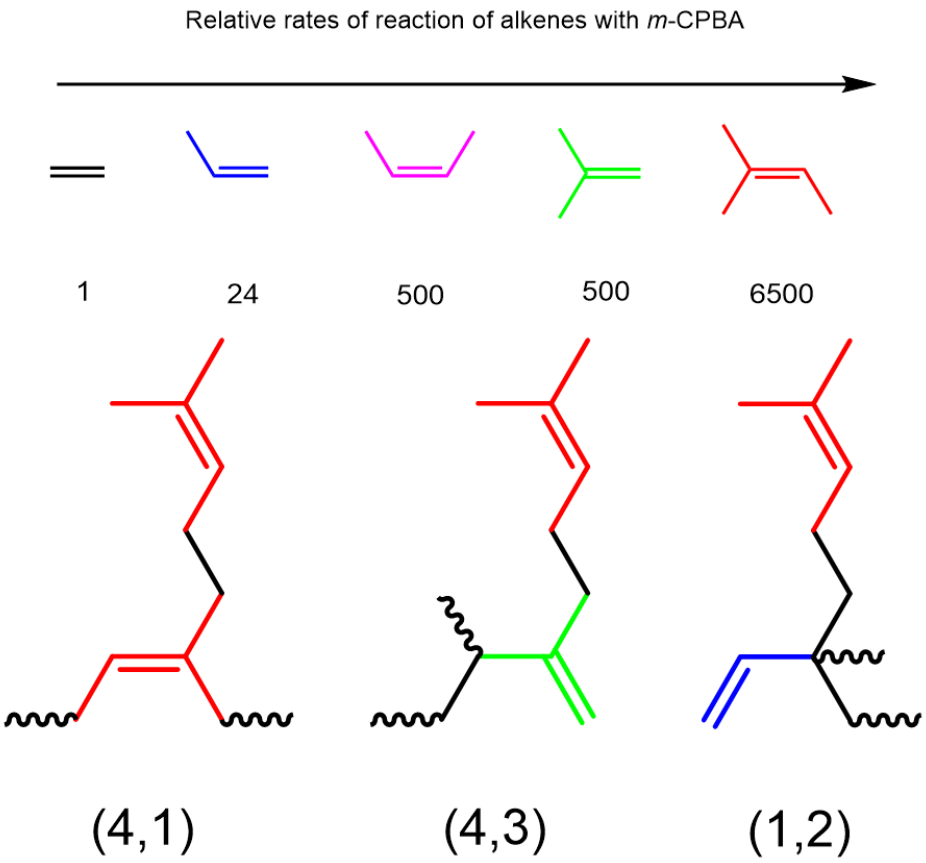

Figure 3.5: Colour-coded diagram of the different possible microstructures of poly(myrcene), relating each of the double bonds to their relative rate of epoxidation.

The extent (and selectivity) of epoxidation of polymyrcene can be calculated using the integral values of the ^{1}H NMR spectra (Table 3.2).

Table 3.2: Summary of integral data for the epoxidised poly(myrcene) sample – PM1 – from the ^{1}H NMR spectrum in Figure 3.4.

Assigned Region	Chemical Shift Range /ppm	Proton Assignment	Integration
M1	1.20 – 1.33	$H_{E9} + H_{E9'} + H_{E10} + H_{E10'}$	11.51
M2	2.65 – 2.75	$H_{E3} + H_{E7} + H_{E7'}$	2.93
M3	4.70 – 4.85	$H_{1'}$	2.00
M4	5.00 – 5.20	$H_3 + H_7 + H_{7'}$	24.14

The situation is rather complex since the epoxidised polymyrcene contains 5 probable repeat units, namely: unreacted 4,1- and 4,3- myrcene repeat units, 4,1- repeat units that are epoxidised at either the 2,3- (backbone) or 7,8- (pendant) alkene and 4,3- repeat units that are epoxidised at the 7,8- alkene (see inset structures, Figure 3.4).

3.2.2.1.1 Calculation of Total Extent of Epoxidation

Although the target extent of epoxidation is described in terms of % double bonds, the total extent of epoxidation will initially be calculated in terms of the % repeat units that have been epoxidised. Thus, the peaks corresponding to assigned regions M2, M3 and M4 (see table 3.4) include signals from each of the possible repeat units in the epoxidised polymer. However, M2 and M4 comprise overlapping signals from multiple protons, and in some cases, protons from the same type of repeat unit appear in different regions. For example, M2 comprises contributions from all three epoxidised repeat units – with 1H from each type of unit contributing to the M2 integral. The underpinning rationale for the initial calculation (Equation 3.5) is that it should calculate a value that is the sum of the integrals arising from the contribution of 1H from each type of repeat unit – an integral value that represents the sum of the contributions of each type of repeat unit.

$$|\text{All Repeat Units}| = \frac{|M2| + \left|\frac{M3}{2}\right| + |M4|}{2} = \frac{2.93 + \frac{2.00}{2} + 24.14}{2} = 14.0$$

Equation 3.5: Equation used to calculate a nominal integral for the relative number of myrcene subunits.

As mentioned above, the peak at 2.65 – 2.75 ppm (M2) comprises a contribution of 1H from each of the three epoxidised repeat units and thus can be used to calculate the overall extent of epoxidation in terms of the percentage of myrcene repeat units that have been epoxidised. – see Equation 3.6.

$$\% \text{ of Myrcene Units Epoxidised} = \frac{|M2|}{|\text{All Repeat Units}|} \text{ X } 100 = \frac{2.93}{14.0} \text{ X } 100 = 21\%$$

Equation 3.6: Equation used to calculate the percentage of myrcene subunits that have been epoxidised.

The calculation above indicates that 21% of the myrcene repeat units contain an epoxidised alkene. Given that each polymyrcene repeat unit comprises two double bonds, we can conclude that approximately 10.5% of double bonds have been epoxidised, in excellent agreement with the expected value of 10%.

3.2.2.1.2 Calculation of Selectivity of Epoxidation

It is also possible to use ^{1}H NMR data to estimate the chemoselectivity of epoxidation and specifically, what proportion of the epoxidation occurs at the pendant -7,8 alkene bond. Thus, the peaks at 1.25 ppm and 1.29 ppm (Region M1 Table 3.2) arise due to the presence of the protons of the -CH_3 groups bonded directly to the (7,8) epoxide ring. This allows the use of Equation 3.7 to calculate the percentage of all epoxidations that occurred at the 7,8-double bond.

$$\% \text{ 7,8-Epoxide Units} = \frac{\left|\frac{M1}{6}\right|}{|M2|} \text{ X } 100 = \frac{\frac{11.51}{6}}{2.93} \text{ X } 100 = 66\%$$

Equation 3.7: Equation used to calculate the percentage of epoxidation that occurred at the 7,8-double bond.

As it can be seen in Equation 3.7 above, there is significant selectivity towards the formation of 7,8-epoxide (66%) compared to the formation of 3,2-epoxides (34%), based on the assumption that an insignificant amount of 2,1-epoxides are synthesised due to the low percentage of 4,3-microstructres and the greatly reduced relative rate of epoxidation of a disubstituted 2,1 alkene double bond, present when 4,3-polymerisation occurs, relative to the trisubstituted bonds present. Based on the aforementioned literature [13], this was

perhaps surprising as both the 3,2-double bond and the 7,8-double bond are trisubstituted and one might expect that, since both double bonds are equally nucleophilic, both the 7,8 and 2,3 epoxides would be present in similar amounts. This would suggest that the increased selectivity of the epoxidation reaction towards the 7,8-alkene could simply be due to the increased steric hindrance associated with the epoxidation of a double bond present on the backbone, meaning the epoxidation of the 7,8-double bond is kinetically more favourable than the 3,2-double bond. However, based on the literature regarding the epoxidation of steroids [18] whereby a decreased selectivity for highly inflexible double bonds (even those that are trisubstituted) was seen, we suggest that there is an increased activation energy for epoxidation of the 3,2-double bond not only due to the increased steric hindrance but also due to the reduced flexibility of the backbone double bond compared to the pendant double bond. Literature reports describing the epoxidation of poly(myrcene) indicate results that are consistent with those observed in the current project. [11]

3.2.2.2 The Epoxidation of Poly(Myrcene) Prepared in the Presence of a Polar Modifier – P(M)2

Due to large differences in microstructure between homopolymers of myrcene that are prepared in the absence and presence of a polar modifier, and given that a key aim of this work was to synthesise and epoxidise an analogue of sSBR-containing myrcene – where polar modifiers are used to 'randomise' the incorporation of styrene and butadiene – it was decided to epoxidise a sample of polymyrcene that had been synthesised in the presence of a polar modifier (TMEDA). This would allow a further investigation of the chemoselectivity of the epoxidation of poly(myrcene) and also provide an opportunity to identify key peaks in the resulting ^{1}H NMR spectrum and to use them to estimate the extent and selectively of epoxidation. As expected, the use of TMEDA in the polymerisation results in a higher proportion of 4,3- microstructure and the addition of 1,2-repeat units. Whereas PM1 (synthesised in the absence of TMEDA) has a microstructure comprising 93 % 4,1- and 7 % 4,3-, PM2 has a microstructure comprising 39 % 4,1-, 58 % 4,3- and 3 % 1,2-. These values were obtained using ^{1}H NMR data (Figure 3.6) and are in line with expectations based on the observed change in the microstructure of polyisoprene when polymerised in the presence of TMEDA. [19] [20] [21] The change in microstructure has significant implications. Firstly, this

change will impact the flexibility of the polymer backbone resulting in massive differences its physical and thermal properties. [19] [22] [23] Secondly, it was expected that the proportion of epoxidation that occurred on the pendant group would increase because the shift from (4,1) to (4,3) microstructures would reduce the number of trisubstituted backbone double bonds and replace them with disubstituted vinyl double bonds, for which the *m*-CPBA has a lower selectivity, according to the literature. [13]

The epoxidation of PM2 was once again carried out using the general procedure described in Section 3.4 with a target 28.4%.

Table 3.3: Conditions used for the epoxidation of PM2.

Polymer Used	Mass of Polymer /g	Volume of DCM /mL	Mass of *m*-CPBA /g	Target Epoxidation / % of 7,8 Double Bonds
PM2	0.25	20	0.12	28.4

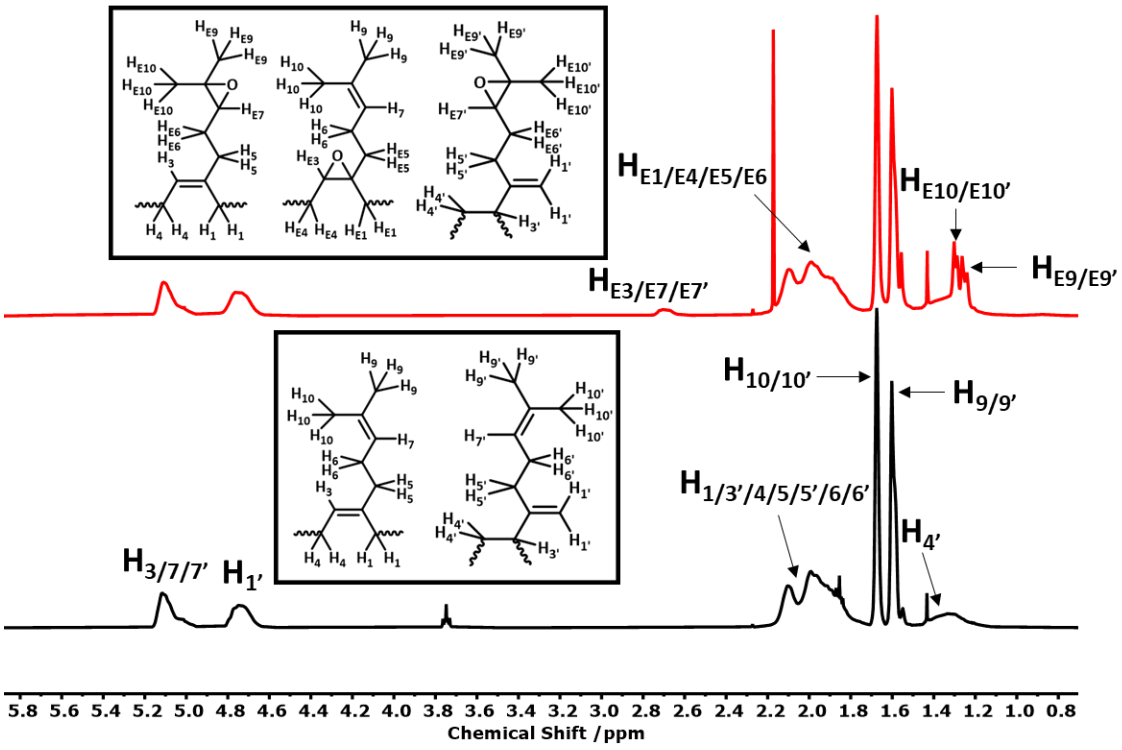

Figure 3.6: Stacked ^{1}H NMR spectra (400 MHz, $CDCl_3$) of poly(myrcene) prepared in the presence of TMEDA - PM2 - (bottom-black) and epoxidised PM2 (red-top).

The stacked ^{1}H NMR spectra shown in Figure 3.6 above conclusively illustrate that the epoxidation reaction was successful, as evidenced by the reduction in the alkene peaks and the appearance of a broad peak at 2.69 ppm, which corresponds to i) H_{E3}, the ring hydrogen

of the 3,2-epoxide derived from epoxidation of the backbone alkene of a 4,1 myrcene repeat unit (*cis or trans)* and ii) both H_{E7} and $H_{E7'}$, the ring hydrogens of the 7,8-epoxide derived from epoxidation of the pendant 7,8 alkene of all microstructures. Moreover, the appearance of new peaks at 1.25 ppm and 1.29 ppm can also be seen in spectrum 3.6, which correspond to the hydrogens (H_{16} and H_{17}) of two methyl groups bonded to the 7,8-epoxide.

Table 3.4: Summary of integral data for the epoxidised poly(myrcene) sample – PM2 - from the ^{1}H NMR spectrum in Figure 3.6.

Assigned Region	Chemical Shift Range /ppm	Proton Assignment	Integration
M1	1.20 – 1.33	$H_{E9} + H_{E9'} + H_{E10} + H_{E10'}$	7.14
M2	2.60 – 2.78	$H_{E3} + H_{E7} + H_{E7'}$	1.00
M3	4.63 – 4.83	$H_{1'}$	4.62
M4	4.95 – 5.20	$H_3 + H_7 + H_{7'}$	5.01

As mentioned above, when myrcene is polymerised in the presence of TMEDA, a small fraction (≤ 5%) of 1,2-polymyrcene is formed. The 1,2-repeat units possess a 7,8-trisubstituted alkene along with a very low-reactive (towards epoxidation) monosubstituted alkene (see figure 3.5). There is no expectation that the monosubstituted alkene would undergo epoxidation, but the 7,8-alkene of a 1,2 repeat unit will be as reactive towards epoxidation as the 7,8 alkene of other microstructures.

Initial calculations to obtain the overall degree of epoxidation and the selectivity of epoxidation were carried out using exactly the same method as described above for PM1 using the integrated peaks within the preselected regions in the ^{1}H NMR spectra (Figure 3.6 and Table 3.4 above). Any contribution from 1,2- repeat units was ignored given the low fraction of 1,2- units present. The calculation making use of regions M2, M3 and M4 (Table 3.6) indicated that 24% of the total number of repeat units were epoxidised, however the subsequent calculation using M1 and M2 indicated that 117 % of the epoxidation occurred at the 7,8-alkene. Whilst the value of 24% for the total extent of epoxidation is in good agreement with the target value of 28.4%, the value of 117% for selectivity towards the 7,8 alkene is clearly incorrect and some other factor must be affecting the accuracy of this calculation. Such factors relate to the presence of 40% 4,3-microstructure, which in turn means that some epoxidation of the 2,1- (less reactive disubstituted) double bond of the 4,3 repeat unit is possible. There is no distinguishable peak for the resulting 2,1-epoxide, although

broadening of the peak at 2.69 ppm could indicate the presence of an overlapping peak relating to the 2,1-epoxide. This means that when we use this data to calculate epoxidation selectivity, we assume that this 2,1-double bond epoxidation does not occur – even though we would definitely expect some of these double bonds to react – so any values that are obtained should be noted to contain this added degree of error, meaning that the overall epoxidation percentage may be overestimated as the 2,1-epoxide contains 2 protons rather than one, meaning the integral for the epoxide units may be exaggerated.

A more likely (and obvious) source of error in calculating selectively towards the 7,8 alkene can be found in Region M1 (Table 3.4 and Figure 3.6). Above in Section 3.2.1, Equation 3.7 uses the integrals of peaks at 1.20-1.30 ppm (Region M1), which can be ascribed to the CH_3 protons of the methyl groups bonded to the 7,8-epoxide. In the case of PM2, with a significantly increased fraction of 4,3-microstructure (40%), a broad peak is observed in the same region and overlapping with the peaks ascribed to the 7,8 epoxide. It is believed that the broad peak arises due to methylene protons $H_{4'}$ on the backbone of 4,3 repeat units. Therefore, the integral for the 7,8-epoxide methyl peaks will be significantly overestimated leading to the incorrect value of 117% for the selectively of epoxidation towards the 7,8 alkene.

It was therefore decided to adopt an alternative approach to calculate % epoxidation of the 7,8-alkene, which accounted for the overlapping peaks at M1. Thus, it is assumed that the sum of the integrals of M3 and M4 in PM2 (the unepoxidised sample) is equal to the sum of the integrals of M2, M3 and M4 in EPM2 (the epoxidised sample) and therefore the integrals for each spectrum are normalised such that the sum of each set of integrals mentioned above are given an equal total value. It can then also be assumed that the integral of protons $H_{4'}$, which are unaffected by the epoxidation reaction, will have the same (normalised) value for both PM2 and EPM2 and therefore this integral value can be subtracted from the integral for Region M1 to provide a more accurate integral value for the peaks ascribed to the CH_3 protons of the methyl groups bonded to the 7,8-epoxide – see Table 3.5 below. Thus a corrected integral value for M1 (EPM2) is equal to 9.28 – 4.22 = 5.06 and this value can be used with an integral value of 1.0 for M2 in Equation 3.7 to calculate a value of 84.3% for the selectivity of epoxidation towards the 7,8 pendant alkene. Thus, to be clear of all the epoxidation that occurs on EPM2, 84% of the epoxidation occurs at a 7,8 double bond.

Table 3.5: Summary of relative integral data for the unepoxidised and epoxidised poly(myrcene) sample – PM2 - from the ^{1}H NMR spectrum in Figure 3.6, whereby the new integral information will be used to increase the accuracy of the epoxidation selectivity calculation.

Assigned Region	Chemical Shift Range /ppm	Proton Assignment		Integration	
		PM2	EPM2	PM2	EPM2
M1	1.20 – 1.40	$H_{4'}$	$H_{E9} + H_{E9'} + H_{E10} + H_{E10'} + H_{4'}$	4.22	9.28
M2	2.60 – 2.78	-	$H_{E3} + H_{E7} + H_{E7'}$	-	1.0

Not only is this value plausible (unlike a value of 117%), but it is also in line with expectations. It was expected that this value would be higher than for the epoxidation of PM1, due to the increased proportion of 4,3-microstructure in EPM2, which sees trisubstituted double bonds in the polymer backbone being replaced by disubstituted alkene bonds, which have a lower relative rate of epoxidation using *m*-CPBA. This in turn results in a higher degree/selectivity of epoxidation (84% v 66%) towards the pendant trisubstituted 7,8 alkene bonds.

In summary, when a sample of poly(myrcene) is synthesised in the presence of a polar modifier such as TMEDA, as it would be if myrcene were to be incorporated into an analogue of sSBR, the resulting changes in microstructure – namely a significant increase in 4,3-units – results in a significantly higher degree of epoxidation of the pendant 7,8-alkene This suggests that this system of selective epoxidation will be highly applicable to the car tyre industry as the amount of control that can be achieved should allow for polar functional groups to be selectively added into the polymer chains at the most sterically available position, to facilitate increased interaction between the silica filler particles and polymer chains with minimal effects on the physical properties that are dominated by the polymer backbone (such as T_g), which are highly desired for tyre formulations.

3.2.3 – The Epoxidation of a Poly(Myrcene-*co*-Styrene) Copolymer – PMS2

Although polystyrene cannot be epoxidised using *m*-CPBA, it was decided to explore whether the incorporation of styrene in a myrcene-styrene copolymer would have any impact on the epoxidation of the myrcene repeat units. This is of particular relevance given that the key aim of the work described herein is to prepare an analogue of sSBR (a random copolymer of styrene and butadiene) containing myrcene. Thus, PMS2 – a copolymer of myrcene and styrene polymerised in the presence of two equivalents of TMEDA with respect to the BuLi

added – was epoxidised using the general procedure described above, with the stoichiometry of the reaction designed to target the epoxidation of 100 % of 7,8 alkene bonds. The full experimental of this epoxidation reaction can be found in Section 3.4.

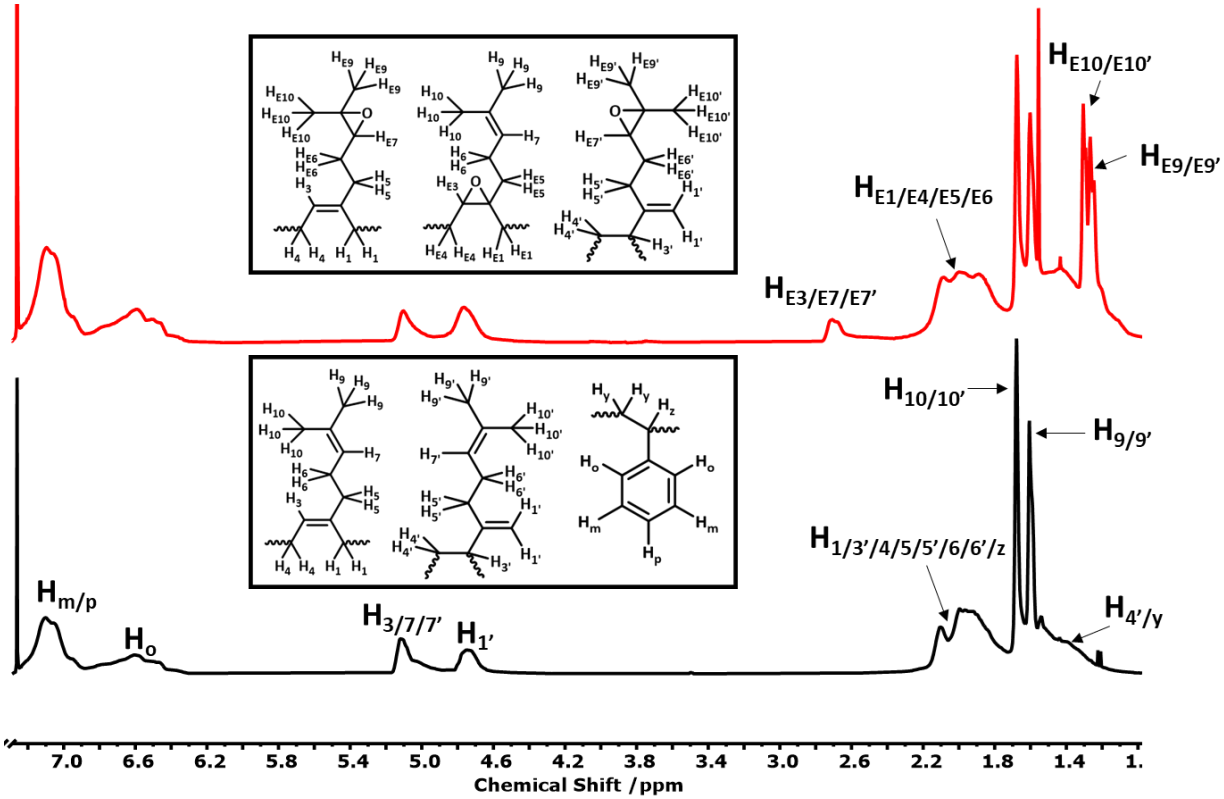

Figure 3.7: Stacked ^{1}H NMR spectra (400 MHz, $CDCl_3$) of poly(myrcene-co-styrene) prepared in the presence of TMEDA -PMS2 - (bottom-black) and epoxidised PMS2 – EPMS1 (red-top).

This epoxidation reaction was once again successful, as can be seen in the stacked ^{1}H NMR spectra (Figure 3.7), shown by the appearance of peaks at 1.27 ppm, 1.31 ppm and 2.70 ppm, although the peaks are very different in shape compared to epoxidised homopolymyrcene – potentially due to the different diad/triad environments that will be present due to the incorporation of styrene into the copolymer.

Table 3.6: Summary of integral data for the epoxidised poly(myrcene-co-styrene) sample – PSM2 – from the ^{1}H NMR spectrum in Figure 3.7.

Assigned Region	Chemical Shift Range /ppm	Proton Assignment	Integration
M1	1.20 – 1.34	$H_{E9} + H_{E9'} + H_{E10} + H_{E10'}$	6.12
M2	2.55 – 2.78	$H_{E3} + H_{E7} + H_{E7'}$	1.00
M3	4.60 – 4.90	$H_{1'}$	1.91
M4	4.90 – 5.20	$H_3 + H_7 + H_{7'}$	1.42

The total extent of epoxidation and the selectivity of epoxidation towards the 7,8 alkene was calculated with a similar (dual) approach adopted to that described above for the characterisation of EPM2. Using Equations 3.5, 3.6 and 3.7 and the integrated peaks within the preselected regions in the ^{1}H NMR spectra (as shown in Table 3.6 above), the total extent of epoxidation of the sample was calculated to be 42% (of all double bonds) and approximately 102% of those alkene bonds were epoxidised on the 7,8 alkene. The total extent of epoxidation (at 42%) was somewhat lower than the target of 50% but considered satisfactory for the purposes of this exercise. There are two possible explanations for these observations. Firstly, it is possible that a higher target extent of epoxidation would require longer reaction times to go to completion and in this case the reaction was not extended beyond that used in previous epoxidation reactions and secondly, completion may have been inhibited due to decreased solubility of the polymer in DCM as the epoxidation proceeded to higher degrees. However, an overlap in the M1 region of the peaks corresponding to both the styrene backbone protons (H_y) and the backbone methylene protons ($H_{4'}$) of the 4,3-microstructure of polymyrcene with signals representing the protons on the two methyl groups next to the 7,8-epoxide ($H_{E9} + H_{E9'} + H_{E10} + H_{E10'}$) results in an impossibly large value for the % 7,8-epoxidation. To overcome this error, the same assumptions and approach was adopted as described above for the characterisation of EPM2, whereby the sum of the integral values of M3 and M4 in PMS2 and the sum of the integrals of M2, M3 and M4 in EPMS1 are assumed to be identical and each normalised to a total integral value of 1.0. The integral values of $H_{4'}$ and H_y can then be subtracted from M1 to give a more accurate value for the % 7,8 epoxidation (see Table 3.9 for integral values). The comparative analysis was carried out using Equations 3.5, 3.6 and 3.7 and the normalised integration data contained in Table 3.9 (which was calculated using the integral values shown in Tables 3.7 and 3.8).

Table 3.7: Summary of relative integral data for the unepoxidised poly(myrcene-co-styrene) sample – PMS2 – from the ^{1}H NMR spectrum in Figure 3.7, whereby the new integral information will be used to increase the accuracy of the epoxidation selectivity calculation.

Assigned Region	Chemical Shift Range /ppm	Proton Assignment	Integration
M1	1.10 – 1.35	$H_{4'} + H_y$	1.35
M2	2.40 – 2.78	-	0.16
M3	4.60 – 4.90	$H_{1'}$	1.50
M4	4.90 – 5.20	$H_3 + H_7 + H_{7'}$	1.86

Table 3.8: Summary of relative integral data for the epoxidised poly(myrcene-co-styrene) sample – EPMS1 – from the ^{1}H NMR spectrum in Figure 3.7, whereby the new integral information will be used to increase the accuracy of the epoxidation selectivity calculation.

Assigned Region	Chemical Shift Range /ppm	Proton Assignment	Integration
M1	1.10 – 1.35	$H_{E9} + H_{E9'} + H_{E10} + H_{E10'} + H_{4'} + H_y$	5.74
M2	2.40 – 2.78	$H_{E3} + H_{E7} + H_{E7'}$	1.00
M3	4.60 – 4.90	$H_{1'}$	1.45
M4	4.90 – 5.20	$H_3 + H_7 + H_{7'}$	1.08

Table 3.9: Summary of the integral differences between PMS2 and EPMS1, whereby the values were calculated by subtracting the integral values of each defined region in Table 3.7 away from the values in Table 3.8.

Assigned Region	Chemical Shift Range /ppm	Integral Difference Between Epoxidised and Unepoxidised
ΔM1	1.10 – 1.35	+4.39
ΔM2	2.55 – 2.78	+0.84
ΔM3	4.60 – 4.90	-0.05
ΔM4	4.90 – 5.20	-0.78

Using Equation 3.7, with both the integral values for ΔM1 (to calculate the 7,8 double bond epoxidation percentage) and ΔM3 ΔM1 (to calculate the 2,1 double bond epoxidation percentage), we can calculate that approximately 3.2% of the epoxidation occurred on the 2,1 double bond, 87% occurred on the 7,8-double bond and 9.8% occurred on the 3,2-double bond. The value for the 7,8-epoxidation is once again higher than we would expect from the literature, due to the high epoxidation degree, but is in line with the trends observed in the epoxidation of a myrcene homopolymer that had been synthesised in the presence of a polar modifier. Once again, due to the high complexity of the calculations that were used for this

copolymer, the difference between our observed 7,8-epoxidation percentage and the expected 7,8-epoxidation may be explainable by the additional errors. However, due to the large difference between the expected and observed values and the continued high 7,8-epoxidation percentage that we have observed across a range of polymers, we can suggest that these values are representative of the chemoselectivity that is brought about by the utilisation of *m*-CPBA for epoxidation.

3.2.4 The Epoxidation of Myrcene-Butadiene Copolymers

A key aim of this work is to produce an analogue of sSBR in which a portion of the butadiene monomer is replaced with myrcene – in effect a statistical terpolymer of styrene, butadiene and myrcene – and to epoxidise that terpolymer. Thus, a series of statistical copolymers of butadiene and myrcene were synthesised in order to explore the selectivity of the epoxidation of the alkene bonds in a butadiene-myrcene copolymer.

3.2.4.1 Epoxidation of PMB3

Initially, the epoxidation of a myrcene-butadiene copolymer that had been prepared in a non-polar solvent in the absence of any polar modifier – PMB3 (see Section 3.4) – was investigated. PMB3 was epoxidised using the general procedure detailed in Section 3.4 using a molar ratio of *m*-CPBA to alkene bond, to enable the epoxidation of 11 % of all alkene bonds present.

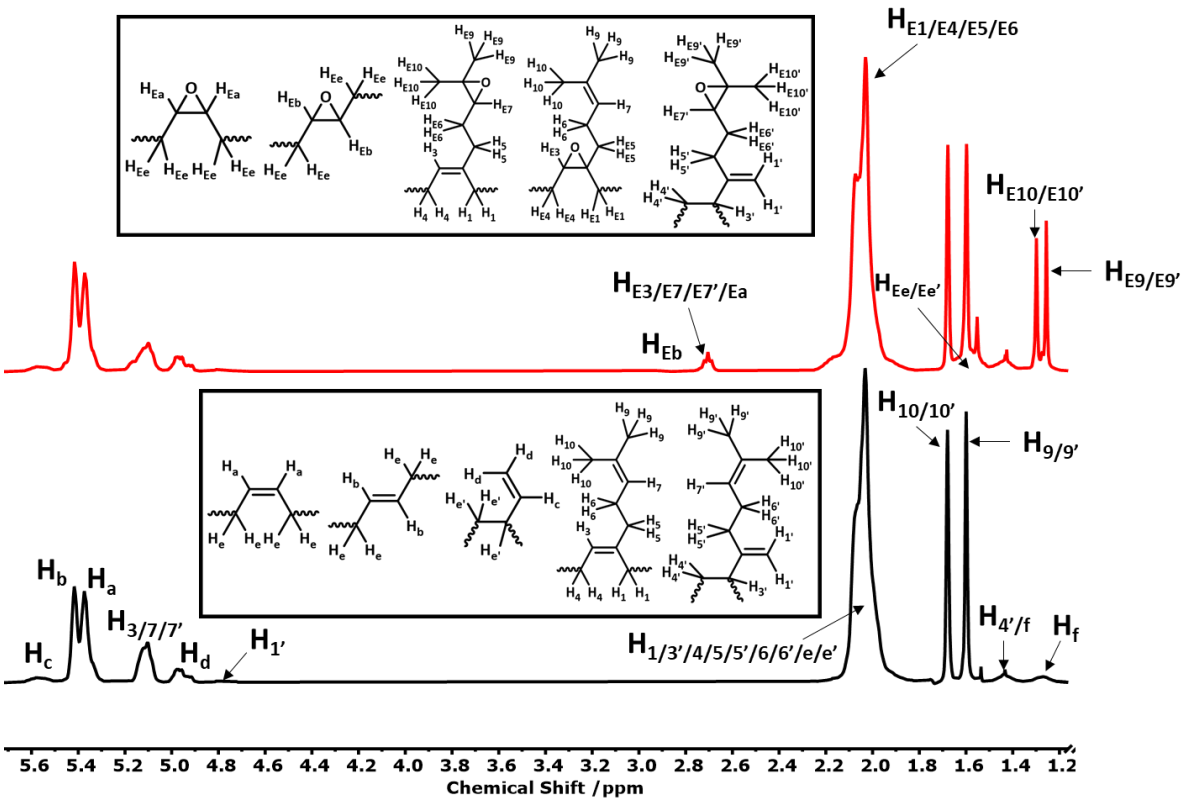

Figure 3.8: Stacked ^{1}H NMR spectra (400 MHz, $CDCl_3$) of poly(myrcene-co-butadiene) prepared in the absence of TMEDA – PMB3 - (bottom-black) and epoxidised PMB3 – EPMB1 (red-top).

New peaks that have appeared at 1.26 ppm ($H_{E9/E9'}$), 1.31 ppm ($H_{E10/E10'}$), 2.70 ppm ($H_{E3/E7/E7'/Ea}$) and 2.93 ppm (H_b), shown in the ^{1}H NMR spectrum in Figure 3.8 above, conclusively show that the epoxidation reaction has been successful, with the epoxidation of both butadiene and myrcene double bonds. Accurate quantitative analysis of the epoxidation reaction becomes increasing complex. However, below, attempts will be made to calculate i) the total extent of epoxidation, ii) the relative extent of epoxidation of butadiene and myrcene double bonds and iii) the overall selectivity of epoxidation towards the 7,8 double bond of myrcene. The key assigned regions and corresponding ^{1}H NMR peak integration values for the (epoxidised) myrcene-butadiene copolymer can be seen in Table 3.10 below.

Table 3.10: Summary of integral data for the epoxidised poly(myrcene-co-butadiene) sample – PMB3 – from the ^{1}H NMR spectrum in Figure 3.8.

Assigned Region	Chemical Shift Range /ppm	Proton Assignment	Integration
M1	1.20 – 1.35	$H_{E9} + H_{E9'} + H_{E10} + H_{E10'}$	6.46
M2-B1	2.63 – 2.78	$H_{E3} + H_{E7} + H_{E7'} + H_{Ea}$	1.39
B2	2.88 – 2.98	H_{Eb}	0.19
M3	4.70 – 4.85	$H_{1'}$	0.41
B3	4.88 – 5.03	H_d	2.00
M4	5.03 – 5.20	$H_3 + H_7 + H_{7'}$	4.27
B4	5.28 – 5.48	$H_a + H_b$	14.19

3.2.4.1.1 Calculation for Total Extent of Epoxidation

Having assigned all of the relevant regions of the ^{1}H NMR spectrum, the integration values can be used to calculate the overall extent of epoxidation, following the same approach as described earlier. As explained above in Section 3.2.2.1.1, although the target extent of epoxidation is described in terms of % double bonds, the total extent of epoxidation will initially be calculated in terms of the % repeat units that have been epoxidised. In the case of PMB3, there are now multiple sites for epoxidation, on two different diene repeat units, each of which has multiple possible microstructures. Again, the underpinning rationale is to calculate a value that is the sum of the integrals arising from the contribution of 1H from each type of repeat unit (epoxidised or not) – an integral value that represents the sum of the contributions of each type of repeat unit. Equation 3.8 (below) is used to estimate an integral value for the total number of repeat units.

$$|\text{All Repeat Units}| = \frac{|\text{M2-B1}|+|\text{B2}|+\left|\frac{\text{M3}}{2}\right|+|\text{B3}|+|\text{M4}|+|\text{B4}|}{2}$$

$$|\text{All Repeat Units}| = \frac{1.39 + 0.19 + \frac{0.41}{2} + 2.00 + 4.27 + 14.19}{2} = 11.1$$

Equation 3.8: Equation used to calculate a nominal integral for the relative number of total subunits.

To estimate the % of epoxidised repeat units, it is necessary to assume that the integral of the peak ascribed to the trans-butadiene epoxide (H_{Eb}) is equal to the integral of the peak ascribed to the cis-butadiene epoxide (H_{Ea}) – which has previously been shown to the case. Using this, we are able to establish that the total extent of epoxidation is given by Equation 3.9.

$$\text{Percentage of Repeat Units Epoxidised} = \frac{|\text{M2-B1}|}{|\text{All Repeat Units}|} \text{ X } 100\ \%$$

$$\text{Percentage of Repeat Units Epoxidised} = \frac{1.39}{11.1} \text{ X } 100\ \%$$

$$\text{Percentage of Repeat Units Epoxidised} = 13\%$$

Equation 3.9: Equation used to calculate the percentage of subunits that have been epoxidised.

From the calculation above, the overall percentage of repeat units that had been epoxidised that was calculated – 13% – was slightly higher than the expected value of 11 %, although as already discussed, this can be explained by the associated errors that we have previously identified.

3.2.4.1.2 Calculation of Selectivity of Epoxidation Towards Myrcene Units

Clearly it is of significant interest to identify the extent to which the epoxidation reaction is selective towards myrcene in preference to butadiene. Once again, assuming that the degree of epoxidation of cis-1,4- and trans-1,4-butadiene is approximately equal and therefore the integral value of $H_{Eb} = H_{Ea}$, it is possible to subtract the contribution of H_{Ea} from the integration of the M2-B1 peak to obtain the integral for $H_{E3} + H_{E7} + H_{E7'}$, which are found in the various repeat units of epoxidised myrcene. With these values, the extent to which the epoxidation reaction is selective towards myrcene units in preference to butadiene units can be calculated – see Equations 3.10 and 3.11.

$$|\text{Epoxidised Myrcene Units}| = |\text{M2-B1}| - |\text{B2}| = 1.39 - 0.19 = 1.20$$

Equation 3.10: Equation used to calculate a nominal integral for the relative number of epoxidised myrcene subunits.

$$\frac{|\text{Epoxidised Myrcene Units}|}{|\text{All Epoxidised Units}|} \text{ X } 100\ \% = \frac{1.20}{1.39} \text{ X } 100\ \% = 86\%$$

Equation 3.11: Equation used to calculate the percentage of epoxidised subunits which are epoxidised myrcene.

The calculations above illustrate that of all the repeat units epoxidised, 86% of those repeat units were myrcene and only 14% were butadiene repeat units. However, the selectivity

towards myrcene is even greater when the composition of this copolymer is considered. PMB3 comprises 26 mol % of myrcene, with butadiene being the major component at 74 mol %. To get a true sense of the selectivity towards the epoxidation of myrcene, it is possible to calculate the outcome of the epoxidation of a copolymer comprising equal numbers of myrcene and butadiene units – see equation 3.12.

$$\text{Relative Selectivity of Myrcene} = \frac{\text{Myrcene epoxidation percentage x Butadiene mol \%}}{\text{Myrcene mol \% x Butadiene epoxidation percentage}}$$

$$\text{Selectivity for Myrcene} = \frac{\text{\% epoxidised units derived from myrcene/mol \% myrcene}}{\text{\% epoxidised units derived from butadiene/mol \% butadiene}}$$

$$\text{Selectivity for Myrcene} = \frac{86.3/26}{13.7/74} = 18$$

Equation 3.12: Equation used to calculate the selectivity of the epoxidation reaction towards the myrcene subunits relative to the butadiene subunits.

The calculation shown in Equation 3.12 indicates the true selectivity of the epoxidation reaction towards myrcene and shows that the reactivity of epoxidation towards a myrcene repeat unit is 18 times that of butadiene. Thus, the epoxidation of a myrcene butadiene copolymer containing equal moles of each monomer would be expected to result in a product in which 95% of the epoxidation occurred on a myrcene repeat unit.

3.2.4.1.3 Calculation of Selectivity of Epoxidation

It is also possible to use NMR spectroscopy data to estimate the proportion of the epoxidation of myrcene repeat units that occurs specifically at the pendant -7,8 alkene bond. Thus, the sharp peaks at 1.25 ppm and 1.29 ppm (M1 Table 3.10) arise due to the presence of the protons of the -CH_3 groups bonded directly to the 7,8-epoxide ring - $H_{E9} + H_{E9'} + H_{E10} + H_{E10'}$. It is not possible to use Equation 3.7 in this case because the two peaks mentioned above overlap with peaks for H_f and $H_{4'}$, however, it is possible to use a modified version of equation 3.7 – namely equation 3.13.

$$\text{Percentage of Myrcene 7,8-Epoxide Units} = \frac{\left|\frac{M1 - B3/2}{6}\right|}{|M2B1 - B2|} \text{ X } 100\ \%$$

$$\text{Percentage of Myrcene 7,8-Epoxide Units} = \frac{\frac{6.46 - 1.0}{6}}{1.39 - 0.19} \text{ X } 100\ \% = 76\%$$

Equation 3.13: Modified equation used to calculate the percentage of epoxidation that occurred at the 7,8-double bond in a myrcene-butadiene copolymer.

As calculated in Equation 3.13 above, 76 % of the epoxidation that occurred on the myrcene subunits occurred on the 7,8-double bond. While slightly higher than the previous epoxidation percentage that occurred on the 7,8-double bond of the homopolymer of polymyrcene – PM1 – this value is in line with expectations and represents the selectivity effect between the backbone double bond and the pendant double bond, which we have ascribed to be due to an increased steric availability and a reduced activation energy to the increased flexibility of the 7,8-double bond.

3.2.4.2 Epoxidation of PMB2

To investigate the impact of butadiene/myrcene microstructure on the selectivity of epoxidation towards myrcene in a myrcene butadiene copolymer, epoxidation of such a copolymer (PMB2) that had been synthesised in the presence of a polar modifier (TMEDA) was carried out. Moreover, the addition of TMEDA to the polymerisation will give a copolymer with a microstructure matching that of the eventual target of this study – a terpolymer analogue of sSBR containing a portion of myrcene. Thus (PMB2**)** was epoxidised using the same general procedure as described above, with a target extent of epoxidation of 100% 7,8 double bonds.

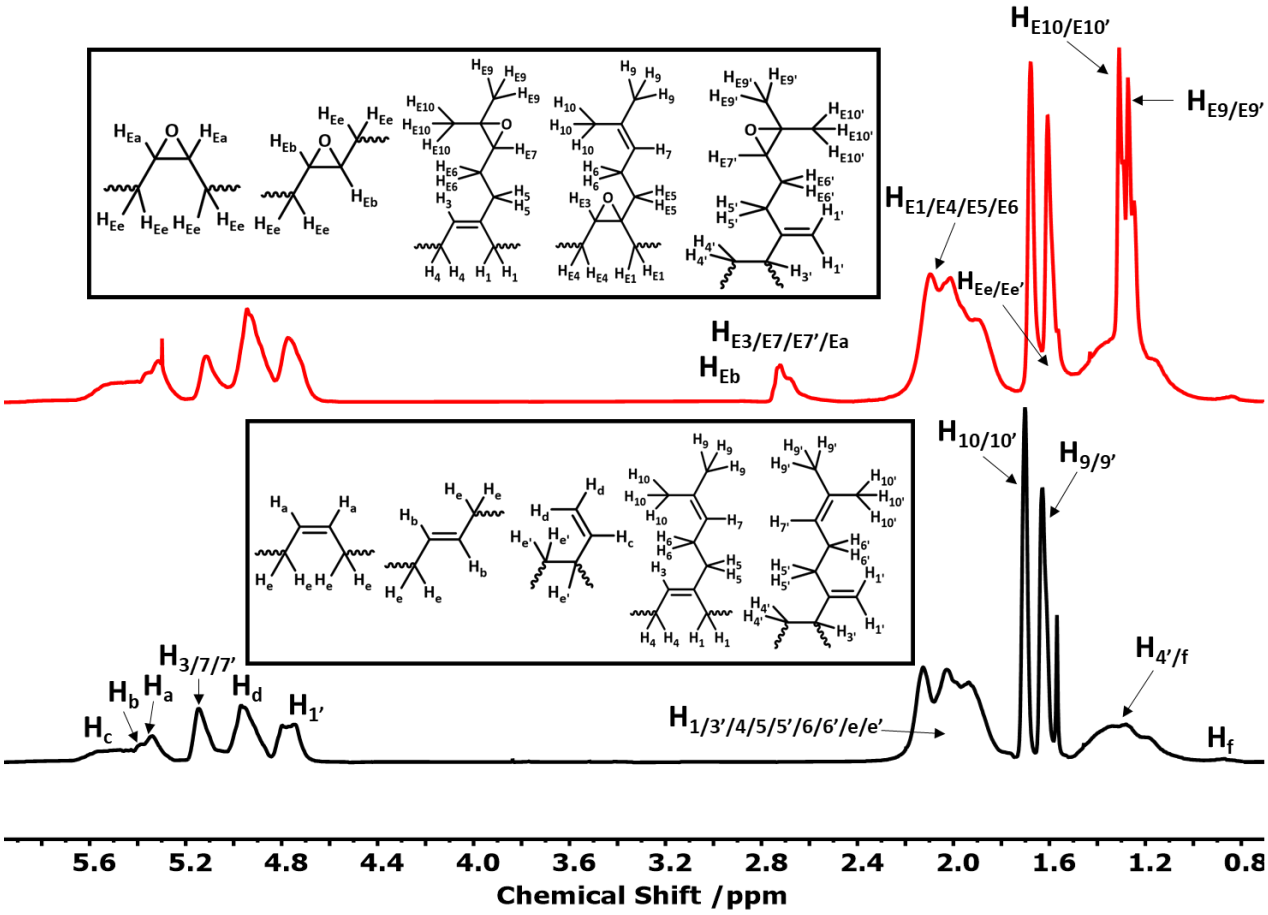

Figure 3.9: Stacked ^{1}H NMR spectra (400 MHz, $CDCl_3$) of poly(myrcene-co-butadiene) prepared in the presence of TMEDA – PMB2 - (bottom-black) and epoxidised PMB2 – EPMB2 (red-top).

Once again, successful epoxidation has occurred, as it can be seen in the stacked ^{1}H NMR spectra in Figure 3.9 above, shown by the appearance of peaks at 1.27 ppm ($H_{E9/E9'}$), 1.31 ppm ($H_{E10/E10'}$) and 2.72 ppm ($H_{E3/E7/E7'/Ea}$). However, once again, the peaks are very different in shape compared to epoxidised poly(myrcene-co-butadiene) that was prepared in the absence of a polar modifier. This is potentially due to the different diad/triad environments, which may be present due to the increase in 4,3-propagation of myrcene and 1,2-propagation of butadiene or due to the increased likelihood of myrcene units that are epoxidised on both the 3,2-double bond and the 7,8-double bond due to a general decrease in the overall substitution of the double bonds, making the 3,2-double bond relatively more epoxidisable. The assigned regions and corresponding ^{1}H NMR peak integration values for the epoxidised myrcene-butadiene copolymer can be seen in Table 3.11 below.

Table 3.11: Summary of integral data for the epoxidised poly(myrcene-co-butadiene) sample – PMB2 – from the ^{1}H NMR spectrum in Figure 3.9.

Assigned Region	Chemical Shift Range /ppm	Proton Assignment	Integration
M1	1.20 – 1.33	$H_{E9} + H_{E9'} + H_{E10} + H_{E10'}$	6.86
M2-B1	2.50 – 2.78	$H_{E3} + H_{E7} + H_{E7'} + H_{Ea}$	1.06
B2	2.78 – 3.00	H_{Eb}	0.11
M3	4.60 – 4.83	$H_{1'}$	2.00
B3	4.83 – 5.03	H_d	3.04
M4	5.03 – 5.20	$H_3 + H_7 + H_{7'}$	1.20
B4	5.20 – 5.40	$H_a + H_b$	1.40*

*Contains a solvent peak of DCM

Using Equations 3.8, 3.9, 3.10, 3.11, and 3.13, we were able to calculate that the polymer was approximately 27% epoxidised, whereby 90% of this epoxidation occurred on the myrcene – 108 % of which occurred on the 7,8-double bond – and 10% occurred on the butadiene. Using the molar composition percentages of both the myrcene and butadiene within this copolymer and Equation 3.12 we can calculate that the relative selectivity for the myrcene over the butadiene was approximately 12 times greater. Due to the unattainable value for the 7,8-double bond epoxidation percentage, the very low relative integral value for the epoxidation – which will see a very low signal to noise ratio – and the overlap of M1 with the 4,3-microstructure vinyl protons of myrcene ($H_{4'}$) and the 1,2-microstructure backbone protons of butadiene (H_f), it was decided that comparative analysis would be trialled in the hope that it would hopefully provide further insight into the epoxidation reaction. The comparative analysis was carried out using Equations 3.8, 3.9, 3.10, 3.11, and 3.13, and the normalised integration data contained in Tables 3.12, 3.13 and 3.14.

Table 3.12: Summary of relative integral data for the unepoxidised poly(myrcene-co-butadiene) sample – PMB2 – from the ^{1}H NMR spectrum in Figure 3.9, whereby the new integral information will be used to increase the accuracy of the epoxidation selectivity calculation.

Assigned Region	Chemical Shift Range /ppm	Proton Assignment	Integration
M1	1.18 – 1.35	$H_{4'} + H_f$	2.85
M2/B1	2.50 – 2.78	-	0.16
B2	2.78 – 3.00	-	0.12
M3	4.60 – 4.83	$H_{1'}$	2.02
B3	4.83 – 5.03	H_d	3.02
M4	5.03 – 5.20	$H_3 + H_7 + H_{7'}$	2.14
B4	5.20 – 5.40	$H_a + H_b$	1.31

Table 3.13: Summary of relative integral data for the epoxidised poly(myrcene-co-butadiene) sample – EPMB2 – from the ^{1}H NMR spectrum in Figure 3.9, whereby the new integral information will be used to increase the accuracy of the epoxidation selectivity calculation.

Assigned Region	Chemical Shift Range /ppm	Proton Assignment	Integration
M1	1.18 – 1.35	$H_{E9} + H_{E9'} + H_{E10} + H_{E10'} + H_{4'} + H_f$	7.70
M2/B1	2.50 – 2.78	$H_{E3} + H_{E7} + H_{E7'} + H_{Ea}$	1.06
B2	2.78 – 3.00	H_{Eb}	0.11
M3	4.60 – 4.83	$H_{1'}$	2.00
B3	4.83 – 5.03	H_d	3.04
M4	5.03 – 5.20	$H_3 + H_7 + H_{7'}$	1.20
B4	5.20 – 5.40	$H_a + H_b$	1.40*

*Contains a solvent peak of DCM

Table 3.14: Summary of the integral differences between PMB2 and EPMB2, whereby the values were calculated by subtracting the integral values of each defined region in Table 3.12 away from the values in Table 3.13.

Assigned Region	Chemical Shift Range /ppm	Integral Difference Between Epoxidised and Unepoxidised
ΔM1	1.18 – 1.35	+4.85
ΔM2/B1	2.50 – 2.78	+0.90
ΔB2	2.78 – 3.00	-0.01
ΔM3	4.60 – 4.83	-0.02
ΔB3	4.83 – 5.03	+0.02
ΔM4	5.03 – 5.20	-0.94
ΔB4	5.20 – 5.40	+0.09

Prior to any calculations being carried out, we can see from Table 3.14 above that it appears that, within the error of ^{1}H NMR, there was no epoxidation that occurred on the butadiene and 100 % of the epoxidation occurred on the myrcene. This lack of butadiene epoxidation can be seen in region B2 (which shows a relative integral for the number of butadiene units), which shows no increase in value, but it can also be seen in the lack of any relative decrease in the number of double bonds of butadiene. When we delve further into the data, using Equations 3.8, 3.9, 3.10, 3.11, and 3.13, we can calculate that of the myrcene epoxidations, approximately 1.05 % of the epoxidations occurred on the 1,2-double bond (found within the 4,3-microstructure of myrcene), 89.8 % of the epoxidations occurred on the 7,8-pendant double bond and 9.1 % occurred on the 3,2-double bond. These percentages are fairly consistent with the data that we have obtained for previous myrcene-containing polymers that were prepared in the presence of TMEDA, further suggesting that the incorporation of

butadiene into this copolymer has little to no effect on the epoxidation of the myrcene units. The lack of any measurable epoxidation occurring on the butadiene repeat units is an incredibly encouraging result for the industrial application of myrcene (especially within the context of SBRs contained within tyre treads) as it suggests that very small amounts of myrcene relative to the amount of butadiene within a rubber can be incorporated into a copolymer before being selectively epoxidised to add functionality into the non-polar chains at selected sites (most likely at the end of the polymer chain, as this provides the most beneficial physical properties for car tyres). This very high selectivity not only reduces the cost of producing any myrcene epoxide-containing polymers (as both the myrcene and epoxidising agent will be fairly expensive relative to the other components of the car tyre) but also limits any negative effects occurring from the epoxidation of the polymer backbone (such as an increase in the T_g of the polymer) as most if not all of the functionalisation will occur selectively at sites that can be installed at positions along the polymer backbone which give the most beneficial property enhancement (for example functionalisation occurring at or near the chain ends of sSBR reduces the energy loss during rolling). [4] [5]

3.2.5 The Epoxidation of Myrcene-Styrene-Butadiene Terpolymers

The final study that had to be undertaken into the chemoselectivity of epoxidation using *m*-CPBA was to investigate whether the 7,8-double bonds could still be selectively epoxidised when myrcene was present in a styrene-butadiene-myrcene terpolymer, as experiments using copolymers of myrcene-butadiene and myrcene-styrene would suggest.

The final copolymer series that was investigated for the epoxidation selectivity of *m*-CPBA, so that the usefulness of myrcene within SBR could be investigated, was myrcene-butadiene-styrene terpolymers. This series of terpolymers provides the most complex study for epoxidation selectivity calculation due to the potential epoxidation sites that are provided by the butadiene and due to the extensive overlap of subunit peaks in the ^{1}H NMR spectra.

3.2.5.1 Epoxidation of PMBS1

Initially, a myrcene-butadiene-styrene terpolymer that had been prepared in a non-polar solvent in the absence of any polar modifier was investigated. To do this, PMBS1 was

epoxidised using the general procedure detailed above and using the amounts of each reactant depicted in the table below.

Table 3.15: Conditions used for the epoxidation of PMBS1.

Polymer Used	Mass of Polymer /g	Volume of DCM /mL	Mass of *m*-CPBA /g	Target Epoxidation / % of 7,8 Double Bonds
PMBS1	0.25	20	0.10	100

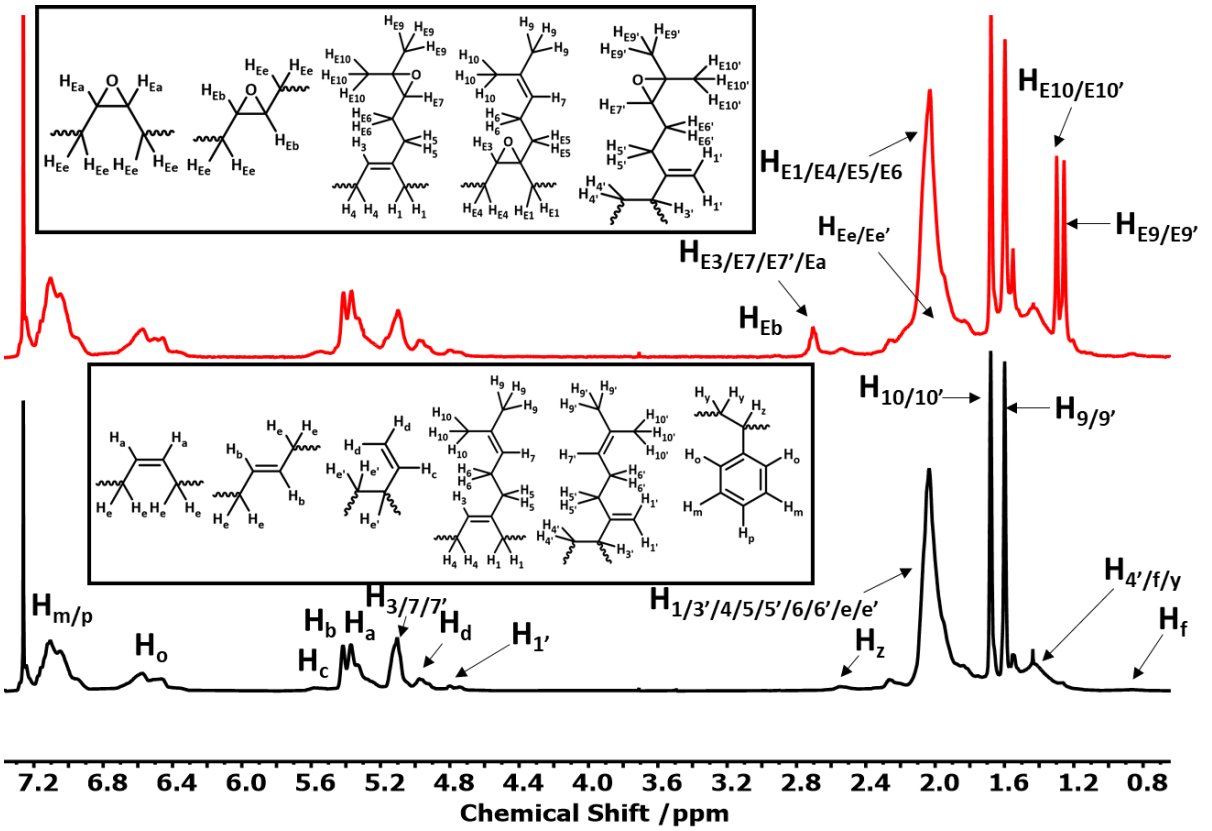

Figure 3.10: Stacked ^{1}H NMR spectra (400 MHz, $CDCl_3$) of poly(myrcene-co-butadiene-co-styrene) prepared in the absence of TMEDA – PMBS1 - (bottom-black) and the epoxidised terpolymer PMBS1– EPMBS1 (red-top), with hydrogen assignments of the peaks.

From the ^{1}H NMR spectra shown in Figure 3.10, it is evident that once again some epoxidation occurred at the butadiene 2,3-double bond (H_{Eb} 2.91 ppm), but the overwhelming majority of epoxidation occurred on myrcene and predominantly at the 7,8 double bonds – evidenced by the appearance of a broad peak at 2.70 ppm ($H_{E3/E7/E7'}$) and the two sharp peaks at 1.25 ppm ($H_{E9/E9'}$) and 1.29 ppm ($H_{E9/E9'}$). However, it should be noted that there is significant overlap of several of the peaks and some of the key peaks have a very low signal to noise ratio, which will result in errors in the integrals and some inaccuracy in the calculations. For consistency,

and to ensure that the values that we get from the comparative analysis are at least within a similar ballpark as the absolute integral values, we would once again start by using the absolute integral values. The assigned regions and corresponding ^{1}H NMR peak integration values for the epoxidised myrcene-butadiene-styrene terpolymer can be seen in Table 3.16 below.

Table 3.16: Summary of integral data for the epoxidised poly(myrcene-co-butadiene-co-styrene) sample – EPMBS1 – from the ^{1}H NMR spectrum in Figure 3.10.

Assigned Region	Chemical Shift Range /ppm	Proton Assignment	Integration
M1	1.23 – 1.33	$H_{E9} + H_{E9'} + H_{E10} + H_{E10'}$	17.42
M2-B1	2.60 – 2.80	$H_{E3} + H_{E7} + H_{E7'} + H_{Ea}$	4.29
B2	2.83 – 3.00	H_{Eb}	0.48
M3	4.65 – 4.85	$H_{1'}$	2.00
B3	4.85 – 5.03	H_d	4.12
M4	5.03 – 5.20	$H_3 + H_7 + H_{7'}$	10.28
B4	5.20 – 5.48	$H_a + H_b$	19.29

Using Equations 3.8, 3.9, 3.10, 3.11, and 3.13, we were able to calculate that approximately 22% of all diene units present in the terpolymer were epoxidised, whereby 89% of this epoxidation occurred on the myrcene – 76% of which occurred on the 7,8-double bond – and 11% occurred on the butadiene. Using the molar composition percentages of both the myrcene and butadiene within this copolymer and Equation 3.12, we can calculate that the relative selectivity for the myrcene over the butadiene was approximately 11 times greater. As mentioned previously, the very low relative integral value for the epoxidation – which will see a very low signal to noise ratio – and the potential overlap of M1 and M2-B1 with the 4,3-microstructure vinyl protons of myrcene ($H_{4'}$), the 1,2-microstructure backbone protons of butadiene (H_f) and the styrenic backbone protons (H_y and H_z) meant that it was decided that once again comparative analysis would be carried out, which would hopefully provide further insight into the epoxidation reaction. The comparative analysis was carried out using Equations 3.8, 3.9, 3.10, 3.11, and 3.13, and the normalised integration data contained in Tables 3.17, 3.18 and 3.19.

Table 3.17: Summary of relative integral data for the unepoxidised poly(myrcene-co-butadiene-co-styrene) sample – PMBS1 – from the ^{1}H NMR spectrum in Figure 3.10, whereby the new integral information will be used to increase the accuracy of the epoxidation selectivity calculation.

Assigned Region	Chemical Shift Range /ppm	Proton Assignment	Integration
M1	1.10 – 1.33	$H_{4'} + H_f + H_y$	3.62
M2/B1	2.60 – 2.83	H_z	0.64
B2	2.83 – 3.00	-	0.30
M3	4.63 – 4.85	$H_{1'}$	2.03
B3	4.85 – 5.03	H_d	4.20
M4	5.03 – 5.20	$H_3 + H_7 + H_{7'}$	13.09
B4	5.20 – 5.48	$H_a + H_b$	18.68

Table 3.18: Summary of relative integral data for the epoxidised poly(myrcene-co-butadiene-co-styrene) sample – EPMBS1 – from the ^{1}H NMR spectrum in Figure 3.10, whereby the new integral information will be used to increase the accuracy of the epoxidation selectivity calculation.

Assigned Region	Chemical Shift Range /ppm	Proton Assignment	Integration
M1	1.10 – 1.33	$H_{E9} + H_{E9'} + H_{E10} + H_{E10'} + H_{4'} + H_f + H_y$	19.14
M2/B1	2.60 – 2.83	$H_{E3} + H_{E7} + H_{E7'} + H_{Ea} + H_z$	4.17
B2	2.83 – 3.00	H_{Eb}	0.46
M3	4.63 – 4.85	$H_{1'}$	2.00
B3	4.85 – 5.03	H_d	3.95
M4	5.03 – 5.20	$H_3 + H_7 + H_{7'}$	9.85
B4	5.20 – 5.48	$H_a + H_b$	18.50

Table 3.19: Summary of the integral differences between PMBS1 and EPMBS1, whereby the values were calculated by subtracting the integral values of each defined region in Table 3.17 away from the values in Table 3.18.

Assigned Region	Chemical Shift Range /ppm	Integral Difference Between Epoxidised and Unepoxidised
ΔM1	1.10 – 1.33	+15.52
ΔM2/B1	2.60 – 2.83	+3.53
ΔB2	2.83 – 3.00	+0.16
ΔM3	4.63 – 4.85	-0.03
ΔB3	4.85 – 5.03	-0.25
ΔM4	5.03 – 5.20	-3.24
ΔB4	5.20 – 5.48	-0.18

Using the calculated integral difference between the epoxidised and unepoxidised terpolymers and Equations 3.8, 3.9, 3.10, 3.11, and 3.13, it is possible to calculate that approximately 4.5% of the epoxidation occurred on the butadiene – whereby 42% of these

epoxides were found on the 2,3-butadiene double bond and 58% of the epoxides were found on the 3,4-butadiene vinyl groups (the value for the vinyl epoxidation was much greater than expected compared to both the literature and previous reactions, and if we look at the change in the regions B3 and B4, it is greater than twice the value of B2, suggesting that there may be some solvent peak within B3 in the unepoxidised sample that is skewing the results) – and approximately 96% of the epoxidation occurred on myrcene – whereby 77% occurred on the 7,8-pendant double bond and approximately 23% of the epoxidation occurred on the 3,2-backbone double bond. Bar the breakdown percentages of the epoxidation occurring on the butadiene, these percentages are fairly consistent with the values that have been calculated for epoxidations of other comparable polymers. Once again, from the comparative analysis, the selectivity of the epoxidation towards myrcene over butadiene was calculated to be even greater than previously calculated – it appears that the large signal to noise ratio leads to an overestimate in the butadiene epoxidation percentage – working out at a selectivity of 33 times towards the myrcene relative to the butadiene.

3.2.5.2 Epoxidation of Styrene-Butadiene-Myrcene Terpolymers prepared in the Presence of TMEDA

The final investigation into the selectivity of epoxidation within myrcene-containing polymers was to look at terpolymers of myrcene, butadiene and styrene that had been synthesised in the presence of TMEDA. For this final study, it was decided to investigate two separate terpolymers, one in which the molar ratios of myrcene, styrene and butadiene were approximately equal and one in which the molar ratios of myrcene, styrene and butadiene were in ratios similar to what would be used as a potential car tyre formulation (70% butadiene, 25% styrene and 5% myrcene).

3.2.5.2.1 Epoxidation of PMBS2

The first investigation began by looking at the equimolar composition terpolymer, as it was believed that this would give the best indication into the absolute selectivity. To do this, PMBS2 was epoxidised using the general procedure detailed in Section 3.4 and using the amounts of each reactant depicted in Table 3.20 below.

Table 3.20: Conditions used for the epoxidation of PMBS2.

Polymer Used	Mass of Polymer /g	Volume of DCM /mL	Mass of *m*-CPBA /g	Target Epoxidation / % of 7,8 Double Bonds
PMBS2	0.25	35	0.10	100

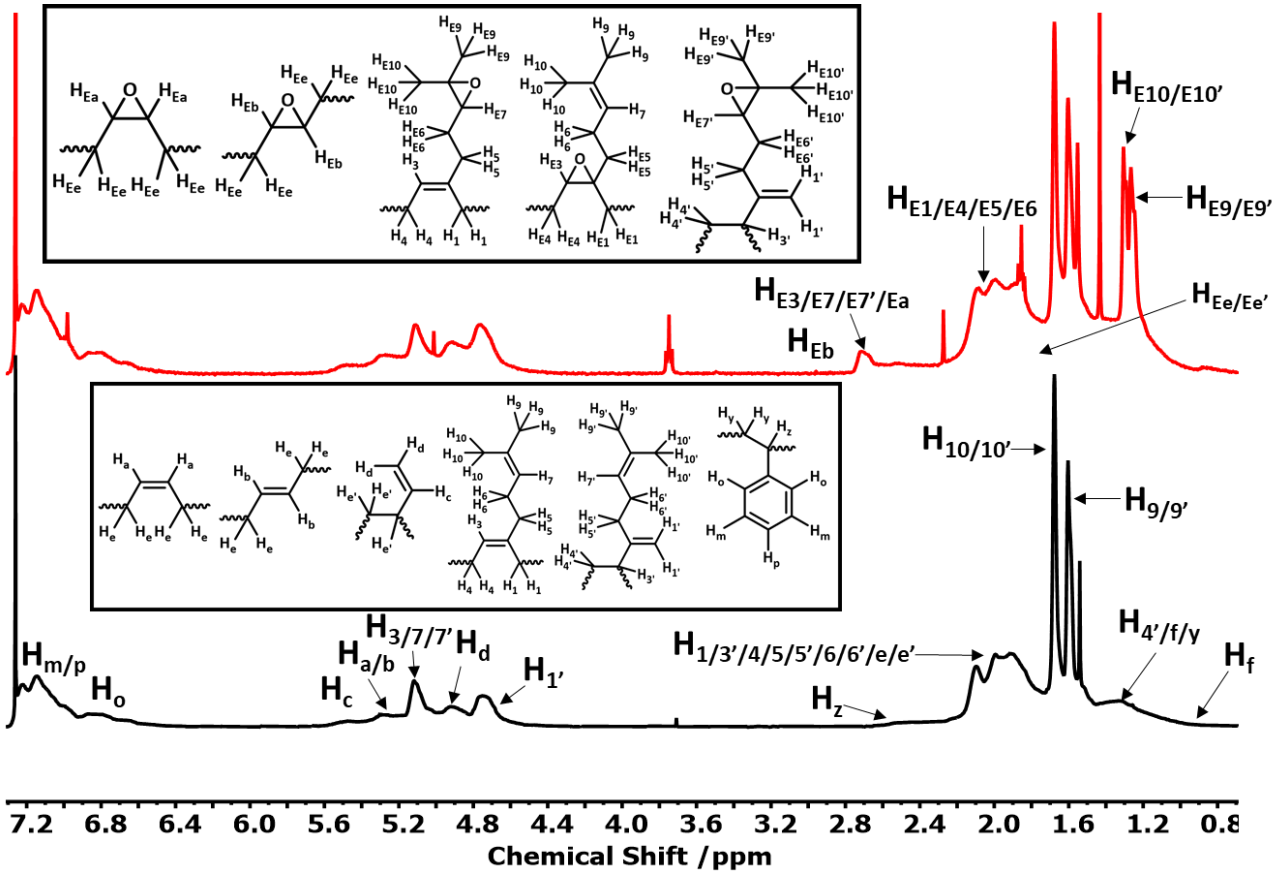

Figure 3.11: Stacked ^{1}H NMR spectra (400 MHz, $CDCl_3$) of poly(myrcene-co-butadiene-co-styrene) prepared in the presence of TMEDA – PMBS2 - (bottom-black) and the epoxidised PMBS2– EPMBS2 (red-top), with hydrogen assignments of the peaks.

As it can be seen in the ^{1}H NMR spectra (Figure 3.11), there is evidence that epoxidation has occurred at the myrcene 3,2 and 7,8 double bonds – due to the presence of the peak at 2.71 ppm ($H_{E3/E7/E7'}$) and the two singlet peaks at 1.26 ppm ($H_{E9/E9'}$) and 1.30 ppm ($H_{E9/E9'}$). However, in the region where it would be expected to see the epoxidised butadiene peak (2.80 ppm – 3.00 ppm), there is once again no observable peak, suggesting no epoxidation has occurred at the butadiene backbone double bond. As it can be seen, there is significant overlap of several of the peaks and some of the peaks have a very low signal to noise ratio, which will probably result in the absolute integrals being fairly inaccurate for calculation. However, it was once again decided that, for consistency and to ensure that the values obtained from the

comparative analysis are at least within a similar ballpark as the absolute integral values, the epoxidation selectivity calculation would once again start by using the absolute integral values. The assigned regions and corresponding ^{1}H NMR peak integration values for the epoxidised myrcene-butadiene-styrene terpolymer that had been prepared in the presence of TMEDA can be seen in Table 3.21 below.

Table 3.21: Summary of integral data for the epoxidised poly(myrcene-co-butadiene-co-styrene) sample – EPMBS2 – from the ^{1}H NMR spectrum in Figure 3.11.

Assigned Region	Chemical Shift Range /ppm	Proton Assignment	Integration
M1	1.20 – 1.35	$H_{E9} + H_{E9'} + H_{E10} + H_{E10'}$	7.63
M2-B1	2.63 – 2.78	$H_{E3} + H_{E7} + H_{E7'} + H_{Ea}$	0.90
B2	2.80 – 3.00	H_{Eb}	0.12
M3	4.50 – 4.83	$H_{1'}$	3.10
B3	4.83 – 5.00	H_d	2.00
M4	5.00 – 5.20	$H_3 + H_7 + H_{7'}$	2.48
B4	5.20 – 5.38	$H_a + H_b$	1.22

Using Equations 3.8, 3.9, 3.10, 3.11 and 3.13, it is possible to calculate that approximately 20% of all diene units present in the terpolymer were epoxidised whereby, when using the integration values in Table 3.21 above, 87% of this epoxidation occurred on the myrcene – 141% of which occurred on the 7,8-double bond – and 13% occurred on the butadiene. Using the molar composition percentages of both the myrcene and butadiene within this copolymer and Equation 3.12, it can be calculated that the relative selectivity for the myrcene over the butadiene was approximately 6 times greater. As mentioned previously, the very low relative integral value for the epoxidation (which will see a very low signal to noise ratio), the potential overlap of M1 and M2-B1 with the 4,3-microstructure vinyl protons of myrcene ($H_{4'}$), the 1,2-microstructure backbone protons of butadiene (H_f) and the styrenic backbone protons (H_y and H_z) and the impossibly large 7,8-double bond myrcene epoxide percentage meant that comparative analysis was required so that further insight into the epoxidation reaction could be achieved. The comparative analysis was carried out using Equations 3.8, 3.9, 3.10, 3.11 and 3.13, and the normalised integration data contained in Tables 3.22, 3.23 and 3.24.

Table 3.22: Summary of relative integral data for the unepoxidised poly(myrcene-co-butadiene-co-styrene) sample – PMBS2 – from the ^{1}H NMR spectrum in Figure 3.11, whereby the new integral information will be used to increase the accuracy of the epoxidation selectivity calculation.

Assigned Region	Chemical Shift Range /ppm	Proton Assignment	Integration
M1	1.10 – 1.38	$H_{4'} + H_f + H_y$	3.56
M2/B1	2.58 – 2.80	H_z	0.16
B2	2.80 – 3.00	-	0.09
M3	4.50 – 4.83	$H_{1'}$	3.20
B3	4.83 – 5.00	H_d	2.05
M4	5.00 – 5.20	$H_3 + H_7 + H_{7'}$	3.30
B4	5.20 – 5.38	$H_a + H_b$	1.24

Table 3.23: Summary of relative integral data for the epoxidised poly(myrcene-co-butadiene-co-styrene) sample – EPMBS2 – from the ^{1}H NMR spectrum in Figure 3.11, whereby the new integral information will be used to increase the accuracy of the epoxidation selectivity calculation.

Assigned Region	Chemical Shift Range /ppm	Proton Assignment	Integration
M1	1.10 – 1.38	$H_{E9} + H_{E9'} + H_{E10} + H_{E10'} + H_{4'} + H_f + H_y$	9.08
M2/B1	2.58 – 2.80	$H_{E3} + H_{E7} + H_{E7'} + H_{Ea} + H_z$	1.13
B2	2.80 – 3.00	H_{Eb}	0.12
M3	4.50 – 4.83	$H_{1'}$	3.10
B3	4.83 – 5.00	H_d	2.00
M4	5.00 – 5.20	$H_3 + H_7 + H_{7'}$	2.48*
B4	5.20 – 5.38	$H_a + H_b$	1.22

*Contains an impurity peak of BHT

Table 3.24: Summary of the integral differences between PMBS2 and EPMBS2, whereby the values were calculated by subtracting the integral values of each defined region in Table 3.22 away from the values in Table 3.23.

Assigned Region	Chemical Shift Range /ppm	Integral Difference Between Epoxidised and Unepoxidised
ΔM1	1.10 – 1.38	+5.52
ΔM2/B1	2.58 – 2.80	+0.97
ΔB2	2.80 – 3.00	+0.03
ΔM3	4.50 – 4.83	-0.10
ΔB3	4.83 – 5.00	-0.05
ΔM4	5.00 – 5.20	-0.82
ΔB4	5.20 – 5.38	-0.02

Using the calculated integral difference between the epoxidised and unepoxidised terpolymers and Equations 3.8, 3.9, 3.10, 3.11 and 3.13, we were able to calculate that

approximately 3.1% of the epoxidation occurred on the butadiene – whereby 29% of these epoxides were found on the 2,3-butadiene double bond and 71% of the epoxides were found on the 3,4-butadiene vinyl groups (again, this value for the vinyl epoxidation was much greater than expected compared to both the literature and previous reactions, and if we look at the change in the regions B3 and B4, it is greater than twice the value of B2, suggesting that there may be some solvent peak within B3 in the unepoxidised sample that is skewing the results) – and approximately 97% of the epoxidation occurred on myrcene – whereby ~ 5.8% of the epoxidation occurred on the on the 2,1-vinyl group and 98% occurred on the 7,8-pendant double bond. This 7,8-pendant double-bond percentage is once again impossibly large – potentially due to the presence of a solvent impurity peak with the M1 region of the epoxidised sample, meaning that the 7,8-epoxidation is slightly exaggerated – but it can be suggested by comparing to previous polymer epoxidations that this value should be approximately 90%, which would mean that the 3,2-epoxdation percentage would be about 4-5%. Once again, from the comparative analysis, the selectivity of the epoxidation towards myrcene over butadiene was calculated to be even greater than previously calculated – it appears that the large signal to noise ratio leads to an overestimate in the butadiene epoxidation percentage – working out at a selectivity of 34 times greater towards the myrcene relative to the butadiene.

3.2.5.2.2 Epoxidation of a Potential sSBR Formulation Modified with Myrcene – PMBS3

The very last myrcene-containing polymer that was investigated was a terpolymer with an approximate 3:1 ratio of diene to styrene (a similar ratio to that used within commercially available car tyre rubbers) whereby a very small amount of the butadiene was replaced by myrcene (< 5 %) in order to simulate a potential formulation that could be made industrially. To do this, PMBS3 was epoxidised using the general procedure detailed above and using the amounts of each reactant depicted in Table 3.25 below.

Table 3.25: Conditions used for the epoxidation of PMBS3.

Polymer Used	Mass of Polymer /g	Volume of DCM /mL	Mass of *m*-CPBA /g	Target Epoxidation / % of 7,8 Double Bonds
PMBS3	0.25	20	0.02	100

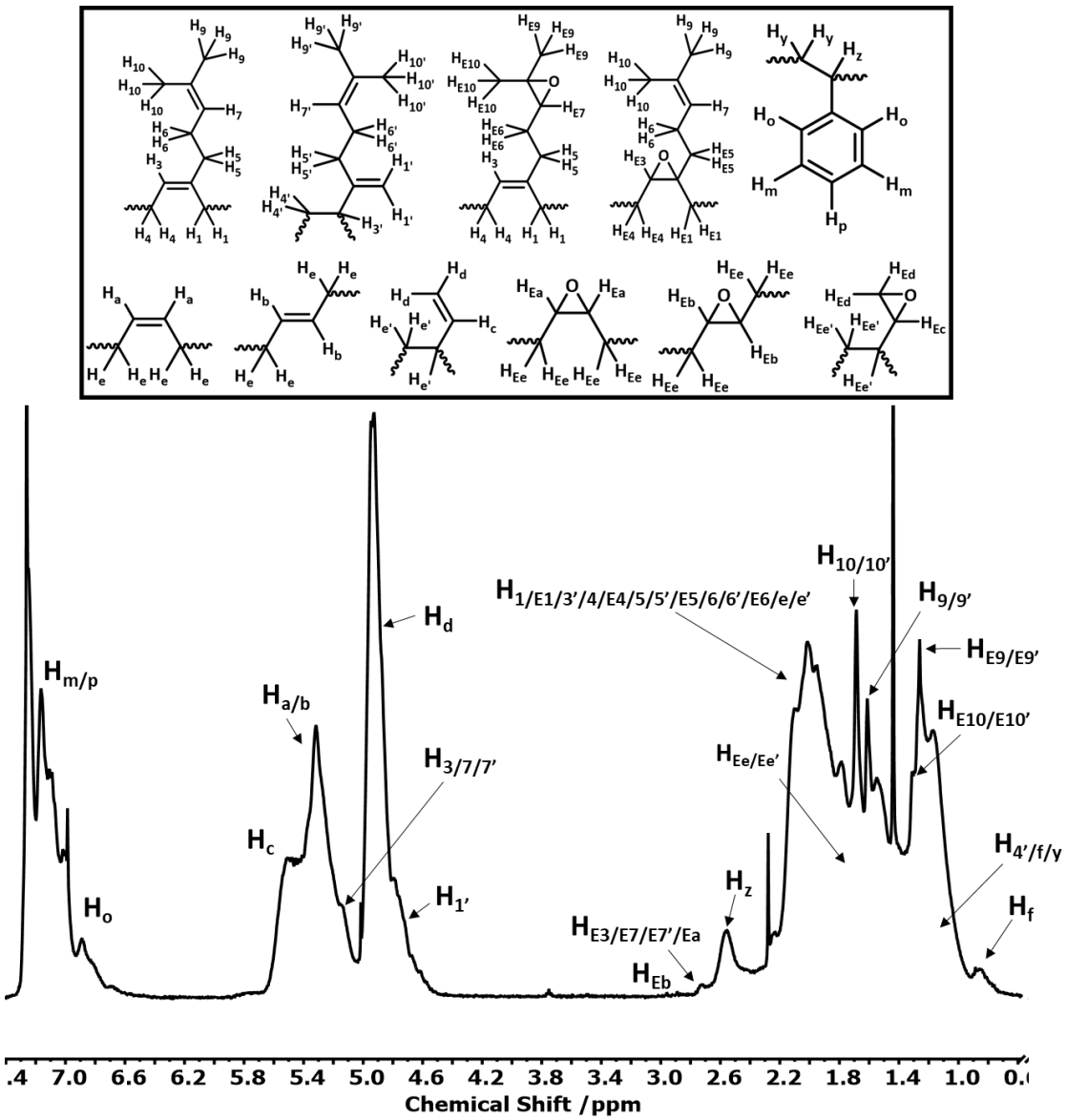

Figure 3.12: Partial 1H NMR spectrum (400 MHz, $CDCl_3$) of the epoxidised terpolymer EPMBS3 with hydrogen assignments of the peaks.

As it can be seen in the ^{1}H NMR spectrum in Figure 3.12 above, the peaks are broad in nature due to the randomisation of butadiene and styrene during the polymerisation and the increase in 1,2-butadiene polymerisation and 4,3-myrcene polymerisation, which were both caused by the addition of TMEDA to the polymerising mixture. It is also evident that, due to this large broadening of peaks and the low myrcene percentage, the separation of peaks that are representative of the myrcene is almost impossible. For this reason, it was decided that this final investigation would be purely qualitative, with reference to previous examples, as any values that would be calculated by a quantitative analysis would be highly inaccurate. Qualitatively, it can be seen that even despite such a small amount of myrcene being present

(5 mol %) in the terpolymer, a myrcene epoxide peak at 2.72 ppm ($H_{E3/E7/E7'}$) and the two myrcene methyl epoxide peaks at 1.26 ppm ($H_{E9/E9'}$) and 1.31 ppm ($H_{E10/E10'}$) are observed, confirming that epoxidation of the myrcene was successful.

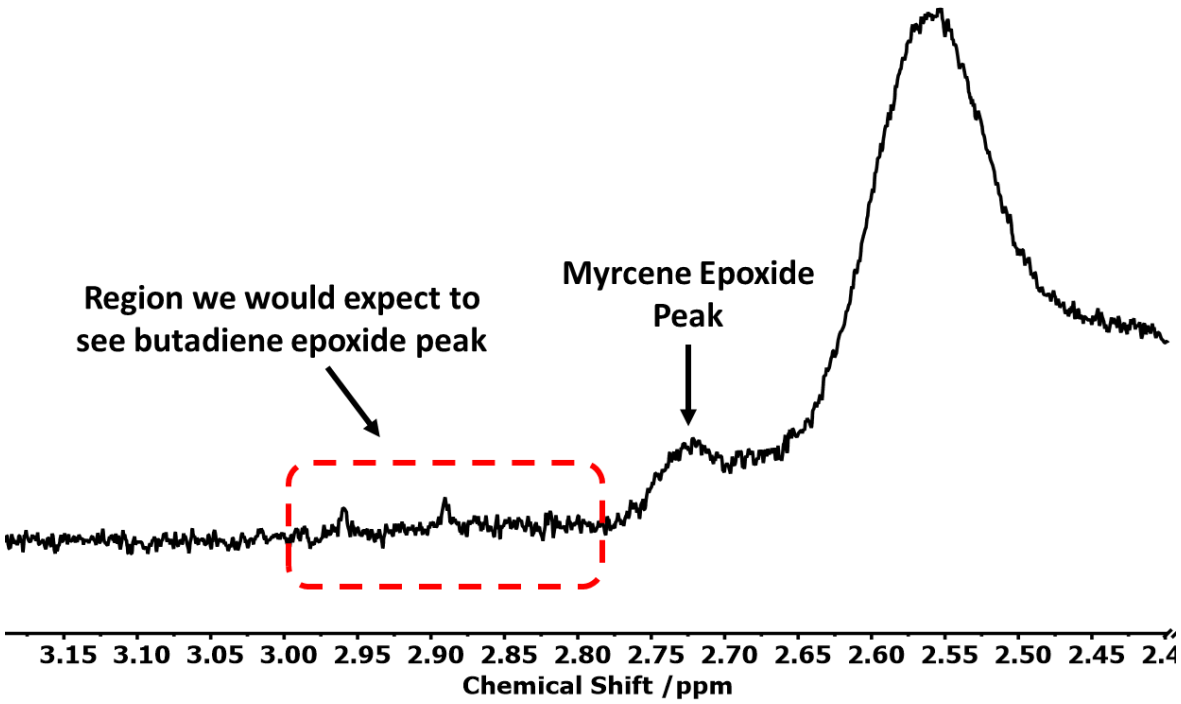

Figure 3.13: Expanded section (2.40 ppm – 3.20 ppm) from the partial ^{1}H NMR spectrum (400 MHz, $CDCl_3$) of the epoxidised terpolymer EPMBS3 seen in Figure 3.12.

Table 3.26: Summary of relative integral data for the unepoxidised and epoxidised poly(myrcene-co-butadiene-co-styrene) sample – PMBS3 - from the ^{1}H NMR spectrum in Figure 3.12.

Chemical Shift Range /ppm	Integral for Unepoxidised Sample	Integral for Epoxidised Sample	Integral Difference Between Epoxidised and Unepoxidised
2.65 – 2.80	0.10	0.20	+0.10
2.83 – 2.95	0.07	0.07	±0.00
6.65 – 6.93	1.00	1.00	-

When zooming in on the ^{1}H NMR spectrum, at the region where one can find the myrcene epoxide peak at 2.72 ppm and where it would be expected to see the butadiene epoxide peak at around 2.90 ppm (shown in Figure 3.13 above), it is possible to see that the peak for the myrcene epoxide is clearly present, but there is no visible peak for any butadiene epoxidation above the noise of the spectrum. This was further verified by comparison of the integrals of the region for butadiene epoxide and the region for myrcene epoxide between the epoxidised

and unepoxidised samples, using the styrenic peak between 6.65 – 6.93 ppm as a reference, the results of which can be seen in Table 3.26 above. From this comparison, it is shown that while there has been an increase in the region where the expected myrcene epoxide peak is to be present, there is no increase in the region where it is expected to see the butadiene epoxide peak. This suggests that even though the butadiene was present in a molar ratio of over 17:1 (based on the initial feed ratio) relative to the amount of myrcene present, the chemoselectivity of the epoxidation reaction using *m*-CPBA results in no significant butadiene epoxidation within the accuracy of the ^{1}H NMR spectroscopic measurement. This observation suggests that the relative selectivity for epoxidation of the myrcene double bonds is so high that through the addition and epoxidation of small amounts of myrcene - 5% or less – into SBR, the myrcene can be used to selectively add functionality with minimal to no effect on the rest of the polymer. This suggests that myrcene will be a viable platform for increasing the dispersion of silica/carbon black within car tyre formulations while limiting the negative impacts that the functionalisation might have on the beneficial physical properties that are provided by SBR by enabling functionalisation to occur at the most beneficial sites so that property improvement can be enhanced at the lowest levels of functionalisation possible.

3.2.6 Ring-Opening of Epoxidised Poly(Myrcene)

Above, it has been shown that myrcene repeat units can be selectively epoxidised when incorporated into copolymers and terpolymers, even when the myrcene constitutes a minor component within the polymer. Below describes an investigation into expanding the utility of this system by exploiting the resulting epoxide as a platform for the introduction of further functionalities. This could allow the introduction of functional groups that have much higher polarity than the epoxide and, therefore, would be useful for the applications previously alluded to.

3.2.6.1 Attempted Base-Catalysed Ring-Opening of Epoxidised Myrcene

Epoxides are generally reactive and (as has been widely reported), the epoxide ring can be susceptible to attack by a wide range of nucleophiles such as sodium hydroxide, leading to the formation of two alcohol groups, which could be used to increase the polarity of a polymer. Alternatively, sodium azide can be used to introduce an azide group, which in turn

can be either used in “click” coupling reactions or reduced to install an amine group. [24] This introduction of an azide group can be tuned through the variation of the experimental conditions such as the pH, or through the addition of different ionic salts to change both the stereoselectivity and regioselectivity of the attack. [25] [26] Selected ring-opening reactions of epoxides are shown in Figure 3.14 below.

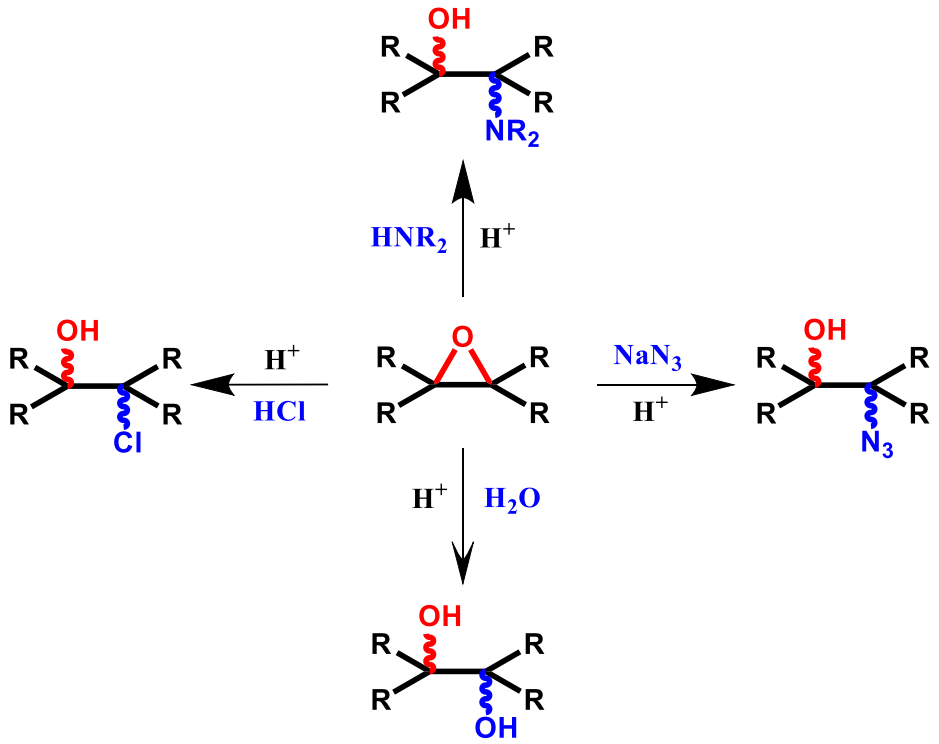

Figure 3.14: Possible ring-opening reactions of epoxides reported in literature. *[24] [13]*

Initial investigations were directed towards base-catalysed ring opening using water as a nucleophile, as the resulting diol would be straightforward to analyse, and would present a viable option for industrial scale-up. Moreover, it was initially decided that the method for ring opening would be explored using myrcene epoxide monomer EM1 (see Chapter 4) as it would allow for much easier analysis of the product, as proton couplings should be visible and individual peaks would be identifiable.

Initially, different solvents were tested to see if biphasic or monophasic basic epoxide ring opening could occur. EM1 was dissolved in the solvents given in Table 3.27 and subjected to basic epoxide ring-opening conditions as described in Section 3.4. The stacked ^{1}H NMR of the recovered epoxidised monomer after being subjected to these conditions can be seen in Figure 3.15 below.

Table 3.27: Summary of the solvents used in each attempted base catalysed epoxide ring-opening reaction.

Product	Solvent
EM-B1	Toluene
EM-B2	Chloroform
EM-B3	THF

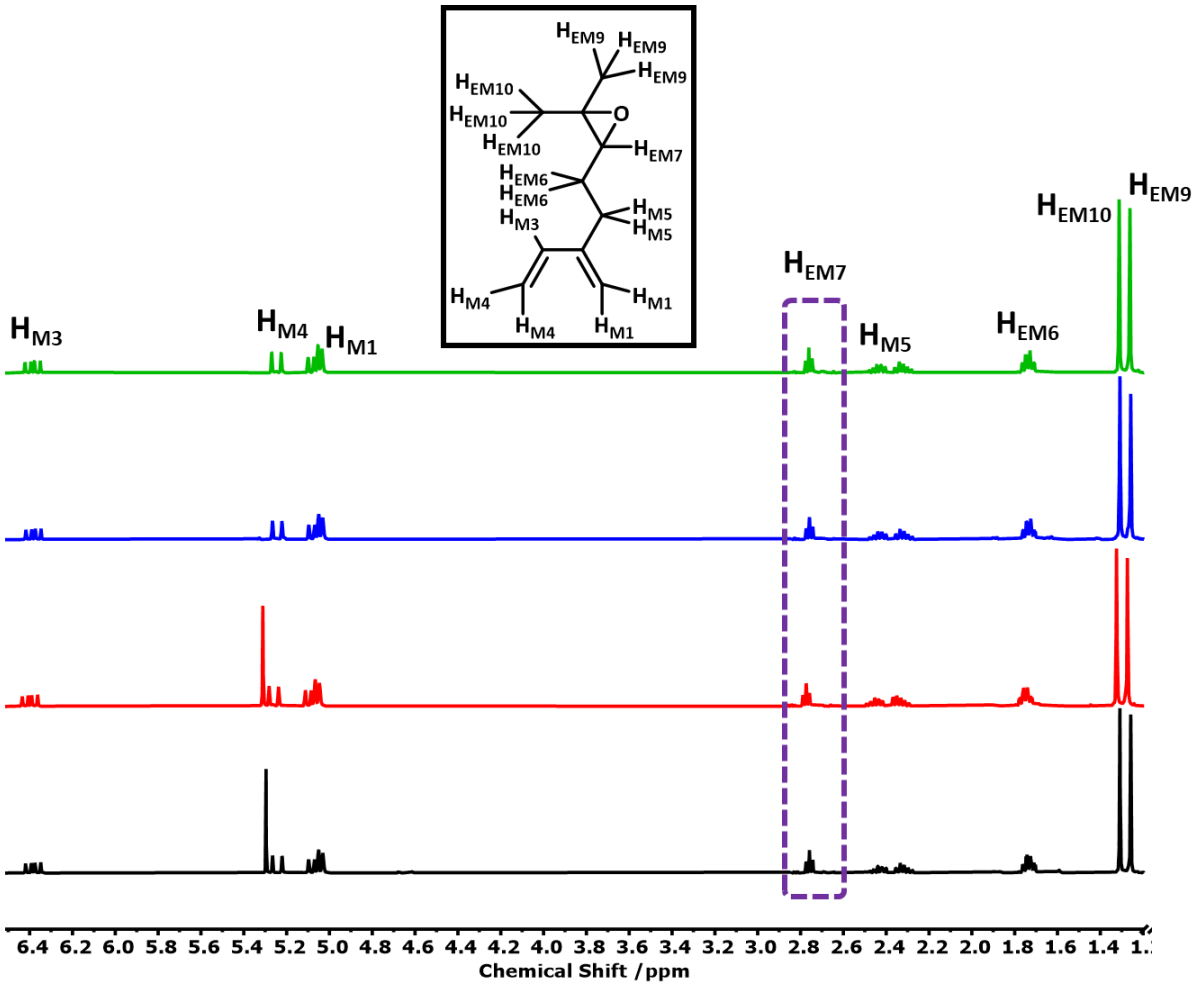

Figure 3.15: Stacked ^{1}H NMR spectra (400 MHz, $CDCl_3$) of epoxidised Myr (Black) with the attempted ring-opening reactions EM-B1 (Red), EM-B2 (Blue), EM-B3 (Green) moving up respectively with proton assignment and the proton next to the epoxide ring highlighted in the purple box.

As it can be seen from Figure 3.15 above, the ring opening of the epoxidised myrcene using sodium hydroxide was unsuccessful – even when using conditions harsher than those that have been utilised in previous literature to ring-open epoxides. [24]

3.2.6.2 Attempted Acid-Catalysed Ring-Opening of Epoxidised Myrcene

Given the electron-rich nature of the epoxide, it was felt that an acid-catalysed approach may be more successful. Thus, EM1 was dissolved in the solvents (and amounts of

water/trifluoroacetic acid) given in Table 3.28 and subjected to acidic epoxide ring-opening conditions, as described in Section 3.4. The stacked ^{1}H NMR of the recovered ring-opened products after being subjected to these conditions can be seen in Figure 3.16 below.

Table 3.28: Summary of the solvents and amount of acid used for each attempted acidic epoxidised ring-opening reaction.

Product Code	Solvent	Amount of Solvent /mL	Amount of Water /mL	Amount of Trifluoracetic Acid /mL
EM-A1	Toluene	10	1	0.5
EM-A2	-	-	5	0.1
EM-A3	THF	5	0.25	0.05

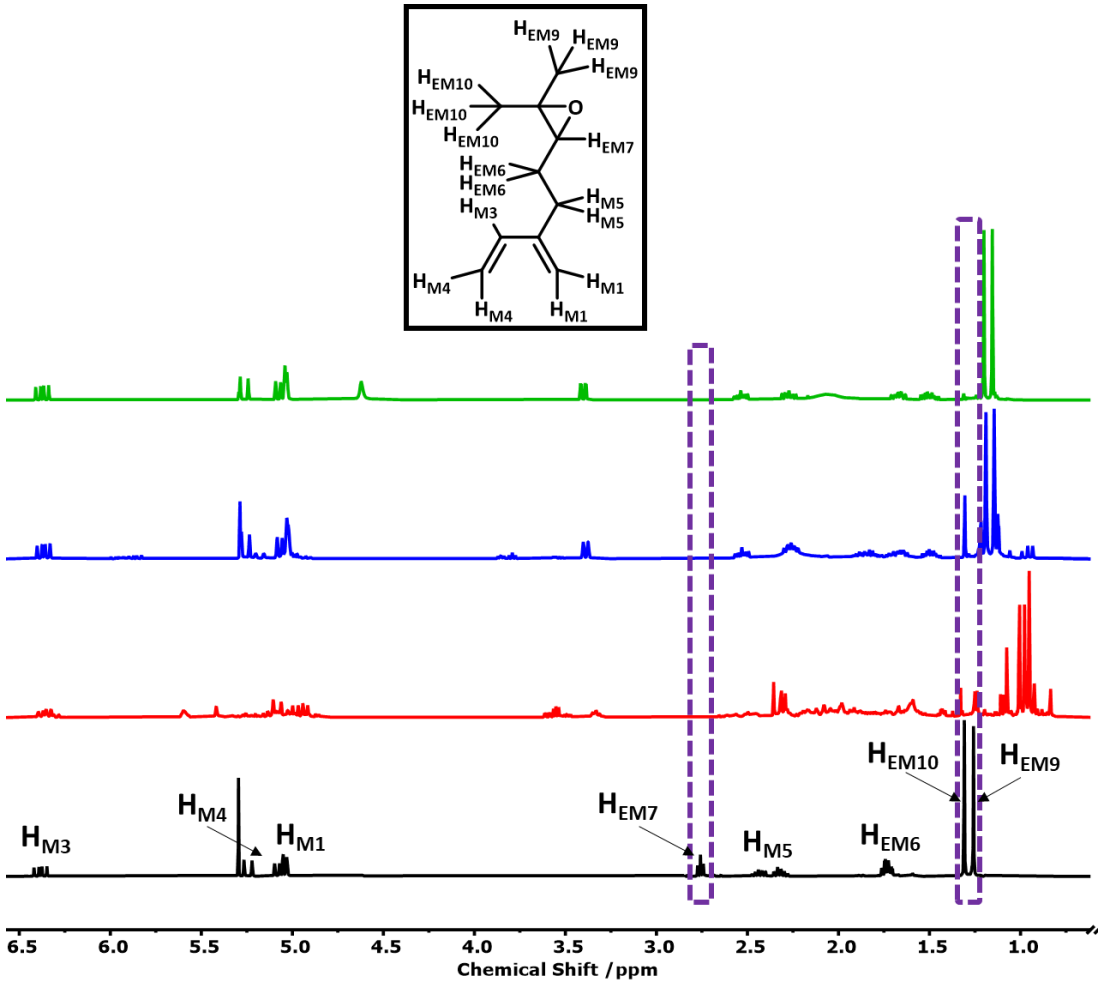

Figure 3.16: Stacked ^{1}H NMR spectra (400 MHz, $CDCl_3$) of epoxidised Myr (Black) with the attempted ring-opening reactions EM-A1 (Red), EM-A2 (Blue), EM-A3 (Green) moving up respectively with proton assignment and the proton next to the epoxide ring and the protons of the methyl groups next to the epoxide highlighted in the purple boxes.

As it can be seen in the stacked ^{1}H NMR spectra above, it is apparent that the epoxide ring has been ring opened using trifluoracetic acid as the catalyst due to the disappearance of the epoxide proton peak at 2.75 ppm and due to the disappearance of the two methyl epoxide peaks at 1.26 ppm and 1.31 ppm. However, if attention is switched to the rest of the spectrum within each sample, it can be seen that under the conditions that were required to allow for the ring opening of the epoxide, there were a whole host of various reactions and side reactions leading to a loss of selectivity. These reactions appear to include Markovnikov and anti-Markovnikov addition of the nucleophile – whereby it appears both water and the acid itself (even when used in a 1:50 ratio with water) have acted as the nucleophile for ring opening – and reaction of unepoxidised double bonds with the trifluoracetic acid. While this established that the epoxide ring can be opened, the loss of selectivity was concerning as the ability to selectively epoxidise would become futile since it would simply be lost upon ring opening. It was decided that we would continue to test the acid catalysed ring opening of an epoxidised poly(myrcene) homopolymer under various conditions to establish whether:

1. The added steric hindrance associated with attack of the backbone double bond resulted in no side reactions of the other double bonds within the system.
2. Under certain conditions the ring opening reaction could be tuned to promote the selective ring opening of the epoxide over any other side reaction.

First, several reactions at different temperatures and in different solvents (as seen in the conditions used for each experiment in Table 3.29 below) were tried using the trifluoracetic acid and water system that was used to open the epoxide ring of the epoxidised myrcene monomer as described in the experimental in Section 3.4.

Table 3.29: Summary of the conditions used for each trifluoracetic acid catalysed epoxide ring-opening reaction of EPM1.

Product Code	Mass of EPM1 /g	Solvent		Volume of water /mL	Volume of CF_3COOH /mL	Temperature /°C	Time /hrs
		Type	Solvent /mL				
EPM-A1	0.26	1,4-dioxane	25	10	3	80	2.5
EPM-A2	0.38	Toluene	30	10	3	95	3
EPM-A3	0.23	1,4-dioxane	30	10	3	100	3

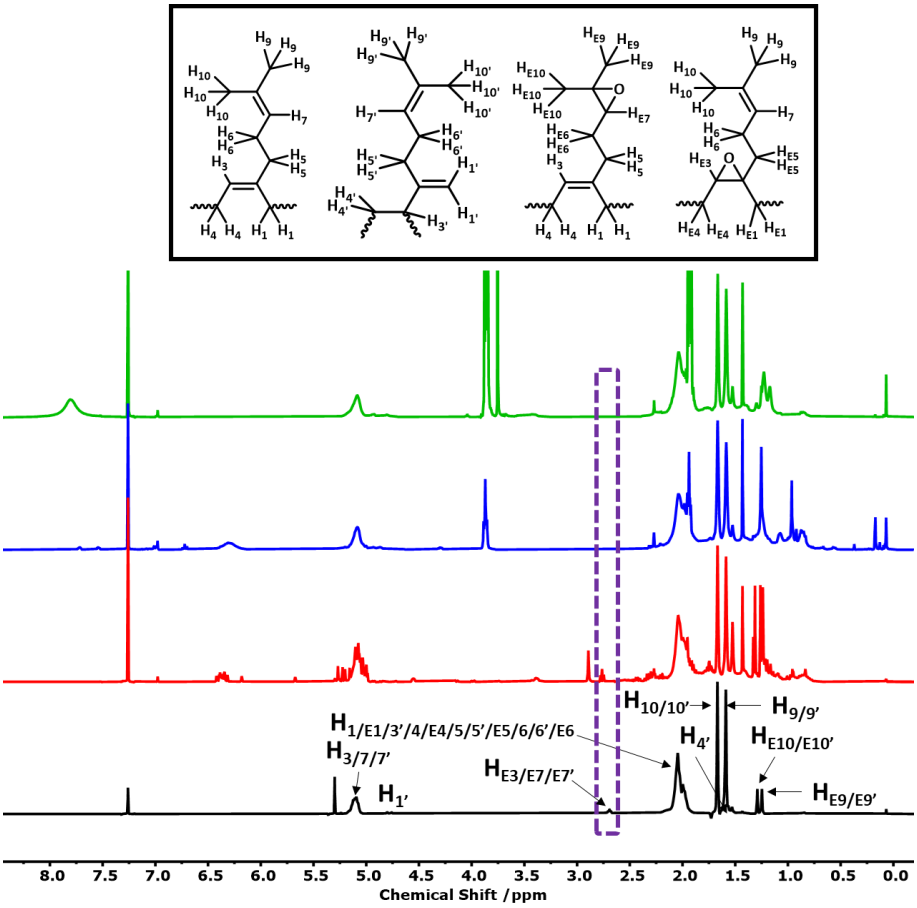

Figure 3.17: Stacked ^{1}H NMR spectra (400 MHz, $CDCl_3$) of epoxidised Poly(Myr) (Black) with the attempted ring-opening reactions EPM-A1 (Red), EPM-A2 (Blue), EPM-A3 (Green) moving up respectively with the proton next to the epoxide ring highlighted by the purple box.

As can be seen in the stacked ^{1}H NMR spectra (Figure 3.17), epoxide ring opening using trifluoracetic acid had occurred, indicated by the disappearance of the epoxide peak at around 2.70 ppm in each of the samples. However, similar to those obtained for the acid-catalysed ring opening of the epoxidised myrcene, the resulting ^{1}H NMR spectra are complex, suggesting that many different products were present and the selectivity that was established through epoxidation was lost, under all the conditions that were tested. It was therefore decided to change the nucleophile from water to benzylamine to determine if a stronger nucleophile could lead to a cleaner reaction. Benzylamine was also chosen as it was believed that it would give a diagnostic signal in the ^{1}H NMR spectrum if it was incorporated into the polymer.

EPM1 was dissolved in a selected solvent system, before benzylamine and a selected catalyst were added and heated, with the condition selection shown in Table 3.30 and the full experimental found in Section 3.4.

Table 3.30: Summary of the conditions used for epoxide ring-opening reaction utilising benzylamine as the nucleophile.

Product Code	Mass of EPM1 /g	Solvent		Catalyst		Temperature /°C
		Type	Volume /mL	Type	Volume /mL	
EPM-Bz1	0.50	DCM	30	None	None	50
EPM-Bz2	0.25	THF/Water (1:1)	20	$NaHCO_3$	10	80
EPM-Bz3	0.10	THF/Water (1:1)	20	Acetic Acid	5	80
EPM-Bz4	0.10	Dioxane/Water (1:1)	15	Acetic Acid	5	100
EPM-Bz5	0.10	Toluene/Water (1:1)	20	Acetic Acid	6	100
EPM-Bz6	0.10	THF	30	Acetic Acid	10	80
EPM-Bz7	0.27	Toluene	40	HCl	4	105

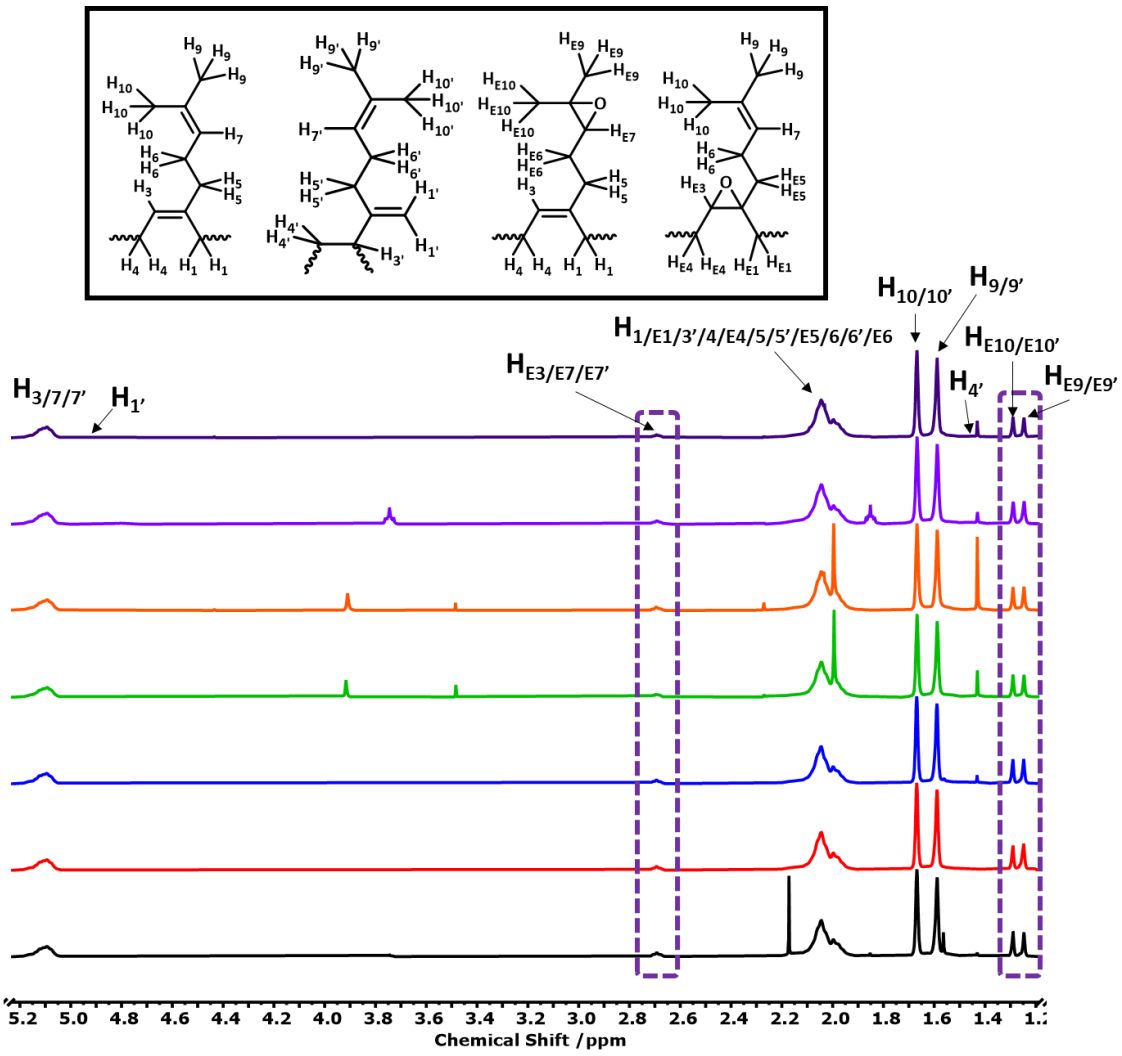

Figure 3.18: Stacked ^1H NMR spectra (400 MHz, $CDCl_3$) of epoxidised Poly(Myr) (Black) with the attempted ring-opening reactions EPM-Bz1 (Red), EPM-Bz2 (Blue), EPM-Bz3 (Green), EPM-Bz4 (Orange), EPM-Bz5 (Violet), EPM-Bz6 (Indigo) moving up respectively with the proton next to the epoxide ring highlighted by the purple box.

As it can be seen in the stacked ^{1}H NMR spectrum in Figure 3.18 above, for the first six experiments in Table 3.30, it appears that the epoxide ring was not ring opened under any of the conditions that were tried using benzylamine as a nucleophile due to the peaks at 2.70 ppm ($H_{E3/E7/E7'}$), 1.26 ppm ($H_{E9/E9'}$) and 1.31 ppm ($H_{E10/E10'}$) still being present at the end of the reaction. However, if we look at the ^{1}H NMR spectrum (shown in Figure 3.19 below) for the final experiment shown in Table 3.30, it can be seen that the epoxide has been ring opened when HCl was used as the catalyst for ring opening.

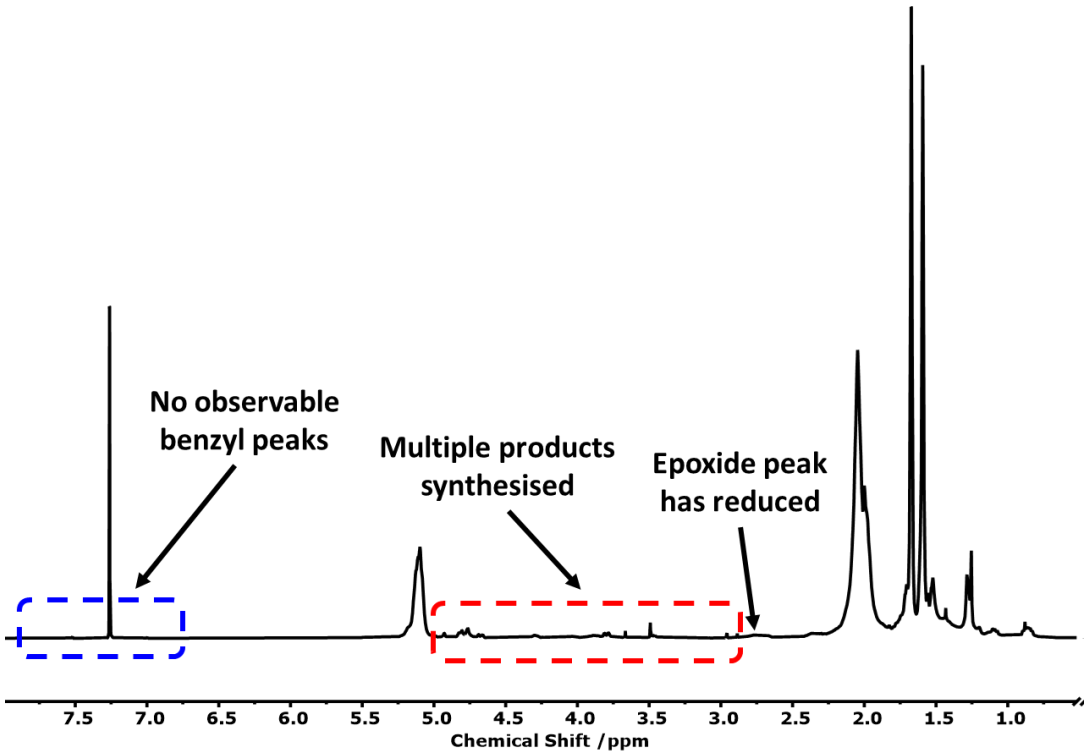

Figure 3.19: ^{1}H NMR spectra (400 MHz, $CDCl_3$) of EPM-Bz7, whereby the area where benzylamine peaks would be expected is highlighted by the blue box and the red box highlights the presence of the by-product signals.

As it can be seen in the ^{1}H NMR spectrum in Figure 3.19 above, despite the peaks at 2.70 ppm ($H_{E3/E7/E7'}$), 1.26 ppm ($H_{E9/E9'}$) and 1.31 ppm ($H_{E10/E10'}$) mostly disappearing, it does not appear that any of the benzylamine has been incorporated into the polymer (as shown by the lack of any phenyl peaks, which would be expected in the range 7.00 ppm – 7.50 ppm). This suggests that the acid and the water in which the acid was dissolved were acting as the nucleophile rather than the benzylamine. This resulted in multiple products being synthesised – much like what was observed in the acid-catalysed ring-opening reactions using water as the nucleophile – whereby both the water and the acid itself acted as the nucleophile in both

Markov and anti-Markovnikov addition reactions. Some of the potential products that could have been synthesised can seen in Figure 3.20 below.

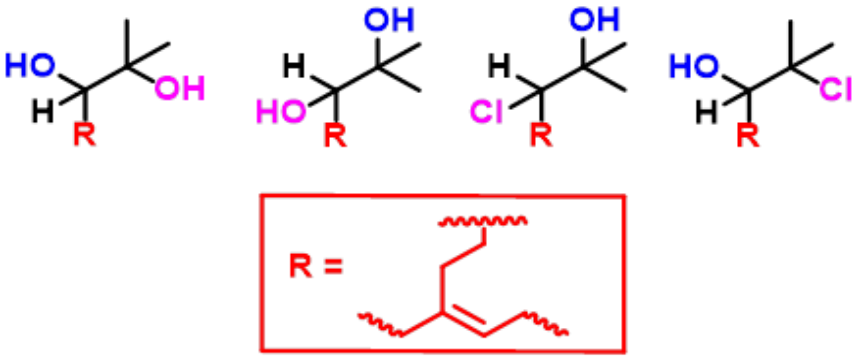

Figure 3.20: Structures of the potential products from the epoxide ring-opening reaction, where the blue hydroxy group represents the group from the epoxide and the pink group represents the added nucleophile.

Due to the lack of any benzylamine being incorporated into the polymer upon epoxide ring-opening, it was decided that we would once again switch the nucleophile being used to sodium azide. Sodium azide was chosen as the new nucleophile as it represented both a stronger nucleophile than benzylamine but also provided a much smaller nucleophile to ensure that it was not the steric bulk of the phenyl group that prevented the incorporation of benzylamine. Initially, very mild conditions were used for the sodium azide reactions due to the fact that in strong acidic conditions, the highly explosive hydrazoic acid could be generated, but also to try and prevent the degradation of the polymer, which was observed in previous acid catalysed reactions.

To do this, EPM1 was dissolved in the selected solvent before the selected catalyst and sodium azide were added. The solution was stirred with heating for a length of time, which has been depicted in Table 3.31 below. The full experimental of this test series can be found in Section 3.4.

Table 3.31: Summary of the conditions used for each ring-opening reaction using sodium azide as the nucleophile.

Product Code	Mass of EPM1 /g	Solvent		Catalyst		Mass of NaN_3 /g	Time /hrs	Temperature/ °C
		Type	Volume /mL	Type	Volume /mL			
EPM-Az1	0.50	Acetonitrile/Water (1:1)	40	-	-	0.15	4	25
EPM-Az2	0.50	THF/Water (1:1)	40	-	-	0.15	4	25
EPM-Az3	0.25	THF/Water (1:1)	40	$NaHCO_3$	10	0.10	4	70
EPM-Az4	0.25	THF/Water (1:1)	40	Acetic A	5	0.15	6	70
EPM-Az5	0.10	Dioxane/Water (1:1)	30	Acetic A	5	0.15	24	100
EPM-Az6	0.20	Toluene/Water (1:1)	40	Acetic A	6	0.20	24	100
EPM-Az7	0.26	Toluene/Water (2:1)	30	Acetic A*	5	0.30	20	100

*0.3 g of NH_4Cl was also added

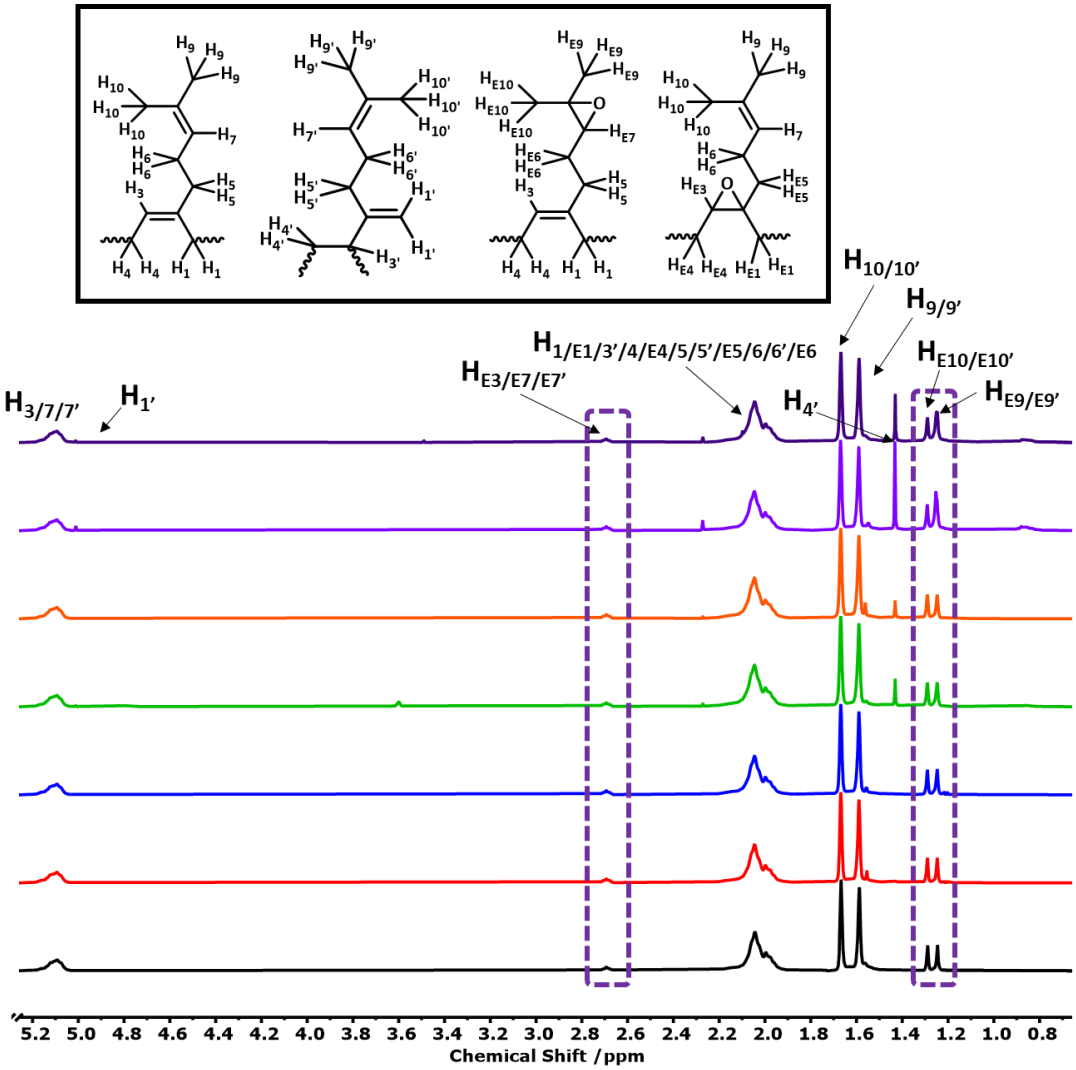

Figure 3.21: Stacked ^1H NMR spectra (400 MHz, $CDCl_3$) of epoxidised Poly(Myr) (Black) with the attempted ring-opening reactions EPM-Az1 (Red), EPM-Az2 (Blue), EPM-Az3 (Green), EPM-Az4 (Orange), EPM-Az5 (Violet), EPM-Az6 (Indigo) moving up respectively with the proton next to the epoxide ring highlighted by the purple box.

As it can be seen in the stacked ^{1}H NMR spectrum in Figure 3.21 above, for the first six experiments in Table 3.31, it appears that the epoxide ring was not ring opened under any of the conditions that were tried using sodium azide as a nucleophile due to the peaks at 2.70 ppm ($H_{E3/E7/E7'}$), 1.26 ppm ($H_{E9/E9'}$) and 1.31 ppm ($H_{E10/E10'}$) still being present at the end of the reaction. However, if we look at the ^{1}H NMR spectrum (shown in Figure 3.22 below), for the final experiment shown in Table 3.31, it can be seen that the epoxide has been ring opened upon the addition of NH_4Cl as a co-catalyst with acetic acid.

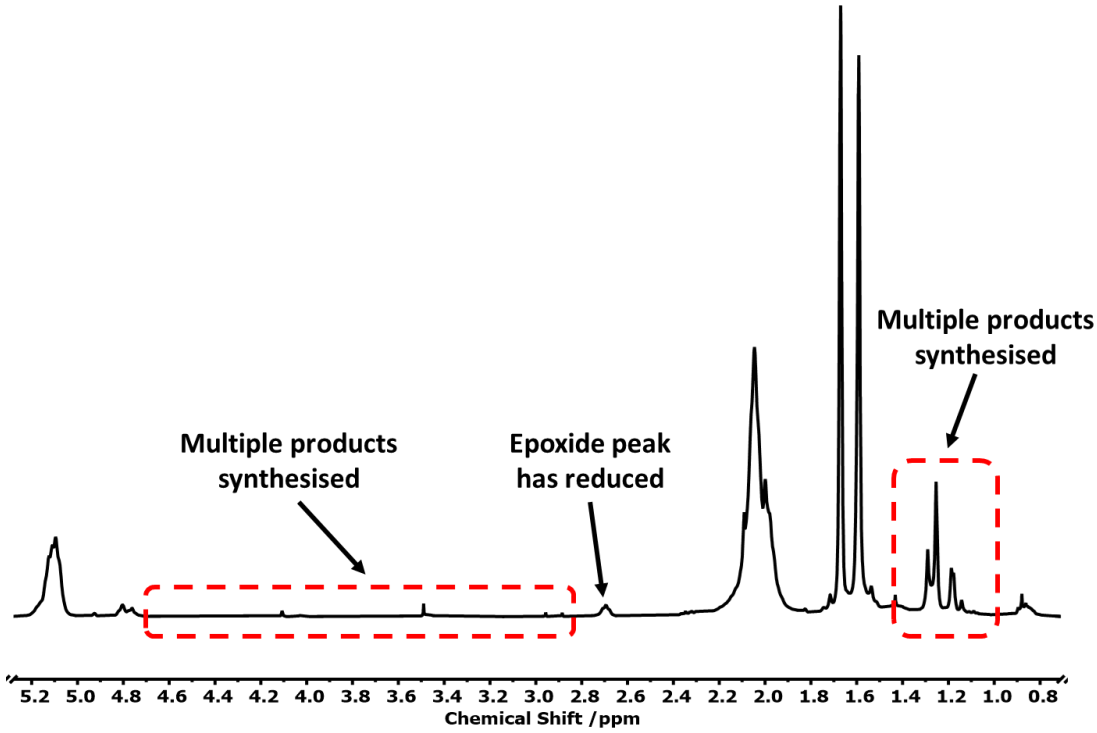

Figure 3.22: ^{1}H NMR spectra (400 MHz, $CDCl_3$) of EPM-Az7, whereby the red box highlights the presence of the by-product signals.

Once again, as it can be seen in the ^{1}H NMR spectrum in Figure 3.22 above, despite the peaks at 2.70 ppm ($H_{E3/E7/E7'}$), 1.26 ppm ($H_{E9/E9'}$) and 1.31 ppm ($H_{E10/E10'}$) being reduced and some peaks appearing, which could indicate the incorporation of the sodium azide, it appears that the chloride from the NH_4Cl and the water in which the acid was dissolved could also be acting as the nucleophile. This resulted in multiple products being synthesised – much like what was observed in the acid-catalysed ring-opening reactions using water as the nucleophile – whereby the water, the azide and the chloride all acted as the nucleophile in both Markov and anti-Markovnikov addition reactions.

Many of the unsuccessful reactions that were tried had been successfully conducted before in the literature, so it was quite surprising that these acid and base catalysed ring-opening reactions were unable to work. [24] Upon revision of the literature that was followed, it was discovered that in each case, the ring-opening reaction had been carried out on an epoxide that either contained an electron withdrawing phenyl group or a reduced degree of substitution. It is therefore proposed that the electron donating effects (and potentially the steric hindrance) of the three alkyl groups on each of the epoxides, together with the lack of the electron withdrawing phenyl group, stabilise the epoxide ring and make it much more difficult to open. This means that harsher conditions were required to allow for the successful incorporation of each of the nucleophiles. After further revision of the literature, it was discovered that under the conditions that were required to open the epoxide ring using acid, it is also possible to cause the hydrolysis of other double bonds that are present – something that was noticed may have been occurring in these systems as well. [27] This has not been evidenced in any of the epoxide ring-opening literature that had been discovered, mainly due to the fact that there is rarely a mixture of epoxides and double bonds. This means that when the epoxides that were synthesised were ring-opened using acid, any selectivity that was brought about by the epoxidation reaction could be lost, making the selective epoxidation reaction useless.

While this work was being conducted, two publications on the epoxidation and subsequent ring-opening reaction using acid as the catalyst were published. [11] [28] In each case, the authors claimed that the diol was synthesised with no mention of by-products. As these publications were each in direct contradiction to observations presented here, the following section will discuss where these papers may in fact contain inaccuracies.

Yang Li *et al.* [28] have claimed to have used trifluoromethanesulfonic acid to open the epoxide rings on an epoxidised poly(myrcene) sample before using the ring-opened product as a macroinitiator to synthesise poly(myrcene)-graft-poly(lactide) copolymers. The stacked ^{1}H NMR for the poly(myrcene), epoxidised poly(myrcene) and hydroxylated poly(myrcene) can be seen in Figure 3.23 below.

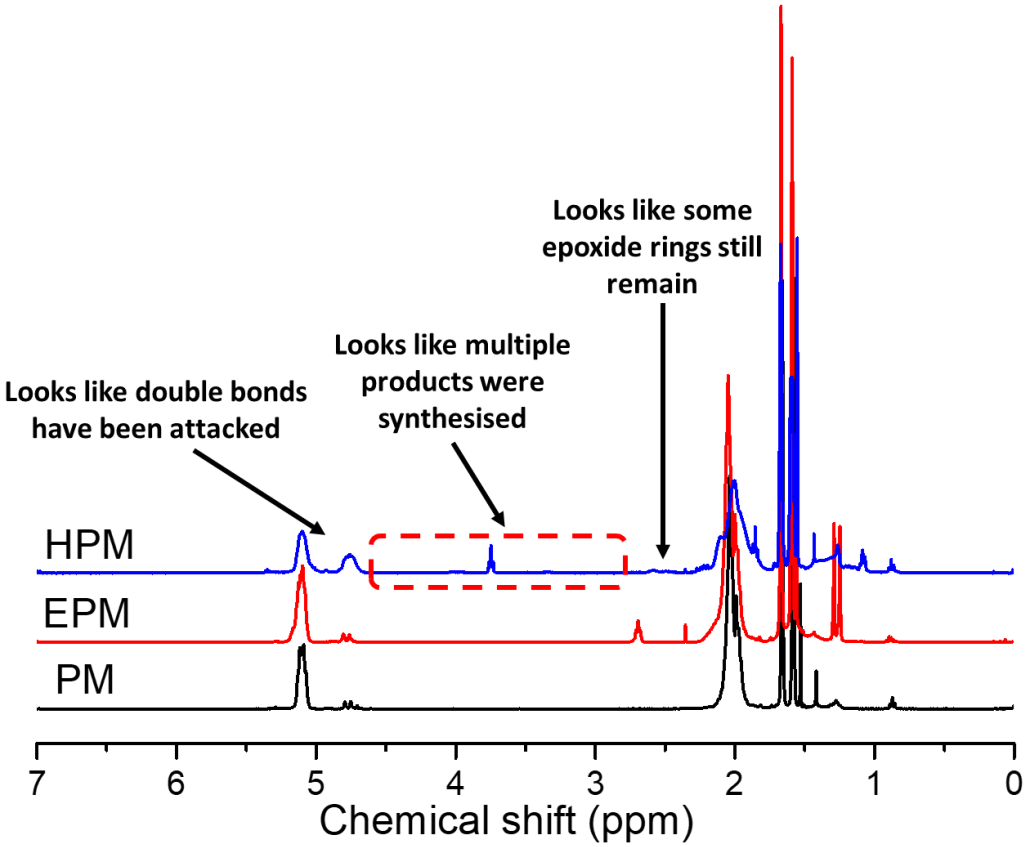

Figure 3.23: Stacked ^{1}H NMR spectra of polymyrcene (black), epoxidised polymyrcene (red) and "ring-opened" epoxidised myrcene (blue) taken from [28] **with areas of interest highlighted.**

Within the hydroxylated poly(myrcene) sample, shown in Figure 3.23 above, the authors of this paper claimed that the peak at around 3.65 ppm was the peak that corresponded to the proton next to the new hydroxyl group. However, it could be argued that due to the presence of the peak at around 1.85 ppm, the peak at 3.65 ppm is actually caused by THF, not the ring-opened product. Two other points that we would like to discuss (which the authors failed to mention) is that the baseline between 3.75 ppm and 4.5 ppm looks fairly messy, and the two peaks relating to the unsaturated poly(myrcene) double bonds have changed significantly in shape (two observations that were also noticed during our investigations). We suggest that based on our observations, both of these factors have been caused by attack of the double bonds and incorporation of multiple nucleophiles, leading to a loss of selectivity, which the authors fail to mention.

The second publication reporting epoxidation of poly(myrcene) is the work conducted by Helmut Schlaad *et al.* whereby poly(myrcene) was epoxidised using *m*-CPBA and the epoxide was then ring-opened using camphorsulfonic acid. [11] The ^{1}H NMR spectra for both the epoxidised poly(myrcene) and ring-opened product can be seen in Figure 3.24 below.

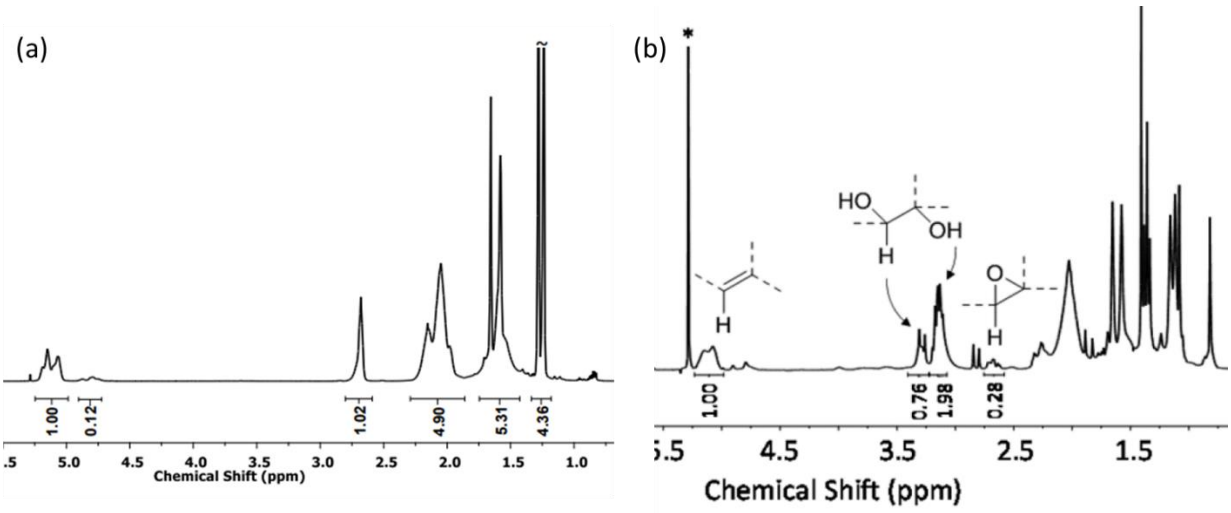

Figure 3.24: ^{1}H NMR spectra of epoxidised polymyrcene (a-left) and "ring-opened" epoxidised myrcene (b-right) taken from [11]**.**

As it can be seen in the ^{1}H NMR spectrum of the hydroxylated poly(myrcene) shown in Figure 3.24 above, the authors of this paper claimed that the peaks at around 3.1 ppm and 3.3 ppm were the peaks corresponding to the new hydroxyl group, while failing to mention that the peaks for the unsaturated double bonds had changed in shape and that the baseline was extremely messy. This suggests that, once again, the double bonds were attacked and multiple nucleophiles were incorporated.

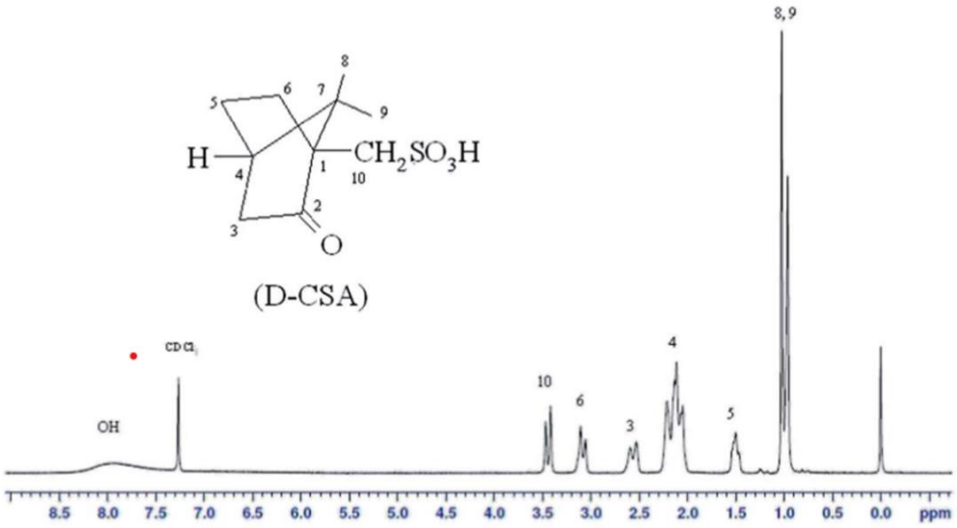

Figure 3.25: ^{1}H NMR spectrum of camphorsulfonic acid taken from [29]**.**

Upon further investigation of the camphorsulfonic acid, which was used in the epoxide ring-opening reaction, an ^{1}H NMR spectrum of which can be seen in Figure 3.25 above, [29] we

reached the further conclusion that the hydroxyl groups identified by Helmut Schlaad *et al.* were actually more likely to be caused by the incorporation of the camphorsulfonic acid due to the almost-perfect alignment of the acid's ^{1}H NMR signals with those that can be seen in the ^{1}H NMR spectrum of the ring-opened poly(myrcene).

Due to the lack of any selective ring-opening reaction by neither us nor the authors of these two publications (despite what the authors may claim), it was decided the search for a selective epoxide ring-opening reaction would continue.

3.2.6.3 The Ring-Opening of EPM1 Using Strong Nucleophiles

Having been unsuccessful in the attempts to selectively ring-open the epoxidised poly(myrcene) sample using conventional acid and base catalysed mechanisms, it was decided to try and explore methods in which neither acid nor base was required for the ring opening. To do this, a range of strong nucleophiles were explored to see whether they could be used to selectively open the epoxide ring.

To do this, EPM-1 was reacted with the nucleophile given in Table 3.32, as described by the experimental found in Section 3.4.

Table 3.32: Summary of the conditions used for each ring-opening reaction using strong nucleophiles.

Product Code	Mass of EPM1 /g	Nucleophile		Time /hrs
		Type	Volume /mL	
EPM-SN1	0.1	*n*-BuLi	0.05	16
EPM-SN2	0.25	Et_3Al	0.1	65
EPM-SN3	0.25	TMEDA and *sec*-BuLi	0.1 of each	65
EPM-SN4	0.25	Allyl MgBr	0.1	65

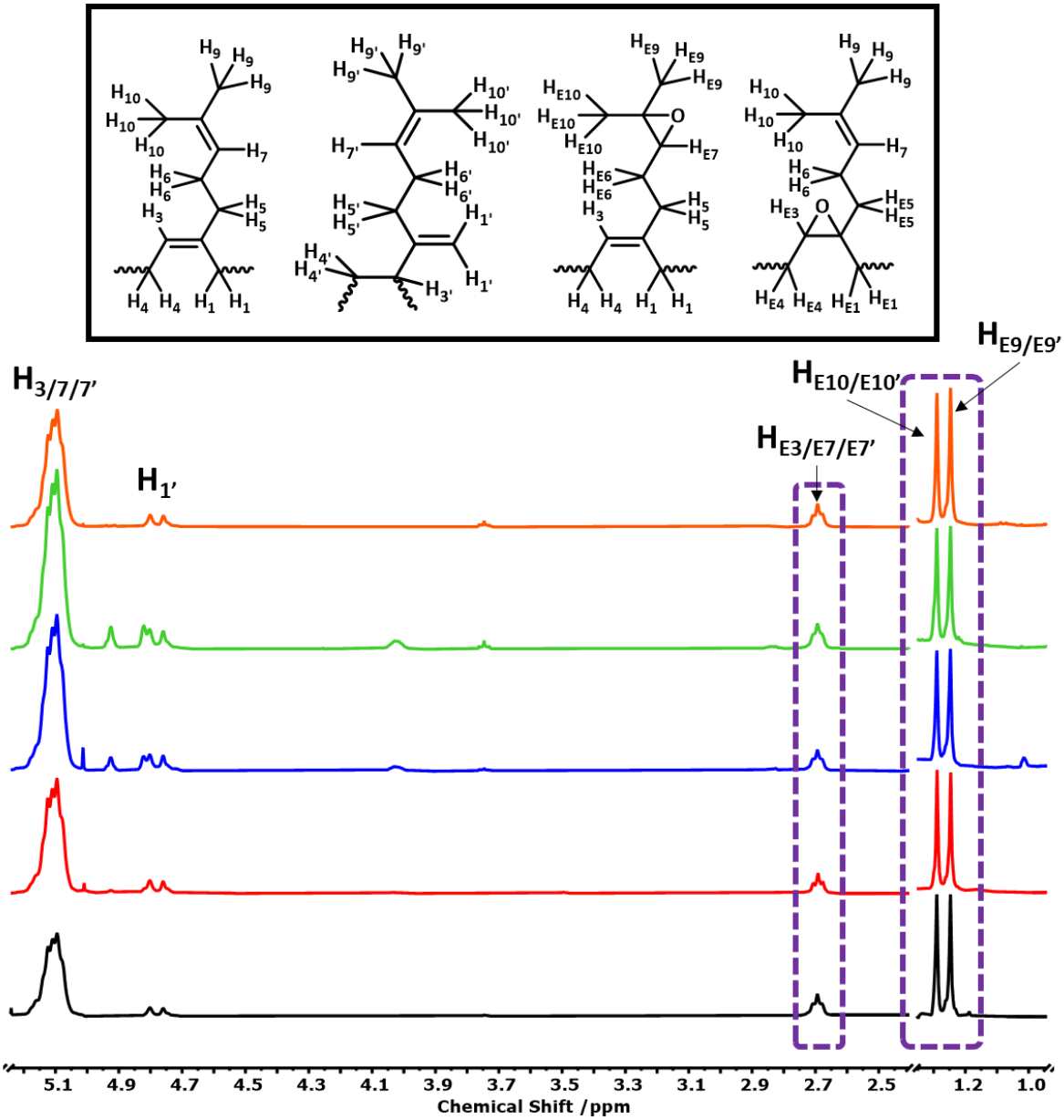

Figure 3.26: Stacked ^{1}H NMR spectra (400 MHz, $CDCl_3$) of epoxidised Poly(Myr) (Black) with the attempted ring-opening reactions EPM-SN1 (Red), EPM-SN2 (Blue), EPM-SN3 (Green) and EPM-SN4 (Orange) moving up respectively with the proton next to the epoxide ring highlighted by the purple box.

As it can be seen in Figure 3.26 above, it appears that, once again, the ring opening reactions using strong nucleophiles were unsuccessful, as evidenced by the peak for the epoxide proton and the two peaks for the methyl epoxide protons remaining even after reaction with an excess of nucleophile for a minimum of 16 h. The percentage epoxidation for each polymer can also be calculated (as shown in Table 3.33 below) and as it can be seen from these percentages, it supports the data shown above as each resulted in less than 38% of the initial epoxides being ring-opened.

Table 3.33: Summary of the ^{1}H NMR spectrum analysis before and after each attempted ring opening reaction using strong nucleophiles.

Product Code	Pre-Reaction Epoxidation Percentage /%	Post-Reaction Epoxidation Percentage /%	Epoxidation Percentage Change /%	Percentage of Epoxides Opened /%
EPM-SN1	23.0	15.3	- 7.7	33.5
EPM-SN2	23.0	14.4	- 8.6	37.4
EPM-SN3	23.0	14.7	- 8.3	36.1
EPM-SN4	23.0	18.1	- 4.9	21.3

Despite these fairly unsuccessful reactions, the fact that some of the epoxide rings had been opened meant that the search for a strong nucleophile that would allow for the selective epoxide ring-opening reaction continued.

3.2.6.4 Ring-Opening Using Lithium Aluminium Hydride as a Reducing Agent

A recent report describing the synthesis of myrcenol used lithium aluminium hydride ($LiAlH_4$) to ring-open the epoxide of myrcene epoxide (see Figure 3.28) with no apparent side reaction occurring at the two double bonds. [30] It was therefore decided that $LiAlH_4$ would be used as a reducing agent in order to try to open the epoxide ring.

It was decided to first repeat the literature reaction on myrcene epoxide (EM1) to ensure that all the products and side reactions that could occur could be identified, the full experimental of which can be found in Section 3.4.

The ^{1}H NMR of the ring-opened epoxidised myrcene (MOH1) can be seen in Figure 3.27 below.

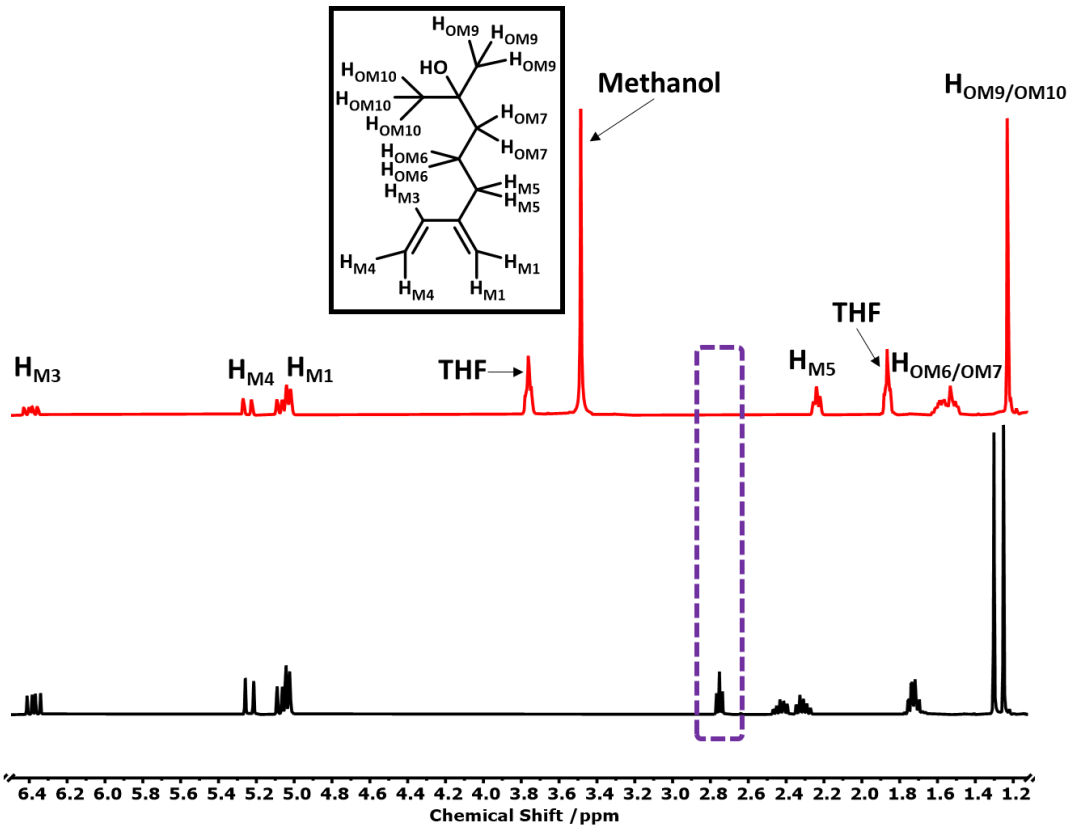

Figure 3.27: Stacked ^{1}H NMR spectra (400 MHz, $CDCl_3$) showing the selective ring opening of EM1 with proton assignment.

Table 3.34: Summary of the ^{1}H NMR analysis of MOH1 showing the expected integrals and those obtained from the ^{1}H NMR spectrum of MOH1.

Chemical Shift Range /ppm	Proton Assignment	Normalised Integration	Expected Integration
1.18 – 1.25	$H_{OM9} + H_{OM10}$	6.08	6
1.45 – 1.65	$H_{OM6} + H_{OM7}$	3.96	4
2.15 – 2.30	H_{M5}	2.00	2
4.98 – 5.30	$H_{M1} + H_{M4}$	3.98	4
6.33 – 6.48	H_{M3}	1.00	1

As can be seen in the overlaid ^{1}H NMR spectra in Figure 3.27 above, it is clear that the epoxide has been completely reduced/ring opened, as evidenced by the disappearance of the peaks at 1.26 ppm and 1.31 ppm (H_{ME9}/H_{ME10}) and 2.75 ppm (H_{Mex}), while two new peaks at 1.23 ppm and 1.55 ppm have appeared in their place. Moreover, the peaks representing the protons on carbon five (H_{M5}) and carbon 6 (H_{OM6}) have been shifted up-field as a result of the epoxide being reduced by hydride attack at carbon 7. The integrals of each of the peaks are in agreement with the predicted outcome. As expected, only one product is seen whereby

the alcohol group is on the most sterically hindered carbon (carbon 8), which shows that not only does the $LiAlH_4$ epoxide ring-opening reaction provide chemoselectivity, but it also has a strong control of the regioselectivity as well. This is brought about by the proposed reaction mechanism whereby the epoxide coordinates to Li^+, which significantly withdraws electronic charge from the epoxide – making it much more susceptible to nucleophilic attack – before a hydride anion attacks at the least substituted carbon (see Figure 3.28 below). This mechanism was known prior to the reaction due to being present in the literature, however, the fact that it appears to have resulted in 100% of the hydroxy group being found on the most substituted carbon (carbon 8) was surprising.

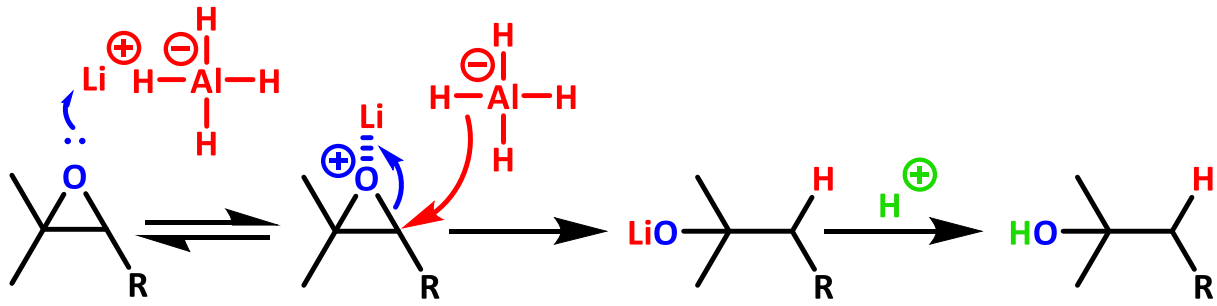

Figure 3.28: Mechanism showing the ring-opening reaction of epoxidised myrcene using $LiAlH_4$ as the strong nucleophile.

The reaction was then repeated (with slightly altered purification) on a sample of epoxidised poly(myrcene). The full conditions of this experiment can be found in Section 3.4 and the ^1H NMR spectrum of PMOH1 can be seen in Figure 3.29 below.

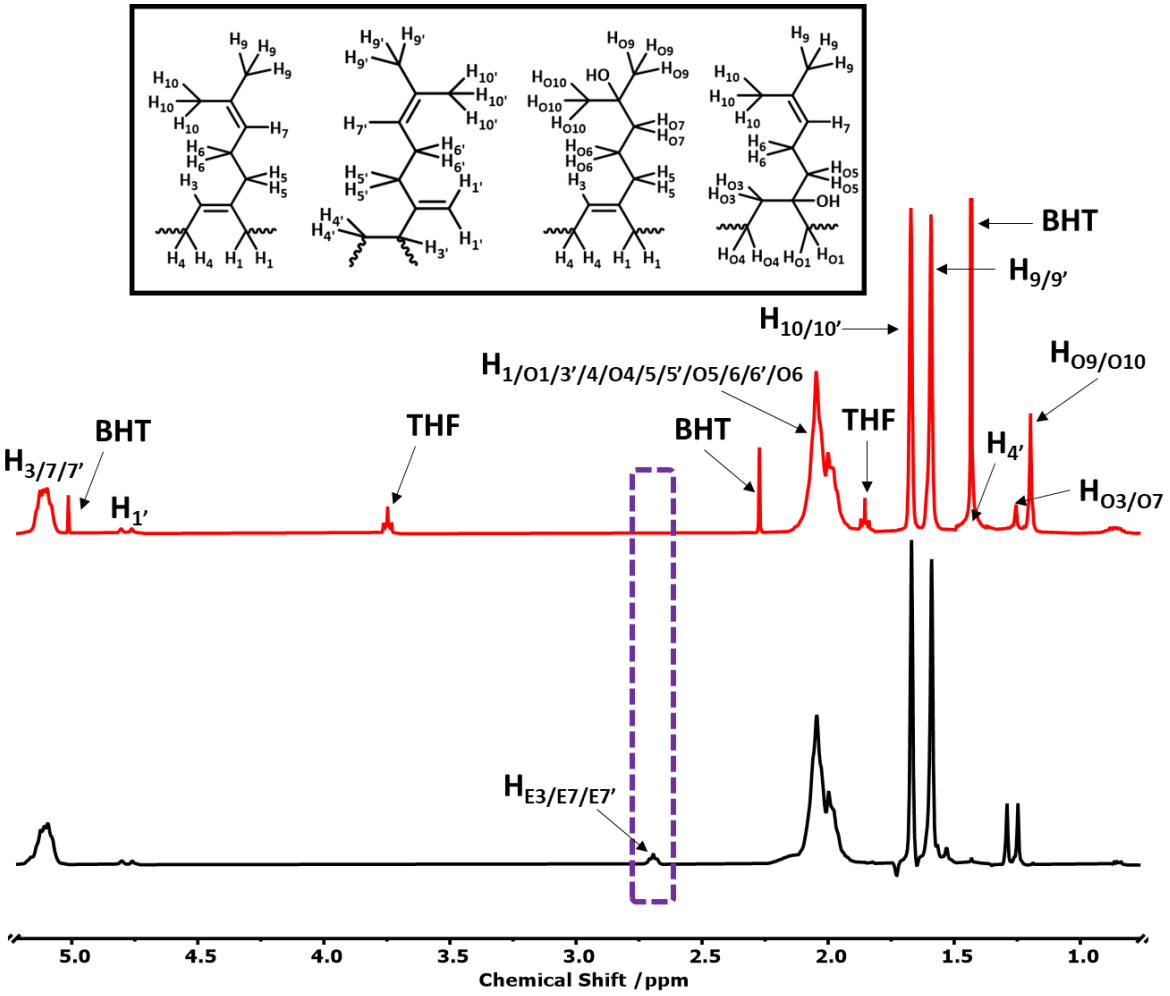

Figure 3.29: Stacked ^{1}H NMR spectra (400 MHz, $CDCl_3$) showing the selective ring opening of EPM1 with proton assignment.

As it can be seen in the stacked ^{1}H NMR spectra (Figure 3.29), the ring-opening reaction has been successful. This is evidenced by the disappearance of the epoxide peak at 2.69 ppm and the epoxidised methyl peaks at 1.25 ppm and 1.29 ppm being exchanged for mostly a single peak representing the methyl peaks that have the alcohol on carbon 8 at 1.20 ppm. There is also a second smaller peak at 1.26 ppm, which could represent either the protons on the carbon that has been attacked by the hydride anion, the product that would be observed if some of the H^- species attacked carbon 8, or – more likely based on the regioselectivity shown with MOH1 – the resulting product of a ring-opened myrcene unit that had been epoxidised on both the 3,2-alkene and the 7,8-alkene. Whatever the case, the epoxide rings appear to have been ring-opened.

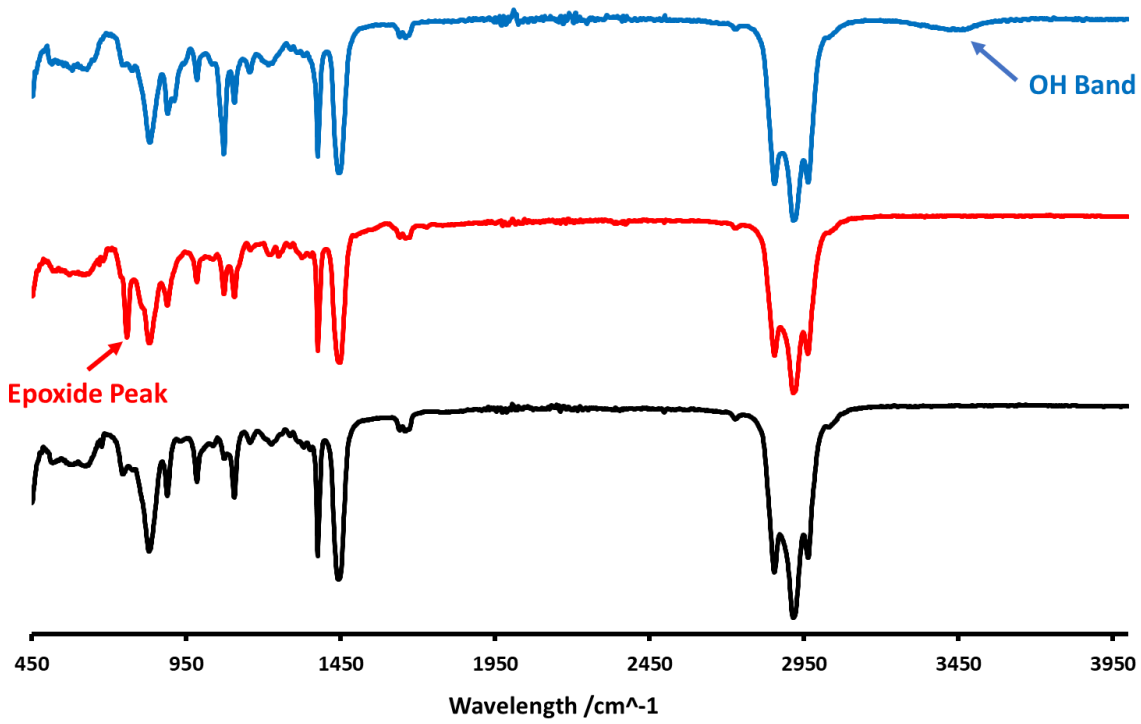

Figure 3.30: Stacked IR spectra of polymyrcene (black), epoxidised polymyrcene (red) and hydroxylated polymyrcene (blue), with the representative peaks for the new functional groups of each highlighted.

The success of the epoxidation and subsequent ring-opening reaction using $LiAlH_4$ was also confirmed through analysis of the FTIR spectrum of a sample of polymyrcene (PM1), epoxidised polymyrcene (PEM1) and hydroxy polymyrcene (PMOH1). As can be seen in the stacked FTIR spectra in Figure 3.30 above, it is evident that the polymyrcene sample is first epoxidised (shown by the appearance of an epoxide peak at around 700 cm^{-1}) and then subsequently the epoxide is ring-opened upon reaction with $LiAlH_4$ (shown by the disappearance of the epoxide peak and the appearance of an OH band at around 3450 cm^{-1}). Further proof of the selectivity of these two reactions can also be demonstrated by FTIR, as it can be seen in Figure 3.30 that the rest of the spectra (apart from the peaks that have been identified) are pretty much identical between each sample (even within the fingerprint region) apart from the alkene/C-O peaks found around 1075 cm^{-1}.

3.3 Conclusion

From the results shown in this Chapter, it is clear to see that the trisubstituted pendant double bond of myrcene shows a preferential rate of epoxidation over the trisubstituted double bond found in the polymer backbone, where it has been shown that approximately 66 % of the epoxidation occurs on the pendant double bond. It was suggested that, even though the majority of chemoselectivity that is observed with *m*-CPBA is based on the electron density of the double bond, the reduced flexibility and reduced steric availability of the myrcene backbone double bonds lead to the preferential epoxidation of the pendant groups.

It was also presented that myrcene can used as a partial/full replacement of petroleum-derived butadiene, whereby when used as a partial replacement, the presence of myrcene's trisubstituted double bonds vs. butadiene's disubstituted double bonds leads to a very strong preference for epoxidation of the myrcene relative to epoxidation of the butadiene. This preference for the epoxidation of myrcene was found to be even greater towards myrcene when the butadiene-myrcene containing polymer was synthesised in the presence of a polar modifier. This enhanced relative epoxidation of the myrcene was attributed to the increased number of vinyl myrcene and butadiene microstructures – which have lower degrees of substitution relative to the backbone bonds found in (1,4) butadiene and (4,1) myrcene – meaning that the number of trisubstituted myrcene double bonds relative to the number of disubstituted double bonds is increased – with a greater proportion of singly substituted alkenes being present, which shows a much reduced rate of epoxidation – due to the pendant double bond being unaffected by the addition of a polar additive. This culminated in the epoxidation of a terpolymer of butadiene, styrene and a very small amount (5 molar %) of myrcene, which was synthesised in the presence of TMEDA in order to provide a model for a potential car tyre formulation, whereby it was shown that the small amount of myrcene present in the sample could be epoxidised preferentially over the butadiene.

This section also looked at the ring-opening potential of the epoxide, to gain an insight into how the epoxide could be used as a platform for further functionalisation. Despite several reports in the literature detailing a variety of different ring-opening reaction conditions and a variety of different nucleophiles that could be incorporated, it was found that the trisubstituted epoxide of myrcene was extremely difficult to ring open, whereby under base-catalysed ring opening, the epoxide remained intact, and under acid-catalysed ring opening,

the unepoxidised double bonds that remained in the sample were attacked, leading to uncontrolled incorporation of a variety of different nucleophiles. It was found, however, that $LiAlH_4$ could be used to open the epoxide, with excellent regio- and chemo-selectivity, leading to hydroxyl modified polymyrcene.

3.4 Experimental

3.4.1 Materials

Food grade myrcene (≥ 95 %, Stabilised, Sigma Aldrich UK), ReagentPlus styrene (≥ 99 %, Sigma Aldrich UK), HPLC grade cyclohexane (99.8 %, Acros Organics) and anhydrous benzene (99.8 %, Sigma Aldrich UK) were dried and degassed, using extra pure calcium hydride (93 %, 0 – 2 mm grain size, Acros Organics) and the freeze-pump-thaw method. 1,3-butadiene (≥ 99.6 %, Sigma Aldrich UK) was purified by passing through molecular sieves before being sacrificially initiated with *n*-butyllithium solution (*n*-BuLi) (2.5 M in hexanes, Sigma Aldrich UK) prior to distillation. 1,1-diphenylethylene (DPE) (97 %, Sigma Aldrich UK) was purified by passing through chromatography grade basic aluminium oxide (Al_2O_3) (Brockmann I, 50-200 µm, Acros Organics) and dried under UHV for 6 hours before being distilled under UHV after titration with *sec*-BuLi. *Sec*-butyllithium (*sec*-BuLi) (1.4 M in cyclohexanes, Sigma Aldrich UK), *N,N,N',N'*-tetramethylethylenediamine (TMEDA) (≥ 99.5 %, Sigma Aldrich UK), analytical reagent grade dichloromethane (DCM) (99.99 %, Fisher Scientific UK), analytical reagent grade methanol (99.99 %, Fisher Scientific UK), analytical reagent grade ethyl acetate (≤ 99.98 %, Fisher Scientific UK), laboratory reagent grade propan-2-ol (99.5 %, Fisher Scientific UK), laboratory reagent grade hexane (fraction from petroleum, Fisher Scientific UK), laboratory reagent grade magnesium sulphate ($MgSO_4$) (dried, Fisher Scientific UK), *n*-butyllithium solution (*n*-BuLi) (2.5 M in hexanes, Sigma Aldrich UK), sodium hydrogen carbonate ($NaHCO_3$) (2.5 % Na_2CO_3, - 40 + 140 mesh, Sigma Aldrich UK) and 3-chloroperbenzoic acid (*m*-CPBA) (≤ 77 %, Sigma Aldrich UK) were all used as supplied.

3.4.2 ^{1}H NMR Measurements

Nuclear Magnetic Resonance (NMR) spectroscopy was carried out using a Bruker Advance III 400 MHz spectrometer with an operating frequency of 400.130 MHz for ^{1}H, using deuterated chloroform ($CDCl_3$) as the solvent.

3.4.3 SEC Measurements

Triple detection Size Exclusion Chromatography (SEC) was carried out using a Viscotek GPC max VE2001 solvent/sample module and a Viscotek TDA 302 (Triple Detector Array) at 35 ^{o}C with a 1 mL min^{-1} flow rate. A dn/dc value of 0.131 mL g^{-1} [31] was used for polymyrcene in

THF, a dn/dc value of 0.185 mL g^{-1} was used for polystyrene in THF and a dn/dc value of 0.124 mL g^{-1} [32] was used for polybutadiene in THF. A weighted average dn/dc value was calculated for each copolymer based on copolymer composition data obtained by ^{1}H NMR spectroscopy.

3.4.4 Polymer Synthesis

PMB3 was synthesised by LAP in benzene at room temperature, under ultra-high vacuum conditions. Dry, degassed myrcene (5.79 g, 42.5 mmol) was mixed with butadiene (6.53 g, 121 mmol), before dissolution in dry, degassed benzene (~100 mL). The polymerisation was then initiated with *sec*-BuLi (0.147 mL, 206 µmol) to synthesise a statistical copolymer, with a target M_n of 60,000 g mol^{-1}. The solution was left to stir for 1200 min at room temperature before termination *via* the injection of an excess of sparged methanol. PMB3 (a clear very viscous liquid) was recovered by precipitation into a large excess of methanol, washed and dried in *vacuo* to yield poly(myrcene-*co*-butadiene) (10.56 g, 86 %); M_n – 58,000 g mol^{-1}, M_w – 59,700 g mol^{-1}, Đ – 1.03 (as calculated by SEC using a dn/dc value of 0.126); 74 % butadiene (13 % (1,2), 47 % (1,4)-cis, 40 % (1,4)-trans), 26 % myrcene (93 % (4,1), 7 % (4,3));

PMBS3 was synthesised by LAP in benzene at room temperature, under ultra-high vacuum conditions. Dry, degassed myrcene (0.47 g, 3.45 mmol) was mixed with butadiene (3.19 g, 58.9 mmol), styrene (1.81 g, 17.4 mmol) and TMEDA (0.05 mL, 330 µmol), before dissolution in dry, degassed benzene (~100 mL). The polymerisation was then initiated with *sec*-BuLi (0.13 mL, 180 µmol) to synthesise a statistical terpolymer, with a target M_n of 30,000 g mol^{-1}. The solution was left to stir for 1200 min at room temperature before termination *via* the injection of an excess of sparged methanol. PMBS3 (a clear very viscous liquid which solidified on drying) was recovered by precipitation into a large excess of methanol, washed and dried in *vacuo* to yield poly(myrcene-*co*-butadiene-*co*-styrene) (5.15 g, 94 % yield); M_n – 34,500 g mol^{-1}, M_w – 35,400 g mol^{-1}, Đ – 1.03 (as calculated by SEC using a dn/dc value of 0.135).

3.4.5 Epoxidation Reactions (adapted from [9])

EPB1 – Poly(butadiene) – (0.30 g, M01122-prepared by Dr Matthew Oti) was dissolved in DCM (15 mL) before being placed under a nitrogen atmosphere and cooled to 0 °C. Afterwards, *m*-CPBA (0.24 g, 1.04 mmol) was dissolved in DCM (5 mL), before being injected into the polymer-containing solution. This solution was then stirred under nitrogen at 0 °C for 2 hours.

This reaction mixture was then washed with 0.1 M $NaHCO_3$ solution (50 mL) before the organic layer was separated, dried with $MgSO_4$ and precipitated into methanol. EPB1 (a white viscous liquid which solidified on drying) was then collected washed and dried in *vacuo* to yield epoxidised poly(butadiene) (0.27 g, 83 %).

EPM1 – PM1 (2.78 g) was dissolved in DCM (50 mL) before being placed under a nitrogen atmosphere and cooled to 0 ^oC. Afterwards, *m*-CPBA (0.98 g, 4.26 mmol) was dissolved in DCM (50 mL), before being injected into the polymer-containing solution. This solution was then stirred under nitrogen at 0 ^oC for 3.5 hours. This reaction mixture was then washed with 0.1 M $NaHCO_3$ solution (100 mL) before the organic layer was separated, dried with $MgSO_4$ and precipitated into methanol. EPM1 (a clear viscous liquid) was then collected, washed and dried in *vacuo* to yield epoxidised poly(myrcene) (2.59 g, 91 %).

EPM2 – PM2 (0.32 g) was dissolved in DCM (30 mL) before being placed under a nitrogen atmosphere and cooled to 0 ^oC. Afterwards, *m*-CPBA (0.22 g, 960 µmol) was dissolved in DCM (30 mL), before being injected into the polymer-containing solution. This solution was then stirred under nitrogen at 0 ^oC for 2 hours. This reaction mixture was then washed with 0.1 M $NaHCO_3$ solution (50 mL) before the organic layer was separated, dried with $MgSO_4$ and precipitated into methanol. EPM2 (a clear viscous liquid) was then collected washed and dried in *vacuo* to yield epoxidised poly(myrcene) (0.25 g, 76 %).

EPMS1 – PMS2 (0.35 g) was dissolved in DCM (30 mL) before being placed under a nitrogen atmosphere and cooled to 0 ^oC. Afterwards, *m*-CPBA (0.13 g, 560 µmol) was dissolved in DCM (30 mL), before being injected into the polymer-containing solution. This solution was then stirred under nitrogen at 0 ^oC for 2 hours. This reaction mixture was then washed with 0.1 M $NaHCO_3$ solution (50 mL) before the organic layer was separated, dried with $MgSO_4$ and precipitated into methanol. EPMS1 (a white solid) was then collected washed and dried in *vacuo* to yield epoxidised poly(myrcene-*co*-styrene) (0.30 g, 83 %).

EPMB1 – PMB3 (0.32 g) was dissolved in DCM (30 mL) before being placed under a nitrogen atmosphere and cooled to 0 ^oC. Afterwards, *m*-CPBA (0.24 g, 1.04 mmol) was dissolved in DCM (30 mL), before being injected into the polymer-containing solution. This solution was

then stirred under nitrogen at 0 ^{o}C for 2 hours. This reaction mixture was then washed with 0.1 M $NaHCO_3$ solution (50 mL) before the organic layer was separated, dried with $MgSO_4$ and precipitated into methanol. EPMB1 (a clear viscous liquid) was then collected washed and dried in *vacuo* to yield epoxidised poly(myrcene-*co*-butadiene) (0.29 g, 87 %).

EPMB2 – PMB2 (0.25 g) was dissolved in DCM (30 mL) before being placed under a nitrogen atmosphere and cooled to 0 ^{o}C. Afterwards, *m*-CPBA (0.16 g, 700 µmol) was dissolved in DCM (30 mL), before being injected into the polymer-containing solution. This solution was then stirred under nitrogen at 0 ^{o}C for 2 hours. This reaction mixture was then washed with 0.1 M $NaHCO_3$ solution (50 mL) before the organic layer was separated, dried with $MgSO_4$ and precipitated into methanol. EPMB2 (a cloudy viscous liquid) was then collected washed and dried in *vacuo* to yield epoxidised poly(myrcene-*co*-butadiene) (0.23 g, 85 %).

EPMBS1 – PMBS1 (0.25 g) was dissolved in DCM (30 mL) before being placed under a nitrogen atmosphere and cooled to 0 ^{o}C. Afterwards, *m*-CPBA (0.10 g, 430 µmol) was dissolved in DCM (30 mL), before being injected into the polymer-containing solution. This solution was then stirred under nitrogen at 0 ^{o}C for 2 hours. This reaction mixture was then washed with 0.1 M $NaHCO_3$ solution (50 mL) before the organic layer was separated, dried with $MgSO_4$ and precipitated into methanol. EPMBS1 (a white solid) was then collected washed and dried in *vacuo* to yield epoxidised poly(myrcene-*co*-butadiene-*co*-styrene) (0.20 g, 74 %).

EPMBS2 – PMBS2 (0.25 g) was dissolved in DCM (30 mL) before being placed under a nitrogen atmosphere and cooled to 0 ^{o}C. Afterwards, *m*-CPBA (0.10 g, 430 µmol) was dissolved in DCM (30 mL), before being injected into the polymer-containing solution. This solution was then stirred under nitrogen at 0 ^{o}C for 2 hours. This reaction mixture was then washed with 0.1 M $NaHCO_3$ solution (50 mL) before the organic layer was separated, dried with $MgSO_4$ and precipitated into methanol. EPMBS2 (a cloudy very viscous liquid which solidified on drying) was then collected washed and dried in *vacuo* to yield epoxidised poly(myrcene-*co*-butadiene-*co*-styrene) (0.22 g, 81 %).

EPMBS3 – PMBS3 (0.23 g) was dissolved in DCM (30 mL) before being placed under a nitrogen atmosphere and cooled to 0 ^{o}C. Afterwards, *m*-CPBA (0.02 g, 90 µmol) was dissolved in DCM

(30 mL), before being injected into the polymer-containing solution. This solution was then stirred under nitrogen at 0 ^{o}C for 2 hours. This reaction mixture was then washed with 0.1 M $NaHCO_3$ solution (50 mL) before the organic layer was separated, dried with $MgSO_4$ and precipitated into methanol. EPMBS3 (a cloudy very viscous liquid which solidified on drying) was then collected washed and dried in *vacuo* to yield epoxidised poly(myrcene-*co*-butadiene-*co*-styrene) (0.19 g, 83 %).

3.4.6 Basic Epoxide Ring Opening

EM-B1 - EM1 (0.50 g, 3.3 mmol) was dissolved in toluene (5 mL) before sodium hydroxide solution (5 mL, 25M, mmol) was added and then placed under argon. The solution was then heated to 70 ^{o}C and stirred for 4.5 hours under argon. Upon cooling, the solvent was removed in *vacuo* before DCM (50 mL) was added and the solution was then washed with HCL (50 mL, 0.1 M), $NaHCO_3$ solution (50 mL, 0.1 M) before the organic layer was separated, dried with $MgSO_4$ and the solvent removed in *vacuo* to yield EM-B1. (0.42 g, 84 %)

EM-B2 - EM1 (0.50 g, 3.3 mmol) was dissolved in chloroform (5 mL) before sodium hydroxide solution (5 mL, 25M, mmol) was added and then placed under argon. The solution was then heated to 70 ^{o}C and stirred for 4.5 hours under argon. Upon cooling, the solvent was removed in *vacuo* before DCM (50 mL) was added and the solution was then washed with HCL (50 mL, 0.1 M), $NaHCO_3$ solution (50 mL, 0.1 M) before the organic layer was separated, dried with $MgSO_4$ and the solvent removed in *vacuo* to yield EM-B2. (0.41 g, 82 %)

EM-B3 - EM1 (0.50 g, 3.3 mmol) was dissolved in THF (5 mL) before sodium hydroxide solution (5 mL, 25M, mmol) was added and then placed under argon. The solution was then heated to 70 ^{o}C and stirred for 4.5 hours under argon. Upon cooling, the solvent was removed in *vacuo* before DCM (50 mL) was added and the solution was then washed with HCL (50 mL, 0.1 M), $NaHCO_3$ solution (50 mL, 0.1 M) before the organic layer was separated, dried with $MgSO_4$ and the solvent removed in *vacuo* to yield EM-B3. (0.42 g, 84 %)

3.4.7 Acidic Epoxide Ring Opening

EM-A1 - EM1 (0.50 g, 3.3 mmol) was dissolved in toluene (10 mL) before water (1 mL) and trifluoracetic acid (0.5 mL) were added and the solution placed under argon. The solution was then heated to 70 ^{o}C and stirred for 4.5 hours under argon. Upon cooling, the solvent was removed in *vacuo* before DCM (50 mL) was added and the solution was then washed with HCL (50 mL, 0.1 M), $NaHCO_3$ solution (50 mL, 0.1 M) before the organic layer was separated, dried with $MgSO_4$ and the solvent removed in *vacuo* to yield EM-A1. (0.39 g, 78 %)

EM-A2 - EM1 (0.50 g, 3.3 mmol) was added to water (1 mL) and trifluoracetic acid (0.5 mL) before the solution was placed under argon. The solution was then heated to 70 ^{o}C and stirred for 4.5 hours under argon. Upon cooling, the solvent was removed in *vacuo* before DCM (50 mL) was added and the solution was then washed with HCL (50 mL, 0.1 M), $NaHCO_3$ solution (50 mL, 0.1 M) before the organic layer was separated, dried with $MgSO_4$ and the solvent removed in *vacuo* to yield EM-A2. (0.41 g, 82 %)

EM-A3 - EM1 (0.50 g, 3.3 mmol) was dissolved in THF (5 mL) before water (0.25 mL) and trifluoracetic acid (0.05 mL) were added and the solution placed under argon. The solution was then heated to 70 ^{o}C and stirred for 4.5 hours under argon. Upon cooling, the solvent was removed in *vacuo* before DCM (50 mL) was added and the solution was then washed with HCL (50 mL, 0.1 M), $NaHCO_3$ solution (50 mL, 0.1 M) before the organic layer was separated, dried with $MgSO_4$ and the solvent removed in *vacuo* to yield EM-A3. (0.41 g, 82 %)

EPM-A1 - EPM1 (0.26 g) was dissolved in 1,4-dioxane (25 mL) before water (10 mL) and trifluoracetic acid (3 mL) were added and the solution placed under argon. The solution was then heated to 80 ^{o}C and stirred for 2.5 hours under argon. Upon cooling, the solution was precipitated into methanol, collected and dried to yield EPM-A1. (0.22 g, 85 %).

EPM-A2 - EPM1 (0.19 g) was dissolved in toluene (30 mL) before water (10 mL) and trifluoracetic acid (3 mL) were added and the solution placed under argon. The solution was then heated to 95 ^{o}C and stirred for 3 hours under argon. Upon cooling, the solution was precipitated into methanol, collected and dried to yield EPM-A2. (0.16 g, 84 %).

EPM-A3 - EPM1 (0.23 g) was dissolved in 1,4-dioxane (30 mL) before water (10 mL) and trifluoracetic acid (3 mL) were added and the solution placed under argon. The solution was then heated to 100 ^{o}C and stirred for 3 hours under argon. Upon cooling, the solution was precipitated into methanol, collected and dried to yield EPM-A2. (0.15 g, 65 %).

EPM-Bz1 - EPM1 (0.25 g) was dissolved in DCM (30 mL) before benzylamine (0.3 mL, 2.75 mmol) was added and the solution placed under argon. The solution was then heated to 50 ^{o}C and stirred for 5 hours under argon. Upon cooling, the solution was precipitated into methanol, collected and dried to yield EPM-Bz1. (0.15 g, 75 %).

EPM-Bz2 - EPM1 (0.10 g) was dissolved in THF (10 mL) and water (10 mL) before $NaHCO_3$ solution (10 mL, 0.1 M, 1 mmol) and benzylamine (0.3 mL, 2.75 mmol) were added and the solution placed under argon. The solution was then heated to 80 ^{o}C and stirred for 5 hours under argon. Upon cooling, the solution was precipitated into methanol, collected and dried to yield EPM-Bz2. (0.08 g, 80 %).

EPM-Bz3 - EPM1 (0.10 g) was dissolved in THF (10 mL) and water (10 mL) before acetic acid (5 mL, 90 mmol) and benzylamine (0.3 mL, 2.75 mmol) were added and the solution placed under argon. The solution was then heated to 80 ^{o}C and stirred for 5 hours under argon. Upon cooling, the solution was precipitated into methanol, collected and dried to yield EPM-Bz3. (0.08 g, 80 %).

EPM-Bz4 - EPM1 (0.10 g) was dissolved in 1,4-dioxane (7.5 mL) and water (7.5 mL) before acetic acid (5 mL, 90 mmol) and benzylamine (0.3 mL, 2.75 mmol) were added and the solution placed under argon. The solution was then heated to 100 ^{o}C and stirred for 5 hours under argon. Upon cooling, the solution was precipitated into methanol, collected and dried to yield EPM-Bz4. (0.05 g, 50 %).

EPM-Bz5 - EPM1 (0.10 g) was dissolved in toluene (10 mL) and water (10 mL) before acetic acid (6 mL, 100 mmol) and benzylamine (0.3 mL, 2.75 mmol) were added and the solution placed under argon. The solution was then heated to 100 ^{o}C and stirred for 5 hours under

argon. Upon cooling, the solution was precipitated into methanol, collected and dried to yield EPM-Bz5. (0.07 g, 70 %).

EPM-Bz6 - EPM1 (0.10 g) was dissolved in THF (30 mL) before acetic acid (10 mL, 170 mmol) and benzylamine (0.3 mL, 2.75 mmol) were added and the solution placed under argon. The solution was then heated to 80 ^{o}C and stirred for 5 hours under argon. Upon cooling, the solution was precipitated into methanol, collected and dried to yield EPM-Bz6. (0.05 g, 50 %).

EPM-Bz7 - EPM1 (0.27 g) was dissolved in toluene (30 mL) before HCl (10 mL, 1 M, 10 mmol) and benzylamine (0.3 mL, 2.75 mmol) were added and the solution placed under argon. The solution was then heated to 105 ^{o}C and stirred for 5 hours under argon. Upon cooling, the solution was precipitated into methanol, collected and dried to yield EPM-Bz7. (0.22 g, 81 %).

3.4.8 Epoxide Ring Opening with Strong Nucleophiles

EPM-SN1 – EPM1 (0.10 g) was dried azeotropically with benzene (3 x 15 mL) before being left under UHV for 18 hours. After 18 hours, the epoxidised polymer was dissolved in dry, degassed benzene (20 mL) before *n*-BuLi (0.05 mL, 1.8 M, 90 µmol) was injected in. The solution was then left to stir at RT under UHV for 16 hours before being precipitated into methanol, collected and dried to yield EPM-SN1. (0.07 g, 70 %).

EPM-SN2 – EPM1 (0.25 g) was dried azeotropically with benzene (3 x 15 mL) before being left under UHV for 18 hours. After 18 hours, the epoxidised polymer was dissolved in dry, degassed benzene (20 mL) before triethylamine (0.1 mL, 700 µmol) was injected in. The solution was then left to stir at RT under UHV for 65 hours before being precipitated into methanol, collected and dried to yield EPM-SN2. (0.19 g, 76 %).

EPM-SN3 – EPM1 (0.25 g) was dried azeotropically with benzene (3 x 15 mL) before being left under UHV for 18 hours. After 18 hours, the epoxidised polymer was dissolved in dry, degassed benzene (20 mL) before TMEDA (0.1 mL, 700 µmol) and *sec*-BuLi (0.1 mL, 1.4 M, 140 mmol) were injected in. The solution was then left to stir at RT under UHV for 65 hours before being precipitated into methanol, collected and dried to yield EPM-SN3. (0.15 g, 60 %).

EPM-SN4 – EPM1 (0.25 g) was dried azeotropically with benzene (3 x 15 mL) before being left under UHV for 18 hours. After 18 hours, the epoxidised polymer was dissolved in dry, degassed benzene (20 mL) before allyl magnesium bromide solution (0.1 mL, 1 M, 100 μmol) was injected in. The solution was then left to stir at RT under UHV for 65 hours before being precipitated into methanol, collected and dried to yield EPM-SN2. (0.19 g, 76 %).

MOH1 – EM1 (0.25 g, 1.64 mmol) was dissolved in dry, degassed benzene (10 mL) before $LiAlH_4$ solution (1 mL, 1.0 M, 1 mmol) was injected in. The solution was then left to stir at RT under UHV for 16 hours before methanol (2 mL) was injected in to terminate the reaction. The solvent was then removed in *vacuo* before the product was collected and dried to yield MOH1. (0.19 g, 76 %).

PMOH1 – EPM1 (0.10 g) was dried azeotropically with benzene (3 x 15 mL) before being left under UHV for 18 hours. After 18 hours, the epoxidised polymer was dissolved in dry, degassed benzene (30 mL) before $LiAlH_4$ solution (1 mL, 1.0 M, 1 mmol) was injected in. The solution was then left to stir at RT under UHV for 68 hours before being precipitated into methanol, collected and dried to yield PMOH1. (0.81 g, 87 %).

3.5 References

[1] C. G. Robertson and N. J. Hardman, “Nature of Carbon Black Reinforcement of Rubber: Perspective on the Original Polymer Nanocomposite,” *Polymers,* vol. 13, no. 538, pp. 1-28, 2021.

[2] R. Bisschop, F. Grunert, S. Ilisch, T. Stratton and A. Blume, “Influence of molecular properties of SSBR and BR types on composite performance,” *Polymer Testing,* vol. 99, p. 107219, 2021.

[3] S. Mihara, D. R. N. and J. W. M. Noordermeer, “Flocculation in Silica Reinforced Rubber Compounds,” *Rubber Chemistry and Technology,* vol. 82, pp. 524-540, 2009.

[4] T. Yuasa, M. Iwano, T. Sone and T. Tominaga, “Improved Silica Dispersibility with functionalised s-SBR for Lower Rolling Resistance,” in *The International Tire Exhibition and Conference*, Ohio, 2008.

[5] D. Kim, G. Yeom, H. Joo, B. Ahn, H.-J. Paik, H. Jeon and W. Kim, “Effect of the Functional Group Position in Functionalized Liquid Butadiene Rubbers Used as Processing Aids on the Properties of Silica-Filled Rubber Compounds,” *Polymers,* vol. 13, p. 2698, 2021.

[6] P. Pinazzi, R. Pautrat and R. Chéritat, “Réactions de carbonyles fortement électrophiles sur les cis 1,4-polyisoprènes et des polyènes analogues,” *Die Makromolekulare Chemie,* vol. 70, pp. 260-283, 1964.

[7] J. Sheng, X. L. Lu and K. D. Yao, “Investigation of Graft Polymerization of Maleic Anhydride Onto Polybutadiene Rubber,” *Journal of Macromolecular Science: Part A - Chemistry,* vol. 27, pp. 167-178, 1990.

[8] K. Sandi, R. W. Lenz and W. J. MacKnight, “Preparation of a Polypentenamer Having Pendant Ionic Groups and Its Hydrogenated Derivatives,” *Journal of Polymer Science: Polymer Chemistry Edition,* vol. 12, pp. 1965-1981, 1974.

[9] R. Pandit, G. H. Michle, R. Lach, W. Grellmann, J. M. Saiter, A. Berkessel and R. Adhikari, “Epoxidation of Styrene/Butadiene Star Block Copolymer by Different Methods and Characterization of the Blends with Epoxy Resin,” *Macromolecular Symposia,* vol. 341, no. 1, pp. 67-74, 2014.

[10] A. D. Asandei, G. Saha and A. Ranade, “Cp2TiCl Catalyzed Grafting of Methyl Methacrylate from Partially Epoxidized Poly(isoprene),” *Polymeric Materials: Science & Engineering,* vol. 51, pp. 569-570, 2006.

[11] A. Matic, A. Hess, D. Schanzenbach and H. Schlaad, “Epoxidized 1,4-polymyrcene,” *Polymer Chemistry,* vol. 11, no. 7, pp. 1364-1368, 2019.

[12] G. Ceska and J. Horgan, “Method for the epoxidation of unsaturated polymers”. International Patent WO 98/28338, 2 July 1999.

[13] J. Clayden, N. Greeves and S. Warren, Organic Chemistry, Oxford University Press, 2012.

[14] L. Shaw, “The synthesis, characterisation and functionalisation of myrcene (co)polymers prepared by living anionic polymerisation.,” University of Durham, 2018.

[15] L. R. Hutchings, “Method of Epoxidation”. International Patent WO2020212492A1, 22 October 2020.

[16] Y. Ren, Q. Gao, C. Zhou, Z. Wei, Y. Zhang and Y. Li, “Facile synthesis of well-defined linear-comb highly branched poly(3-caprolactone) using hydroxylated polybutadiene and organocatalyst,” *RSC Advances,* vol. 5, p. 27421–27430, 2015.

[17] H. L. Hsieh and R. P. Quirk, Anionic Polymerization: Principles and Practical Applications, New York: Marcel Dekker, 1996.

[18] E. Ma, H. Kim and E. Kim, “ Epoxidation and reduction of cholesterol, 1,4,6-cholestatrien-3-one and 4,6-cholestadien-3-ol,” *Steroids,* vol. 70, no. 4, pp. 245-250, 2005.

[19] S. Habibu, N. M. Sarih and A. Mainal, “Synthesis and characterisation of highly branched polyisoprene: exploiting the “Strathclyde route” in anionic polymerisation,” *RSC Advances,* vol. 8, no. 21, pp. 11684-11692, 2018.

[20] C. C. Chang, A. F. Halasa and J. W. Miller JR., “The reaction engineering of the anionic polymerization of isoprene,” *Journal of Applied Polymer Science,* vol. 47, no. 9, pp. 1589-1599, 1993.

[21] A. F. Halasa and W. L. Hsu, “Synthesis of high vinyl elastomers via mixed organolithium and sodium alkoxide in the presence of polar modifier,” *Polymer,* vol. 43, no. 25, pp. 7111-7118, 2002.

[22] J. M. Widmaier and G. C. Meyer, “Glass transition temperature of anionic polyisoprene,” *Macromolecules,* vol. 14, no. 2, pp. 450-452, 1981.

[23] M.-H. Klopffer, L. Bokobza and L. Monnerie, “Effect of vinyl content on the viscoelastic properties of polybutadienes and polyisoprenes — monomeric friction coefficient,” *Polymer,* vol. 39, no. 15, pp. 3445-3449, 1998.

[24] A. Padwa and S. S. Murphee, “Epoxides and aziridines - A mini review,” *Arkivoc,* vol. 3, pp. 6-33, 2006.

[25] F. Fringuelli, O. Piermatti, F. Pizzo and L. Vaccaro, “Ring Opening of Epoxides with Sodium Azide in Water. A Regioselective pH-Controlled Reaction,” *Organic Chemistry,* vol. 64, pp. 6094-6096, 1999.

[26] R. Munirathinam, D. Joe, J. Huskens and W. Verboom, “Regioselectivity Control of the Ring Opening of Epoxides With Sodium Azide in a Microreactor,” *Flow Chemistry,* vol. 2, no. 4, pp. 129-134, 2012.

[27] K. B. Wiberg and D. J. Wasserman, “Enthalpies of Hydration of Alkenes,” *American Chemical Society,* vol. 103, pp. 6563-6566, 1981.

[28] C. Zhou, Z. Wei, C. Jin, Y. Wang, Y. Yu, X. Leng and Y. Li, “Fully biobased thermoplastic elastomers: Synthesis of highly branched linear comb poly(beta-myrcene)-graft-poly(L-lactide) copolymers with tuneable mechanical proberties,” *Polymer,* vol. 138, pp. 57-64, 2018.

[29] X. Rao, J. Zhang, J. Zheng, Z. Song and S. Shang, “Chiral ionic liquid crystals with a bulky rigid core from renewable camphorsulfonic acid,” *RSC Advances,* vol. 4, no. 48, pp. 25334-25340, 2014.

[30] A. Behr and L. Johnen, “Myrcene as a Natural Base Chemical in Sustainable Chemistry: A Critical Review,” *ChemSusChem,* vol. 2, pp. 1072-1095, 2009.

[31] C. Pittman and B. Culbertson, “New Monomers and Polymers,” *Polymer Science and Technology,* vol. 25, 2012.

[32] L. R. Hutchings, P. P. Brooks, D. Parker, J. A. Mosely and S. Sevinc, “Monomer Sequence Control via Living Anionic Copolymerization: Synthesis of Alternating, Statistical, and Telechelic Copolymers and Sequence Analysis by MALDI ToF Mass Spectrometry,” *Macromolecules,* vol. 48, no. 3, pp. 610-628, 2015.

[33] L. Li, S. Li and D. Cui, “Highly Cis-1,4-Selective Living Polymerization of 3-Methylenehepta1,6-diene and Its Subsequent Thiol−Ene Reaction: An Efficient Approach to Functionalized Diene-Based Elastomer,” *Macromolecules,* vol. 49, pp. 1242-1251, 2016.

[34] M. A. Peters, A. M. Belu, R. W. Linton, L. Dupray, T. J. Meyer and J. M. DeSimone, “Termination of Living Anionic Polymerizations Using Chlorosilane Derivatives: A General Synthetic Methodology for the Synthesis of End-Functionalized Polymers,” *Journal of American Chemistry Society ,* vol. 117, pp. 3380-3388, 1995.

[35] P. Sarkar and A. K. Bhowmick, “Green Approach toward Sustainable Polymer: Synthesis and Characterization of Poly(myrcene-co-dibutyl itaconate),” *Sustainable Chemistry and Engineering,* vol. 4, pp. 2129-2141, 2016.

[36] A. Hirao, R. Goseki and T. Ishizone, “Advances in Living Anionic Polymerization: From Functional Monomers, Polymerization Systems, to Macromolecular Architectures,” *Macromolecules ,* vol. 47, pp. 1883-1905, 2014.

[37] D. Baskaran, “Strategic developments in living anionic polymerization of alkyl (meth)acrylates,” *Progress in Polymer Science,* vol. 28, pp. 521-581, 2003.

[38] J. Herzberger, K. Niederer, H. Pohlit, J. Seiwert, M. Worm, F. R. Wurm and H. Frey, “Polymerization of Ethylene Oxide, Propylene Oxide, and Other Alkylene Oxides: Synthesis, Novel Polymer Architectures, and Bioconjugation,” *Chemical Reviews,* vol. 116, pp. 2170-2243, 2016.

[39] S. Nakahama and A. Hirao, “Protection and Polymerization of Functional Monomers - Anionic Living Polymerization of Protected Monomers,” *Progress in Polymer Science,* vol. 15, pp. 299-335, 1990.

Chapter 4 – The Synthesis and Anionic Polymerisation of Epoxidised Myrcene

4.1 Introduction

Living Anionic Polymerisation (LAP), first reported in 1956 [1] [2], is the gold-standard polymerisation mechanism for the synthesis of polymers that are well-controlled in terms of molar mass, dispersity and molecular architecture. [3] However, due to the very reactive nature of the propagating carbanion in LAP, initiators and propagating chains have very low tolerance for presence of functional groups. Commercially, this largely restricts carbanionic LAP to the use of non-functional monomer families such as styrenics and dienes and more recently the anionic polymerisation of (meth)acrylate monomers have been commercialised, although the latter requires specific reaction conditions to inhibit unwanted side reactions with the ester carbonyl group. Although the synthesis of functional polymers and copolymers by LAP presents additional challenges, there are numerous applications where a combination of the molecular control offered by LAP and the presence of chemical functionality is highly desirable. One of the most relevant and globally significant applications that exemplifies the potential advantages of functionalised polymers produced by LAP (butadiene rubber and solution styrene-butadiene rubber) is the use of functional polymers to enhance the dispersion of filler particles in tyre rubber. There are numerous literature reports focussing on the benefits of elastomeric polymers decorated with polar/reactive functional groups in tyre rubber formulations, in terms of uniformity of dispersion of filler particles and improved viscoelastic properties, which in turn result in enhanced tyre performance. [4] [5] [6] [7]

In practice, there are two types of polymer functionalisation: chain-end functionalisation and in-chain functionalisation. Moreover, functionalisation can be achieved as part of the polymerisation reaction or post-polymerisation. Although these are topics that have been frequently discussed, herein briefly outlines the key features of the different approaches to chain functionalisation, in the context of LAP, with some typical examples.

As the name implies, chain-end functionalisation decorates the resulting polymer with functional groups at one or both chain ends for a linear polymer and at the multiple free chain ends in branched polymers. Generally speaking, such functionalities are introduced via the

initiation and/or termination steps, whereby functionalities may need to be protected to avoid reaction with the carbanion.

Organolithium initiators with a silyl-protected hydroxyl functionality, such as 3-(*t*-butyldimethylsilyloxy)-1-propyllithium, [8] [9] [10] [11] [12] or acetal-protected hydroxyl functionalities, such as (6-lithiohexyl)acetaldehyde acetal, [13] and (3-lithiopropyl)acetaldehyde acetal, [13] [14] have been used to obtain hydroxyl end-functionalised polymers, following post-polymerisation deprotection. Amino functional groups have also been introduced by the use of *p*-lithio-*N*,*N*-bis(trimethylsilyl)aniline, [15] 3-(*N*,*N*-dimethylamino)propyl-lithium [16] and 2-(*N*,*N*-dimethylamino)methylphenyl-lithium. [17] Even though 100% chain functionalisation is assured with a (protected) functionalised initiator, limited availability and often limited solubility of the initiators strongly impact the practical application of this strategy. [3] [18]

Chain-end functionalisation via end-capping and/or termination can be achieved by reaction of the living anionic chain-end with an electrophilic species carrying the desired functional group. Numerous functionalities may be introduced by the controlled termination of alkyllithium-initiated living polymers with special reagents. For example, a carboxylic acid group can be introduced by the addition of gaseous carbon dioxide to the living solution of the polymeric organolithium compound, [19] [20] hydroxyl-terminated polymers can be obtained by reaction with ethylene oxide, [18] [21] [22] and amino groups can be added through protected α-halo-ω-aminoalkanes. [23] [24] [25] Sulfonate end-capped polymers have been synthesised through the reaction of polymeric organolithium compounds directly with sultones. [26] [17] [26] However, many of these reactions are affected by side reactions, usually leading to a lower degree of functionalisation. [3]

Also, of interest for the introduction of functionalisation in LAP are functionalised derivatives of 1,1-diphenylethylene (DPE) (See Figure 4.1). DPE, a styrene derivative is a functional monomer that, due to steric bulk and a stable carbanion, is unable to homopolymerise [3] and only monoaddition occurs, even with an excess of DPE. [27] Functionalised derivatives of DPE can be added as an end-capping agent, prior to termination, [28] [29] [30] or it can be activated by butyllithium and the adduct used to initiate the polymerisation. [30] Moreover, since after the addition of DPE (or functional derivative), the polymer is still a living chain, the resulting polymeric 1,1-diphenylalkyllithium can be used as a macro-initiator to synthesise (block)copolymers by the sequential addition of monomers, an example of in-chain

functionalisation. DPE derivatives with amino groups on the aromatic rings, e.g. 1-(4-dimethylaminophenyl)-1-phenylethylene and 1-(4-(*N*,*N*-bis(trimethylsilyl)-amino)phenyl)-1-phenylethylene, have been used to obtain amino-functionalised chains of styrene and dienes with examples of such kind of functionalisation introduced at the beginning of the chain, [31] the terminus of the chain, [32] [33] [34] in-chain, [35] [36] or to prepare telechelic copolymers. [32] [37] The carboxyl functionalisation can be achieved by the use of a DPE carboxyl derivative, protected as an oxazoline group or a diisopropylamide. [3] [38] Similarly, DPE derivatives have been used to introduce a phenol group at the chain terminus [39] and 1,1-bis(4-tert-butyldimethylsiloxyphenyl)ethylene (DPE-OSi) has been used as both initiator or end-capping agent in living anionic polymerisation. [11] [40] [41] [42] The use of functionalised DPE monomers has also been exploited in the synthesis of functionalised statistical copolymers by LAP. [27] [43] [44] [45] [46] [47] [48] Although the use of functional derivatives of DPE is a widely used, valuable and effective strategy to produce functionalised (co)polymers and in particular, end-functionalised polymers, there are challenges associated the use of DPE derivatives if the objective is to produce chains with 100% end functionalisation. [49]

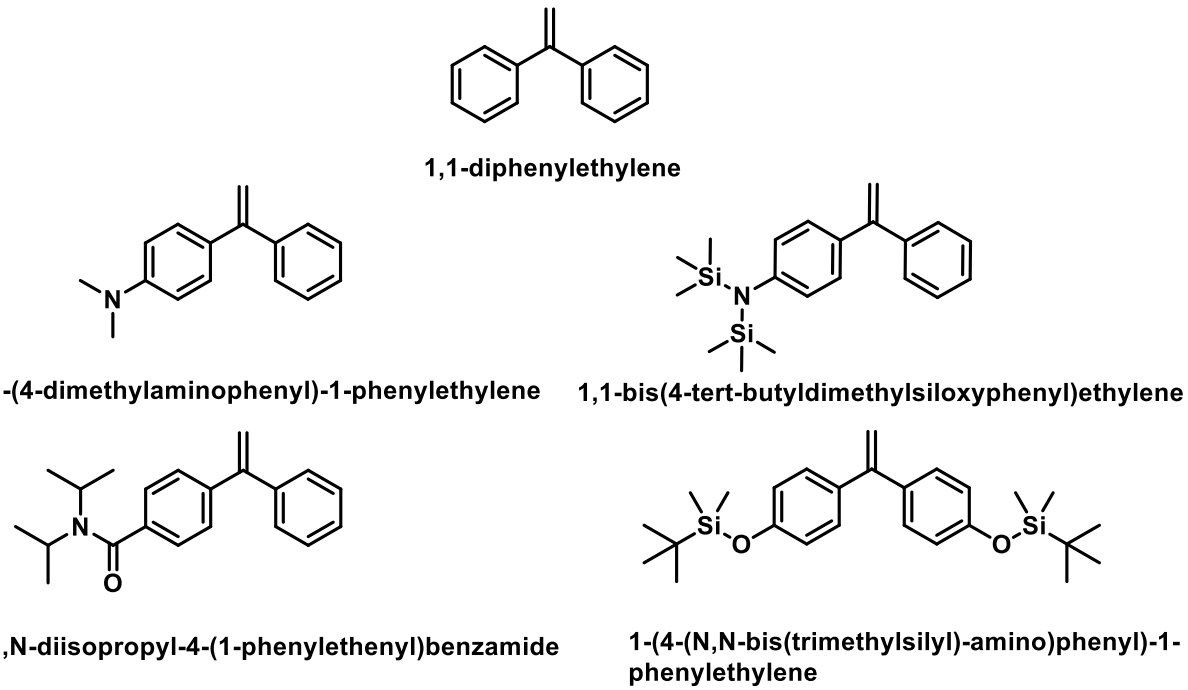

Figure 4.1: Protected functionalised derivatives of 1,1-diphenylethylene which have been used to add polarity into polymers synthesised by LAP, whereby post-polymerisation deprotection steps are required to deprotect the required functionality.

As alluded to above, it is also possible to introduce functionality onto polymers and copolymers prepared by LAP after polymerisation. Common examples include the maleinisation of polybutadiene, [50] [51] the sulfonation of polystyrene [52] [53] and the epoxidation of dienes [54] [55] [56] and the result might be considered an in-chain functionalised polymer.

As discussed previously, the use of bio-based terpene monomers such as myrcene and farnesene has been growing in prominence, in both academia and industry, [57] [58] [59] due to enhancements in the efficient extraction and industrial synthesis of these terpenes. [60] [61] [62] [63] We and others have recently reported the synthesis of myrcene-containing copolymers by LAP, with reactivity ratios reported for the statistical copolymerisation of myrcene with isoprene, styrene and 4-methylstyrene in cyclohexane. [64] Reactivity ratios have also been reported for the statistical copolymerisation of myrcene and styrene in cyclohexane in the presence of TMEDA [65] and DTHFP. [66] In a non-polar solvent and the absence of a polar modifier, the polymerisation of myrcene is strongly favoured over styrene (r_{Myr} = 36; r_S = 0.028). [64] However, the addition of even very small quantities of a polar modifier can result in a reversal of the monomer reactivity and styrene is consumed in preference to myrcene. With a ratio of BuLi:TMEDA of 1:2, reactivity ratios of r_{Mry} = 0.15 and r_{Sty} = 17.52 were reported [67] whereas the impact of DTHFP as a modifier was even more pronounced with reactivity ratios of r_{Mry} = 0.067 and r_{Sty} = 15.3 report for BuLi:DTHFP ratio of 1:1. [66] In each case the comonomer sequence can be tuned as a function of BuLi:modifier.

A couple of broader reviews covering the living anionic polymerisation of terpene monomers have recently been published by Holger Frey *et al*. [68] [69]

The use of bio-based terpene monomers as a (partial) replacement for oil-based monomers in both tyre-rubber applications and in thermoplastic elastomers is now an established concept and therefore the potential to produce functionalised polyterpenes by LAP is an attractive proposition. As mentioned in Chapter 3, a small number of reports on the synthesis of functionalised polymyrcene have been published. Schlaad *et al.* described the post-polymerisation epoxidation of high 1,4- (or more correctly 4,1-) polymyrcene produced by LAP. [70] Epoxidation was carried out using *meta*-chloroperbenzoic acid (*m*-CPBA) to varying extent of functionalization. It was noted that for partially epoxidised samples, epoxidation was selective towards the 7,8-double bond in the side chain. It was also noted that the resulting trisubstituted epoxide rings were extremely stable towards nucleophilic attack

under basic conditions, but ring-opening was possible under acidic conditions. Schlaad also reported the regioselective photochemical functionalization with various thiols using thiol-ene chemistry, although the thiol-ene addition was accompanied by chain coupling reactions and in some cases in the formation of insoluble crosslinked material. [71] Frey *et al.* took a different (in-chain) approach and synthesised silyl-protected *β*-myrcenol from *β*-myrcene in two steps, and then used LAP to polymerise the protected, hydroxyl-functionalised monomer. Homopolymers and statistical copolymers with myrcene were prepared, although it was reported that side reactions occur during polymerisation, resulting in increasing dispersity at higher molar mass. [72]

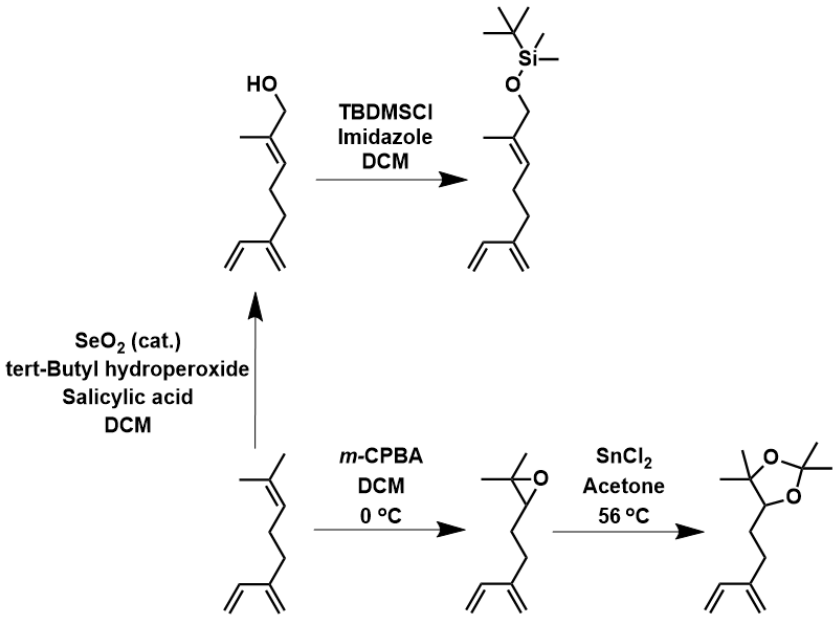

Figure 4.2: Scheme showing two protected myrcenol-based monomers that have been synthesised for use in LAP by Frey *et al.* [72] *[73]*

Combining all of this means that while an understanding of the polymerisation of myrcene and it copolymerisation with styrene has been established – in the search of a butadiene replacement with enhanced thermal and physical properties for its intented use – and protocols have been devised to selectively add functionality onto myrcene-containing polymer chains post polymerisations, there still appears to be scope for introducing functionality into the polymer through functionalised terpene-based monomers which don't require a post polymerisation step. This section will therefore be used to outline the synthesis and anionic polymerisation of a new functionalised monomer – epoxidised myrcene.

4.2 Results and Discussion

It was initially believed that epoxidised myrcene could be used as an unprotected functional monomer to be used in LAP, where the epoxide could also be used as a site for further modification if required. For this to work, the epoxide must be stable to attack by a commonly used initiator such as butyllithium (BuLi) or at least have a rate of polymerisation much quicker than any potential side or termination reactions.

4.2.1 Attempted Ring Opening of Epoxidised Polymyrcene

To ensure that any epoxidised myrcene monomer synthesised was suitable for polymerisation by LAP, it was decided to first test the stability of the epoxide in a sample of epoxidised polymyrcene (EPM3) towards nucleophilic attack (by *n*-BuLi). This was achieved by mixing EPM3 with an excess of *n*-BuLi (see Section 4.4). EPM3 was prepared using the experimental found in Section 4.4, which was a modified version of the epoxidation reaction utilised by Pandit *et al.* [55] As discussed previously, the epoxidation of polymyrcene was researched in the recent publication by Schlaad *et al.* where it was found that approximately two thirds of the epoxidation occurred on the pendant double bond. [70] This was in great agreement to the 74 % of epoxidation that was found to have occurred on the pendant double bonds in EPM3.

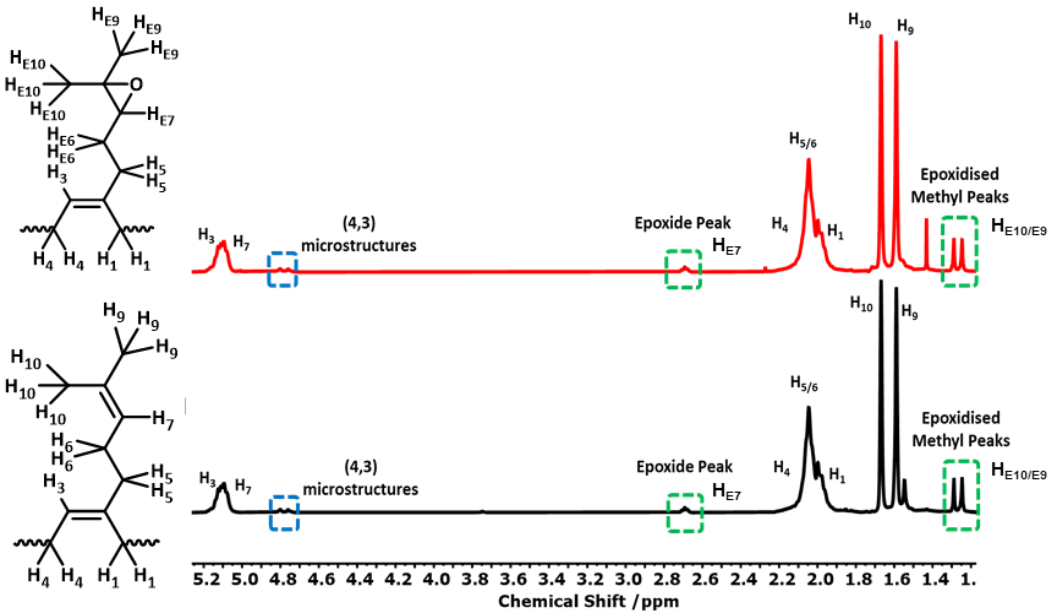

Figure 4.3: Stacked ^{1}H NMR spectra of EPM3 (Black - Bottom) and EPM-BuLi (Red - Top) with proton assignment.

As it can be seen in the stacked ^{1}H NMR spectra in Figure 4.3, there is only a little change to EPM3 when it is reacted with *n*-BuLi, with no observable peaks for the ring-opened product. This is confirmed by the epoxidation percentage being 16 % and 15 % in EPM3 and EPM-BuLi respectively, which was calculated using Equations 3.5 and 3.6 found in Section 3.2.2.1.1, indicating that very little observable epoxide ring opening has occurred (within the accuracy of the ^{1}H NMR used) despite a very long reaction time and enough *n*-BuLi to ring open most of the epoxide units. This suggests that the epoxidised myrcene monomer would be suitable for LAP, as it suggests that on the timescale of the polymerisation, very little termination through epoxide ring would occur.

4.2.2 Synthesis of Epoxidised Myrcene

As discussed previously, Schlaad *et al*. showed that by epoxidising polymyrcene with meta-chloroperoxybenzoic acid (*m*-CPBA), high selectivity (~ 66 %) towards the pendant double bond could be achieved. [70] However, it was proposed that the presence of some backbone epoxides may still impact the T_g – while due to the reduction of accessibility of the epoxide does not provide the full extent of benefit which is possible – and the process requires a post-polymerisation functionalisation, which can prove costly for industry due to the requirement for large amounts of solvents to solubilise the polymer.

The idea behind the polymerisation of epoxidised myrcene was therefore to remove the post-polymerisation functionalisation step that has had to be employed previously and to ensure that 100 % of the epoxide rings were situated on the 7,8 double bond of myrcene, rather than having to rely on the relative rates of reactions of the different myrcene double bonds.

To prepare the epoxidised myrcene (EM), myrcene is reacted with *m*-CPBA similar to the reaction used by Schlaad *et al.* to synthesise the epoxidised polymyrcene. However, within myrcene, there are three different double bonds of varying degrees of substitution, and this epoxidation reaction is not 100 % selective towards the 7,8 double bond but instead follows the expected trend in relative rates of reaction (Figure 4.4) [74]

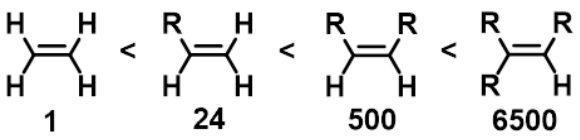

Figure 4.4: Rates of epoxidation by m-CPBA for a variety of alkene substrates, relative to an unsubstituted alkene (ethylene). *[74]*

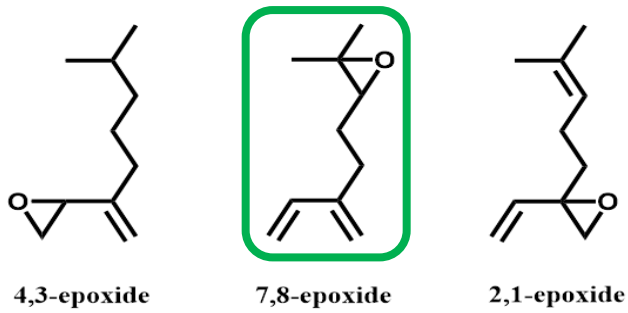

Figure 4.5: Diagram showing the potential sites of epoxidation with the required epoxidised myrcene highlighted in green.

This means that there are three different potential sites of the epoxide ring, as seen in Figure 4.5 above, where the ratios of each would follow the rates shown in Figure 4.4 where the 7,8-epoxide would be expected to predominate. For the purpose of LAP and our requirements, only the 7,8-epoxide is desired, as neither the 4,3-epoxide nor the 2,1-epoxide would have the required diene to allow them to be polymerised by LAP, and both have a significant decrease in the steric hindrance around the epoxide, which could result in termination of the LAP through the ring opening of the epoxide. However, chromatographic separation of the 7,8-epoxides from the 2,1-epoxides and 4,3-epoxides would be extremely difficult if not impossible due to all epoxides having approximately the same polarity. It was therefore decided to epoxidise the myrcene using 1.1 eqv. *m*-CPBA (Figure 4.6).

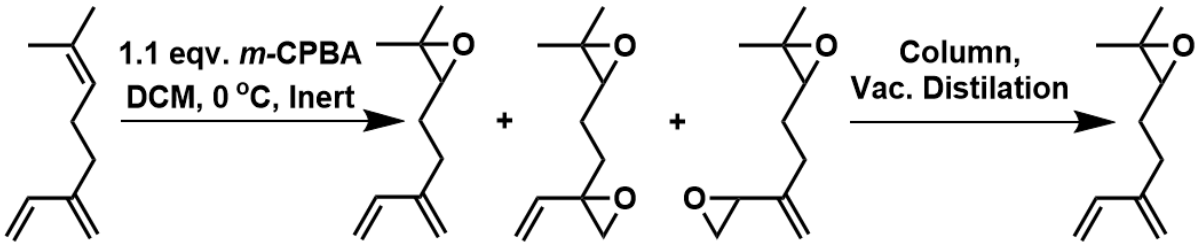

Figure 4.6: Scheme showing how high purity 7,8-epoxidised myrcene could be prepared for polymerisation by LAP.

This approach would help ensure that all 7,8-double bonds were epoxidised and any other epoxides formed should have a 7,8-epoxide also present in myrcene. This would allow the 7,8-epoxidised myrcene to be removed from any di-epoxide impurities using a silica column to separate the products based on polarity, followed by a vacuum distillation. The full experimental and characterisation of EM1 can be found in Section 4.4.

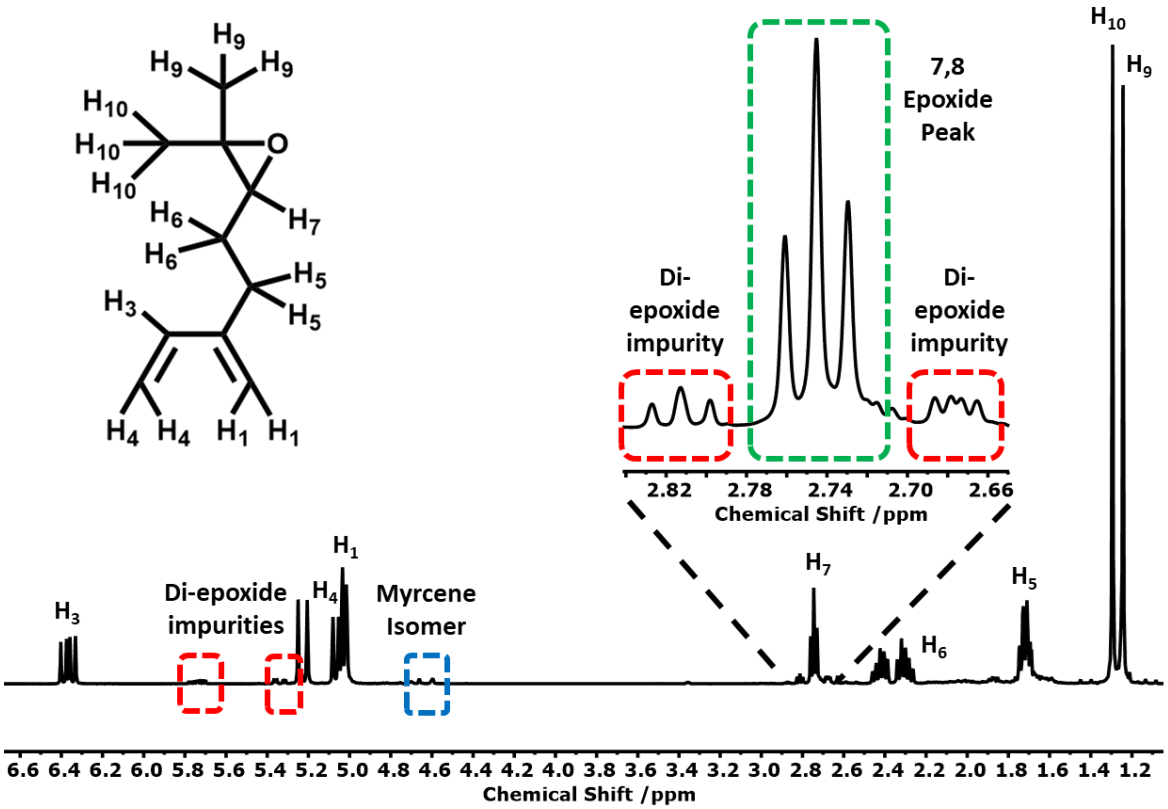

Figure 4.7: ^{1}H NMR spectrum (400 MHz, $CDCl_3$) of crude EM1.

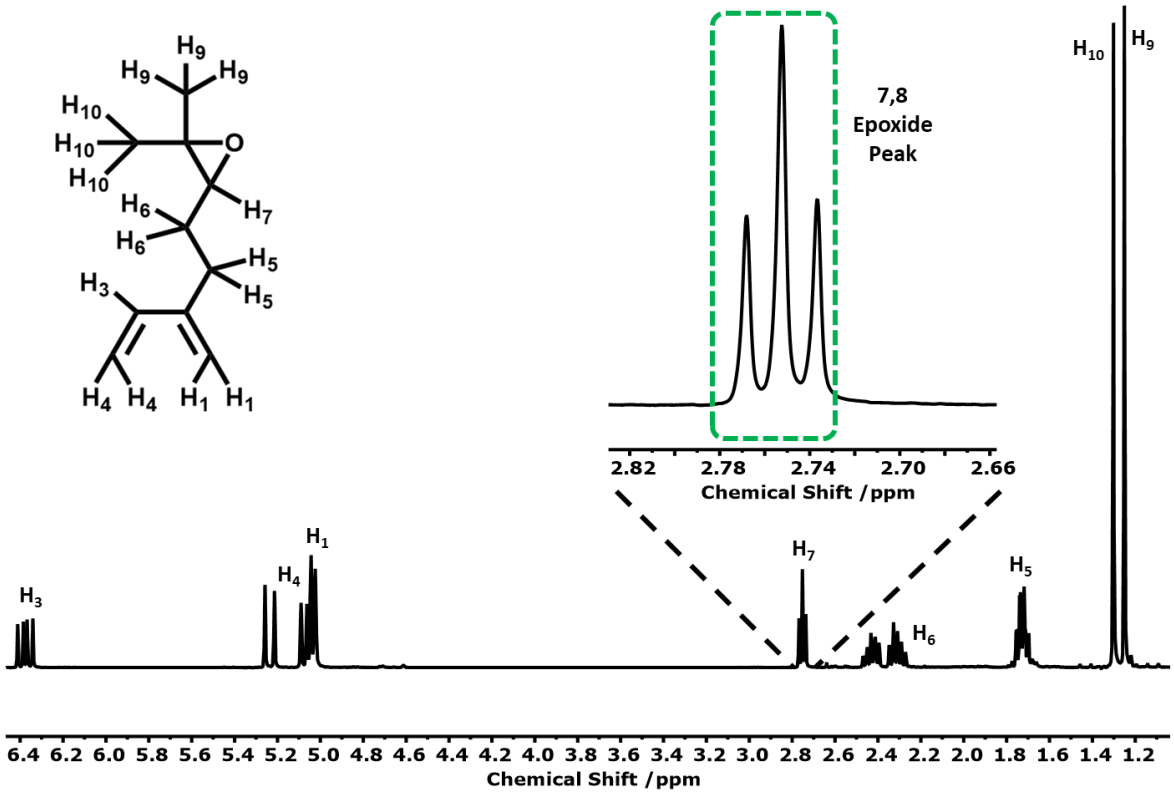

Figure 4.8: ^{1}H NMR spectrum (400 MHz, $CDCl_3$) of EM1 after purification of the monomer by both a column and vacuum distillation, with hydrogen assignment.

As it can be seen in Figure 4.8 above, the EM contained no detectable di-epoxide impurities left in the monomer mixture. This suggests that this synthetic route may be suitable for preparation of monomer for subsequent LAP.

4.2.3 Statistical Copolymerisation of Epoxidised Myrcene

Having proven that the epoxide was stable to attack by *n*-BuLi and having synthesised pure EM, the next step was to try to synthesise polymers via LAP. Due to potential problems associated with the solubility of EM and 100 % epoxidised polymyrcene, it was decided to copolymerise EM with myrcene. Not only would this help prevent any problems associated with the solubility of the final polymer, but it would allow us to increase the amount of BuLi initiator used relative to amount of impurities that could be introduced through our synthesised monomer, making the reaction more robust.

Initially, it was believed that by carrying out the polymerisation at -78 ^{o}C, much like in the LAP of methyl methacrylate and its derivatives (most interestingly methyl glycidyl methacrylate [75]), the polymerisation would occur and the reduced temperature would help reduce any potential side or chain-end reactions. [76]

The attempted synthesis of PEM1 was carried out at -78 ^{o}C in toluene (full experimental can be found in Section 4.4), however, the polymerisation was unsuccessful, with the ^{1}H NMR spectrum indicating the presence of only unreacted monomer. It was therefore decided to raise the temperature to RT and try the polymerisation again.

The second attempted LAP of EM1 was carried out at RT in benzene, with the full experimental details being found in Section 4.4.

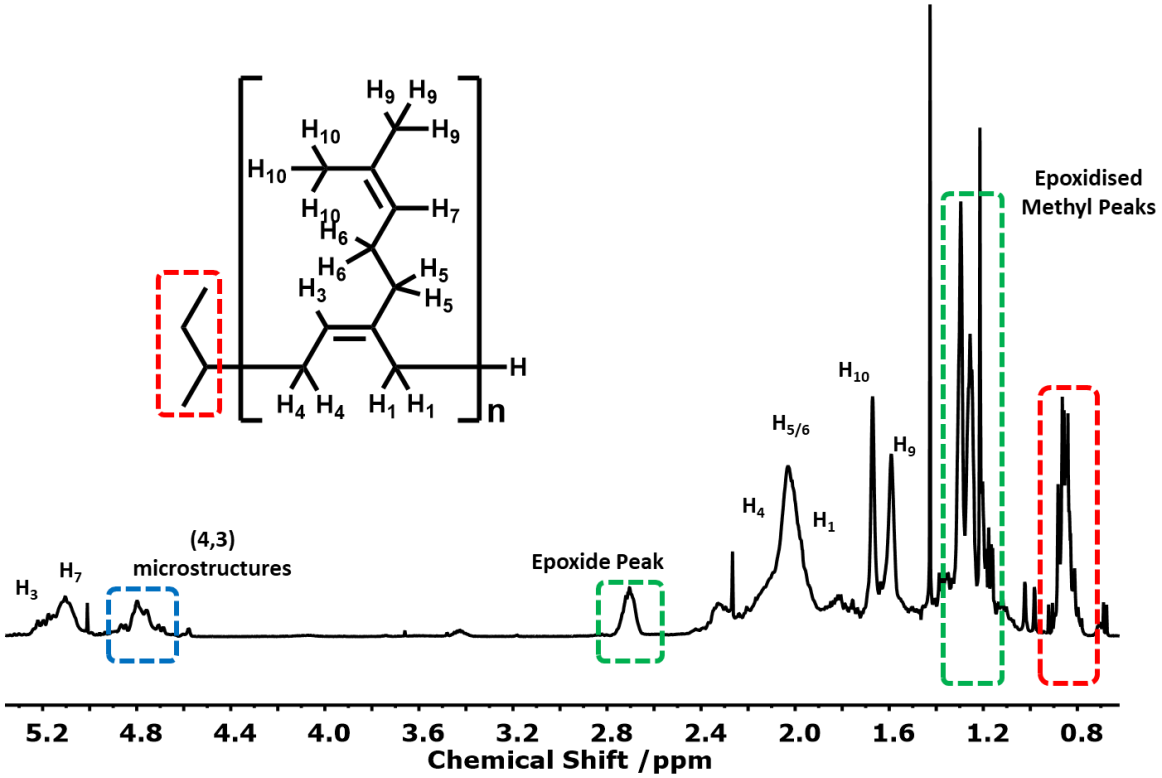

Figure 4.9: Partial ^{1}H NMR (400 MHz, $CDCl_3$) spectrum of PEM2 with proton assignment.

As it can be seen in Figure 4.9 above, polymerisation has occurred during this reaction as evidenced by the presence of the polymer peaks that are observed in polymyrcene when compared to a ^{1}H NMR spectrum of polymyrcene [77]. We can also see, when compared to the ^{1}H NMR spectrum in Figure 4.3, that both a peak representing the hydrogen next to the epoxide at 2.70 ppm and two peaks representing the hydrogens on the methyl peaks next to the epoxide at 1.26 ppm and 1.30 ppm are present. The broad nature of the epoxide peak at 2.70 ppm and the absence of monomer peaks in the ^{1}H NMR spectrum indicate that EM has been incorporated into the polymer, demonstrating that EM can in fact be polymerised by LAP. From the integrals of the NMR spectrum, it can be estimated that there is 39 % (4,3) microstructures (far higher than the usual 7 % and far closer to those observed in polymerisations occurring in the presence of a polar modifier [217]) and 61 % (4,1) microstructures. It can also be calculated that the polymer is composed of 64 % EM, which is significantly higher than the feed ratio of 14 % EM, suggesting a gradient copolymerisation.

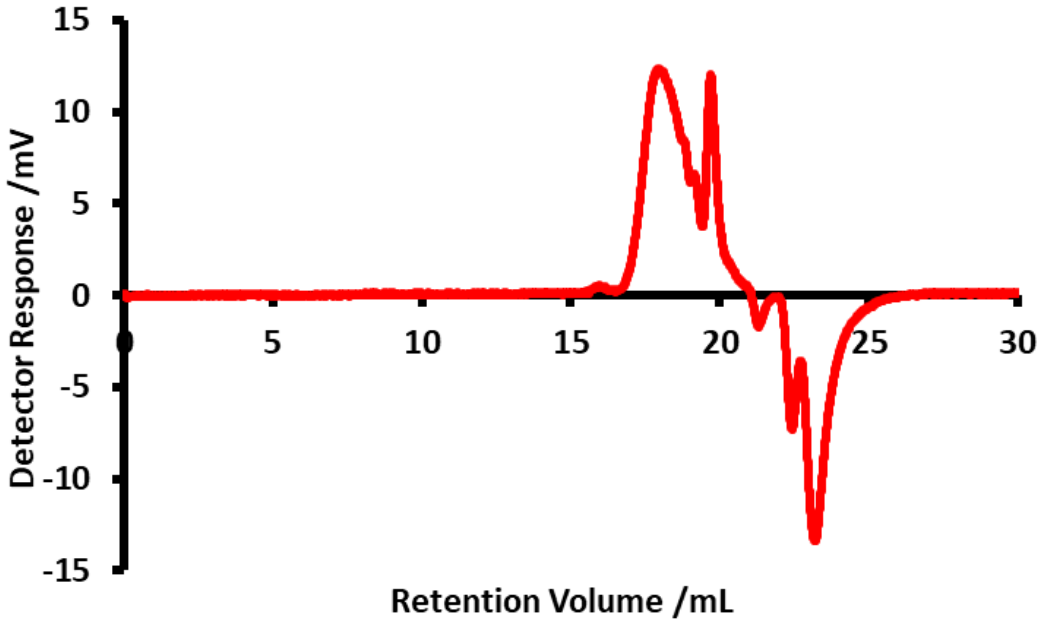

Figure 4.10: RI SEC trace of PEM2.

No numerical data was obtained from the SEC, suggesting that the oligomers were too small to be assigned a molecular weight by the detector. We can, however, gather some qualitative information about PEM2 from the RI trace in Figure 4.10 above. Firstly, supporting the presence of polymer peaks in the ^{1}H NMR spectrum, it is shown that some degree of polymerisation has occurred due to the wide trace (with several shoulders present) observed. Secondly, it can be suggested that the dispersity is very high – due to the broad nature of the trace – and the actual M_n of the collected polymer did not reach the theoretical M_n of 5,000 g mol^{-1} – as one would expect the peak at a lower retention volume based on previous polymyrcene polymerisations – suggesting some form of termination mechanism may be occurring.

Based on both the high (4,3) microstructure content and the higher-than-expected epoxide content, we propose that not only is the EM being polymerised as a monomer in LAP but also acting as its own polar modifier, in a similar way in which the ether tetrahydrofuran (THF) acts as a polar modifier. This hypothesis not only explains the higher-than-would-be-expected (4,3) microstructure for a polymerisation carried out in a non-polar solvent in the absence of a polar modifier but also leads to the preferential incorporation of the EM at the start of the reaction. Despite both myrcene and EM having a diene, which will be almost electronically identical, the presence of the epoxide and its co-ordination to the lithium counter cation leads

to an increased local concentration of the EM at the active anion. This coordination could be expected to lead to the $k_{M\text{-}EM}$ rate constant being higher than the $k_{EM\text{-}M}$ rate constant, where $k_{M\text{-}M}$ and $k_{EM\text{-}EM}$ are approximately equal due to the electronic similarity of the dienes in each. This is turn would lead to the reactivity ratio r_{EM} being greater than r_M, resulting in the preferential incorporation of the EM at the beginning of the polymerisation. To the best of our knowledge, this is the first time that a monomer that can act as its own polar modifier through co-ordination to the lithium counter ion has been copolymerised by LAP in a non-polar solvent. These observations may yield some insight into the importance that local concentration may play in the kinetics of copolymerisation, but further investigation is needed to provide a complete explanation.

In an attempt to synthesise a polymer with a higher molar mass to enable collection by precipitation and to eliminate any effect that the initiator might have on the EM, it was decided to stagger the monomer feed with only myrcene present during initiation, and epoxidised myrcene added after a short period of time. PEM3 was synthesised by allowing the polymerisation of myrcene to occur for 10 mins before the epoxidised myrcene was added, the full experimental of which can be found in Section 4. 4.

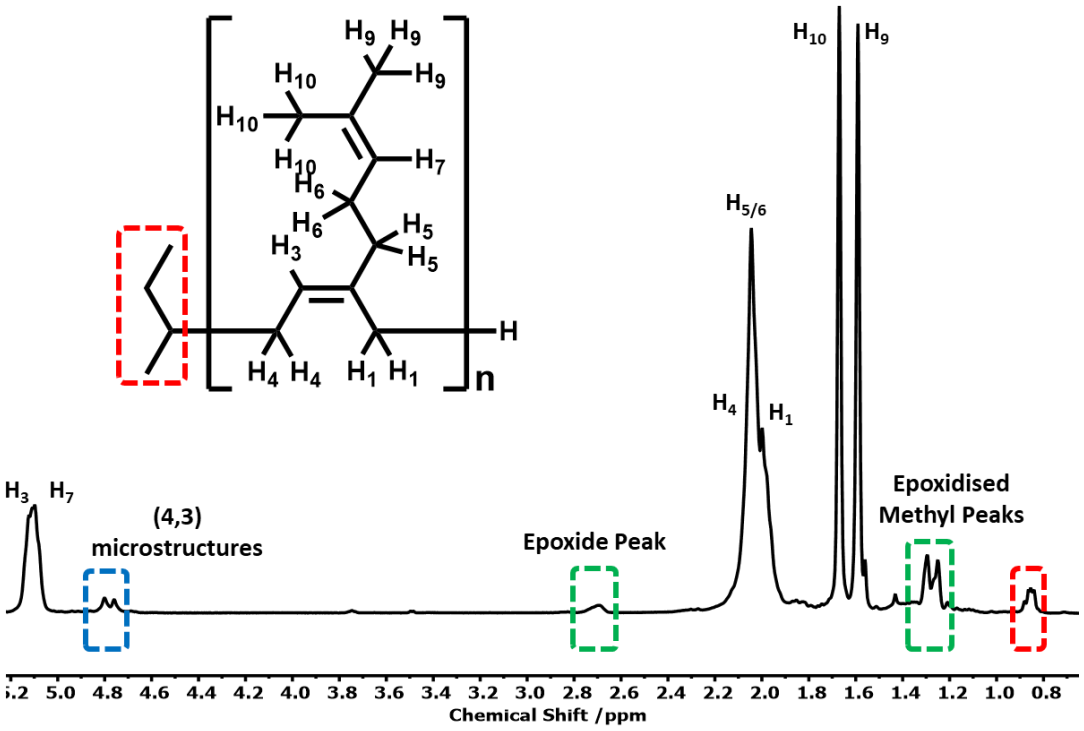

Figure 4.11: Partial ^{1}H NMR spectrum (400 MHz, $CDCl_3$) of PEM3 with proton assignment.

As it can be seen in Figure 4.11 above, it is evident that polymerisation has once again occurred, as evidenced by the presence of the polymer peaks that are observed in polymyrcene when compared to a ^{1}H NMR spectrum of myrcene [77]. From the integrals of the ^{1}H NMR spectrum, it can be calculated that there is 11 % (4,3) microstructures (slightly higher than the usual 7 %) and 89 % (4,1) microstructures. It can also be calculated that 14 % of the polymer is the epoxidised monomer, which is just slightly less than the proposed amount of epoxidised monomer that is present in the reaction mixture (18 %). This potentially suggests that the polymer has been terminated slightly early.

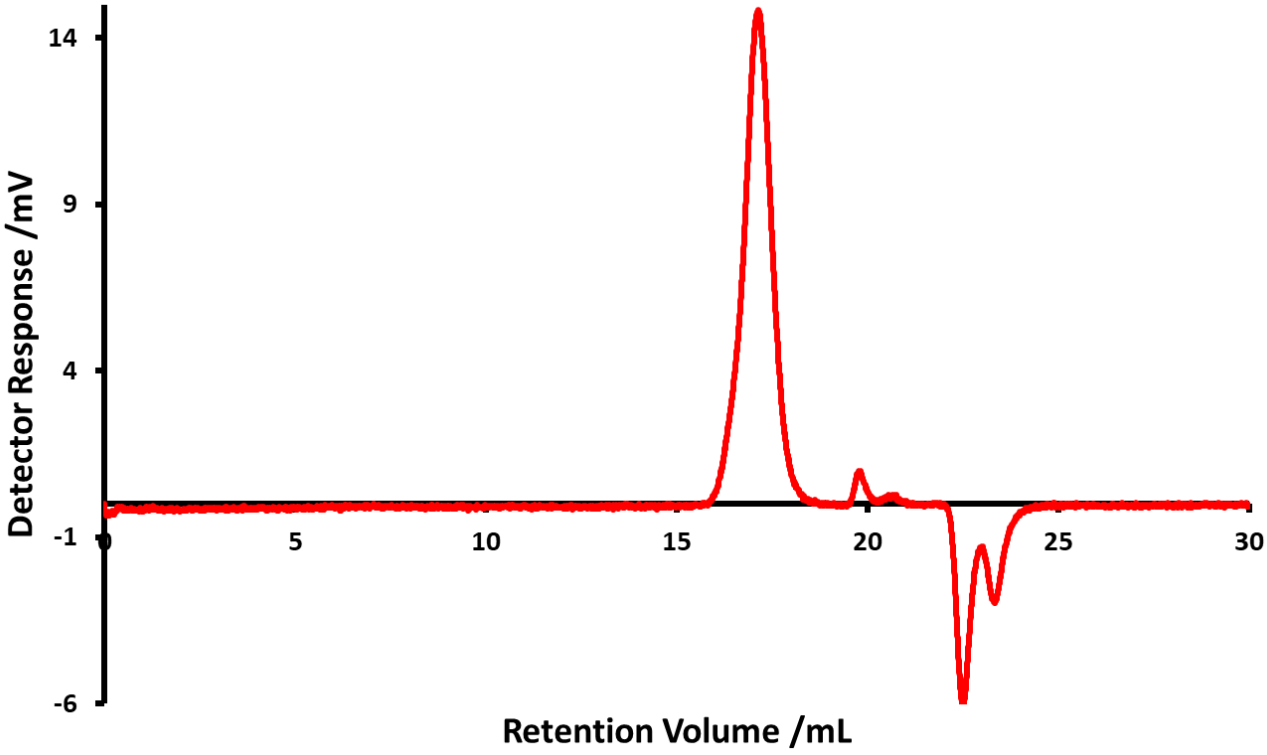

Figure 4.12: RI SEC trace of PEM3.

M_n = 3,700 g mol^{-1} M_W = 4,400 g mol^{-1} Đ = 1.19

The M_n of the polymer is slightly lower than the target M_n which again suggests that the polymerisation may have terminated early. However, at this point, we would also suggest that due to the increased polarity of the epoxide rings present in the polymer, the dn/dc value of 0.1311 [78] may no longer be correct. The Đ of 1.19 is also slightly higher than expected for LAP, which suggests that either air was getting into the reaction flask (potentially due to the

double puncturing of the septum for initiation and addition of the EM) or that the polymerisation was being terminated early though some other mechanism. Even though the polymerisation may not have gone to completion, with this reaction and PEM2, it has been shown that 100 % 7,8 EM can be incorporated into polymers synthesised by LAP, giving increased selectivity and further control over the position of the epoxide in the polymers synthesised.

By using the information from both the ^{1}H NMR spectrum in Figure 4.11, the values for M_n associated with the RI SEC trace in Figure 4.12 and Equations 4.1, 4.2, and 4.3 below, it is possible to estimate the average number of epoxidised myrcene units per chain.

$$\overline{M} = M_{Myr} \text{ x Myr percentage} + M_{EM} \text{ x EM percentage}$$

$$\overline{M} = 136 \text{ g mol}^{-1} \text{ x } 0.86 + 152 \text{ g mol}^{-1} \text{ x } 0.14 = 138 \text{ g mol}^{-1}$$

Equation 4.1: Equation used to calculate the Average Molar Mass of a Monomer Unit ($\bar{M}$), where M_{Myr} is the Molar Mass of a myrcene unit and M_{EM} is the Molar Mass of an EM unit.

$$\overline{X} = \frac{M_n}{\overline{M}}$$

$$\overline{X} = \frac{3{,}700 \text{ g mol}^{-1}}{138 \text{ g mol}^{-1}} = 27 \text{ g mol}^{-1}$$

Equation 4.2: Equation used to calculate the Average Number of Units per Chain ($\bar{X}$), where M_n is the Number Average Molecular Weight of the polymer chains and $\bar{M}$ is the Average Molar Mass of a Monomer Unit.

$$X_{EM} = \overline{X} \text{ x EM Percentage}$$

$$X_{EM} = 27 \text{ x } 0.14 = 3.8$$

Equation 4.3: Equation used to calculate the Average Number of EM Units per Chain (X_{EM}), where $\bar{X}$ is the Average Number of Units per Chain.

The average number of EM Units per polymer chain was calculated as ~ 3.8, meaning that compared to simple chain-end functionalisation, the amount of functionality that can be added is between 3 and 4 times more while also providing some degree of polarity without any deprotection required and proving to be 100 % selective. It is believed that this method of functionalisation offers advantages over both chain-end functionalisation methods and in-chain functionalisation methods, which are commonly used for LAP. The epoxide group can

also be utilised as a platform for further functionalisation, such as to install an azide through acid catalysed epoxide ring opening, or to synthesise a diol through base catalysed epoxide ring opening with water. [79] However, as evidenced by the lower-than-expected M_n for both PEM2 and PEM3, we believe that there is some form of termination mechanism, which limits this method of functionalisation in a statistical copolymerisation and therefore we must change our approach to how it is utilised.

4.2.4 Potential Mechanisms of Termination

Previous observations suggest that there is some form of termination during the polymerisation of EM, which limits the use of this monomer in LAP. There are two potential mechanisms that could account for the termination:

1. Ring Opening of the Epoxide Ring – Despite the experiment shown in Section 4.2.1 above, where it was shown that there was little epoxide ring opening when a sample of epoxidised polymyrcene was reacted with *n*-BuLi, there are a number of variables that mean we believe that the ring opening of the epoxide may still be possible and is therefore a potential reason for the termination of the LAP of EM. Firstly, the experiment mentioned above was carried out on a sample of epoxidised polymyrcene rather than the epoxidised monomer where there is a much greater amount of steric hindrance compared to the monomer. Secondly, due to the fact that the EM may act as both a monomer and its own polar modifier, as evidenced by the increased (4,3) microstructure of the myrcene polymers, the anion may have a far greater nucleophilicity (due to the increased C-Li bond length), which could result in the attack and ring opening of the epoxide ring. If the epoxide ring was attacked by the anion, the propagation of the anion would result in the negative charge being located on the oxygen. If this occurred, the resulting O-Li bond would effectively result in the termination of the LAP, as the bond is too strong to continue to propagate. The mechanism of this reaction can be seen in Figure 4.13 below.

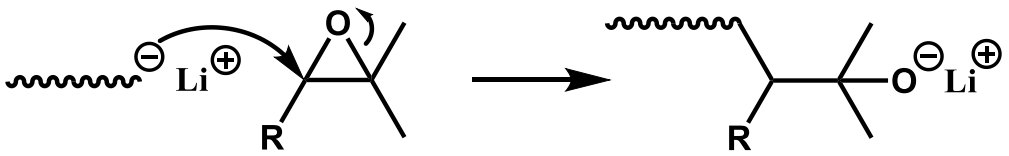

Figure 4.13: Potential mechanism for the termination of the LAP through attack of the epoxide by the propagating carbanion.

This epoxide ring opening could also be a result of a beta hydrogen abstraction to the epoxide whereby the resulting alkene formation would result in the opening of the epoxide ring and formation of the Li-O bond. Although these ring-opening termination mechanisms are possible, there is no detectable evidence of any ring-opened products in the ^{1}H NMR spectra of the epoxidised polymyrcene in Figures 4.9 and 4.11. This suggests that either the amount of ring-opened product is in such low yields that it is unobservable by ^{1}H NMR spectroscopy, or this method of termination is not occurring and some other method of termination is occurring in its place.

2. Lithiation of the Epoxide Ring – Another potential explanation for the early termination of propagation could be due to lithiation of the EM. It is well known that during LAP in THF, the THF can be lithiated through partial coordination of the lithium to the ether oxygen before hydrogen abstraction (Figure 4.14). The lithiated product can rearrange to yield ethene and acetaldehyde lithium enolate [80]. This lithiation reaction causes early termination of LAP.

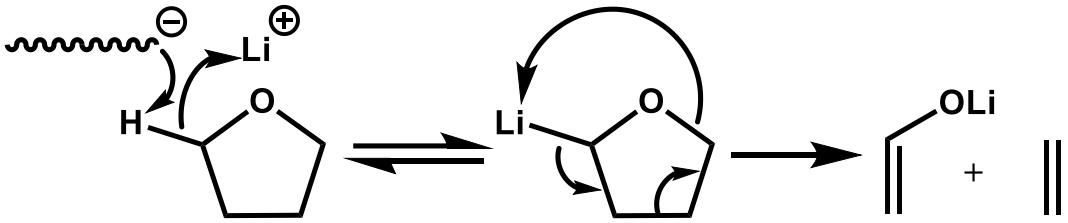

Figure 4.14: Mechanism for the termination of LAP through lithiation of tetrahydrofuran. *[81]*

Due to the fact that the EM appears to be acting as a polar modifier (and therefore coordinating to the lithium), the hydrogen adjacent to the epoxide could potentially be abstracted, resulting in termination of the polymerisation (Figure 4.15). This lithiated product would then simply reform EM when terminated by protonation.

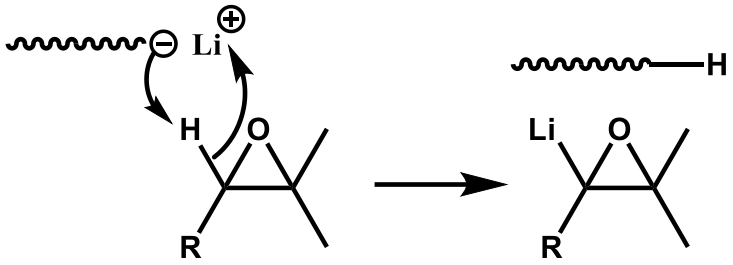

Figure 4.15: Potential mechanism for the termination of the LAP through lithiation of epoxidised myrcene/polymyrcene.

During LAP in THF, the temperature is generally reduced, especially with methacrylates to reduce the termination that is caused by the lithiation of THF. [3] Unfortunately, this does not appear to be a solution in this system, as shown in the experiment in Section 4.2.3 where there appeared to be no polymerisation at lower temperatures.

Due to the presence of two potential mechanisms for the termination of the LAP of EM, trying to stop termination becomes very difficult, as stopping one type of termination may lead itself to an increase in another. For example, to prevent the lithiation termination, a sodium or potassium counter cation could be used, however, this could potentially lead to an increased nucleophilicity of the living chain end, leading to increased termination through epoxide ring opening. For this reason, the statistical copolymerisation of EM may be limited, especially within industry, and may require a lot more work to find conditions for the most efficient polymerisation. However, based on the experiments in Section 4.2.3, it has been proven that not only can EM be polymerised by LAP, but when a delayed injection of EM is used, a polymer with a fairly narrow dispersity and fairly sizable epoxidation percentage can be achieved.

4.2.5 Chain-End Polymerisation Functionalisation

LAP could also be used to introduce a short block of a few (functionalised) repeat units at the chain end. As a novel type of functionalisation for LAP, this approach would provide many of the benefits of both in-chain and chain-end functionalisation with far fewer negatives. The way in which it is believed this novel functionalisation will work is through an almost block-like copolymerisation where initially a polymer chain can be synthesised before a small EM chain is added to the chain end at the end of the polymerisation. This should provide multiple epoxide groups at the end of each polymer chain, which can then be used on their own as a method of functionalisation or as a site for further functionalisation. [81] As the

functionalisation occurs at the end of the polymerised chain, any termination, through either potential method, will have little impact on the dispersity or characteristics of the primary polymer chain.

4.2.5.1 End-Functionalisation of Polymyrcene.

It was decided to first explore the multi-chain-end functionalisation of poly(myrcene) with EM, as the delayed injection polymerisation approach had worked well for the synthesis of copolymers. A chain-end multi-functionalisation approach was therefore attempted whereby a polymyrcene sample was end-functionalised/terminated with a small block of polymerised epoxidised myrcene. The full experimental of this functionalised polymer can be found in Section 4.4.

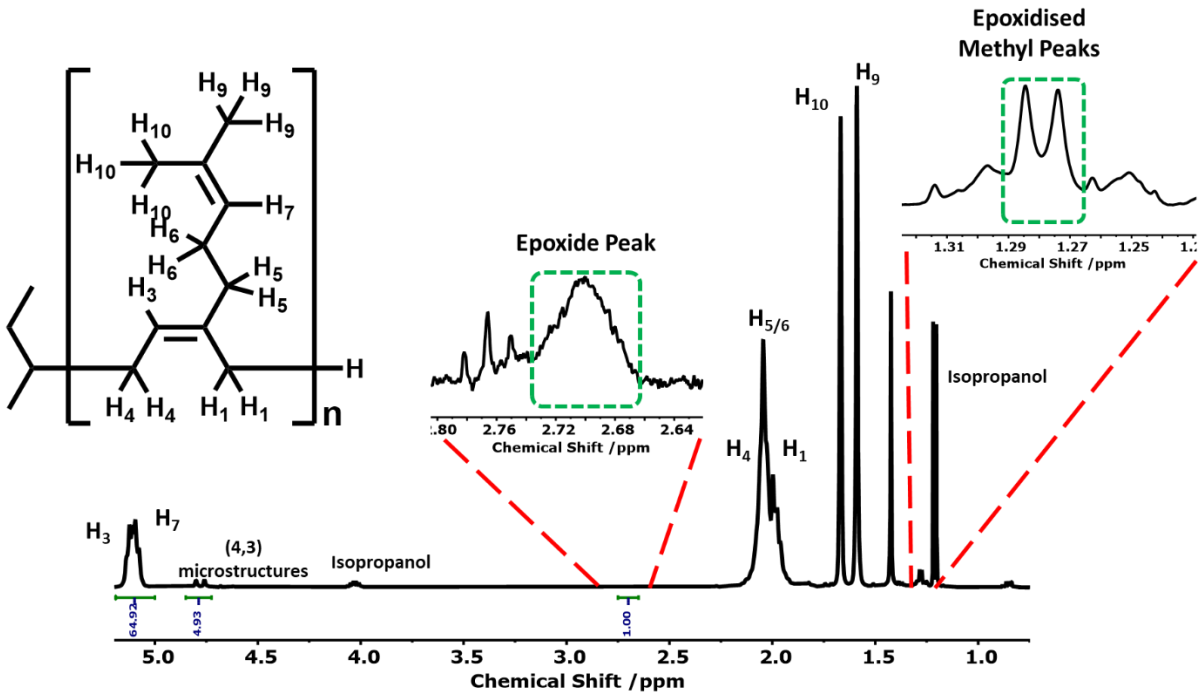

Figure 4.16: ^{1}H NMR spectrum (400 MHz, $CDCl_3$) of PM(*b*)EM1 with proton assignment.

As it can be seen in Figure 4.16 above, some of the EM has been incorporated into the polymer chain. Again, due to the method of collection for this polymer (i.e. precipitation into isopropanol), the broad nature of the epoxide peak at 2.70 ppm and the lack of monomer peaks in the ^{1}H NMR spectrum, we can be confident that the epoxidised monomer has been incorporated into the polymer. From the integrals of the ^{1}H NMR spectrum, it can be calculated that there is 7 % (4,3) microstructures and 93 % (4,1) microstructures, which is

fairly consistent with the percentages that would be expected for an LAP of myrcene carried out in a non-polar solvent in the absence of a polar modifier. By using the integral data associated with the ^{1}H NMR spectrum in Figure 4.16 above and using Equations 3.5 and 3.6 found in Section 3.2.2.1.1, we calculated that 3 mol % of the polymer is the epoxidised monomer.

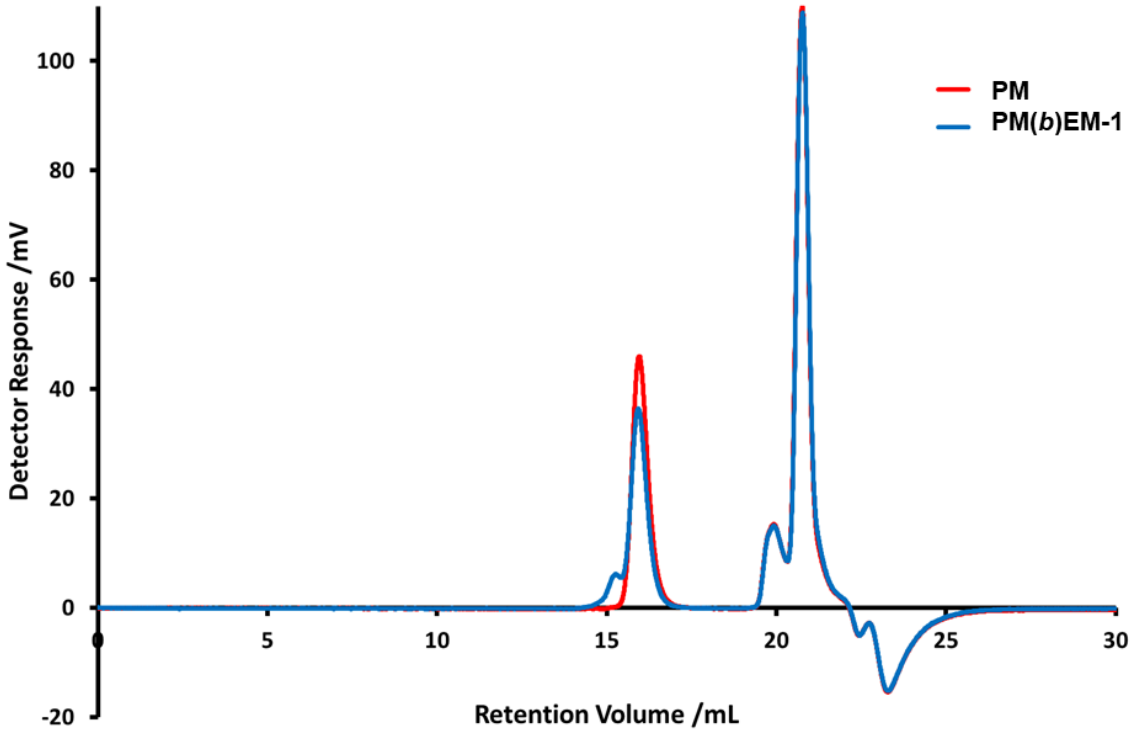

Figure 4.17: RI SEC trace of PM(*b*)EM1.

For PM:

M_n = 15,500 g mol^{-1} M_W = 15,900 g mol^{-1} Đ = 1.03

For PM(*b*)EM1:

M_n = 17,500 g mol^{-1} M_W = 19,500 g mol^{-1} Đ = 1.11

From the SEC trace in Figure 4.17 above and the associated values for M_n, it is shown that compared to the statistical copolymerisation of the EM, this new method for multi-chain-end functionalisation appears to be much more controlled, leading to an actual M_n that is close to the target (the value of M_n is slightly higher than the target, but this may be due to impurities introduced at the beginning of the polymerisation or due to a *sec*-BuLi concentration that is lower than expected) and a Đ that is much lower than previous polymerisations and more

consistent with expectations for LAP. As it can be seen in the SEC trace in Figure 4.17 above, there is a shoulder on the trace of PM(*b*)EM1 (compared with the trace of the sample before EM was added – PM), which generally signifies a doubling of the M_n, most commonly caused by oxygen coupling of two 'living' chains upon termination. This coupling is more prominent with dienes (especially those activated by an R group on the carbon adjacent to the carbanion – such as myrcene and isoprene), where the increased polymerisation time along with the addition of a second monomer and sampling is believed to have caused this increase in oxygen coupled chains (compared to PM) that were observed. This increase in the oxygen coupled chains (which have a molecular weight $2M_n$) is believed to also be the leading contributor to the increase in overall M_n and Đ. For this reason, and due to the fact that a sample was taken before the addition of EM, it was decided that rather than using the Equations 4.1, 4.2, and 4.3 in Section 4.2.3 to calculate X_{EM}, new equations would be devised that did not require a final M_n. These equations can be seen below.

$$\bar{X}(S) = \frac{M_n(S)}{M(S)}$$

$$\bar{X}(S) = \frac{15{,}500\ \mathrm{g\ mol^{-1}}}{136\ \mathrm{g\ mol^{-1}}} = 114$$

Equation 4.4: Equation used to calculate the Average Number of Units per Chain in the Sample ($\bar{X}(S)$), where $M_n(S)$ is the Number Average Molecular Weight of the Polymer Sample and M(S) is the Molar Mass of a Monomer Unit.

$$X_{EM} = \frac{\bar{X}(S)}{\text{Unepoxidised Monomer Percenatge}} - \bar{X}(S)$$

$$X_{EM} = \frac{114}{0.97} - 114 = 3.5$$

Equation 4.5: Equation used to calculate the Average Number of EM Units per Chain (X_{EM}), where $\bar{X}(S)$ is the Average Number of Units per Chain in the Sample.

By using the information from both the ^{1}H NMR spectrum in Figure 4.16, the value for M_n associated with the SEC trace of PM in Figure 4.17 and Equations 4.4 and 4.5 above, we are able to estimate the average number of epoxide myrcene units at the end of each polymer chain. The average number of EM units at the end of each chain was calculated as ~ 3.5, which means on average every chain that was synthesised had between 3 and 4 functional epoxide

units at the end of it. This means that, once again, polymer chains have been synthesised with a fairly large amount of 100 % selective functionalisation in a non-polar solvent under ambient temperatures (conditions that could be utilised within industry) without the requirement for any protection of the functional group. We have now also shown that the polymers synthesised can be extremely well controlled which, we believe, makes this new method of functionalisation a useful addition to the arsenal of LAP scientists.

4.2.5.2 Chain-End Functionalisation of Polybutadiene.

To ensure that this method of functionalisation was not limited to just myrcene homopolymers, it was decided to test it as a chain-end multi-functionaliser for another commonly used diene – butadiene – which differs from myrcene through the lack of an activating R group on the carbon adjacent to the carbanion.

Again, a chain-end multi-functionalisation approach was therefore attempted whereby this time a polybutadiene sample was end-functionalised/terminated with a small block of polymerised epoxidised myrcene. The full experimental of this functionalised polymer can be found in Section 4.4.

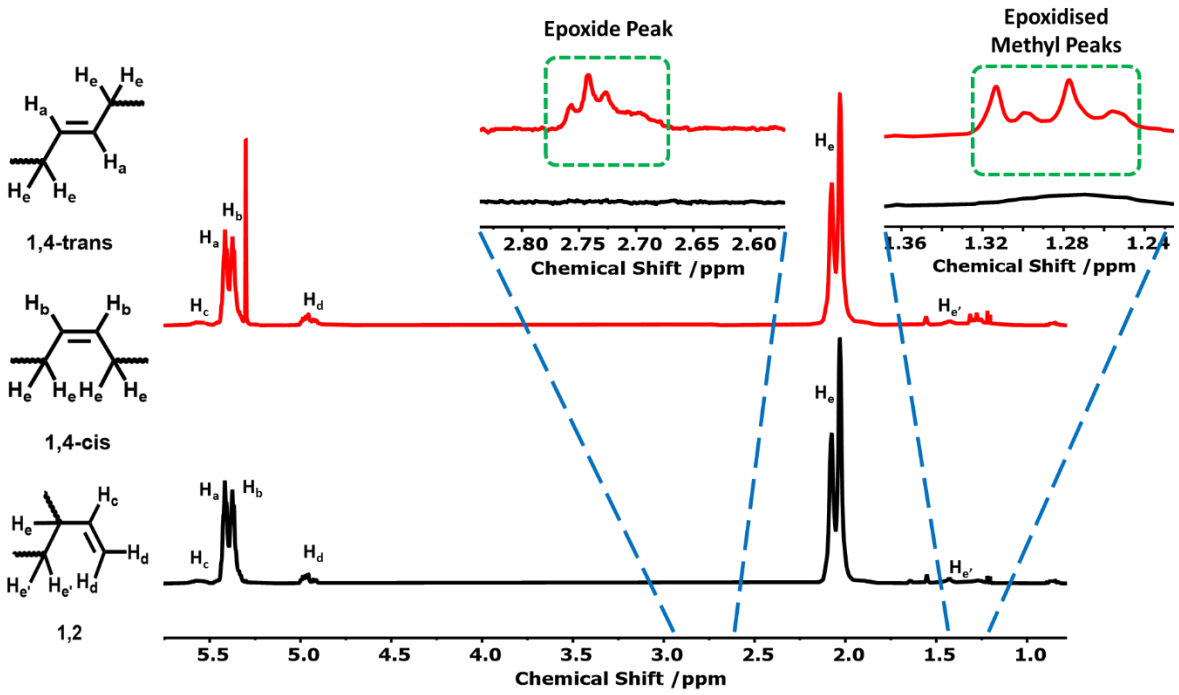

Figure 4.18: Stacked ^{1}H NMR spectra (400 MHz, $CDCl_3$) of PB (Black - Bottom) and PB(*b*)EM1 (Red - Top) with proton assignment.

The ^{1}H NMR spectrum (Figure 4.18) demonstrates that above some of the EM has been incorporated into the polybutadiene copolymer. Again, due to the method of collection for this polymer (i.e. precipitation into isopropanol), with the broad nature of the epoxide peak at 2.72 ppm, we can be confident that the epoxidised monomer has been incorporated into the polymer. From the integrals of the ^{1}H NMR spectrum, it can be calculated that there is 10 % (1,2) microstructures and 90 % (1,4) microstructures, which is fairly consistent with the percentages that would be expected for an LAP of butadiene carried out in a non-polar solvent in the absence of a polar modifier. By using the integral data associated with the ^{1}H NMR spectrum in Figure 4.18 above and Equations 3.5 and 3.6 found in Section 3.2.2.1.1, it can be calculated that 2 mol % of the polymer is the epoxidised monomer.

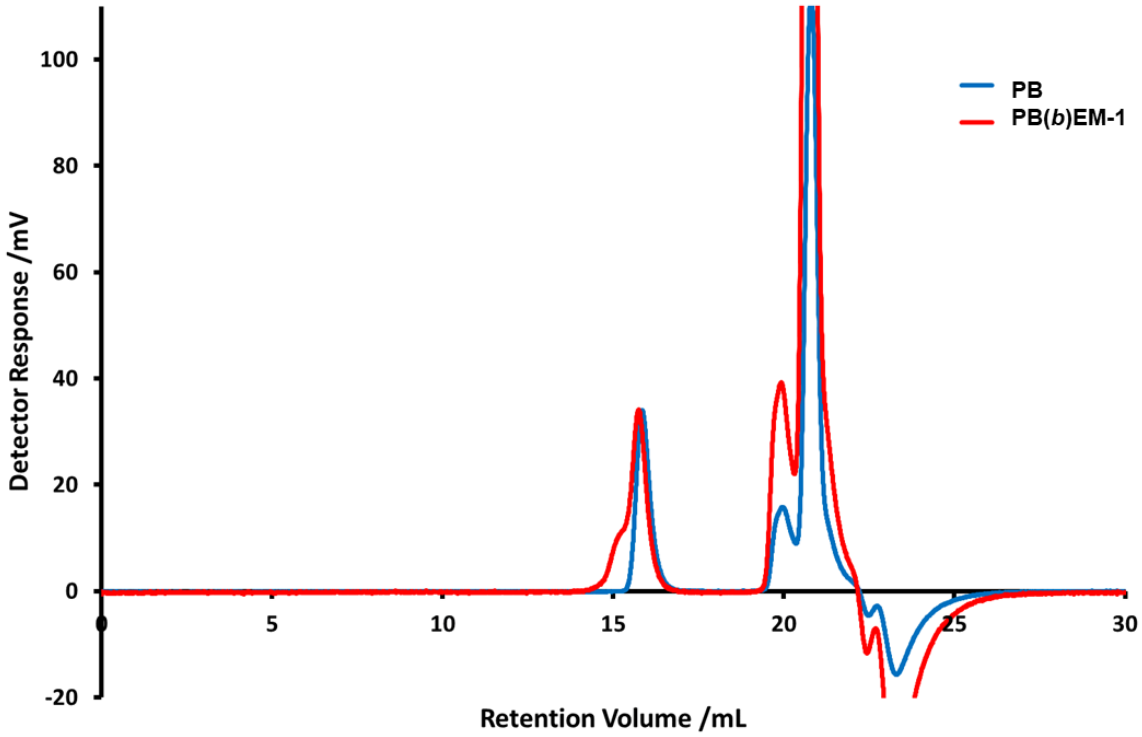

Figure 4.19: RI SEC trace of PB(b)EM-1.

For PB:

M_n = 11,500 g mol^{-1} M_W = 11,600 g mol^{-1} Đ = 1.01

For PB(*b*)EM1:

M_n = 14,400 g mol^{-1} M_W = 16,000 g mol^{-1} Đ = 1.11

The RI SEC trace (Figure 4.19) and the associated values for M_n suggest that when compared to the statistical copolymerisation of EM, this new method for multi-chain-end functionalisation appears to be much more controlled, leading to an actual M_n that is close to the target and a Đ that is much lower than previous polymerisations and more consistent with a Đ that is expected for LAP. As it can be seen in the RI SEC trace in Figure 4.19 above, there is once again a significant shoulder on the trace of PB(*b*)EM1 (compared with the trace of the sample before EM was added – PB), which as discussed before, generally signifies a doubling of the M_n, most commonly caused by chain coupling of two 'living' chains upon termination, due to the introduction of air (oxygen and CO_2) with the EM monomer. Again, this increase in the oxygen coupled chains is believed to be the leading contributor to the increase in overall M_n and Đ. For this reason, and due to the fact that a sample was taken before the addition of EM, it was decided to calculate X_{EM} using Equations 4.4 and 4.5 above.

By using the information from both the ^{1}H NMR spectrum in Figure 4.18, the value for M_n associated with the SEC trace of PB in Figure 4.19 and Equations 4.4 and 4.5 above, it was possible to calculate a rough approximate for the average number of EM units at the end of each polymer chain. The average number of EM units at the end of each chain was calculated as ~ 4.3, which means on average every chain that was synthesised had between 4 and 5 functional epoxide units at the end of it.

4.2.5.3 End-Functionalisation of Polystyrene

Following the successful 'end-functionalisation' of both polymyrcene and polybutadiene, the approach attempted with polystyrene was not possible under the same procedure and conditions. It was believed that this lack of reaction was due to the increased stability of the carbanion at the living polystyrene chain end compared to the stability of the carbanion at the living polydiene chain end. This increased stability could be leading to an increased bond length of the carbon-lithium bond at the propagating chain end of the polystyrene compared to the propagating chain end of polydiene. This in turn would lead to a weaker carbon-lithium bond, which in-turn increases the carbon-lithium bond length. This increased bond length could lead to an increased rate of lithiation of the epoxide due to an increase in the availability of the lithium and a reduced steric hindrance associated with the abstraction of the hydrogen or an increased rate of epoxide attack and ring opening due to a more accessible carbanion. Another potential explanation for the lack of polymerisation of the EM at the end of a

polystyrene chain end could be demonstrated by looking at the kinetics of the polymerisation of myrcene and styrene in the presence of a polar modifier. As shown previously, the rate of myrcene and styrene incorporation during their copolymerisation almost completely inverts when the copolymerisation is carried out in the presence of a polar modifier compared to when the copolymerisation is carried out in a non-polar solvent in the absence of a polar modifier. [64] [65] This may suggest that in the presence of a polar modifier, $k_{Sty\text{-}Myr}$ decreases significantly. If we assume that EM polymerises in a similar fashion to myrcene (due to the fact that the epoxide is far enough removed from the diene that it has little to no influence on the electronic nature of the diene) and assume that EM is acting as both a monomer and its own polar modifier, this would suggest that $k_{Sty\text{-}EM}$ would be significantly decreased compared to $k_{Myr\text{-}EM}$ or $k_{But\text{-}EM}$, and the rate of polymerisation of EM may become comparable to or less than the rate of either lithiation of the epoxide or ring opening of the epoxide, which results in no observable EM being incorporated into the polymer.

To try to establish both the leading cause of termination and different methods to allow the synthesis of functionalised styrenic polymers (without the need for short diene blocks, which have been utilised in other methods of functionalisation and polymer star formation [3]), it was decided that a sample of 1,1-diphenylethylene (DPE) end-capped polystyrene would be synthesised and reacted with EM to see if the increased steric hindrance and reduced nucleophilic character of the DPE anion (relative to the styrene anion) would allow the EM to be polymerised (see Figure 4.20).

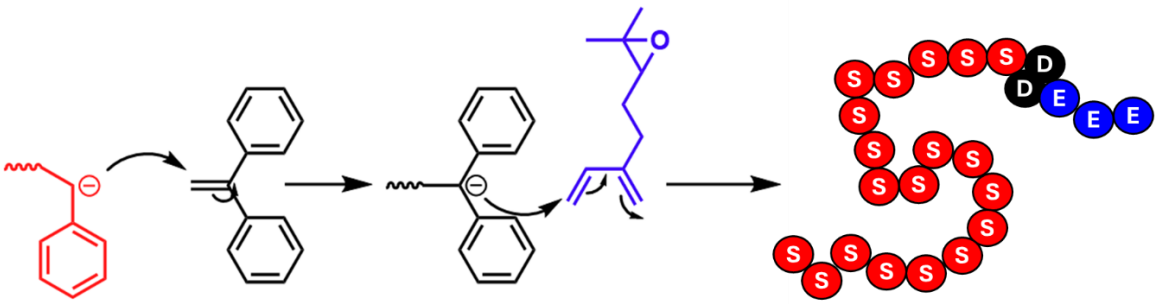

Figure 4.20: Schematic showing the concept behind how styrenic polymers could be functionalised with epoxidised myrcene by utilising a single monomeric unit of DPE at the chain end to prevent early termination of the polymerisation.

The full experimental of this functionalised polymer can be found in Section 4.4.

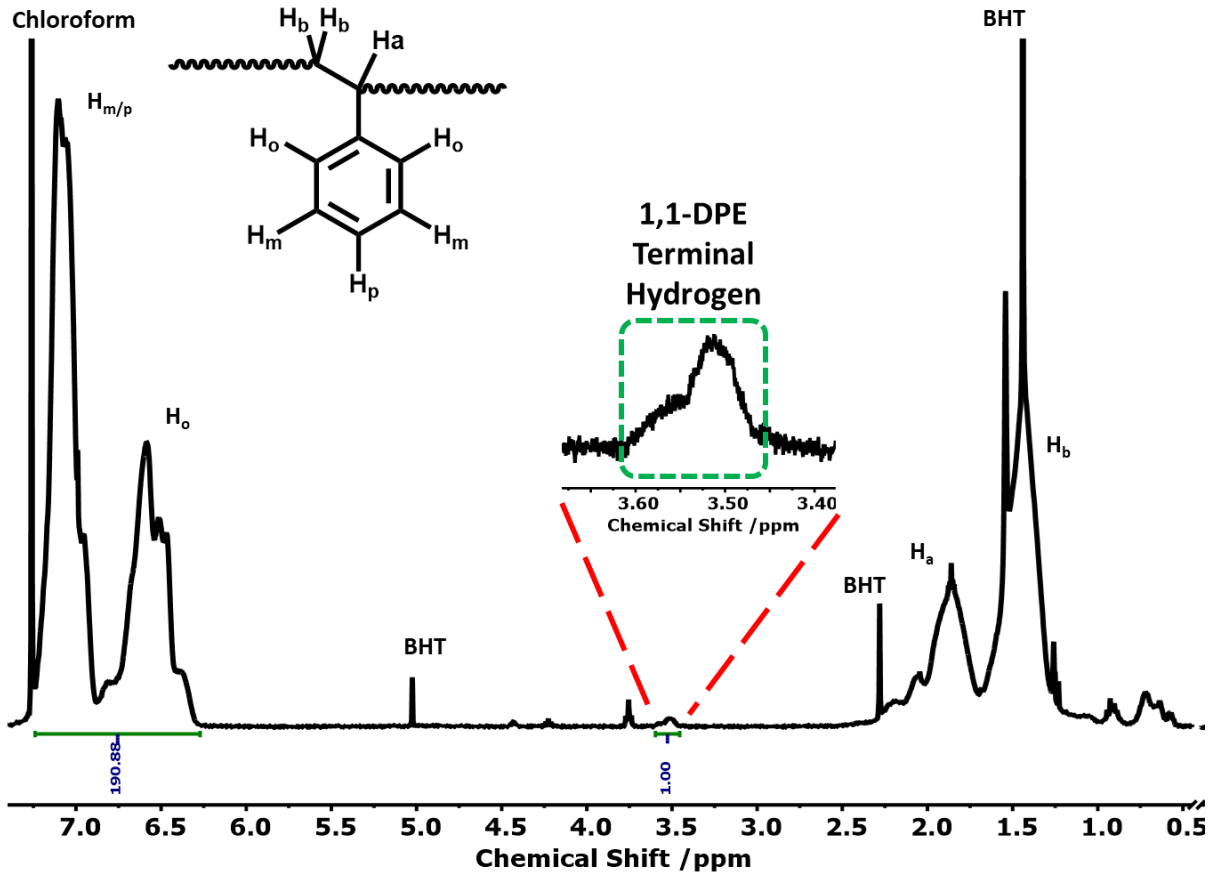

Figure 4.21: ^{1}H NMR spectrum (400 MHz, $CDCl_3$) of PS(DPE) with proton assignment.

The ^{1}H NMR spectrum (Figure 4.21) indicates that DPE was incorporated at the end of the polystyrene, as evidenced by the presence of a peak at 3.52 ppm, which represents the terminal hydrogen atom on the tertiary carbon between the two phenyl groups of DPE. By integration analysis, it can be determined that there is approximately 1 DPE unit for every 36 styrene units.

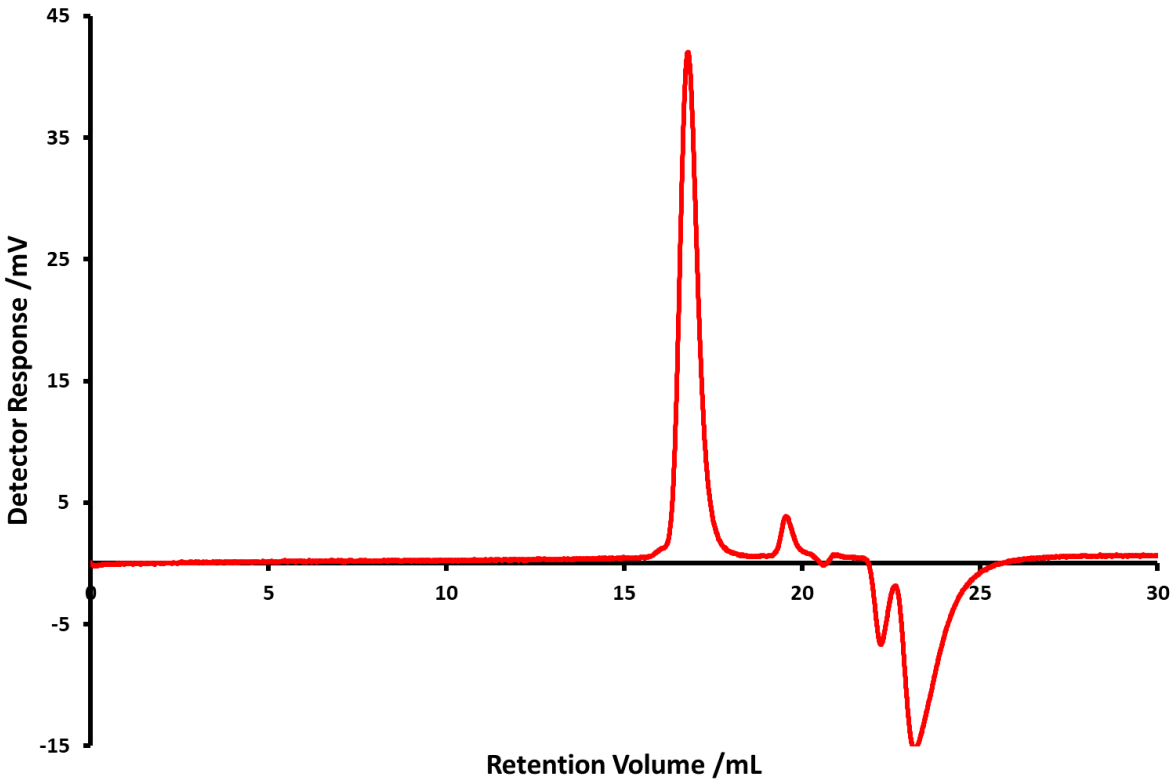

Figure 4.22: RI SEC trace of PS(DPE).

For PS(DPE):

M_n = 5,100 g mol^{-1} M_W = 5,500 g mol^{-1} Đ = 1.08

As it can be seen in the SEC trace of PS(**DPE**) in Figure 4.22 above, and the associated values for the M_n and Đ, the LAP of styrene has been successful and well controlled with both a very accurate M_n and low Đ. Using the value of M_n obtained from the RI SEC trace and the molar mass of both styrene and DPE, it is possible to calculate that in a 100 % DPE-terminated sample of polystyrene, there would be 1 DPE unit for every 47 units of styrene. This is far lower than the ratio that was calculated to be found in PS(**DPE**) by ^{1}H NMR spectroscopy. It is proposed that this is due to the low signal to noise ratio of the 1,1-DPE terminal hydrogen atom found in the ^{1}H NMR spectrum of PS(**DPE**), which gives a ratio of DPE to styrene that may be far higher than the true value. Despite this discrepancy, we suggest that a considerable amount of DPE chain-end functionalisation has occurred, meaning that an indication into the usefulness of a DPE linker for the multi-chain-end functionalisation of polystyrene will be determined when PS(**DPE**) is reacted with EM.

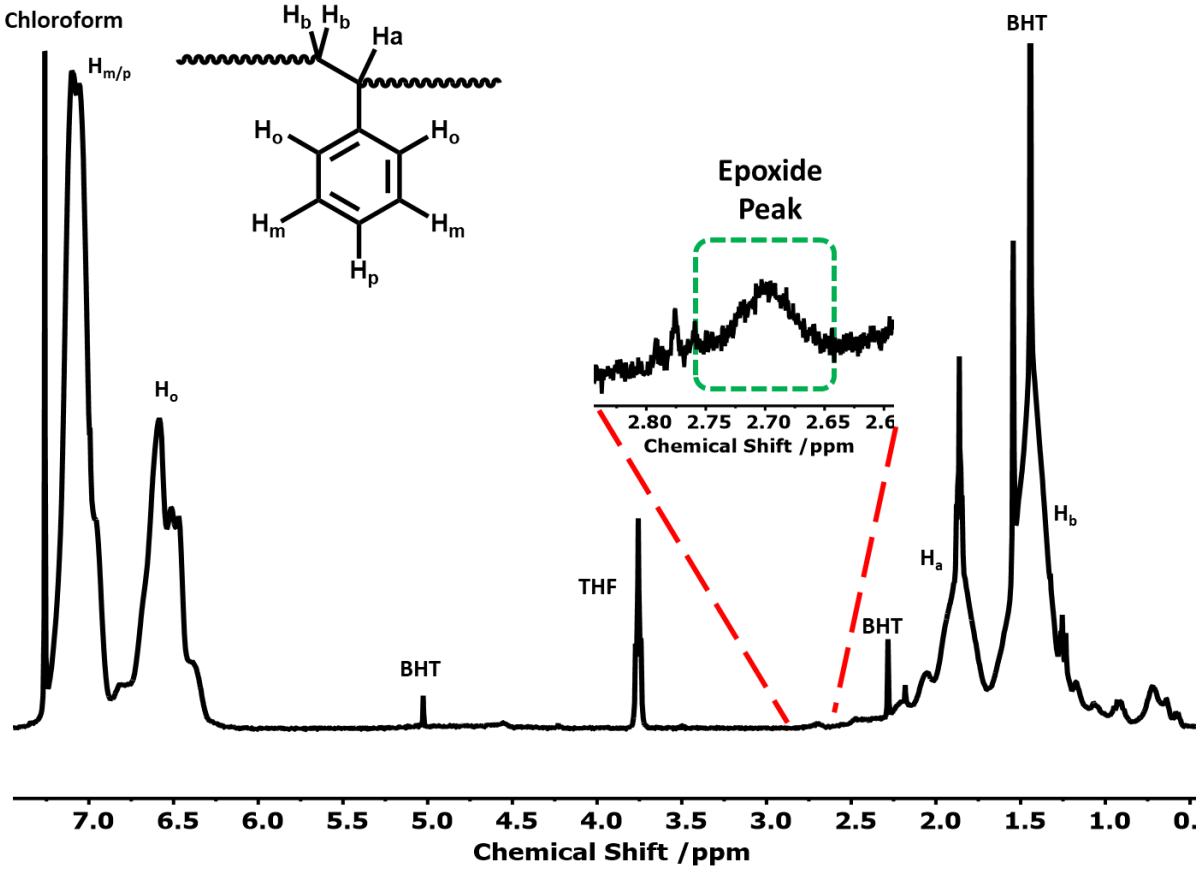

Figure 4.23: ^{1}H NMR spectrum (400 MHz, $CDCl_3$) of PS(DPE)EM-1 with proton assignment.

^{1}H NMR spectroscopic analysis (Figure 4.23) suggests that some of the EM has been incorporated into the DPE terminated polystyrene sample Again, due to the method of collection for this polymer (i.e. precipitation into isopropanol), with the broad nature of the epoxide peak at 2.70 ppm, we can be confident that the epoxidised monomer has been incorporated into the polymer. Using the relative integrals, associated with the ^{1}H NMR spectrum in Figure 4.23 above, we can calculate that approximately 2 mol % of the polymer was epoxidised. We could also calculate that the ratio of epoxidised myrcene units to styrene units was approximately 1 to 46. One final thing that we can observe from the ^{1}H NMR spectrum is that there is no detectable peak at 3.52 ppm, which suggests that there are very few to no chains that have a terminal DPE unit.

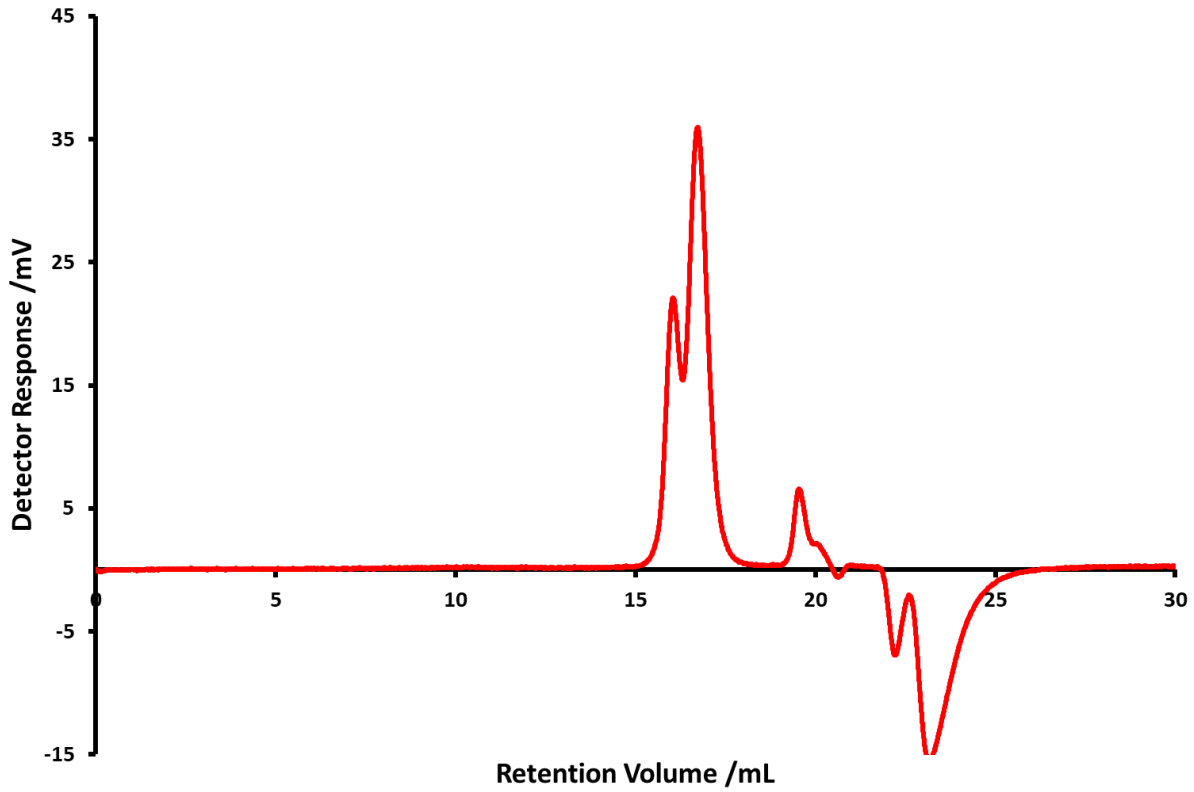

Figure 4.24: RI SEC trace of PS(DPE)EM-1.

For PS(DPE)EM1:

M_n = 6,600 g mol^{-1} M_W = 7,900 g mol^{-1} Đ = 1.20

From the SEC trace in Figure 4.24 above, we can see that once again when compared to the SEC trace of PS(**DPE**), there is a significant shoulder on the trace of PS(**DPE**)EM1 (compared with the trace of the sample before EM was added – PS(**DPE**)), which as discussed before, generally signifies a doubling of the M_n, most commonly caused by oxygen coupling of two 'living' chains upon termination. Again, this increase in the oxygen coupled chains is believed to be the leading contributor to the increase in overall M_n and Đ – where the dispersity increase for this copolymerisation was much higher than would be expected for LAP. For this reason, and due to the fact that a sample was taken before the addition of EM, it was decided to calculate X_{EM} using Equations 4.4 and 4.5 above.

By using the information from both the ^{1}H NMR spectrum in Figure 4.23, the value for M_n associated with the SEC trace of PS(**DPE**) in Figure 4.24 and Equations 4.4 and 4.5 above, the average number of EM units at the end of each polymer chain can be estimated. The average number of EM units at the end of each chain was calculated as ~ 1.0, which means every chain

that was synthesised had on average 1 functional epoxide unit at the end of it. Although still far lower than the number of epoxide units added to polydiene polymers, we have proven that EM can be added to styrene living homopolymers. Due to the fact that no DPE terminal hydrogen peak at 3.52 ppm could be observed in the ^{1}H NMR spectrum (Figure 4.23), and the average number of EM units per chain being equal to 1.0, we can suggest that within the accuracy of the ^{1}H NMR spectroscopy, every (or nearly every) polystyrene chain that has been terminated with a DPE unit has also got an EM unit after. This suggests that the steric hindrance associated with DPE and the increased stability of the DPE carbanion have a beneficial impact on the termination reactions that occurred when polystyrene was not end-capped with DPE. However, due to the fact that the average number of EM per chain is reduced compared to that of EM terminated polydiene chains, we can suggest that the styrenic monomers may still have an impact on the termination reaction even when the carbanion is situated on the EM. For this reason, we suggest that having a small polydiene chain after the polystyrene chain will have a far greater impact on increasing the amount of EM units that can be added to the chain end than by simply having a DPE linker.

4.3 Conclusion

It has been shown that LAP grade EM can be synthesised and purified through common laboratory experiments and purification methods. It has also been proven that once purified, this EM can be used as a novel multi-chain-end functionaliser, which, unlike most methods used for the functionalisation of polymer chains synthesised by LAP, requires no post-polymerisation modifications to add polarity, but which can also be used as a site for further functionalisation. Using this method of functionalisation, between 3 and 4 epoxide units can be incorporated into polydiene polymer chains including polybutadiene and polymyrcene. However, due to the increased nucleophilicity of the carbanion at the end of a living polystyrene chain end and the decreased cross-polymerisation rate of styrenic monomers to diene monomers in the presence of a polar additive, this method of functionalisation did not show any observable functionalisation of polystyrene polymer chains. To overcome this limitation, it is proposed that much like during the synthesis of 4-armed stars (using a $SiCl_4$ terminator), a small block of butadiene (or other diene monomer) can be added to the end of the polymer chain before the EM is added. Finally, it was shown that by adding a DPE linker to the end of the polystyrene polymer chain end, ~ 1.0 epoxide unit can be incorporated into the polystyrene polymer chains.

4.4 Experimental

4.4.1 Materials

Food grade myrcene (≥ 95 %, Stabilised, Sigma Aldrich UK), ReagentPlus styrene (≥ 99 %, Sigma Aldrich UK), HPLC grade cyclohexane (99.8 %, Acros Organics) and anhydrous benzene (99.8 %, Sigma Aldrich UK) were dried and degassed, using extra pure calcium hydride (93 %, 0 – 2 mm grain size, Acros Organics) and the freeze-pump-thaw method. 1,3-butadiene (≥ 99.6 %, Sigma Aldrich UK) was purified by passing through molecular sieves before being sacrificially initiated with *n*-butyllithium solution (*n*-BuLi) (2.5 M in hexanes, Sigma Aldrich UK) prior to distillation. 1,1-diphenylethylene (DPE) (97 %, Sigma Aldrich UK) was purified by passing through chromatography grade basic aluminium oxide (Al_2O_3) (Brockmann I, 50-200 µm, Acros Organics) and dried under UHV for 6 hours before being distilled under UHV after titration with *sec*-BuLi. *Sec*-butyllithium (*sec*-BuLi) (1.4 M in cyclohexanes, Sigma Aldrich UK), *N,N,N',N'*-tetramethylethylenediamine (TMEDA) (≥ 99.5 %, Sigma Aldrich UK), analytical reagent grade dichloromethane (DCM) (99.99 %, Fisher Scientific UK), analytical reagent grade methanol (99.99 %, Fisher Scientific UK), analytical reagent grade ethyl acetate (≤ 99.98 %, Fisher Scientific UK), laboratory reagent grade propan-2-ol (99.5 %, Fisher Scientific UK), laboratory reagent grade hexane (fraction from petroleum, Fisher Scientific UK), laboratory reagent grade magnesium sulphate ($MgSO_4$) (dried, Fisher Scientific UK), *n*-butyllithium solution (*n*-BuLi) (2.5 M in hexanes, Sigma Aldrich UK), sodium hydrogen carbonate ($NaHCO_3$) (2.5 % Na_2CO_3, - 40 + 140 mesh, Sigma Aldrich UK) and 3-chloroperbenzoic acid (*m*-CPBA) (≤ 77 %, Sigma Aldrich UK) were all used as supplied.

4.4.2 ^{1}H NMR Measurements

Nuclear Magnetic Resonance (NMR) spectroscopy was carried out using a Bruker Advance III 400 MHz spectrometer with an operating frequency of 400.130 MHz for ^{1}H, using deuterated chloroform ($CDCl_3$) as the solvent.

4.4.3 SEC Measurements

Triple detection Size Exclusion Chromatography (SEC) was carried out using a Viscotek GPC max VE2001 solvent/sample module and a Viscotek TDA 302 (Triple Detector Array) at 35 ^{o}C with a 1 mL min^{-1} flow rate. A dn/dc value of 0.131 mL g^{-1} [78] was used for polymyrcene in

THF, a dn/dc value of 0.185 mL g^{-1} was used for polystyrene in THF and a dn/dc value of 0.124 mL g^{-1} [27] was used for polybutadiene in THF. A weighted average dn/dc value was calculated for each copolymer based on copolymer composition data obtained by ^{1}H NMR.

4.4.4 Polymer Synthesis

PM3 was synthesised by LAP in benzene at room temperature, under ultra-high vacuum conditions. Dry, degassed myrcene (11.73 g, 86.1 mmol) was mixed with dry, degassed benzene (~60 mL). The polymerisation was then initiated with *sec*-BuLi (0.168 mL, 1.4 M in cyclohexane, 235 µmol) to synthesise a statistical copolymer, with a target M_n of 50,000 g mol^{-1}. The solution was left to stir for 3 hours min at room temperature before termination *via* the injection of an excess of sparged methanol. PM3 (a clear very viscous liquid) was recovered by precipitation into a large excess of methanol, washed and dried in *vacuo* to yield poly(myrcene) (8.83 g, 75 %); M_n – 76,900 g mol^{-1}, M_w – 79,900 g mol^{-1}, Đ – 1.04 (as calculated by SEC using a dn/dc value of 0.131); (94 % (4,1), 6 % (4,3)).

PEM1 was synthesised by LAP in toluene at -78 °C, under ultra-high vacuum conditions. Dry, degassed EM1 (0.90 g, 5.91 mmol) was mixed with dry, degassed myrcene (1.68 g, 12.3 mmol) and dry, degassed toluene (~ 50 mL). The polymerisation was then initiated with *sec*-BuLi (0.185 mL, 1.4 M in cyclohexane, 259 µmol) to synthesise a statistical copolymer, with a target M_n of 10,000 g mol^{-1}. The solution was then left to stir for 18 hours at -78 °C under UHV, before the polymerisation was terminated *via* the injection of an excess of sparged methanol. PEM1 (a clear liquid) was collected by rotary evaporator and dried under vacuum (1.17 g, 45 %).

PEM2 was synthesised by LAP in benzene at RT, under UHV conditions. Dry, degassed myrcene (2.91 g, 21.4 mmol) and dry, degassed EM1 (0.53 g, 3.48 mmol) (which had been purified by the addition of 50 µL of *n*-BuLi just prior to distillation) were distilled into dry, degassed benzene (~150 mL) before the addition of *sec*-BuLi (0.49 mL, 1.4 M in cyclohexane, 686 µmol), injected *via* syringe, to synthesise a polymer with a target M_n of 5,000 g mol^{-1}. The solution was then left to stir for 72 h at RT before the polymerisation was terminated *via* the injection of an excess of sparged methanol. PEM2 (a clear liquid) was collected by rotary evaporator and dried under vacuum (0.98 g, 28 %); 61 % (4,1), 39 % (4,3).

PEM3 was synthesised by LAP in benzene at RT, under UHV conditions. Dry, degassed myrcene (3.58 g, 26.3 mmol) was distilled into dry, degassed benzene (~ 100 mL) before being initiated with *sec*-BuLi (0.511 mL, 1.4 M in cyclohexane, 715 µmol), injected *via* syringe, to synthesise a polymer with a target M_n of 5,000 g mol^{-1}. After 10 minutes dry, degassed EM1 (1 mL, 1.02 g, 6.70 mmol) was also injected into the propagating polymer mixture. The solution was then left to stir for 18 hours at RT, before the polymerisation was terminated *via* the injection of an excess of sparged methanol. PEM3 (a clear viscous liquid) was recovered by precipitation into a large excess of methanol, washed and dried in *vacuo* to yield poly(myrcene) (1.19 g, 26 %); M_n – 3,700 g mol^{-1}, M_w – 4,400 g mol^{-1}, Đ – 1.19 (as calculated by SEC using a dn/dc value of 0.131); 89 % (4,1), 11 % (4,3).

PM(*b*)EM1 was synthesised by LAP in cyclohexane at RT, under ultra-high vacuum conditions. Dry, degassed myrcene (10.98 g, 80.6 mmol) was distilled into dry, degassed cyclohexane (~200 mL) before being initiated with *sec*-BuLi (0.78 mL, 1.4 M in cyclohexane, 1.09 mmol), injected *via* syringe, to synthesise a polymer with a target M_n of 10,000 g mol^{-1}. After stirring for 1.5 hours at RT, dry, degassed EM1 (0.80 g, 5.26 mmol) was distilled into the polymer mixture. At this point, the solution changed from a very pale yellow to a dark yellow colour. The solution was then left to stir for 60 hours at RT, before the polymerisation was terminated *via* the injection of an excess of sparged isopropanol. PM(*b*)EM1 (a clear viscous liquid) was recovered by precipitation into a large excess of isopropanol, washed and dried in *vacuo* to yield poly(myrcene-*block*-epoxidised myrcene) (9.70 g, 82 %); **PM** – M_n – 15,500 g mol^{-1}, M_w – 15,900 g mol^{-1}, Đ – 1.03, **PM(*b*)EM1 –** M_n – 17,500 g mol^{-1}, M_w – 19,500 g mol^{-1}, Đ – 1.11 (as calculated by SEC using a dn/dc value of 0.131); 93 % (4,1), 7 % (4,3).

PB(*b*)EM1 was synthesised by LAP in cyclohexane at RT, under ultra-high vacuum conditions. Dry, butadiene (8.92 g, 165 mmol) was distilled into dry, degassed cyclohexane (~200 mL) before being initiated with *sec*-BuLi (0.64 mL, 1.4 M in cyclohexane, 896 µmol), injected *via* syringe, to synthesise a polymer with a target M_n of 10,000 g mol^{-1}. After 6.5 hours being stirred at RT, dry, degassed EM1 (0.42 g, 2.76 mmol) was distilled into the polymer mixture. At this point the solution changed from a very, very pale yellow to a dark yellow colour, reminiscent of living polymyrcene. The solution was then left to stir for 18 hours at RT, before the polymerisation was terminated *via* the injection of an excess of sparged isopropanol.

PB(*b*)EM1 (a clear viscous liquid) was recovered by precipitation into a large excess of isopropanol, washed and dried in *vacuo* to yield poly(butadiene-*block*-epoxidised myrcene) (8.62 g, 92 %); **PB** – M_n – 11,500 g mol^{-1}, M_w – 11,600 g mol^{-1}, Đ – 1.01, **PB(*b*)EM1 –** M_n – 14,400 g mol^{-1}, M_w – 16,000 g mol^{-1}, Đ – 1.11 (as calculated by SEC using a dn/dc value of 0.124); 10 % (1,2), 90 % (1,4).

PS(DPE)EM1 was synthesised by LAP in cyclohexane at RT, under ultra-high vacuum conditions. Dry, degassed styrene (6.06 g, 58.2 mmol) was distilled into dry, degassed cyclohexane (~150 mL) before being initiated with *sec*-BuLi (0.87 mL, 1.4 M in cyclohexane, 1.22 mmol), injected *via* syringe, to synthesise a polymer with a target M_n of 5,000 g mol^{-1}. After 3 hours being stirred at RT, 1,1-diphenylethylene (DPE) (0.21 mL, 1.19 mmol, ~ 1 equivalent with respect to *sec*-BuLi) was added to the solution and left to stir at RT, under UHV. After 6 hours, dry, degassed EM1 (1.18 g, 7.76 mmol) was distilled into the polymer mixture. The solution was then left to stir for 4 hours at RT, before the polymerisation was terminated *via* the injection of an excess of sparged isopropanol. PS(DPE)EM1 (a white solid) was recovered by precipitation into a large excess of isopropanol, washed and dried in *vacuo* to yield poly(butadiene-*block*-epoxidised myrcene) (6.13 g, 82 %); **PS(DPE)** – M_n – 5,100 g mol^{-1}, M_w – 5,500 g mol^{-1}, Đ – 1.08, **PS(DPE)EM1 –** M_n – 6,600 g mol^{-1}, M_w – 7,900 g mol^{-1}, Đ – 1.21 (as calculated by SEC using a dn/dc value of 0.185).

4.4.5 Epoxidation Reactions (adapted from [55])

EM1 - Myrcene (33.60 g, 247 mmol) was passed through basic Al_2O_3 before being mixed with chloroform (200 mL), placed under argon and cooled to 0 ^oC. *m*-CPBA (62.71 g, ≤ 77 % purity, 280 mmol), which had been dissolved in chloroform (200 mL) was then added slowly. This solution was then stirred at 0 ^oC for 3 hours under argon. The reaction mixture was then washed with 0.1 M $NaHCO_3$ solution (250 mL x 2) before the organic layer was separated, dried with $MgSO_4$ and the DCM removed under vacuum. The EM was then columned to remove any di-epoxidised impurities using a gradient solvent approach starting at 100 % hexane and with a final solvent mixture of 90 % hexane and 10 % ethyl acetate. Solvents were removed in *vacuo* before the solution was distilled under vacuum where EM1 (27.29 g, 179 mmol, 73 % yield) was collected at 78 ^oC. ^1H NMR (400 MHz, $CDCl_3$): δ 6.38 (ddd, J = 17.6,

10.8, 0.7 Hz, 1H), 5.24 (dd, J = 17.8, 1.0 Hz, 1H), 5.12 – 4.99 (m, 3H), 2.75 (t, J = 6.3 Hz, 1H), 2.50 – 2.24 (m, 2H), 1.81 – 1.64 (m, 2H), 1.28 (d, J = 20.3 Hz, 6H).

EPM3 – PM3 (0.50 g) was dissolved in DCM (15 mL) before being place under argon and being cooled to - 78 ^{o}C. Afterwards, *m*-CPBA (0.17 g, ≤ 77 % purity, 759 µmol) was dissolved in DCM (10 mL) and slowly added to the polymer containing solution. This solution was then stirred at -78 ^{o}C for 3 hours under argon. The reaction mixture was then washed with 0.1 M $NaHCO_3$ solution (250 mL x 2) before the organic layer was separated, dried with $MgSO_4$ and precipitated into a large excess of methanol. EPM3 (a clear viscous liquid) was then collected, washed and dried in *vacuo* to yield epoxidised poly(myrcene) (0.43 g, 81 %).

4.4.6 Attempted Epoxide Ring Opening with BuLi

EPM-BuLi – EPM3 (0.15 g, 0.87 µmol) was first dried with 3 cycles of benzene azeotropic drying (3 x 10 mL) and then left under ultra-high vacuum for 18 hours to ensure it was completely dry. EPM-1 was then dissolved in dry benzene (20 mL) before an excess of *n*-BuLi (0.05 mL, 2.5 M in hexanes, 130 µmol) was added and the solution was left to stir at room temperature under UHV for 18 hours. EPM-BuLi (a clear viscous liquid) was recovered by precipitation into a large excess of methanol, washed and dried in *vacuo* to yield epoxidised poly(myrcene) (0.11 g, 73 %).

4.5 References

[1] M. Szwarc, “Living Polymers,” *Nature,* vol. 178, pp. 1168-1169, 1956.

[2] M. Szwarc, M. Levy and R. Milkovich, “Polymerization Initiated by Electron Transfer to Monomer. A New Method of Formation of Block Polymers,” *Communications to the Editor,* vol. 78, pp. 2636-2637, 1956.

[3] H. L. Hsieh and R. P. Quirk, Anionic Polymerization - Principles and Practical Applications, New York: Marcel Dekker, Inc., 1996.

[4] J. Gheller Jr, M. V. Ellwanger and V. Oliveira, “Polymer–filler interactions in a tire compound reinforced with silica,” *Elastomer and Plastics,* vol. 48, no. 3, pp. 217-226, 2016.

[5] M. Hassanabadi, M. Najafi, G. H. Motlagh and S. S. Garakani, “Synthesis and characterization of end-functionalized solution polymerized styrene-butadiene rubber and study the impact of silica dispersion improvement on the wear behavior of the composite,” *Polymer Testing,* vol. 85, p. 10643, 2020.

[6] W. Kaewsakul, K. Sahakaro, W. K. Dierkes and J. W. M. Noordermeer, “Factors influencing the flocculation process in silica-reinforced natural rubber compounds,” *Journal of Elastomers,* vol. 48, no. 5, p. 426, 2016.

[7] T. Yuasa, M. Iwano, T. Sone and T. Tominaga, “Improved Silica Dispersibility with functionalised s-SBR for Lower Rolling Resistance,” in *The International Tire Exhibition and Conference*, Ohio, 2008.

[8] S. M. Kimani and L. R. Hutchings, “A Facile Route to Synthesize Well-Defined Polybutadiene DendriMacs,” *Macromolecular Rapid Communications,* vol. 29, no. 8, pp. 609-683, 2008.

[9] J. M. Dodds, E. D. Luca, L. R. Hutchings and N. Clarke, “Rheological properties of HyperMacs—long-chain branched analogues of hyperbranched polymers,” *Journal of Polymer Science Part B: Polymer Physics,* vol. 45, no. 19, pp. 2762-2769, 2007.

[10] J. Hwang, M. D. Foster and R. P. Quirk, “Synthesis of 4-, 8-, 12-arm star-branched polybutadienes with three different chain-end functionalities using a functionalized initiator,” *Polymer,* vol. 45, no. 3, pp. 873-880, 2004.

[11] S. Agostini and L. R. Hutchings, “Synthesis and Temperature Gradient Interaction Chromatography of model asymmetric star polymers by the “macromonomer” approach,” *European Polymer Journal,* vol. 49, no. 9, pp. 2769-2784, 2013.

[12] C. L. Elkins, K. Viswanathan and T. E. Long, “Synthesis and Characterization of Star-Shaped Poly(ethylene-co-propylene) Polymers Bearing Terminal Self-Complementary Multiple Hydrogen-Bonding Sites,” *Macromolecules,* vol. 39, no. 9, pp. 3099-3472, 2006.

[13] M. Gauthier, L. Tichagwa, J. S. Downey and S. Gao, “Arborescent Graft Copolymers: Highly Branched Macromolecules with a Core-Shell Morphology,” *Macromolecules,* vol. 29, no. 2, pp. 519 - 527, 1996.

[14] A. Búcsi, J. Forcada, S. Gibanel, V. Héroguez, M. Fontanille and Y. Gnanou, “Monodisperse Polystyrene Latex Particles Functionalized by the Macromonomer Technique,” *Macromolecules,* vol. 31, no. 7, pp. 2087-2097, 1998.

[15] D. N. H. A. F. Schulz, “Anionic polymerization initiators containing protected functional groups. II,” *Journal of Polymer Science Part A: Polymer Chemistry,* vol. 15, no. 10, pp. 2401-2410, 1977.

[16] S. Pispas and N. Hadjichristidis, “End-Functionalized Block Copolymers of Styrene and Isoprene: Synthesis and Association Behavior in Dilute Solution,” *Macromolecules,* vol. 27, no. 7, pp. 1891-1896, 1994.

[17] A. Bozanko, W. D. Carswell, L. R. Hutchings and R. W. Richards, “Synthesis of a,v-macrozwitterionic polymers. End group analysis by SEC,” *Polymer,* vol. 41, no. 23, pp. 8175-8182, 2000.

[18] C. Tonhauser and H. Frey, “A Road Less Traveled to Functional Polymers: Epoxide Termination in Living Carbanionic Polymer Synthesis,” *Macromolecular Rapid Communications,* vol. 31, no. 22, p. 1938–1947, 2010.

[19] R. P. Quirk and J. Yin, “Carbonation of polymeric organolithium compounds: Effects of chain end structure,” *Journal of Polymer Science Part A: Polymer Chemistry,* vol. 30, no. 11, pp. 2349-2355, 1992.

[20] R. P. Quirk, J. Yin and L. J. Fetters, “Carbonation and related reactions of poly(styryl)lithium,” *Macromolecules,* vol. 22, no. 1, pp. 85-90, 1989.

[21] R. P. Quirk and J.-J. Ma, “Characterization of the functionalization reaction product of poly(styryl)lithium with ethylene oxide,” *Journal of Polymer Science Part A: Polymer Chemistry,* vol. 26, no. 8, pp. 2031-2037, 1988.

[22] J. Bowers, A. Zarbakhsh, J. R. P. Webster, L. R. Hutchings and R. W. Richards, “Structure of a Spread Film of a Polybutadiene−Poly(ethylene oxide) Linear Diblock Copolymer at the Air−Water Interface As Determined by Neutron Reflectometry,” *Langmuir,* vol. 17, no. 1, pp. 131-139, 2001.

[23] K. Ueda, A. Hirao and S. Nakahama, “Synthesis of polymers with amino end groups. 3. Reactions of anionic living polymers with α-halo-ι-aminoalkanes with a protected amino functionality,” *Macromolecules,* vol. 23, no. 4, pp. 939-945, 1990.

[24] R. P. Quirk and Y. Lee, “Quantitative amine functionalization of polymeric organolithium compounds with 3-dimethylaminopropyl chloride in the presence of lithium chloride,” *Journal of Polymer Science Part A: Polymer Chemistry,* vol. 38, no. 1, pp. 145-151, 2000.

[25] M. Ganß, B. K. Satapathy, M. Thunga, U. Staudinger, R. Weidisch, D. Jehnichen, J. Hempel, M. Rettenmayr, A. Garcia-Marcos and H. H. Goertz, “Morphology and mechanical response of S–B star block copolymer – Layered silicate nanocomposites,” *European Polymer Journal,* vol. 45, no. 9, pp. 2549-2563, 2009.

[26] R. P. Quirk and J. Kim, “Anionic synthesis of model ionomers: ι-lithium poly(styrene)sulfonates,” *Macromolecules,* vol. 24, no. 16, pp. 4481-4732, 1991.

[27] L. R. Hutchings, P. P. Brooks, D. Parker, J. A. Mosely and S. Sevinc, “Monomer Sequence Control via Living Anionic Copolymerization: Synthesis of Alternating, Statistical, and Telechelic Copolymers and Sequence Analysis by MALDI ToF Mass Spectrometry,” *Macromolecules,* vol. 48, no. 3, pp. 610-628, 2015.

[28] L. R. Hutchings and S. J. Roberts-Bleming, “DendriMacs. Well-Defined Dendritically Branched Polymers Synthesized by an Iterative Convergent Strategy Involving the Coupling Reaction of AB2 Macromonomers,” *Macromolecules,* vol. 39, no. 6, pp. 2144 - 2152, 2006.

[29] L. R. Hutchings, J. M. Dodds and S. J. Roberts-Bleming, “HyperMacs: Highly Branched Polymers Prepared by the Polycondensation of AB2 Macromonomers, Synthesis and Characterization,” *Macromolecules,* vol. 38, no. 14, pp. 5970-5980, 2005.

[30] L. R. Hutchings, J. M. Dodds, D. Rees, S. M. Kimani, J. J. Wu and E. Smith, “HyperMacs to HyperBlocks: A Novel Class of Branched Thermoplastic Elastomer,” *Macromolecules,* vol. 42, no. 22, pp. 8675-8687, 2009.

[31] X. Fan, Q. Zhou, C. Xia, W. Cristofoli, J. Mays and R. Advincula, “Living Anionic Surface-Initiated Polymerization (LASIP) of Styrene from Clay Nanoparticles Using Surface Bound 1,1-Diphenylethylene (DPE) Initiators,” *Langmuir,* vol. 18, no. 11, pp. 4511-4518, 2002.

[32] R. P. Quirk and L.-F. Zhu, “Anionic synthesis of dimethylamino-functionalized polystyrenes and poly (methyl methacrylates) using 1 - (4-dimethylaminophenyl) - 1 - phenylethylene,” *Polymer International,* vol. 23, no. 1-2, pp. 47-54, 1990.

[33] R. P. Quirk and T. Lynch, “Anionic synthesis of primary amine-functionalized polystyrenes using 1-[4-[N,N-bis(trimethylsilyl)amino]phenyl]-1-phenylethyleneClick,” *Macromolecules,* vol. 26, no. 6, pp. 1206 - 1212, 1993.

[34] S. Pispas and N. Hadjichristidis, “Block copolymers with Zwitterionic groups at specific sites: Synthesis and aggregation behavior in dilute solutions,” *Journal of Polymer Science Part A: Polymer Chemistry,* vol. 38, no. 20, pp. 3791-3801, 2000.

[35] L. Wu, Y. Wang, Y. Wang, K. Shen and Y. Li, “In-chain multi-functionalized polystyrene by living anionic copolymerization with 1,1-bis(4-dimethylaminophenyl)ethylene: Synthesis and effect on the dispersity of carbon black in polymer-based composites,” *Polymer,* vol. 54, no. 12, pp. 2958-2965, 2013.

[36] A. Hirao, Y. Karasawa, T. Higashihara, Y. Zhao and K. Sugiyama, “Synthesis of block co-polymers and star-branched polymers consisting of conducting polyacetylene segments via ionic interaction to form ionic bonds,” *Designed Monomers & Polymers,* vol. 7, no. 6, pp. 647-660, 2004.

[37] M. Hayashi, “Design and Synthesis of Functionalized Styrene-Butadiene Copolymers by Means of Living Anionic Polymerization,” *Macromolecular Symposia,* vol. 215, no. 1, pp. 29-40, 2004.

[38] G. J. Summers and R. P. Quirk, “Anionic synthesis of aromatic amide and carboxyl functionalized polymers. Chain-end functionalization of poly(styryl)lithium with N,N-diisopropyl-4-(1-phenylethenyl)benzamide,” *Journal of Polymer Science Part A: Polymer Chemistry,* vol. 36, no. 8, pp. 1233-1241, 2000.

[39] R. P. Quirk and L.-f. Zhu, “Anionic synthesis of chain-end functionalized polymers using 1,1-diphenylethylene derivatives. Preparation of 4-hydroxyphenyl-terminated polystyrenes,” *Macromolecular Chemistry and Physics,* vol. 190, no. 3, pp. 487-493, 1989.

[40] N. Clarke, E. D. Luca, J. M. Dodds, S. M. Kimani and L. R. Hutchings, “HyperMacs – long chain hyperbranched polymers: A dramatically improved synthesis and qualitative rheological analysis,” *European Polymer Journal,* vol. 44, no. 3, pp. 665-676, 2008.

[41] R. P. Quirk, T. Yoo, Y. Lee, M. Morton, J. Kim and B. Lee, “Application of 1,1-Diphenylethylene Chemistry in Anionic Synthesis of Polymers with Controlled Structures.,” in *Biopolymers · PVA Hydrogels Anionic Polymerisation Nanocomposites*, Berlin, Springer Science & Business Media, pp. 67-162, 2000.

[42] R. P. Quirk and Y. Wang, “Anionic difunctionalization with 1,1-bis(4-t-butyldimethylsiloxyphenyl) ethylene. Synthesis of ω,ω-bis(phenol)-functionalized polystyrene condensation macromonomers,” *Polymer International,* vol. 31, no. 1, pp. 51-59, 1993.

[43] P. P. Brooks, A. Natalello, J. N. Hall, E. A. L. Eccles, S. M. Kimani, K. Bley and L. R. Hutchings, “Monomer Sequencing in Living Anionic Polymerization Using Kinetic Control,” *Macromolecular Symposia,* vol. 323, no. 1, pp. 42-50, 2013.

[44] A. Natalello, J. N. Hall, E. A. L. Eccles, S. M. Kimani and L. R. Hutchings, “Kinetic Control of Monomer Sequence Distribution in Living Anionic Copolymerisation,” *Macromolecular Rapid Communications,* vol. 32, no. 2, pp. 233 - 237, 2011.

[45] P. Liu, H. Ma, W. Huang, H. Shen, L. Wu, Y. Li and Y. Wang, “The determination of sequence distribution in the living anionic copolymerization of styrene and strong electron-donating DPE derivative-1,1-bis(4-N,N-dimethylanimophenyl)ethylene,” *Polymer,* vol. 97, pp. 167-173, 2016.

[46] P. Liu, H. Ma, W. Huang, L. Han, X. Hao, H. Shen, Y. Bai and Y. Li, “Sequence regulation in the living anionic copolymerization of styrene and 1-(4-dimethylaminophenyl)-1-phenylethylene by modification with different additive,” *Polymer Chemistry,* vol. 8, no. 11, p. 1778–1789, 2017.

[47] A. Natalello, M. Werre, A. Alkan and H. Frey, “Monomer Sequence Distribution Monitoring in Living Carbanionic Copolymerization by Real-Time 1H NMR Spectroscopy,” *Macromolecules,* vol. 46, no. 21, pp. 8467-8471, 2013.

[48] H. Ma, L. Han and Y. Li, “Sequence Determination and Regulation in the Living Anionic Copolymerization of Styrene and 1,1-Diphenylethylene (DPE) Derivatives,” *Macromolecular Chemistry and Physics,* vol. 218, no. 12, p. 1600420, 2017.

[49] A. Pagliarulo and L. R. Hutchings, “End-Functionalized Chains via Anionic Polymerization: Can the Problems with Using Diphenylethylene Derivatives be Solved by using Bisphenol F?,” *Macromolecular Chemistry and Physics,* vol. 19, no. 1, p. 1700386, 2018.

[50] M. Panthakkal, A. Muthalif and Y. Choe, “Influence of Maleinized Polybutadiene on Adhesive Strength and Toughness of Epoxy Resins,” *International Journal of Polymer Science,* vol. 2022, no. 1, p. 8, 2022.

[51] B. Yang, P. Li, Z. Luo, J. Zhong and L. Yin, “Influence of thermal oxidation and maleinized liquid polybutadiene on dynamic and static performance of short aramid fiber-reinforced carbon black-ethylene propylene diene monomer composites,” *Polymer Composites,* vol. 41, no. 5, pp. 2036 - 2045, 2020.

[52] A. E. Holboke and R. P. Pinnell, “Sulfonation of polystyrene: Preparation and characterization of an ion exchange resin in the organic laboratory,” *Journal of Chemical Education,* vol. 66, no. 7, pp. 535-618, 1989.

[53] J. E. Coughlin, A. Reisch, M. Z. Markarian and J. B. Schlenoff, “Sulfonation of polystyrene: Toward the “ideal” polyelectrolyte,” *Journal of Polymer Science Part A: Polymer Chemistry,* vol. 51, no. 11, pp. 2319-2526, 2013.

[54] F. R. De Risi, L. D'Ilario and A. Martinelli, “Synthesis and Characterization of Epoxidized Polybutadiene/Polyaniline Graft Conducting Copolymer,” *Polymer Science,* vol. 42, no. 12, pp. 3082-3090, 2004.

[55] R. Pandit, G. H. Michle, R. Lach, W. Grellmann, J. M. Saiter, A. Berkessel and R. Adhikari, “Epoxidation of Styrene/Butadiene Star Block Copolymer by Different Methods and Characterization of the Blends with Epoxy Resin,” *Macromolecular Symposia,* vol. 341, no. 1, pp. 67-74, 2014.

[56] K. Sengloyluan, K. Sahakaro, W. Dierkes and J. W. M. Noordermeer, “Silica-reinforced tire tread compounds compatibilized by using epoxidized natural rubber,” *European Polymer Journal,* vol. 51, pp. 69-79, 2014.

[57] P. Sarkar and A. K. Bhowmick, “Synthesis, characterization and properties of a bio-based elastomer: polymyrcene.,” *Royal Society of Chemistry Advances,* vol. 4, pp. 61343-61354, 2014.

[58] C. Iacob, T. Yoo and J. Runt, “Molecular Dynamics of Polyfarnesene,” *Macromolecules,* vol. 51, no. 13, pp. 4917-4922, 2018.

[59] P. Sahu and A. K. Bhowmick, “Redox Emulsion Polymerization of Terpenes: Mapping the Effect of the System, Structure, and Reactivity.,” *Industrial & Engineering Chemistry Research,* vol. 58, no. 46, pp. 20946-20960, 2019.

[60] A. Behr and L. Johnen, “Myrcene as a Natural Base Chemical in Sustainable Chemistry: A Critical Review,” *ChemSusChem,* vol. 2, pp. 1072-1095, 2009.

[61] X. Yang, C. Wang, S. Li, K. Huang, M. Li, W. Mao, S. Cao and J. Xia, “Study on the synthesis of bio-based epoxy curing agent derived from myrcene and castor oil and the properties of the cured products,” *RSC Advances,* vol. 7, pp. 238-247, 2017.

[62] E.-M. Kim, J.-H. Eom, Y. Um, Y. Kim and H. M. Woo, “Microbial Synthesis of Myrcene by Metabolically Engineered Eschericha coli,” *Agricultural and Food Chemistry,* vol. 63, pp. 4606-4612, 2015.

[63] W. Li, J. Zhao, X. Zhang and D. Gong, “Capability of PN3-type Cobalt Complexes toward Selective (Co-)Polymerization of Myrcene, Butadiene, and Isoprene: Access to Biosourced Polymers,” *Industrial and Engineering Chemistry Research ,* vol. 58, pp. 2792-2800, 2019.

[64] E. Grune, J. Bareuther, J. Blankenburg, M. Appold, L. Shaw, A. H. E. Muller, G. Floudas, L. R. Hutchings, M. Gallei and H. Frey, “Towards bio-based tapered block copolymers: the behaviour of myrcene in the statistical anionic copolymerisation,” *Polymer Chemistry,* vol. 10, pp. 1213-1220, 2019.

[65] L. Shaw and L. R. Hutchings, “Tales of the unexpected. The non-random statistical copolymerisation of myrcene and styrene in the presence of a polar modifier,” *Polymer Chemistry,* vol. 11, pp. 7020-7025, 2020.

[66] D. A. H. Fuchs, H. Hübner, T. Kraus, B.-J. Niebuur, M. Gallei, H. Frey and A. H. E. Müller, "The effect of THF and the chelating modifier DTHFP on the copolymerisation of β-myrcene and styrene: kinetics, microstructures, morphologies, and mechanical properties," *Polymer Chemistry,* vol. 12, no. 32, pp. 4632-4642, 2021.

[67] E. Grune, J. Bareuther, J. Blankenburg, M. Appold, L. Shaw, A. H. E. Muller, G. Floudas, L. R. Hutchuings and H. Frey, "Towards bio-based tapered block copolymers: the behaviour of myrcene in the statistical anionic copolymerisation," *Polymer Chemistry,* vol. 10, pp. 1213-1220, 2019.

[68] C. Wahlen and H. Frey, "Anionic Polymerization of Terpene Monomers: New Options for Bio-Based Thermoplastic Elastomers," *Macromolecules,* vol. 54, no. 16, pp. 7323 - 7336, 2021.

[69] M. Rauschenbach, M. Meier-Merziger and H. Frey, "Green perspective drives the renaissance of anionic diene polymerization," *Polymer Chemistry,* vol. 15, no. 42, pp. 4297-4311, 2024.

[70] A. Matic, A. Hess, D. Schanzenbach and H. Schlaad, "Epoxidized 1,4-polymyrcene," *Polymer Chemistry,* vol. 11, no. 7, pp. 1364-1368, 2019.

[71] A. Matic and H. Schlaad, "Thiol-ene photofunctionalization of 1,4-polymyrcene," *Polymer International,* vol. 67, no. 5, pp. 500-505, 2018.

[72] C. Wahlen, M. Rauschenbach, J. Blankenburg, E. Kersten, C. P. Ender and H. Frey, "Myrcenol-Based Monomer for Carbanionic Polymerization: Functional Copolymers with Myrcene and Bio-Based Graft Copolymers," *Macromolecules,* vol. 53, no. 20, pp. 9008-9017, 2020.

[73] C. Wahlen, M. Rauschenbach, J. Blankenburg, E. Kersten, C. P. Ender and H. Frey, "Myrcenol-Based Monomer for Carbanionic Polymerization: Functional Copolymers with Myrcene and Bio-Based Graft Copolymers," *Macromolecules,* vol. 53, no. 20, pp. 9008-9017, 2020.

[74] J. Clayden, N. Greeves and S. Warren, Organic Chemistry, Oxford University Press, 2012.

[75] L. Leemans, R. Fayt and P. Teyssie, "Controlled "Living" Anionic Polymerization of Glycidyl Methacrylate," *Journal of Polymer Science: Part A Polymer Chemistry,* vol. 28, pp. 2187-2193, 1990.

[76] D. Baskaran, “Strategic developments in living anionic polymerization of alkyl (meth)acrylates,” *Progress in Polymer Science,* vol. 28, pp. 521-581, 2003.

[77] S. Georges, M. Bria, P. Zinck and M. Visseaux, “Polymyrcene microstructure revisited from precise high-field nuclear magnetic resonance analysis,” *Polymer,* vol. 55, pp. 3869-3878, 2014.

[78] C. Pittman and B. Culbertson, “New Monomers and Polymers,” *Polymer Science and Technology,* vol. 25, 2012.

[79] A. Padwa and S. Murphree, “Epoxides and aziridines - A mini review,” *Arkivoc,* vol. 3, pp. 6-33, 2006.

[80] J. Corset, M. Castella-Ventura, F. Froment, T. Strzalko and L. Wartski, “Formation mechanism of acetaldehyde lithium enolate by reaction of n-butyllithium with tetrahydrofuran: infrared and Raman spectroscopy and density functional theory calculations,” *Journal of Raman Spectroscopy,* vol. 33, pp. 652-668, 2002.

[81] S. Monticelli, L. Castoldi, I. Murgia, R. Senatore, E. Mazzeo, J. Wackerlig, E. Urban, T. Langer and V. Pace, “Recent advancements on the use of 2-methyltetrahydrofuran in organometallic chemistry,” *Monatsh Chemistry,* vol. 147, pp. 37-48, 2017.

Conclusions and Future Works

From the results presented in this thesis it has been shown that the bio-available monomer myrcene can be both homopolymerised and copolymerised by LAP. It was shown that in the copolymerisation of myrcene with styrene that a strong preference for the incorporation of myrcene is displayed – resulting in a tapered block copolymer – while in the copolymerisation of myrcene with butadiene there is a very slight preference for the incorporation of myrcene – resulting in gradient copolymers. This preference for the enhanced relative incorporation of myrcene was found to be completely inverted in both cases of copolymerisation when a polar modifier, such as TMEDA, was added to the reaction mixture. In the presence of two molar equivalents of TMEDA it was shown that in both sets of copolymerisations the relative rate of myrcene incorporation is massively reduced leading to the synthesis of tapered block-like copolymers.

This thesis also presented results regarding the epoxidation of myrcene-containing polymers to demonstrate that myrcene can be utilised as a selective site of epoxidation in conventional styrene-butadiene rubbers. It was shown that despite the backbone and pendant double bond of myrcene being equally substituted, that there is a preference for epoxidation to occur on the pendant double bond (~ 66 %). It was also shown that small amounts of myrcene can be incorporated into sSBR and selectively epoxidised with minimal effect on the double bonds of butadiene present in the sample – allowing for the exact positioning of the epoxidation to occur based on where the myrcene is present in the polymer. Attempted ring-opening reactions also lead to the realisation that the trisubstituted epoxide of polymyrcene is fairly resistant against nucleophilic attack whereby only $LiAlH_4$ was found to allow for the ring-opening of the epoxides without side reactions occurring at the unepoxidised double bonds in the sample.

The realisation that the epoxide of myrcene was fairly resistant against nucleophilic attack also led to the research of epoxidised myrcene as a functionalised monomer that could be polymerised by LAP. Despite only marginal levels of success in the anionic polymerisation of this epoxidised monomer it was found that the epoxidised monomer could be utilised as a multi-chain end functionalising unit to provide on average up to 3/4 epoxidised units compared to conventional chain-end functionalisation methods that usually provide 1 (or 2 if a functional initiator is used too) functional group(s) per chain.

Whilst this thesis focussed solely on myrcene and its selective epoxidation, other types of bio-available monomer and other methods of selective functionalisation were also investigated but due to the limitation of space and time, this work was excluded. This work included the anionic polymerisation and copolymerisation of farnescene and ocimene – two other bio-available terpenes – and the selective epoxidation of the resulting copolymers. Both of these monomers showed interesting kinetics, whereby the ocimene was found to copolymerise almost completely randomly with styrene in the absence of any polar modifier but suffered from competing side reactions which limited its usefulness. Other selective functionalisation methods that were trialled included bromination – which was investigated to provide selective sites for the initiation of ATRP – and triazolinedione functionalisation – which was investigated as part as a collaboration with Filip Du Prez but suffered from oxidative crosslinking reactions. Given more time the work around these monomers and methods of functionalisation would be expanded upon to further enhance the selective functionalisation toolbox of LAP scientists whilst also continuing the ever-pressing hunt for sustainable polymers. During the investigation of this thesis only the synthesis of functionalised polymers that can be utilised industrially were investigated and given more time, the effect of the functionalisation of the polymers would be investigated to ensure that the benefit of functionalisation that has been alluded to was present in commercial samples of the functionalised sSBR.

Several projects were also conceived during the duration of this study which could provide the foundations for further research and utilisation of selectively functionalised polymers synthesised by LAP that were not investigated due to restrictions in time but based on observations provided by this thesis would be of significant interest. A project which looked at the selective functionalisation of styrenic monomers – utilising the differences in rates of aromatic electrophilic substitution reactions along with a range of methyl-substituted styrenes – would be highly interesting as this would provide a completely separate class of selectively fuctionisable polymers for when diene monomers may not be applicable and potentially allows for investigation of two orthogonal selective functionalisation methods for sSBR that could provide separate property enhancements to the formulation.

Finally, it is believed that vast improvements could be made to the polymerisation of functional monomers by LAP through a couple of different modifications to the system that was presented in the polymerisation of epoxidised myrcene shown in Chapter 4 but were not

possible during the time of study. These improvements include using a methyl substituted aziridine (which can be synthesised directly from the epoxide - See Figure C.1) below instead of the epoxide as the functional diene monomer that could be polymerised by LAP. It is believed that this aziridine would have a greater degree of incorporation before any potential termination reactions (if any termination reactions are still possible) could occur due to the lower electronegativity of the nitrogen compared to oxygen and due to the reduced internal bond strain of the aziridine compared to the epoxide which should reduce the likelihood of any potential termination reactions that were identified. This could mean that this methyl-aziridine could be a highly interesting monomer to investigate potential monomers that provide polymer polarity without the requirement for deprotection post-polymerisation.

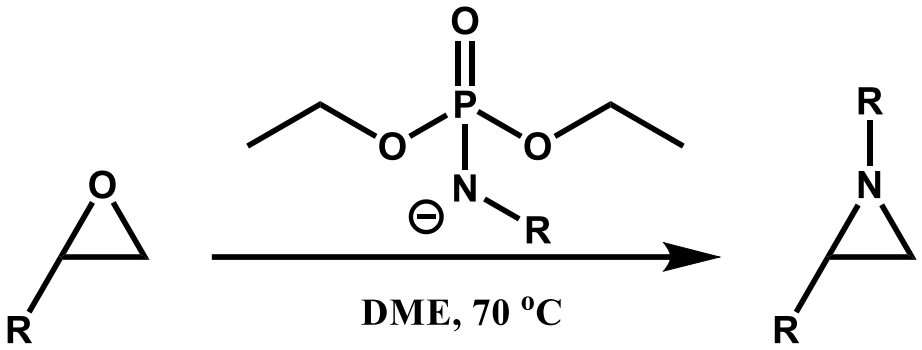

Figure C.1: Schematic showing the conditions required for the direct synthesise of a substituted aziridine from the corresponding epoxide. [1]

The final project that was conceived, while potentially highly speculative but theoretically possible based on all of the available knowledge and understanding that has been gained throughout the investigations conducted during this thesis, regards the use of lithium as a "pseudo"-protecting group for alcohols during LAP. It is common knowledge that in LAP systems the Li-O bond represents a strong ionic bond that once formed in the system generally results in termination (for example the LAP of ethylene oxide is possible using a sodium counterion but polymerisations using a lithium counterion are generally terminated after one ring opening of a ethylene oxide monomer due to the formation of a lithium oxygen bond unless other additives which "activate" the monomer are added). [2] It is believed that due to this phenomenon that it would be theoretically possible to ring open the epoxide that was presented in Chapter 4 of this thesis (or treat another monomer with hydroxyl

functionality) using a lithiating agent such as $LiAlH_4$ to provide a Li-O at the resulting hydroxyl sites. If rather than working this lithiated monomer up – through the addition of a protic solvent – that this monomer was used directly in an LAP system (without exposure to air) it is believed that the Li-O bond would act as a "pseudo"-protecting group during the polymerisation which would then be removed to provide the corresponding hydroxyl functionalisation through standard termination of the LAP reaction – through addition of a protic solvent – without the requirement for an additional deprotection step. While highly speculative any success that could be provided from a project such as this would be of great interest to academia and industry as it would provide a brand-new concept for introducing functionality into polymers synthesised by LAP without any requirement for costly deprotection steps.

[1] F. Minicone, W. J. Rogers, J. F. J. Green, M. Khan, G. M. T. Smith, C. D. Bray, "Direct conversion of epoxides into aziridines with N-arylphosphoramidates," *Tetrahedron Letters,* vol. 55, no. 43, pp. 5890-5891, 2014.

[2] J. Herzberger, K. Niederer, H. Pohlit, J. Seiwert, M. Worm, Fr. R. Wurm, H. Frey, "Polymerization of Ethylene Oxide, Propylene Oxide, and Other Alkylene Oxides: Synthesis, Novel Polymer Architectures, and Bioconjugation," *Chemical Reviews,* vol. 116, no. 4, pp. 2170-2243, 2016.